Scientific Research Support Fund

The Hashemite Kingdom of Jordan

The University of Jordan

المجلة الأردنية في العلوم الصيدلانية

مجلة علمية عالمية متخصصة تصدر بدعم من صندوق دعم البحث العلمي والابتكار

Jordan Journal of PHARMACEUTICAL Sciences

Specialized International Refereed Journal

Issued by the Scientific Research Support Fund

This title is indexed in Scopus

مجلد (16) العدد (2)، ملحق (1) 2023

Volume 16, No. 2, Supplement 1, 2023

Established 2007

ISSN: 1995-7157

EISSN: 2707-6253

Publisher

The University of Jordan
Deanship of Scientific Research
Amman 11942 Jordan
Fax: +962-6-5300815

National Deposit
(23.3/2008/D)
(Journal's National Deposit Number at the Jordanian National Library)

Jordan Journal of Pharmaceutical Sciences

Volume 16, Number (2) Supplement 1, 2023

Jordan Journal of Pharmaceutical Sciences

Aims & Scopes:

***Jordan Journal of Pharmaceutical Sciences* (*JJPS*)** is a bimonthly open-access peer reviewed journal funded by the Scientific Research Fund at Ministry of Higher Education and Research and hosted by the Deanship of Research at the University of Jordan. JJPS is dedicated to various disciplines of pharmaceutical and allied sciences. JJPS publishes manuscripts on original work, either experimental or theoretical in the following areas:

- Pharmaceutics & Biopharmaceutics
- Drug Delivery systems
- Nanotechnology & Nanomedicine
- Organic & Medicinal Chemistry
- Pharmacognosy & Phytochemistry
- Pharmacology, Toxicology, and Experimental Therapeutics
- Pharmaceutical Biotechnology
- Microbiology
- Pharmacy Practice
- Clinical Pharmacy & Hospital Pharmacy
- Pharmacovigilance & Drug Safety
- Health Outcomes and Economics
- Pharmaceutical Health Care Services
- Natural Product Research
- Drug Regulatory Affairs
- Health Policy
- Pharmaceutical Marketing

Instructions to Authors

Preparation and Submission of Manuscripts

Type of Manuscripts

JJPS publishes original research articles, full reviews, research reports, short communications, case studies, commentaries, and short reviews.

Manuscript Preparation

Research paper should be typed on the computer; double spaced, and shouldn't exceed 15 pages (3000 words, font size 12). Spelling, punctuation, sentence structure, spacing, length, and consistency in form and descriptions should be checked before submission. References should also be checked for accuracy. Ensure that all figures and tables are mentioned in the text, and that all references are cited in the text.

Title Page

A separate title page should be submitted separately with the manuscript. The title should be followed by the author(s) name(s) and full affiliations including institution name and address. The title, author(s) name(s), and affiliations should all appear on their own respective line of text. Place an asterisk after the name of the author to whom enquiries regarding the paper should be directed and include that author's telephone and fax numbers and e-mail address. Author(s) affiliation (s) must be mentioned for each one in order.

Abstract

Authors should submit with their research two abstracts, one in English and it should be typed at the beginning of the paper followed by the keywords before the introduction.

The abstract, detailing in one paragraph the problem, experimental approach, major findings, and conclusions, should appear on the second page. It should be double spaced and should not exceed 200 words for **Full Papers and Reviews or l00 words for Case Studies and Short Communications.**

Compounds mentioned in the abstract, given as specific Arabic numbers in the text, should also be accompanied in the abstract by that same numeral. The abstract should appear on a separate page and should be untitled.

Authors are required to submit an Arabic abstract (Required only for Arab native speakers) which should be appended at the end of the submitted manuscript on a separate sheet, including author(s) name(s) and affiliation(s).

Keywords

Should be included at the end of the abstract page, separated by semicolons, not exceeding seven both in Arabic and in English.

Introduction

The manuscript should include an introduction stating the purpose of the research detailed in the manuscript and summaries previous literature leading to the idea and method described in the manuscript.

Results

The results should be presented concisely. Tables and figures should be designed to maximize the presentation and comprehension of the experimental data. Data present in tables and figures should not be redundant in the manuscript's text.

Discussion

The discussion section should interpret the results and relate them to existing knowledge in the field in as clearly and brief as possible. For Full Papers, subheadings may be included within the Results and Discussion sections.

Bolded structural code numbers should only be used for new compounds and for those known compounds for which new biological data or spectroscopic values are being reported. Other known compounds should be referred to in the text by name, wherever necessary.

Experimental Section

The presentation of specific details about instruments used, sources of specialized chemicals and related experimental details should be incorporated into the text of the Experimental Section as a paragraph headed General Experimental.

Acknowledgments

The Acknowledgments section should include credits [initial(s) and last name(s)] for technical assistance, and other appropriate recognition.

Conflict of Interest

Authors should declare any pertaining conflicts in their work, otherwise the authors should clearly indicate that no conflict is present.

Funding

Authors should declare any received funding, indicating the funding institution and grant number. Otherwise, the receipt of no funding should be indicated.

References and Notes

References to the literature and all notes, regardless of their nature, should be numbered in order of appearance in the manuscript, and then cited under the heading References and Notes with superscript numbers. Each reference may have its own citation number, then should be assigned its own number in this section. References and notes should follow the format shown:

Journal

Taha M., Al-Bakri A. and Zalloum W. Discovery of potent inhibitors of pseudomonal quorum sensing via pharmacophore modeling and silico screening. *Bioorg. Med. Chem. Lett.* 2006; 16:5902-5906.

Book

Ancel H. C., Allen L. V. and Popovich N. G. *Pharmaceutical Dosage Forms and Drug Delivery Systems*; Lippicott Williams & Wilkins: New York. 1999, p 45.

Chapter in a Book

Aburjai T., Natsheh F. and Qasem A.: *In: Contemporary Perspective on Clinical Pharmaceutics*. Kohli K. (Ed).; Elsevier New York, 2006; 1st edition, Chapter 57, pp 623-633.

Chemical or Biological Abstract

Al-Hiari Y., Qaisi A., El-Abadelah M. and Wolfgamg V., *Monatshefte fuer Chemei*. 2006; 137(2) 243-248, *Chem. Abstr*. 2007; 145, 397308.

Ph.D. or M. Sc. Thesis

Alkhalil S. The Alkaloids of *Thalictrum isopyroides*. Ph.D. Thesis, Pittsburgh University, PA. 1986, p 115.

Patent

Davis R. U.S. Patent 5,708,591, 1998.

The author is responsible for the accuracy and completeness of all references.

All references must be numbered and written "superscript "without parentheses in the Manuscript (*e.g....according to guidelines pertaining to these techniques*[5,6,7] **);but with parentheses around in the references list (***e.g. (1) Alkhalil S. The Alkaloids of Thalictrum isopyroides. Ph.D. Thesis, Pittsburgh University, PA. 1986, p 115).*

Nomenclature

It is the responsibility of the author(s) to provide correct nomenclature.

Insofar as possible, authors should use systematic names similar to those used by Chemical Abstracts Service.

Abbreviations

Standard abbreviations should be used throughout the manuscript. All nonstandard abbreviations should be kept to a minimum and must be defined in the text following their first use. The preferred forms of some of the more commonly used abbreviations are: mp, bp, °C, K, s, min, h, mL, . **μ**L, kg, g, mg, ng, **μ**g, cm, mm, nm, mnl, mmol, , **μ**mol, ppm, TLC, GC, HPLC, NMR, MS, UV, and IR.

Graphics

The quality of the illustrations printed depends on the quality of the originals provided. Figures cannot be modified or enhanced by the journal production staff. Whenever possible, the graphic files furnished by authors on CD with revised submissions of accepted manuscripts are used in production of the Journal.

A- Layout

In preparing structures for direct photoreproduction, layout is critical. Equations, schemes and blocks of structures are presented in the Journal either in one-column or two-column format.

B- Content

Abbreviations such as Me for CH_3, Et for C_2H_5 and Ph (but not Φ) for C_6H_5 are acceptable.

C- Dimensions

For best results, illustrations should be submitted in the actual size at which they should appear in the Journal. Only original work or high quality photographic prints of originals should be submitted; photocopies do not reproduce well.

Chemical Structures

Structures should be produced with the use of a drawing program such as Chem-Draw. Structure drawing preferences are as follows:

1- Drawing settings:

Chain angle 120°

Bond spacing 18% of width

Fixed length 14.4 pt (0.508 cm, 0.2 in.), Bold width 2.0 pt (0.071 cm, 0.0278 in.), Line width 0.6 pt (0.021 cm, 0.0084 in.), Margin width 1.6 pt (0.056 cm, 0.0222 in.), Hash spacing 2.5 pt (0.088 cm, 0.0347 in.)

2- Text settings:

Font: Arial/Helvetica

Size: 10 pt

3- Preference:

Units: points

Tolerance: 3 pixels

4- Page setup:

Paper: US Letter

Scale: 100%

Tables

These should be numbered consecutively with Arabic numerals and should be arranged within the manuscript.

Footnotes in tables should be given lowercase letter designations and be cited in the table by italic superscript letter.

Figures

Figures should be constructed in keeping with the column width and line width. All illustrations should be numbered as "Figures", with Arabic numerals.

The Arabic numbers (not the roman ones or the alphabets) are used to number the Tables and Figures which are not abbreviated into Fig. or Tab.

Informed Consent

All manuscripts reporting the results of experimental investigation involving human subjects should include a statement confirming that an informed consent was obtained from each subject or subject's guardian, after the approval of the experimental protocol by a local human ethics committee or IRB.

Copyright Status Form

A properly completed Copyright Status Form with an original signature in ink must be provided for each submitted manuscript.

Manuscript Submission

Manuscripts (in English), together with a cover letter from the corresponding author, should be submitted. A valid e-mail address should be listed when submitting manuscripts.

Manuscript submission via **Website**: **https://jjournals.ju.edu.jo/index.php/jjps/**

Galley Proofs

Page proofs will be sent to the author who submitted the paper. The standard delivery method for galley proofs is by mail.

Correspondence

Correspondence regarding accepted papers and proofs should be directed to Jordan Journal of Pharmaceutical Sciences.

Deanship of Scientific Research
The University of Jordan
Amman 11942, Jordan
Phone: +962 6 5355000 Ext. 25106
Fax: 00962 6 5300815
E-mail: jjps@ju.edu.jo
Website: **https://jjournals.ju.edu.jo/index.php/jjps/**

INTRODUCTION

The Jordan Journal of Pharmaceutical Sciences (**JJPS**) is a peer-reviewed Journal, which publishes original research work that contributes significantly to further the scientific knowledge in pharmaceutical sciences' fields including pharmaceutical/medicinal chemistry, drug design and microbiology, biotechnology and industrial pharmacy, instrumental analysis, phytochemistry, biopharmaceutics and pharmacokinetics, clinical pharmacy and pharmaceutical care, pharmacogenomics, bioinformatics, and also **JJPS** is welcoming submissions in pharmaceutical business domain such as pharmacoeconomics, pharmaceutical marketing, and management. Intellectual property rights for pharmaceuticals, regulations and legislations are also interesting topics welcomed from our colleagues in Schools of Law.

On a current topic in Pharmaceutical Sciences are also considered for publication by the Journal. **JJPS** is indexed in SCOPUS (Q3). It's a journal that publishes 4 issues per year since 2021 in (**March, June, September, December**). The Editorial Team wishes to thank all colleagues who have submitted their work to JJPS). If you have any comments or constructive criticism, please do not hesitate to contact us at jjps@ju.edu.jo. We hope that your comments will help us to constantly develop **JJPS** as it would be appealing to all our readers.

Prof Ibrahim Alabbadi
Editor-in-Chief
School of Pharmacy- The University of Jordan
Amman 11942- Jordan

Volume 16, 2023

Letter from the Editor-in-Chief

After a full year of getting back to normal life in 2022, with all work including editorial board meetings performed face to face, the Jordan Journal of Pharmaceutical Sciences (JJPS) will continue to publish 4 issues annually at regular times i.e., quarterly, but the good news that each issue every quarter will have 15 accepted articles to be published per issue (instead of 10). The latter indicates the good achievement of JJPS last year as much more submissions were received from international countries representing 70% of total submissions while 30% were received from Jordan. Furthermore, this will decrease waiting times for researchers in receiving decisions regarding whether their submissions are either accepted or not. Also increasing the number of articles published per issue will again increase researchers' satisfaction and not delay publishing their accepted work, for example, the waiting time from receiving the submission through the decision to publishing decreased from 34 weeks in (2019-2020) to 22 weeks in (2021-2022) on average.

On the other hand, the number of citations exceeded 2 folds of the number of articles published looking forward to reaching the Q2 category in SCOPUS soon; thanks to all colleagues on the editorial board, local as well as international advisory board scientists, also special thanks to all researchers for their belief and trust in JJPS.

One important issue worth mentioning this year is the challenge of using Artificial Intelligence in writing scientific papers using new applications such as Chat GPT which since launched last November was spread not only very fast but in acceleration way all over the world. We are observing and will try to meet with all stakeholders in our field very soon to have deep discussions hoping to reach a solution to such a threat mainly in similarity percentages reports for the submissions.

In JJPS, we will continue encouraging researchers to submit their original research as well as systematic reviews and commentaries emphasizing our commitment to complete reviewing the submissions by a group of excellent scholars in a scientific logical transparent way in a short time.

Best regards

Prof Ibrahim Alabbadi
Editor-in-Chief

Editorial Commentary

Dear Researchers,

It is my privilege to write this narration for the issuance of this special issue of the prestigious "**Jordan Journal of Pharmaceutical Sciences (JJPS)**". This special issue includes the extract of the scientific work that was presented at the **8th International Pharmaceutical Conference (ZIPC-2022)** that is held at **Al-Zaytoonah University of Jordan** and organized on regular basis by the endeavor and teamwork of the great colleagues at the Faculty of Pharmacy at Al-Zaytoonah University of Jordan. The theme of this event was "***Promising Prospective in Pharmaceutical Sciences***".

It is our pride that ZIPC-2022 was the first pharmaceutical scientific event to be held in Jordan after the breakdown and the closures sadly caused by COVID. The Faculty of Pharmacy at Al-Zaytoonah University of Jordan has been holding ZIPC periodically on a regular basis every two years, since 2006 until our eighth conference this year, which comes to emphasize the University's mission of improving the reality of scientific research, learning and teaching processes.

It is our honor to host 26 presentations and 75 posters presented by elite scientists from Jordan and globally in the different fields of Pharmacy: Pharmaceutics and Drug Delivery, Pharmaceutical Biotechnology, Pharmaceutical Chemistry and Phytochemistry, Drug Design and Discovery, Pharmaceutical Analysis, Pharmacology and Toxicology, Clinical Pharmacy and Pharmacy Practice, and Pharmaceutical Marketing and Pharmacoeconomics.

Immense gratitude is conferred to the Editorial team at JJPS for their great efforts and communication to publish the fruit of the hard work imposed in our conference, and for reviewing and editing the accepted papers and abstracts, which we are so confident will contribute to spreading the valuable scientific findings presented at ZIPC-2022 to the maximum.

Finally, I'm very thankful to every team member at the Faculty of Pharmacy in Al-Zaytoonah University of Jordan, members of organizing and scientific Committees, presenters, and attendees of ZIPC-2022 for their significant role in making this event a great success.

Dr Abdel Qader Al Bawab
Associate Professor of Clinical Pharmacy and Pharmacokinetics
Dean of Faculty of Pharmacy
Al-Zaytoonah University of Jordan
Tel: + 962-6-429 1511, ext. 305/ + 962-797 974 023
Email: pharmacy@zyj.edu.jo

CONTENTS

Jordan Journal of Pharmaceutical Sciences, Volume 16, No. 2, Supplement 1, 2023

Hemophilia in Jordan: An Economic Burden Dilemma of Rare Disease

Ibrahim Alabbadi[1]*, Abdel Karim Al-Oweidi[2], Amirah Daher[2], Ayah BaniHani[3], Abdallah Awidi[2]

[1] Faculty of Pharmacy, The University of Jordan, Amman, Jordan.
[2] Faculty of Medicine, The University of Jordan, Amman, Jordan.
[3] International Society for PharmacoEconomics and Outcomes Research (ISPOR)-Jordan Chapter-General Secretary.

ABSTRACT

Jordan is an upper-middle-income country with high expenditures on pharmaceuticals. The development of new rare disease (e.g. hemophilia) therapies has encountered significant obstacles with respect to economic the cost of the disease and treatment. The aim of this overview was to estimate current annual spending on hemophilia treatment in Jordan and estimate the financial impact of adapting a new medication (Emicizumab) recently used for treating hemophilia patients in Jordan. **Methods:** based on the literature review, direct medical costs were quantified, required items' costs from the actual practice in Jordan were elicited from an expert panel, and a focus group meeting with the same was conducted one month later to determine the current estimated number of hemophilia Patients in Jordan, identify current treatment on demand quantities and their prices. All related medical costs were also identified (e.g. bleeding, the estimated number of hospital days, and/or Intensive Care Unit per bleeding episodes). Estimation of the annual consumption of current on-demand treatment quantities and cost were calculated and compared with scenarios of adding the new therapy (Emicizumab). **Results**: showed that the financial impact of using Emicizumab S.C. instead of Recombinant Factor VIIa I.V. on the budget of the Jordanian government will be 425,747 JOD ($601,338) annually. **Conclusions**: the economic advantages of a new hemophilia treatment might be very substantial for patients.

Keywords: Hemophilia, Jordan, Economic burden, 2019.

INTRODUCTION

Jordan is an upper middle-income country located in the western Asia part of the Middle East in an area of political instability, with a population of 10.554 million (4.966 million females=47.1% and 5.588 million males=52.9%) and an average annual live birth of 197,280 (2019). The Gross Domestic Product (GDP) amounted to be 31.435 billion JODs ($ US$44.4 billion), and Jordan GDP Per Capita reached 2,990 JOD ($4,222) in 2019. Jordan has a small economy with limited natural resources[(1)]. The total expenditure on health in Jordan amounted to be 2.566 billion JOD ($ 3.6 billion), and the per capita expenditure was 255 JOD ($ 361) in 2017 accounted for 8.9 percent of the GDP which is considered high for an upper middle-income country.

Expenditures on pharmaceuticals were high and reached 593 million JOD (US $ 838 million) in 2017 accounting for 2.05 % of the GDP and 23.13 % of the total health expenditures. Public expenditures on curative care accounted for 73.7 % while expenditures on primary care accounted for 19.6 % in 2017[(2)].

The health sector in Jordan is subdivided into multiple health providers including public, private, international and charity sectors. Two major public programs that finance and deliver healthcare in Jordan are the Ministry

[*]***Corresponding author: Ibrahim Alabbadi***
i.abbadi@ju.edu.jo
Received: 16/3/2022 Accepted: 21/6/2022.
DOI: https://doi.org/10.35516/jjps.v16i2.1462

of Health (MoH) and Royal Medical Services (RMS). Other smaller public programs include universities-based programs, namely the University of Jordan, and Jordan University of Science and Technology. In addition, several non-governmental organizations and donors own and operate facilities such as the United Nations Relief Works Agency (UNRWA), which provides care mostly to Palestinian refugees and the United Nations High Commissioner for Refugees (UNHCR), which with the support of MoH, provides medical care to Syrian refugees inside camps. Those outside the camps pay out of pocket at the same rate as uninsured Jordanians, which are highly subsidized. Yet, this might account for a considerable burden on them [(3)].

Many rare diseases cause chronic or progressive physical deterioration, disability, or premature death. Usually they start in childhood, creating a huge burden on parents and caregivers. Mostly, rare diseases are thought to be genetic in nature. Although there is increasing demand for therapies for rare diseases, drug companies were not interested in adopting them to develop treatments, and as such became known as orphan diseases. The development of new rare disease therapies has encountered significant obstacles with respect to understanding the incidence and prevalence (epidemiology), patient reported burden of disease, economic cost of the disease and treatment, health technology assessment, and patient access [(4)].

There is no universal agreed on definition of what constitutes a rare" disease. A recent survey of definitions from more than 1,100 organizations worldwide found significant variations, ranging from prevalence thresholds of five to 76 cases per 100,000 population [(5)]. Individual rare diseases affect less than 5 to 7 individuals in 10,000[(6)].Hemophilia is a rare congenital blood disorder that primarily affects males and causes potentially fatal internal bleeding in the brain and the gastrointestinal tract as well as frequent bleeding in joints and soft tissues [(7)] [(8)]. The two forms of the condition are Hemophilia A (Factor VIII deficiency) and Hemophilia B (Factor IX deficiency); Hemophilia A is approximately four times more common than Hemophilia B [(9)].

For individuals with hemophilia, acute bleeding episodes can occur spontaneously and after trauma or surgery. Repeated bleeding in joints may eventually lead to debilitating and painful chronic hemophilic arthropathy, limiting mobility [(8)]. The clinical severity of hemophilia A and B is best correlated with the factors VIII, IX activity level. Patients with severe and milder clinical hemophilia who have factor VIII, IX activity levels below 30-40% of normal and they are at risk for excessive bleeding when undergoing a major surgical procedure. Female carriers of hemophilia A can also be at risk of excessive surgical bleeding. About 10% of female carriers have factor VIII activity below 30%.

Hemophilia is characterized by frequent hemarthrosis, leading to acute/chronic joint pain. Patients with chronic pain, particularly those with both acute/chronic pain, frequently experience psychological issues, functional disability and reduced Health Related Quality of Life (HRQoL) [(10)].

Severe hemophilia patients experience chronic hemophilic joint disease, characterized by chronic inflammation and progressive joint deformity, in one or more major joints by the age of 30. Furthermore, the latter experience significant acute pain during bleed events and chronic pain due to arthropathy, leading to disability and impaired quality of life in more than half of cases [(9)].

The overall weighted prevalence of hemophilia was 3.6 per 100,000 and the prevalence among males was 5.5 per 100,000. The prevalence based on community studies was 2.9 per 100,000 in mainland China, lower than the prevalence worldwide [(11)]. The prevalence of hemophilia in India, Russia, Taiwan and Turkey was 2.27 per 100 000, 5.12 per 100 000, 3.61 per 100 000 and 4.93 per 100 000 respectively [(12)].

Global incidence of hemophilia A is approximately 1

in every 5000 male births; hemophilia B is approximately six times rarer than hemophilia A (13, 14).

Individuals with severe hemophilia (have factor levels less than 1% of that expected in a healthy person) representing approximately one-third of the hemophilia population in Europe [9]. Hemophilia affects approximately 20,000 individuals in the United States (more than 80% are of A type) [8]. Without prophylactic treatment, patients with severe disease have an average of 20 to 30 episodes per year of spontaneous bleeding or excessive bleeding after minor trauma [15].

Joint damage remains a major complication associated with hemophilia and as one of the most debilitating symptoms for persons with severe hemophilia. The presence of chronic synovitis has a significant negative impact on HRQoL for adults with severe hemophilia. Approximately 80% of bleeding events are intra-articular in nature, two-thirds of which are reported in the knees, elbows, and ankles (9, 10, 15, 16). In the absence of effective treatment, either with bypass therapies or through 'training' the body to accept factor concentrate ('immune tolerance induction' or ITI), the presence of an inhibitor can significantly increase bleed frequency and accelerate joint damage [16].

Hemophilic arthropathy (HA) is a major complication in patients with hemophilia (PWH), however, studies of age-specific prevalence and severity of HA are very limited in Asian countries. Although severe arthropathy of the six major joints was rare in PWH aged <30 years, it increased rapidly in PWH after 30 years [17].

Hemophilia A and B are X-linked diseases that predominantly affect male patients. Patients can develop coagulation factor inhibitors, which exponentially increases the treatment cost. The factor replacements were derived from plasma (48.4%), recombinant concentrates (22.9%), both sources (14.6%), or fresh frozen plasma (14.1%). Factor VIII inhibitors were observed in (29.3%). Most patients who developed inhibitors had severe hemophilia (90.9%), and inhibitors were also common among patients who received recombinant product 32.6%[18].

Central venous access devices (CVADs) facilitate repeated or urgent treatments for pediatric hemophilia patients but are associated with complications. Pediatric hemophilia patients with CVADs experienced greater infection rates, healthcare utilization and higher hospitalization costs compared with non-CVAD patients[14].

Longer length of Stay (LOS) in hospitals and higher total hospital costs for the CVAD cases were also found[14].

TREATMENT OF HEMOPHILIA:

Administering the missing coagulation factors by replacement therapy is the treatment option. In the 1960s, the use of plasma-derived factor concentrates made these disorders manageable and made the first significant impact on life expectancy. After that, recombinant factor concentrates have been introduced that guarantee a high degree of safety. A further important innovation in hemophilia treatment in the last 20 years has been the increasing use of prophylactic therapy rather than on-demand replacement therapy [19].

The major risk associated with the use of clotting factor replacement therapy is the development of inhibitors due to production of neutralizing antibodies that inhibit factor uptake leading to poor control of bleeds associated with more mortality and decrease in HRQoL. The formation of inhibitors is multifactorial being associated with both genetic and environmental factors [20]; treating patients with inhibitor is a lengthy process with high costly regimens of ITI with large risk uncertain success [9].

Inhibitors can be low or high titer based on the maximum titers developed by a patient after repeated exposure to FVIII. A person with high-titer inhibitors is someone with a titer >5 Bethesda units (BU), whereas a low-titer person is someone with <5 BU. The Scientific and Standardization Committee of the International

Thrombosis and Hemostasis Society has recommended that inhibitor titers equal to or greater than 5 BU be considered as high titer. These antibodies, especially in cases of high titer, can modify the pharmacokinetics of replacement therapy, reducing the effectiveness of treatment. In addition, even after increasing the frequency and dose of FVIII, in some patients it is not possible to control bleeding episodes, making necessary the use of alternative therapies, immune tolerance induction (ITI) as an option to eradicate inhibitors, or bypassing agents, either activated prothrombin complex concentrate (aPCC) or activated recombinant factor VII (rFVIIa) [(21)].

Prevention, early diagnosis and treatment of target joints should be an important consideration for clinicians and patients when managing hemophilia [(16)]. Prevention of bleeding through prophylaxis, rather than the on-demand treatment of bleeding events when they occur, is considered the gold standard of treatment for severe hemophilia by trying to maintain factor activity above a trough of 1% baseline factor activity level [(22)].

Economic Aspects of Hemophilia

Target joints are a common complication of severe hemophilia as mentioned above, while factor replacement therapy constitutes the majority of costs in hemophilia, prevention and management of target joints should be an important consideration for managing hemophilia patients[(13)].

Main concerns for hemophilia healthcare are shifting from the pure clinical aspects to the economic considerations of long-term replacement therapy, equity considerations are relevant as well[(23)]. Hemophilia is a condition whose treatment requires a large amount of financial resources associated with the cost of hemostatic factors and care of hemorrhage, the latter being lower in patients on prophylaxis relative to on-demand [(24)].

Cost-of-illness (COI) studies quantify the economic burden of a disease, including direct healthcare and non-healthcare costs and productivity losses. COI studies are useful to inform policymakers about the magnitude of a disease. To correctly support the decision-making process, it is necessary to identify the cost-drivers through COI studies with robust design and standardized methodology. There is a lack of COI studies in the field of rare diseases.

The major cost driver accounting for more than 70-95% of the direct medical costs for treating hemophilia are due to clotting factor usage [(8)] i.e. costs of factor replacement therapy account for the vast majority of the cost burden in severe hemophilia. However, the importance of the indirect impact of hemophilia on the patient and family should not be overlooked [(9)]. On the other hand, it is estimated that 99.8% of the calculated cost corresponds to coagulation factors and bypassing agents. This evidence will allow countries to continue generating policies to offer access to technologies, under the assumption of system sustainability [(21)].

The large observed variability in hemophilia prevalence prevents robust estimation of burden of disease. Establishing prevalence at birth is a milestone toward assessing years of life lost, years of life with disability, and burden of disease [(25)].

Only a small share of new drugs is truly innovative; 85% to 90% of all new health technologies have little or no advantage over existing therapeutic alternatives. Although higher price levels are usually associated with higher investments in R&D, there is still a need to improve access to new technologies and to guarantee that they provide more health benefits than they displace in consequence of their costs[(26)]. Health economic evaluations can be used to inform decision makers in this regard to achieve economic efficiency by maximizing value for money.

OBJECTIVES

The aim of this overview was to:

- Estimate current annual spending on Hemophilia treatment in Jordan.

- Estimate the financial impact of adapting a new medication (Emicizumab) recently used for treating hemophilia patients in Jordan

METHODOLOGY

In order to estimate the economic burden of hemophilia in Jordan, at first literature review showed that the direct medical costs that have to be quantified-if available or if applicable- are of the following items (27, 28):

– **Clotting factor and bypassing agent**, **Healthcare service** (Comprehensive care, Clinician visit including Hematologist, Rheumatologist, Orthopedic surgeon, Infectious disease specialist, Physical therapy, Social worker and Psychology), **Hospitalization, Emergency department**, **Outpatient procedure.**

– **Lab tests** (laboratory, radiological and diagnostic)**,** MRI Ultrasound, Other tests (e.g., bone scan, immunology test) **and other hemophilia-related medication(s)**

The second step was to identify the required items' costs from the actual practice in Jordan. The latter requires expert opinion elicitation in which one to one interview with six consultants, who usually treat hemophilia patients in Jordanian big hospitals (MoH Albashir and Prince Hamza Hospitals, Royal Medical Services Hospitals, Jordan University Hospital and King Abdallah University Hospital) was conducted [(29)]. Furthermore, a focus group meeting with the same panel of experts was conducted one month later. The latter ended up with a consensus of the expert panel identifying the following required data to be collected:

1. Determine current estimated number of Hemophilia Patients in Jordan (classified in 3 age groups), estimated number of severe patients (average), estimated number of patients with inhibitors, estimated number of patients with inhibitors low titer and high titer and estimated number of patients treated on demand.
2. Identify current treatment on demand and its price obtained from the Joint Procurement Directorate (JPD) (the governmental body responsible for buying medications for the treatment of rare diseases patients in Jordan).
3. Determine current annual estimated number of bleeding episodes, the estimated number of hospital days per bleeding episodes per year (as average), estimated number of inpatient ward days per bleeding episodes and estimated number of Intensive Care Unit (ICU) days per bleeding episode.
4. Estimate total on demand ideal current need as practiced; annual consumption of Recombinant Factor VIIa I.V. (Novoseven® 2 mg) (2019) for estimated age groups with severe hemophilia patients with inhibitors high titer only (as the major cost driver)
5. Calculate total estimated on demand real current annual quantities consumed of Recombinant Factor VIIa I.V. (Novoseven® 2 mg) (2019 tender) for estimated age groups with severe hemophilia patients with inhibitors high titer
6. Estimate real practice scenarios for annual quantities consumed of Emicizumab = Hemlibra® S.C. for the same estimated age groups with severe hemophilia patients with inhibitors high titer
7. Estimate real practice scenarios of annual cost of Emicizumab = Hemlibra® S.C. for estimated age groups with severe hemophilia patients with inhibitors high titer (based on data on item number 6 above) in JODs

RESULTS

Table 1 shows the total current cases of Hemophilia in Jordan including number of hemophilia patients, severe cases number with and without inhibitors and consequently estimated number of annual bleeding episodes, hospital length of stay (days), specific length of stay (days) within inpatient wards and ICU per bleeding episode.

Table 1: Hemophilia in Jordan: current situational analysis [29]

Category (annual)	**%**	**JUH**	**MoH**	**KAUH**	**DRMS**	**Total**
Estimated number of Hemophilia Patients	100%	280		50	70	**400**
Estimated number of Hem B	≈ 10%	20		10	10	**40**
Estimated number of Hem A	≈ 90%	260		40	60	**360**
Estimated number of severe patients (average) [A]	60%	140		32	44	**216**
Estimated number of patients with inhibitors (9% of all)	15%	23		4	6	**33**
Estimated number of patients with inhibitors low titer	≈ (1/3)	7-9		1-3	2- 4	**11**
Estimated number of patients with inhibitors high titer	≈ (2/3)	18		2	3	**23**
Estimated number of patients treated on demand	(in case of symptoms or elective surgery) **23**					
Estimated age groups: Severe patients with inhibitors high titer	**23**					
< 5 years	**5** (average weight = 12 kg)					
5 - 15 years	**8** (average weight = 25 kg)					
> 15 years	**10** (average weight = 50 kg)					
Estimated number of patients on prophylaxis	**NONE**					
Current treatment on demand	Novoseven® 2 mg (Recombinant Factor VIIa) **I.V.**					
Estimated number of bleeds annually	12.5 (average of 10-15)					
Estimated number of hospital days/bleed/year (average of 2-3 days)	2.5 X 12.5 = 31.25 **total** hospital days/year due to S.E.					
Estimated number of **inpatient ward** days/bleed	28.125 (90%) **inpatient ward** days/year due to S.E					
Estimated number of **ICU** days / bleed (10%)	3.125 (10% of 31.25)					

Total annual estimated on demand ideal (current **need as practiced)** cost of using of Recombinant Factor VIIa I.V. (Novoseven® 2 mg) i.e., annual consumption if all patients treated (acquisition cost of the drug only for 2019 tender prices obtained from JPD) is 7,939,036 JOD ($11,213,328) for different estimated age groups with severe hemophilia (patients with inhibitors high titer) are shown in Table 2.

Table 2: **Estimated on demand ideal current need as practiced; annual consumption of Novoseven® 2 mg (Recombinant Factor VIIa I.V.) (2019) for estimated age groups with severe hemophilia patients with inhibitors high titer (Tender prices from JPD)**

Estimated age groups: Severe with inhibitors high titer	Number of patients	Average weight (Kg)	Average each dose 90 µg / Kg / Patient in (µg)	Average of each dose/ Patient (vial)	Average of each dose/ Patient i.e. TID/ Bleed (vial)	Average dose/ Patient/Bleed (total of 5) (vial)	Annual consumption/ Patient (aver. of 12.5 bleeds) (vial)	Annual consumption/ number of patients (vial)	Unit tender price (JOD) / vial	Total annual cost (JOD) for total number of patients
< 5 years	5	12	1080	≈ 1	≈ 3	≈ 15	≈ 188	≈ 940	1,281.730	1,204,826
5 – 15 years	8	25	2250	≈ 1	≈ 3	≈ 15	≈ 188	≈ 1504	1,281.730	1,927,722
> 15 years	10	50	4500	≈ 2	≈ 6	≈ 30	≈ 375	≈ 3750	1,281.730	4,806,488
Total annual current cost of using **Novoseven® 2 mg** (acquisition cost of the drug only)										**7,939,036**

However, not all patients were treated in Jordan, and not all treated patients took the required full doses of Recombinant Factor VIIa I.V. (Novoseven® 2 mg). Table 3 shows the real current total annual estimated cost of using Recombinant Factor VIIa I.V. (Novoseven® 2 mg) on demand i.e. real purchased quantities accounting for 2,498,589 JOD ($3,529,080): the medication cost of 2,307,114 JOD ($3,258,635) and inpatient & ICU length of stay cost of 191,475 JOD ($270,445) for different age groups with severe hemophilia (patients with inhibitors high titer).As the new medication, Emicizumab (Hemlibra®) S.C. is available in four dose strengths (30 mg, 60mg, 105mg, 150mg), the possible scenarios of using any of these doses as per the recommended dose of 1.5mg/kg/week or 3mg/kg/2weeks after excluding doses when not applicable or resulted in higher prices or if the full dose was not needed. Table 4 shows the estimated real practice of two scenarios of the annual quantities consumed of Emicizumab (Hemlibra®) S.C:

A. Scenario A: 676 of 30 mg vials and 520 of 60 mg vials

B. Scenario B: 130 of 30 mg vials and 208 of 60 mg vials and 260 of 150 mg.

Table 3: **Estimated on-demand real current annual consumption of Novoseven® 2 mg (Recombinant Factor VIIa I.V.) (2019 tender) for estimated age groups with severe hemophilia patients with inhibitors high titer**

	MoH	**JUH**	**KAUH**	**RMS**	**Total quantity**	**JPD Unit price**	**Total JOD**
JPD tender 2019	**1,010**					**1281.730**	**1,294,547**
Real purchases (+ direct purchase)	**200 Converted to JUH**	**880**	**770**	**800**	-	-	-
For inhibitors ONLY		**700**	**700**	**400**	**1800**	**1281.730**	**2,307,114**
			Unit cost*	**Cost/patient**	**Number of patients**	**Cost/all patients**	
Estimated number of **inpatient ward** days/bleed		28.125	**254**	**7143.75**	**23**	**164306.25**	
Estimated number of **ICU** days / bleed		**3.125**	**378**	**1181.25**	**23**	**27168.75**	
						191475	**2,498,589**

*(37)

In order to calculate the estimated annual cost of using either scenario A or B of Emicizumab (Hemlibra®) S.C; quantities mentioned in Table 4 above are used considering available pharmacy prices i.e. whole sales prices (not tender price of JPD because Emicizumab is not yet a national formulary item) obtained from Jordan Food and Drug Administration (JFDA) website [30]. Results showed that scenario a costs 3,621,469 JOD ($5,115,069) while scenario B costs 3,895,822 JOD ($5,502,573).

As regulated in Jordan; any new medication listed in the Jordan National Drug formulary (so it can be purchased by JPD for public hospitals) lose 5 % of its price immediately. In addition, any new medication participated alone in the JPD tender must not bid more than 15% less than its pharmacy price [31].

Table 4: Estimated real practice scenarios annual consumption of Emicizumab = Hemlibra® S.C. for estimated age groups with severe hemophilia patients with inhibitors high titer (Prices from JFDA website)

Estimated age groups: Severe with inhibitors high titer	**Average weight (Kg)**	**Real practice scenarios Either - OR** **NA=Not applicable or higher price, NN=not needed**									
		(A): 1.5mg/kg/week					**(B):** 3mg/kg/2weeks				
		Dose	**30mg**	**60mg**	**105mg**	**150mg**	**Dose**	**30mg**	**60mg**	**105mg**	**150mg**
< 5 years	12	18mg	≈ 1	NA	NA	NA	36 mg	≈ 1	NA	NA	NA
5 – 15 years	25	37.5 mg	≈ 1	NA	NA	NA	75 mg	NA	≈ 1	NA	NA
> 15 years	50	75mg	NA	≈ 1	NA	NA	150 mg	NA	NA	NA	≈ 1
No. of vials/patient/year							**No. of vials/patient/year**				
< 5 years			**52**	NA	NA	NA		**26**	NA	NA	NA
5 – 15 years			**52**	NA	NA	NA		NA	**26**	NA	NA
> 15 years			NA	**52**	NA	NA		NA	NA	NA	**26**
No. of vials/all patients/year							**No. of vials/all patients/year**				
No. of patients			**30mg**	**60mg**	**NN**	**NN**		**30mg**	**60mg**	**NN**	**150mg**
< 5 years	5		**260**	NA				**130**	NA		NA
5 – 15 years	8		**416**	NA				NA	**208**		NA
> 15 years	10		NA	**520**				NA	NA		**260**

Accordingly, scenario A costs 2,924,336 JOD ($4,130,418) while scenario B costs 3,145,876 JOD ($4,443,327) (Table 5).

Table 5: Estimated real practice scenarios annual cost of Emicizumab = Hemlibra® S.C. for estimated age groups with severe hemophilia patients with inhibitors high titer (based on Table 4 quantities) in JODs

	Scenario A			Scenario B		
Emicizumab dosage form	30 mg	60mg	150mg	30 mg	60mg	150mg
Total vials/year	676	520	0	130	208	260
Hospital unit price	2110.41	4220.83	10552.06	2110.41	4220.83	10552.06
Total cost for each	1,426,637	2,194,832	0	274,353	877,933	2,743,536
Total cost			**3,621,469**	**Total cost**		**3,895,822**
Cost less by 5% (formulary inclusion)	2004.89	4009.79	10024.46	2004.89	4009.79	10024.46
Total cost for each	1,355,305.3	2,085,090	0	260,635.64	834,036	2,606,358.82
Total cost			**3,440,395.32**	**Total cost**		**3,701,030.46**
Maximum allowed tender prices (cost less by 15% of the new cost)	1704.155	3408.32	8520.79	1704.155	3408.32	8520.79
	1,152,010	1,772,327	0	221,540	708,931	2,215,405
Total cost			**2,924,336**	**Total cost**		**3,145,876**

The lower the cost the better the scenario, as scenario A was selected; annual cost of using Emicizumab (Hemlibra®) S.C is 2,924,336 JOD ($4,130,418) for the same number of hemophilia patients treated with current medication; Recombinant Factor VIIa I.V. (Novoseven® 2 mg) that costs 2,498,589 JOD ($3,529,080). The latter means that the financial impact of using Emicizumab S.C. instead of Recombinant Factor VIIa I.V. on the budget of the Jordanian government will be 425,747 JOD ($601,338) annually (without any discount from the whole sale price or what is called pharmacy price).

DISCUSSION

Use of so-called "orphan" drugs to treat rare diseases are poised to represent more than one-fifth of pharmaceutical expenditures by 2022. Worldwide sales of orphan drugs first reached $100 billion in 2015 but are expected to be more than double by 2022 and will represent more than one-fifth of all prescription drug sales by that time. High acquisition cost is the main factor driving the trend in spending on orphan drugs.

Effort to understand whether rare diseases require special considerations on their part and how to adapt traditional methods of health technology assessment and economic evaluation to accommodate these situations is badly needed [32]. Accordingly, patient access to medicines for rare diseases varies across countries even among high income countries such as in Europe [33].

It was estimated that average per-patient annual direct cost of severe hemophilia in some European countries (France, Italy, Spain, Germany and UK) range from €129,365 in the UK up to €313,068 in Germany, approximately 34 to 87 times higher than the mean per-capita health expenditure in these countries [9].

Public populations would support giving priority to a smaller but more severely ill group of patients over a larger group when prioritizing the needs of the few is life-saving, extends life enough to give hope of future improvement, and relieves otherwise intractable symptoms, especially pain (34-35).

There is simply no magic solution to the conundrum of assessing the evidence on clinical effectiveness, economic impact, and value of drugs to treat rare diseases [5]. Although it has been ascertained that on demand treatment can the long-term complications, but it does not prevent them, whereas prophylaxis in patients with severe hemophilia from early childhood prevents such complications. Moreover, even if prophylaxis requires one or two infusions per week, it is associated with improved quality of life [19]. Given that as hemophilia begins at birth, the illness has an impact on the lives of caregivers [36].

CONCLUSION

Although the efficacy and safety profiles of novel treatments (e.g., Emicizumab) warrant long-term clinical studies, the economic advantages of these new compounds might be very substantial both in patients with inhibitors and in those at risk of developing inhibitors [36].

REFERENCES

(1) Alabbadi, I., Massad, E., Taani, N. et al. (2022). Exploring the Economic Aspects of β-Thalassemia in Jordan in. Jordan J. Pharm. Sci. 2019; 15(3), 390–404. https://doi.org/10.35516/jjps.v15i3.412

(2) High Health Council-Jordan. Jordan National Health Accounts for 2016 – 2017 Fiscal Years 2019. [https://jordankmportal.com/resources/jordan-national-health-accounts]. Accessed in Oct 2020

(3) Ministry of Health-Jordan. Ministry of Health Annual Report. 2019. [https://www.moh.gov.om/en/web/statistics/annual-reports] Accessed in Oct 2020

(4) Copley-Merriman K. Rare Diseases: Addressing the Challenges in Diagnosis, Drug Approval, and Patient Access. Value in Health. 2018; 21: 491-92.

(5) Richter T, Nestler-Parr S, Babela R. et al. Rare Disease Terminology and Definitions-A Systematic Global Review: Report of the ISPOR Rare Disease Special Interest Group. Value in Health. 2015; 18: 906-14.

(6) Auvin S, Irwin J, Abi-Aad P. et al. The Problem of Rarity: Estimation of Prevalence in Rare Disease. Value Health. 2018; 21: 501-07.

(7) Berntorp E. Future of haemophilia outcome assessment: registries are key to optimized treatment. Journal of Internal Medicine. 2016; 279: 498-501.

(8) Chen CX, Baker JR, Nichol MB. Economic Burden of Illness among Persons with Hemophilia B from HUGS Vb: Examining the Association of Severity and Treatment Regimens with Costs and Annual Bleed Rates. Value in Health. 2017; 20: 1074-82.

(9) O'Hara J, Hughes D, Camp C. et al. The cost of severe haemophilia in Europe: the CHESS study. Orphanet Journal of Rare Diseases. 2017; 12: 8.

(10) Self-reported prevalence, description and management of pain in adults with haemophilia: methods, demographics and results from the Pain, Functional Impairment, and Quality of life (P-FiQ) study.

(11) The Prevalence and Treatment Status of Hemophilia in India, Russia, Taiwan and Turkey: A Systematic Review and Meta-Analysis.

(12) O'Hara J, Walsh S, Camp C. et al. The relationship between target joints and direct resource use in severe haemophilia. Health Economics Review. 2018; 8.

(13) Buckley B, Dreyfus J, Prasad M. et al. Burden of illness and costs among paediatric haemophilia patients with and without central venous access devices treated in US hospitals. Haemophilia. 2018; 24: E93-E102.

(14) Institute for Clinical and economic review (ICER). Emicizumab for Hemophilia A: Effectiveness and value. 2017. [https:icer.org] on line data base accessed in Dec 2020

(15) O'Hara J, Walsh S, Camp C. et al. The impact of severe haemophilia and the presence of target joints on health-related quality-of-life. Health and Quality of Life Outcomes. 2018; 16.

(16) Prevalence and severity by age and other clinical correlates of haemophilic arthropathy of the elbow, knee and ankle among Taiwanese patients with haemophilia.

(17) The prevalence of factor VIII and IX inhibitors among Saudi patients with hemophilia Results from the Saudi national hemophilia screening program.

(18) Cavazza M, Kodra Y, Armeni P. et al. Social/economic costs and quality of life in patients with haemophilia in Europe. European Journal of Health Economics. 2016; 17: 53-65.

(19) Mousavi SH, Mesbah-Namin SA, Rezaie N. et al. Prevalence of factor VIII inhibitors among Afghan patients with hemophilia A: a first report. Blood Coagul Fibrinolysis. 2018; 29: 697-700.

(20) Sánchez-Vanegas G, Linares A, Sarmiento I. et al. Cost of Patients With Hemophilia A and High-Titer Inhibitors in Colombia. Value Health Reg Issues. 2019; 20: 164-71.

(21) Jimenez-Yuste V, Auerswald G, Benson G. et al. Achieving and maintaining an optimal trough level for prophylaxis in haemophilia: the past, the present and the future. Blood Transfusion. 2014; 12: 314-19.

(22) Castro HE, Briceno MF, Casas CP. et al. The History and Evolution of the Clinical Effectiveness of Haemophilia Type A Treatment: A Systematic Review. Indian Journal of Hematology and Blood Transfusion. 2014; 30: 1-11.

(23) Carlos-Rivera F, Gasca-Pineda R, Majluf-Cruz A. et al. Economic Impact of Hemophilia type A and B in Mexico. Gaceta Medica De Mexico. 2016; 152: 19-29.

(24) Establishing the Prevalence and Prevalence at Birth of Hemophilia in Males A Meta-analytic Approach Using National Registries.

(25) Santos AS, Guerra-Junior AA, Noronha KVMS, et al. The Price of Substitute Technologies. Value Health Reg Issues. 2019; 20: 154-58.

(26) Zhou ZY, Koerper MA, Johnson KA. et al.Burden of illness: direct and indirect costs among persons with hemophilia A in the United States. Journal of Medical Economics. 2015; 18: 457-65.

(27) Heemstra HE, Zwaan T, Hemels M.et al. Cost of severe haemophilia in Toronto. Haemophilia. 2005; 11: 254-60.

(28) Team JH. Personal interview with each member of the Jordanian Hemophilia Team followed by a discussion forum reaching a consensus about topics of discussion. 2019.

(29) Administration JFaD. Medication prices in the private sector. 2019.

(30) Jordan. The Hashemite kingdom of Jordan - Jordan Food and Drug Administration Laws and regulations. In: Administration JFaD, ed., 2008.

(31) Ollendorf DA, Chapman RH, Pearson SD. Evaluating and Valuing Drugs for Rare Conditions: No Easy Answers. Value in Health. 2018; 21: 547-52.

(32) Detiček A, Locatelli I, Kos M. Patient Access to Medicines for Rare Diseases in European Countries. Value Health. 2018; 21: 553-60.

(33) Magalhaes M. Can Severity Outweigh Smaller Numbers? A Deliberative Perspective from Canada. Value Health. 2018; 21: 532-37.

(34) Pocoski J, Benjamin K, Michaels LA. et al. An overview of current trends and gaps in patient-reported outcome measures used in haemophilia. European Journal of Haematology. 2014; 93: 1-8.

(35) Ibrahim Alabbadi: Budget impact of adding one Dipeptidyl peptidase-4 inhibitor to Ministry of Health Jordan tender list in the treatment of Type II Diabetes Mellitus. Jordan J. Pharm. Sci. 2015; 8, 3: 173-180.

(36) Messori A. Inhibitors in Hemophilia A: A Pharmacoeconomic Perspective. Seminars in Thrombosis and Hemostasis. 2018; 44: 561-67.

(37) Hammad EA, Fardous T, Abbadi I. Costs of hospital services in Jordan. International Journal of Health Planning and Management. 2017; 32: 388-99.

الهيموفيليا في الأردن: معضلة العبء الاقتصادي للأمراض النادرة

إبراهيم العبادي[1*]، عبدالكريم العويدي[2]، أميرة ضاهر[2]، آية بني هاني[3]، عبد الله العويدي[2]

[1] كلية الصيدلة، الجامعة الأردنية، عمان، الأردن.

[2] كلية الطب، الجامعة الأردنية، عمان، الأردن.

[3] الجمعية العالمية للاقتصاد الصيدلاني (ISPOR)، فرع الأردن.

ملخص

الأردن بلد من الشريحة العليا من البلدان متوسطة الدخل ذات الإنفاق العالي على المستحضرات الصيدلانية. واجه تطوير علاجات جديدة للأمراض النادرة (مثل الهيموفيليا) عقبات كبيرة فيما يتعلق بالتكلفة الاقتصادية للمرض والعلاج. هدفت هذه الدراسة لتقدير الإنفاق السنوي الحالي على علاج الهيموفيليا في الأردن والأثر المالي لإستخدام دواء جديد (Emicizumab) استخدم مؤخرا لعلاج مرضى الهيموفيليا في الأردن. **الأساليب:** بناء على مراجعة الأدبيات، تم تحديد التكاليف الطبية المباشرة، وتم استخلاص عناصر التكاليف المطلوبة من الممارسة الفعلية في الأردن من لجنة خبراء، وتم عقد اجتماع لهذه اللجنة مع مجموعة من المختصين بعد شهر واحد من أجل تقدير عدد مرضى الإيموفيليا في الأردن، والتعرف على كميات العلاج حسب الطلب وأسعارها لهؤلاء المرضى. كما تم تحديد جميع التكاليف الطبية ذات الصلة (مثل النزيف، والعدد المقدر لأيام المكوث في المستشفى و/ أو وحدة العناية المركزة لكل حالة نزيف). تم حساب تقدير الاستهلاك السنوي لكميات وتكلفة العلاج الحالي عند الطلب ومقارنته بسيناريوهات إضافة العلاج الجديد (Emicizumab). أظهرت **النتائج** أن الأثر المالي لاستخدام Emicizumab S.C. بدلا من Recombinant Factor VIIa IV على ميزانية الحكومة الأردنية سيكون 425,747 دينار أردني (601,338 دولار) سنويا. **الإستنتاج:** قد تكون المزايا الاقتصادية لعلاج الهيموفيليا الجديد كبيرة جدا للمرضى.

الكلمات الدالة: الهيموفيليا، الأردن، العبء الأقتصادي، 2019.

المؤلف المراسل:

i.abbadi@ju.edu.jo

تاريخ الإستلام 2022/3/16 تاريخ قبول النشر 2022/6/21.

Jordan Journal of Pharmaceutical Sciences, Volume 16, No. 2, Supplement. 1, 2023

Design, Synthesis, and Biological Activity of Coniferyl Aldehyde Derivatives as Potential Anticancer and Antioxidant Agents

Worood H. Ismail[1] †, Osama H. Abusara[1] †*, Balqis Ikhmais[1], Hassan Abul-Futouh[2], Suhair Sunoqrot[1], Ali I. M. Ibrahim[1]*

[1] Faculty of Pharmacy, Al-Zaytoonah University of Jordan, Amman, Jordan.
[2] Department of Chemistry, Faculty of Science, The Hashemite University, Zarqa, Jordan.
† Worood H. Ismail and Osama H. Abusara contributed equally to this work.

ABSTRACT

Natural products are known to exhibit antimicrobial, anticancer, and antioxidant activities. Among these natural products is cinnamon which contains cinnamaldehyde. Cinnamaldehyde and its derivatives have been reported to have anticancer and antioxidant activities. Coniferyl aldehyde, a non-cytotoxic compound and a cinnamaldehyde derivative, has also been shown to have anticancer activity. In this study, several derivatives of coniferyl aldehyde were synthesized and evaluated for their anticancer and antioxidant activities. Compounds 1, 2, 4, and 8-11 showed cytotoxic activity against H1299 cell line, a non-small cell lung cancer cells, with 4 being the most potent with IC_{50} value of 6.7 μM. The antioxidant assay experiment showed that compounds 1, 2, and 4 resulted in half the scavenging activity of vitamin C at all tested concentrations. The coniferyl aldehyde itself showed dose-dependent antioxidant activity, with a proposed free radical stabilization mechanism. Thus, our study showed that the synthesized coniferyl aldehyde derivatives exhibit anticancer and antioxidant activities, which might act as potential therapeutic agents.
Keywords: Coniferyl aldehyde, Anticancer, Antioxidant, DPPH.

1. INTRODUCTION

The use of natural products for the treatment of several conditions, such as cancer, bacterial infections, fungal infections, and as antioxidants is widely reported[1-11]. Among these natural The use of natural products for the treatment of several conditions, such as cancer, bacterial infections, fungal infections, and as antioxidants is widely reported[1-11]. Among these natural products is the cinnamon spice. Cinnamon spice is obtained from the inner bark of several *Cinnamomum* trees[12,13]. A major constituent of cinnamon spice is cinnamaldehyde[12].

Corresponding author:
Osama H. Abusara ; Ali I. M. Ibrahim
o.abusara@zuj.edu.jo ; *a.ibrahim@zuj.edu.jo*
Received: 28/12/2022 Accepted: 8/3/2023.
DOI: https://doi.org/10.35516/jjps.v16i2.1463

Cinnamaldehyde and its derivatives have been reported to show several pharmacological properties. Among the commonly studied properties are the anticancer[14-17] and antioxidant[18-21] activities. The anticancer activity of cinnamaldehyde has been observed in several cancer cell lines, such as leukemia (K562) and breast cancer (MCF7)[22,23]. It has also shown to enhance anticancer effects in combination treatments[24-26]. Moreover, cinnamaldehyde has shown to have a glucolipid lowering effects in diabetic animals leading to enhancement of glucose and lipid homeostasis[27]. Cinnamaldehyde has also shown to be involved in fatty acid metabolism and has alleviated steatosis, *in vivo*[28]. It has also shown to possess antibacterial[29-31] and antifungal[32] activities. Cinnamaldehyde also has an emerging role in the treatment of inflammatory bowel diseases[33].

Cinnamaldehyde (**Figure 1**) has conjugated systems of benzene ring and α,β-unsaturated carbonyl system. Similarly, coniferyl aldehyde (**Figure 1**) has also the same systems along with the presence of the hydroxyl group. The ability of these conjugated systems to be stabilized by resonance[34] upon accepting electrons give rise for their biological activity, such as anticancer and/or antioxidant.

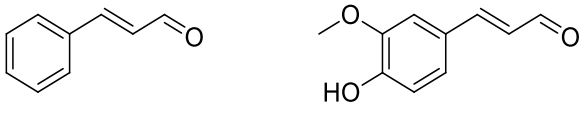

Figure 1: Chemical structure of cinnamaldehyde and coniferyl aldehyde

Coniferyl aldehyde is a derivative of cinnamaldehyde and its derivatives have shown to exhibit anticancer activity[35, 36] variably. The anticancer activity of coniferyl aldehyde derivatives has been reported in non-small cell lung cancer (NSCLC) cell line (H1299)[35], but was non-toxic on breast (MCF7) and small cell lung cancer (NCI-H187) cell lines[36].

As mentioned above, cinnamaldehyde and coniferyl aldehyde along with their derivatives possess multiple pharmacological activities. Hence, further development of derivatives of these compounds would be needed to explore their pharmacological activities. Along with the reported anticancer and antioxidant activities of cinnamaldehyde and its derivatives, further investigation of different coniferyl aldehyde derivatives is worth studying. Herein, we aimed to synthesize different coniferyl aldehyde and cinnamaldehyde derivatives to investigate their potential anticancer and antioxidant activity.

2. RESULTS AND DISCUSSION

As cinnamaldehyde and its derivative coniferyl aldehyde considered among the components of natural products that possess therapeutic uses, several derivatives were synthesized to investigate further anticancer and antioxidant effects.

2.1 Chemistry

The synthesis of coniferyl aldehyde derivatives (compounds **1**, **2**, **4**, and **8-11**) and 4-(Dimethylamino) cinnamaldehyde (DA) derivatives **(**compounds **5** and **6)** were achieved using 4-hydroxy-3-methoxy cinnamic aldehyde (coniferyl aldehyde) and DA as starting materials as presented in **Scheme 1**.

Briefly, **1**, **2**, **8**, and **11** were synthesized via acetylation reactions by reacting coniferyl aldehyde with various benzoyl chloride derivatives under basic conditions, using trimethylamine (TEA), at room temperature (RT). These reactions afforded the desired products with 33, 32, 30 and 57 % yield, respectively. Similar procedure was carried out for the synthesis of **10** but using phenyl acetyl chloride with a yield of 56 %. Compounds **4** and **9** were synthesized via alkylating the phenolic oxygen of coniferyl aldehyde by reacting it with various benzyl halides under reflux conditions, which provided 84 and 40 % yield of the target compounds, respectively. It was noticed that the % yields of the alkylation reactions were generally higher than acetylation reactions, probably due to the high incidence of acid chlorides' hydrolysis during the reaction, which can be optimized by using anhydrous conditions. Compounds **5** and **6** were formed via crossed aldol condensation reactions of DA with acetone and 4′-fluoroacetophenone, respectively, under basic conditions using sodium hydroxide, at RT. It was also noticed that the % yield for compound **5** was 15 %, while for **6** was 70 %, which was likely related to both the volatility of the ketone used and the electron withdrawing power to stabilize the anionic intermediate.

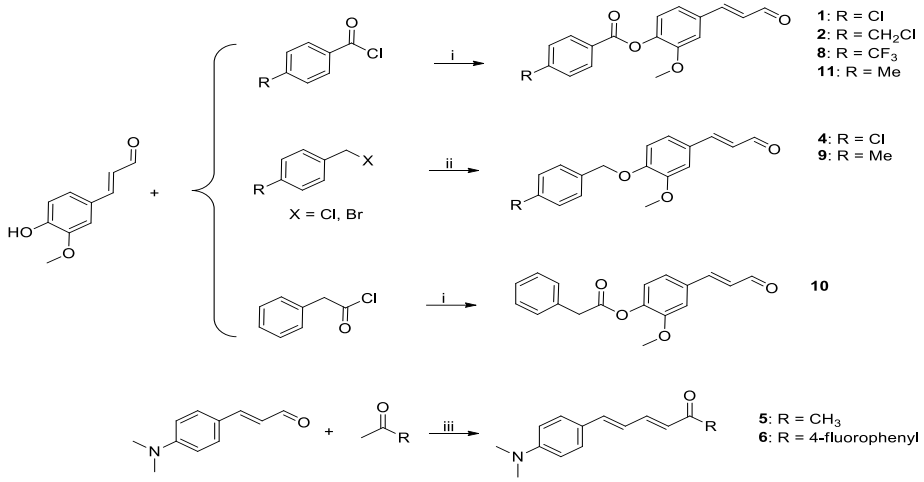

Scheme 1: The synthetic pathways for coniferyl aldehyde and 4-(Dimethylamino) cinnamaldehyde derivatives; i: TEA, DMF, RT, overnight; ii: K_2CO_3, DMF, reflux; iii: NaOH, RT, overnight**.**

All compounds were structurally characterized by ^{1}H and ^{13} C NMR, with aid of melting points, as described at the experimental section. **Figure2** shows the ^{1}H NMR spectrum for compound **2** as an example to generally show the logical assignment of the peaks to their corresponding atoms.

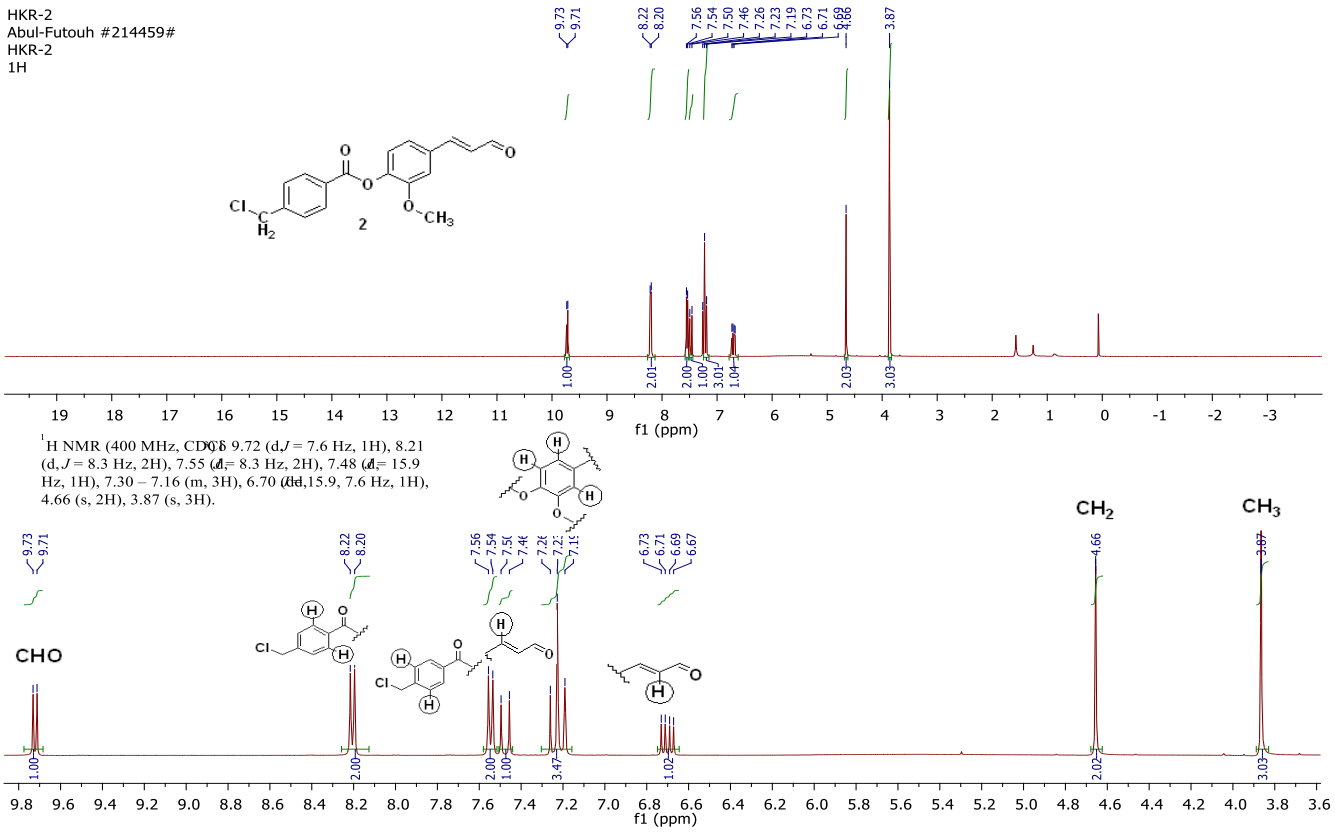

Figure 2: ^{1}H NMR spectrum for compound 2.

2.2 Cytotoxicity Assays

The antiproliferative activity of the synthesized compounds was investigated on two NSCLC cell lines; A549 and H1299. In previous work, we have found that coniferyl aldehyde derivatives that contain cinnamaldehyde nucleus has shown to have promising cytotoxic activity against H1299 cell line, but insignificantly against A549 cell line[35]. Hence, the cytotoxicity of the new derivatives was also investigated on these cell lines.

In our previous work[35], coniferyl aldehyde derivatives were synthesized to evaluate their inhibitory effect against aldehyde dehydrogenase enzyme (ALDH) isoforms (ALDH1A1, ALDH1A3, and ALDH3A1), which are expressed variably in cancer cell lines and are known to be involved in cancer proliferation. Although H1299 cell line lacks these ALDH isoforms in contrast to A549 cell line, coniferyl aldehyde derivatives were cytotoxic against them. It has been suggested that these derivatives might be detoxified in A549 cells via these isoforms, thus preventing their cytotoxic effect[35]. Hence, more coniferyl aldehyde derivatives were synthesized to check their cytotoxicity against these cell lines that variably express ALDH isoforms. This is also to check whether structure changes might interfere with activity on both cell lines.

Table 1 represents the IC_{50} values for the synthesized compounds on A549 and H1299 cell lines after being treated for 96 hours. Compounds **2** and **8** showed cytotoxic activity on A549 cell line, with IC_{50} values of 32.5 and 58.0 μM, respectively. On H1299 cell line, except for compounds **5** and **6**, all other compounds showed relative cytotoxicity with compounds **2** and **4** having the lowest IC_{50} values (9.6 and 6.7 μM, respectively). These results generally were found aligned with our previous work, in which A549 cells were considered as resistant cells, and with the opposite for H1299 cell line[35].

Table 1: Cytotoxicity (IC_{50} ± SEM) of **1**, **2**, **4-6** and **8-11** on A549 and H1299 cell lines after treatment for 96 h; n = 3.

Compound	**CytotoxicityIC_{50} ± SEM (μM)**	
	A549	**H1299**
1	>60	**18 ± 4**
2	**32.5 ± 2.5**	**9.6 ± 0.4**
4	>60	**6.7 ± 1.2**
5	>60	>60
6	>60	>60
8	**58 ± 1.5**	**12.5 ± 0.5**
9	>60	**30.5 ± 1.5**
10	>60	**58.3 ± 1.7**
11	>60	**48.3 ± 2.8**

The main nucleus for these derivatives is cinnamaldehyde. Cinnamaldehyde has shown to be cytotoxic on a number of cancer cell lines (K562[22] and MCF7[23]) as discussed above. In addition, cinnamaldehyde has shown to be a promising adjuvant compound to be combined with 5-fluorouracil and oxaliplatin against colorectal carcinoma[24]. Moreover, cinnamaldehyde has also shown to enhance apoptosis induced by hyperthermia and doxorubicin on A549 and U87MG (glioblastoma) cell lines, respectively[25, 26]. The presence of α,β-unsaturated aldehyde (electrophilic Michael acceptor) pharmacophore on cinnamaldehyde has shown to negatively affect the proliferation and tumor growth of melanoma cells[37]. Hence, the cytotoxicity of the synthesized compounds on A549 and H1299 cell line may be due to the presence of this pharmacophore as they are considered also cinnamaldehyde derivatives. In addition to that our compounds are cinnamaldehyde derivatives, compound **2** has a benzyl chloride moiety (as shown in **Scheme 1**), which could act as an alkylating agent and perhaps explain why it showed the highest cytotoxic activity on A549 cells. Furthermore, compound **8** showed also a considerable activity on both cell lines, which may be due to the presence of CF_3 moiety, whereby numerous

pharmacologically active compounds have been found to have flourin-containing functional groups[38].

Moreover, most of the newly synthesized coniferyl aldehyde derivatives were cytotoxic on H1299 cell line while non-cytotoxic on A549 cell line, which is similar with our previous results indicating possible detoxification of compounds via ALDH isoforms in A549 cell line[35]. It may be concluded that coniferyl aldehyde derivatives may be effective against ALDH non-expressing cells and they might act as substrates for ALDH enzymes in line with our previous work[35].

2.3 Antioxidant activity

Nucleophiles, such as free radicals, do exist inside our body. The balance between their production and elimination is essential to maintain normal physiologic functions[39]. When the body becomes unable to control these free radicals, state of oxidative stress occurs, causing the spreading of various diseases[39]. The synthesized compounds exhibit the electrophilic Michael acceptor pharmacophore (α,β-unsaturated carbonyl system) that is susceptible to nucleophilic attack at its β-carbon. Hence, the investigation of the synthesized compounds as antioxidants was performed.

The 2,2-Diphenyl-1-picrylhydrazyl (DPPH) assay[40] is a common antioxidant assay that works by the reduction of DPPH radical, in its stable form (DPPH*) (purple-colored), to DPPH-H (yellow-colored) through the presence of radical species or antioxidants. DPPH* absorbs light at 515-517 nm[41] and absorption disappears upon reduction. Therefore, free radical scavenging activity testing was performed to test the antioxidant activity of the synthesized compounds.

Vitamin C is known to be a potent antioxidant[42]. The antioxidant activity for the synthesized compounds was measured in relative to vitamin C as a reference along with the use of coniferyl aldehyde (the starting material). **Figure 3** represents the scavenging activity of vitamin C, coniferyl aldehyde, and the new compounds as referenced to vitamin C.

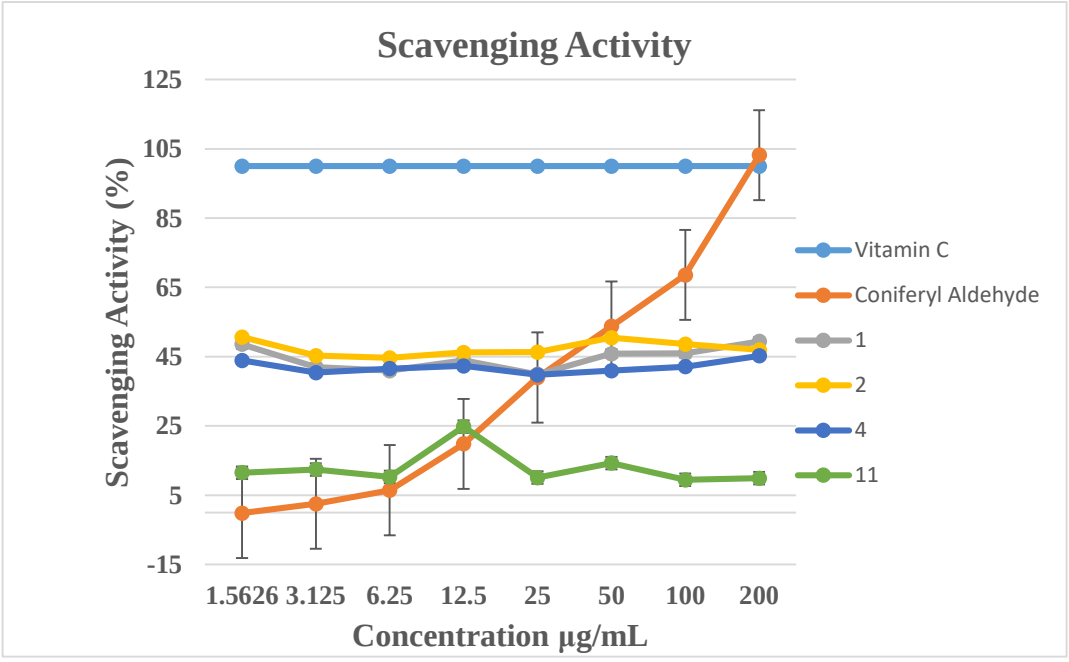

Figure 3: The scavenging activity of vitamin C, coniferyl aldehyde, 1, 2, 4 and 11 as referenced to vitamin C; n = 3.

The scavenging activity of vitamin C was found to be ~ 40% in our experiments. For the purpose of this study, the scavenging activity of the tested compounds was referenced to vitamin C, which was considered to have 100% scavenging activity, as presented in **Figure 3**. The scavenging activity of coniferyl aldehyde increased by increasing its concentration to finally meet the scavenging activity of vitamin C around the concentration of 200 µg/mL, showing a dose-dependent scavenging activity (**Figure 3**). This may be justified due to the presence of the conjugated systems; the α,β-unsaturated carbonyl system and the aromatic ring in coniferyl aldehyde and the tested compounds, along with the presence of hydroxyl group in coniferyl aldehyde, in which accepting the free electron of DPPH* cause resonance stabilization within the structure[34] (**Figure 4**), in a similar pattern to how vitamin C reduces the free radicals.

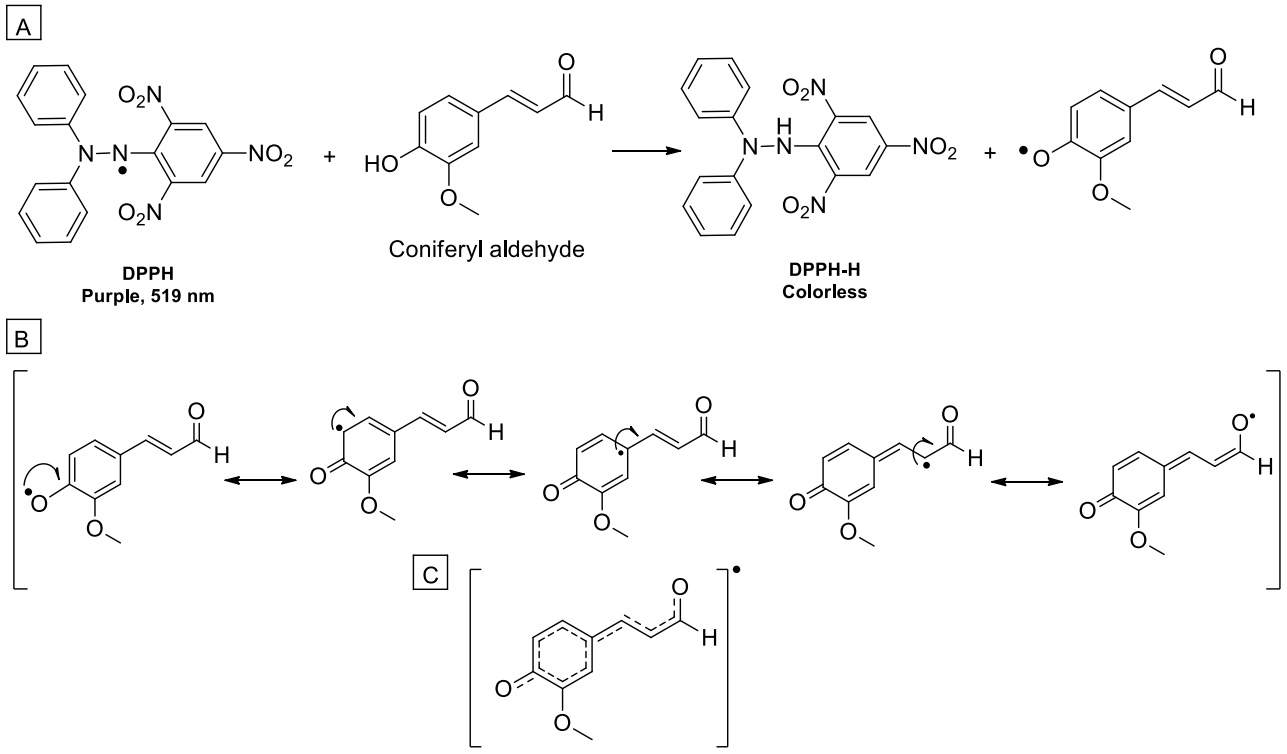

Figure 4: **The proposed mechanistic antioxidant activity of coniferyl aldehyde (panel A), with electronic delocalization of the formed free radical (panel B) and the hybrid form (panel C).**

Compounds **1**, **2**, and **4** have around the half scavenging activity of vitamin C as presented in **Figure 3**, at all tested concentrations resulting in almost consistent effect regardless of the concentration used. Interestingly, it can be realized that all those compounds contain chlorine, either aliphatic or aromatic, which may provide a structurally related clue for biological activity. Although, more analogues with variable substitutions should be synthesized and investigated to prove this conclusion and optimize the structure-activity relationship. Compound **11** showed the lowest scavenging activity with a value of ~ 5% at 200 µg/mL. Compounds **5**, **6**, and **8-10** showed no scavenging activity.

Although there are variations in the scavenging activity among the synthesized compounds, these results indicated that coniferyl aldehyde derivatives could exhibit potential

scavenging activity, which may be justified due to the presence of the α,β-unsaturated carbonyl system and the aromatic ring on them.

Compounds **1**, **2**, **8**, **10**, and **11** has an ester within their structure as presented in **Scheme 1**. Esterases, which break ester bonds, are expressed in human tissues and perform various functions, such as the metabolism of endogenous molecules and drugs[43]. Theoretically, breaking the ester bond in **1**, **2**, **8**, **10**, and **11** will release a metabolite like coniferyl aldehyde that might have similar scavenging activity to coniferyl aldehyde. Thus, compounds **1**, **2**, **8**, **10**, and **11** may act as prodrugs and be metabolized to deliver an effective antioxidant. Although only compounds **1**, **2**, and **11** (to a lower extent) showed antioxidant activity via DPPH assay *in vitro*, further *in vivo* studies are required to validate the esterases' effect hypothesis. *In vivo* studies might show that compounds **8**, **10**, and **11** possess antioxidant activity in contrast to the DPPH *in vitro* assay.

3. EXPERIMENTAL

3.1 Materials

Coniferyl aldehyde, 4-(Dimethylamino) cinnamaldehyde, 4-hydroxy-3-methoxy cinnamic aldehyde, 4-chlorobenzoyl chloride, 4-(Chloromethyl) benzoyl chloride, 4-Chlorobenzyl chloride, 4′-Fluoroacetophenone, 4-(Trifluoromethyl) benzoyl chloride, 4-Methylbenzyl bromide, phenyl acetyl chloride, p-toluoyl chloride, acetone, hexane, ethyl acetate, methanol, magnesium sulfate ($MgSO_4$), dichloromethane (DCM), triethylamine (TEA), potassium carbonate (K_2CO_3), dimethylformamide (DMF), sodium hydroxide (NaOH), (3-4,5-dimethylthiazole-2-yl)-2,5-diphenyltetrazolium bromide (MTT), vitamin C (ascorbic acid), and DPPH were purchased from Sigma (Dorset, UK); A549 [A549 (ATCC CCL-185)] and H1299 [NCI-H1299 (ATCC CRL-5803)] human NSCLC cell lines were purchased from ATCC (USA); PBS, RPMI-1640 medium, fetal bovine serum (FBS) and L-glutamine were purchased from Euroclone (Pero, Italy); DMSO was purchased from TEDIA (USA). Chemical reactions were monitored by analytical thin layer chromatography (TLC) using Merck 9385 silica gel 60 F254 aluminum-backed plates through visualizing the spotted plates under ultraviolet (UV) at 254 and 366 nm. Intermediates and final products were purified by column chromatography using silica gel (pore size 60 Å, 40–63 µm particle size). Proton and carbon NMR were analyzed for all intermediates and final products on Bruker AMX400 (400 MHz) nuclear magnetic resonance spectrometer. Chemical shifts were reported in parts per million (δ, ppm) downfield from internal TMS. Coupling constants (*J*) were expressed in Hertz (Hz). Melting points were measured with a Gallenkamp melting point apparatus.

3.2 Chemistry

3.2.1 (E)-2-methoxy-4-(3-oxoprop-1-en-1-yl)phenyl 4-chlorobenzoate (1)

To 530 mg (1.68 mmol, 1.0 eq) 4-hydroxy-3-methoxy cinnamic aldehyde in 4 mL DMF was added 585 mg (3.36 mmol, 2.0 eq) 4-chlorobenzoyl chloride and (2.52 mmol,1.5 eq) TEA. The reaction was stirred at RT for overnight. The reaction was followed up by TLC, and when was completed, 25 mL water was added to quench the reaction. The precipitate was then filtered, washed frequently with distilled water and dried. The crude was then purified by column chromatography using 70:30 (hexane:ethyl acetate) affording 33% of the titled product as a white solid, melting point 134-136 °C. ^{1}H NMR (400 MHz, $CDCl_3$) δ 9.72 (d, *J* = 7.6 Hz, 1H, C*H*O), 8.25 – 8.08 (m, 2H, Ar*H*), 7.57 – 7.47 (m, 2H, Ar*H*), 7.30 – 7.13 (m, 3H, Ar*H* & C*H*=CH-CHO), 6.70 (dd, *J* = 15.9, 7.6 Hz, 1H, CH=C*H*-CHO), 3.87 (s, 3H, CH_3). ^{13}C NMR (101 MHz, $CDCl_3$) δ 193.54, 163.73, 151.92, 151.90, 142.42, 140.47, 133.28, 131.88, 129.14, 128.99, 127.60, 123.72, 122.05, 111.64, 56.16.

3.2.2 (E)-2-methoxy-4-(3-oxoprop-1-en-1-yl)phenyl 4-(chloromethyl)benzoate (2)

To 500 mg (2.8 mmol, 1.0 eq) 4-hydroxy-3-methoxy

cinnamic aldehyde in 4 mL DMF was added 1.12 g (5.6 mmol, 2.0 eq) 4-(Chloromethyl) benzoyl chloride and (4.2 mmol,1.5 eq) TEA. The reaction was stirred at RT for overnight. The reaction was followed up by TLC, and when was completed, 25 mL water was added to quench the reaction. The precipitate was then filtered, washed frequently with distilled water, and dried. The crude was then purified by column chromatography using 100% DCM affording 32% of the titled product as an off-white solid, melting point 125-127 ^{o}C. ^{1}H NMR (400 MHz, $CDCl_3$) δ 9.70 (d, *J* = 7.6 Hz, 1H, C*H*O), 7.36 (q, *J* = 8.5 Hz, 4H, Ar*H*), 6.98 (d, *J* = 2.1 Hz, 1H, Ar*H*), 6.87 (dd, *J* = 8.3, 2.0 Hz, 1H, Ar*H*), 6.80 (d, *J* = 8.2 Hz, 1H, Ar*H*), 6.55 (d, *J* = 15.8 Hz, 1H, C*H*=CH-CHO), 6.26 (dt, *J* = 15.9, 5.9 Hz, 1H, CH=C*H*-CHO), 5.12 (s, 2H, CH_2), 3.91 (s, 3H, CH_3). ^{13}C NMR (101 MHz, $CDCl_3$) δ 194.16, 173.69, 149.89, 147.87, 135.70, 133.79, 131.11, 130.72, 128.86, 128.75, 127.08, 119.65, 114.23, 109.68, 63.91, 56.07.

3.2.3(E)-3-(4-((4-chlorobenzyl)oxy)-3-methoxyphenyl) acrylaldehyde (4)

To 500 mg (2.8mmol, 1.0 eq) 4-hydroxy-3-methoxy cinnamic aldehyde in 4 mL DMF was added 1.12 g (5.6 mmol, 2.0 eq) 4-Chlorobenzyl chloride and (4.2mmol, 1.5 eq) K_2CO_3. The reaction was stirred at reflux for overnight. The reaction was followed up by TLC, and when was completed, 25 mL water was added and a precipitate was formed. The precipitate was then filtered, washed frequently with distilled water, and dried. The crude was then purified by column chromatography using 100% DCM affording 83.88% of the titled product as a white solid, melting point 110-112 ^{o}C. ^{1}H NMR (400 MHz, $CDCl_3$) δ 9.64 (d, *J* = 7.4 Hz, 1H, C*H*O), 7.43 – 7.18 (m, 3H, Ar*H*), 7.00 – 7.15 (m, 4H, Ar*H*), 6.86 (d, *J* = 15.3 Hz, 1H, C*H*=CH-CHO), 6.59 (dd, *J* = 15.3, 7.3 Hz, 1H, CH=C*H*-CHO), 5.15 (d, *J* = 6.0 Hz, 2H, CH_2), 3.94 (s, 3H, CH_3). ^{13}C NMR (101 MHz, $CDCl_3$) δ 193.55, 152.65, 150.79, 149.95, 134.88, 134.00, 128.92, 128.62, 127.67, 127.01, 123.13, 113.49, 110.52, 70.17, 56.06.

3.2.4 (3E,5E)-6-(4-(dimethylamino)phenyl)hexa-3,5-dien-2-one (5)

To 300 mg (1.7 mmol, 1.0 eq) 4-(Di methylamino) cinnamaldehyde in 10 mL acetone was added (3.4 mmol, 2.0 eq) NaOH. The reaction was stirred under N_2 for overnight. The reaction was followed up by TLC, and when was completed, 25 mL water was added and then extracted three times with DCM (25 mL), the organic layer was dried over anhydrous $MgSO_4$ then the organic solvent was evaporated under reduced pressure to obtain the product. The crude was then purified by column chromatography using 100% DCM affording 15% of the titled product as a bright yellow solid, melting point 110-112 ^{o}C. ^{1}H NMR (400 MHz, $CDCl_3$) δ 7.32 (d, *J* = 8.6 Hz, 2H, Ar*H*), 6.89 (d, *J* = 8.6 Hz, 2H), 6.68 (dt, *J* = 14.2, 6.1 Hz, 3H, CH=C*H*-CO), 6.17 (t, *J* = 14.2 Hz, 1H, C*H*=CH-CO), 3.02 (s, 6H, NCH_3), 2.30 (s, 3H, COCH_3). ^{13}C NMR (101 MHz, $CDCl_3$) δ 198.61, 151.22, 145.10, 142.35, 128.94, 128.08, 122.20, 112.16, 40.33, 27.27.

3.2.5 (2E,4E)-5-(4-(dimethylamino)phenyl)-1-(4-fluorophenyl)penta-2,4-dien-1-one (6)

To 300 mg (1.7 mmol, 1.0 eq) 4-(Dimethylamino)cinnamaldehyde in 10 mL methanol was added (3.4 mmol, 2.0 eq) NaOH, and (1.7 mmol, 1.0 eq) 4′-Fluoroacetophenone. The reaction was stirred under N_2 for overnight. The reaction was followed up by TLC, and when was completed, 25 mL water was added and then extracted with DCM. The organic layer was dried over anhydrous $MgSO_4$ then the organic solvent was evaporated under reduced pressure to obtain the product. The crude was then purified by column chromatography using 50:50 (DCM : hexane) affording 70% of the titled product as a red solid, melting point 128-130 ^{o}C. ^{1}H NMR (400 MHz, $CDCl_3$) δ 7.99 (dd, *J* = 8.5, 5.6 Hz, 2H, Ar*H*), 7.62 (dd, *J* = 14.8, 11.0 Hz, 1H, HC=C*H*-CH=CH), 7.48 – 7.28 (m, 2H, ArH & *H*C=CH-CH=CH), 7.13 (t, *J* = 8.5 Hz, 2H, Ar*H*), 7.07 – 6.86 (m, 1H, HC=CH-CH=C*H*), 6.82 (dd, *J* = 14.8, 5.6 Hz, 1H, HC=CH-C*H*=CH), 6.67 (d, *J* = 8.6 Hz, 2H, Ar*H*), 3.02

(s, 6H). ^{13}C NMR (101 MHz, $CDCl_3$) δ 189.00, 165.5 (d, *J* = 254.5 Hz, 1C), 151.31, 146.75, 143.54, 135.19, 130.97, 130.78 (d, *J* = 24.24, 1C), 129.10, 124.26, 122.42, 122.20, 115.77, 115.55, 112.16, 111.89, 77.41, 40.33, 40.21.

3.2.6 (E)-2-methoxy-4-(3-oxoprop-1-en-1-yl)phenyl 4-(trifluoromethyl)benzoate (8)

To 250 mg (1.4 mmol, 1.0 eq) 4-hydroxy-3-methoxy cinnamic aldehyde in 4 mL DMF was added (2.8 mmol, 2.0 eq) 4-(Trifluoromethyl)benzoyl chloride and (2.1 mmol, 1.5 eq) TEA. The reaction was stirred at RT for overnight. The reaction was followed up by TLC, and when was completed, 25 mL water was added to quench the reaction then extracted with DCM, the organic layer was dried over anhydrous $MgSO_4$ then the organic solvent was evaporated under reduced pressure to obtain the product. The crude was then purified by column chromatography using 100% DCM affording 30% of the titled product as a yellow solid, melting point 78-80 °C. ^{1}H NMR (400 MHz, $CDCl_3$) δ 9.64 (d, *J* = 7.8 Hz, 1H, C*H*O), 7.62 (d, *J* = 8.1 Hz, 2H, Ar*H*), 7.53 (d, *J* = 8.0 Hz, 2H, Ar*H*), 7.39 (dd, *J* = 14.6, 11.7 Hz, 1H, CH=C*H*-CHO), 7.07 (d, *J* = 9.3 Hz, 2H, Ar*H*), 6.85 (d, *J* = 8.1 Hz, 1H, Ar*H*), 6.59 (dd, *J* = 15.8, 7.7 Hz, 1H, C*H*=CH-CHO), 3.92 (s, 3H, CH_3). ^{13}C NMR (101 MHz, $CDCl_3$) δ 198.29, 157.31, 155.38, 154.73, 145.23, 132.62, 132.01, 131.88, 131.22, 130.48, 130.44, 127.85, 127.46, 118.23, 117.22, 115.33, 60.83.

3.2.7(E)-3-(3-methoxy-4-((4-methylbenzyl) oxy)phenyl) acrylaldehyde (9)

To 250 mg (1.4 mmol, 1.0 eq) 4-hydroxy-3-methoxy cinnamic aldehyde in 4 mL DMF was added (2.8 mmol, 2.0 eq) 4-Methylbenzyl bromide and (2.1 mmol, 1.5 eq) K_2CO_3. The reaction was stirred at reflux for overnight. The reaction was followed up by TLC, and when was completed, 25 mL water was added and a precipitate was formed. The precipitate was then filtered, washed frequently with distilled water and dried. The crude was then purified by column chromatography using 100% DCM affording 40% of the titled product as a yellow solid, melting point 98-100 °C. ^{1}H NMR (400 MHz, $CDCl_3$) δ 9.64 (d, *J* = 7.8 Hz, 1H, C*H*O), 7.38 (d, *J* = 15.8 Hz, 1H, C*H*=CH-CHO), 7.31 (d, *J* = 7.6 Hz, 2H, Ar*H*), 7.17 (d, *J* = 7.6 Hz, 2H, Ar*H*), 7.00 – 7.15 (m, 2H, Ar*H*), 6.89 (d, *J* = 8.5 Hz, 1H, Ar*H*), 6.59 (dd, *J* = 15.6, 7.8 Hz, 1H, CH=C*H*-CHO), 5.16 (s, 2H, CH_2), 3.91 (s, 3H, OCH_3), 2.34 (s, 3H, ArCH_3). ^{13}C NMR (101 MHz, $CDCl_3$) δ 188.19, 147.47, 144.50, 132.52, 127.90, 123.98, 121.92, 121.35, 117.84, 107.99, 105.05, 71.96, 71.88, 71.64, 71.32, 65.39, 50.64, 15.81.

3.2.8 (E)-2-methoxy-4-(3-oxoprop-1-en-1-yl)phenyl 2-phenylacetate (10)

To 530 mg (1.68 mmol, 1.0 eq) 4-hydroxy-3-methoxy cinnamic aldehyde in 4 mL DMF was added 585 mg (1.68 mmol, 1.0 eq) phenyl acetyl chloride and (2.52 mmol,1.5 eq) TEA. The reaction was stirred at RT for overnight. The reaction was followed up by TLC, and when was completed, 25 mL water was added to quench the reaction. The precipitate was then filtered, washed frequently with distilled water and dried. The crude was then purified by column chromatography using 100% DCM affording 56 % of the titled product as a white solid, melting point 112-114 °C. ^{1}H NMR (400 MHz, $CDCl_3$) δ 9.68 (d, *J* = 7.6 Hz, 1H, C*H*O), 7.46 – 7.33 (m, 5H, Ar*H*), 7.33 – 7.26 (m, 1H, Ar*H*), 7.16 – 7.08 (m, 2H, Ar*H* & C*H*=CH-CHO), 7.06 (d, *J* = 7.9 Hz, 1H, Ar*H*), 6.64 (dd, *J* = 15.8, 7.6 Hz, 1H, CH=C*H*-CHO), 3.89 (s, 2H, CH_2), 3.79 (s, 3H, CH_3). ^{13}C NMR (101 MHz, $CDCl_3$) δ 188.10, 163.92, 146.52, 146.21, 136.94, 127.94, 127.56, 124.01, 123.33, 123.27, 121.98, 118.02, 116.48, 106.00, 50.53, 35.59.

3.2.9 (E)-2-methoxy-4-(3-oxoprop-1-en-1-yl)phenyl 4-methylbenzoate (11)

To 530 mg (1.68 mmol, 1.0 eq) 4-hydroxy-3-methoxy cinnamic aldehyde in 4 mL DMF was added 585 mg (1.68 mmol, 1.0 eq) p-toluoyl chloride and (2.52 mmol,1.5 eq) TEA. The reaction was stirred at RT for overnight. The

reaction was followed up by TLC, and when was completed, 25 mL water was added to quench the reaction. The precipitate was then filtered, washed frequently with distilled water and dried. The crude was then purified by recrystallization using 1:1 methanol:water affording 57% of the titled product as an off-white solid, melting point 118-120 °C. ^{1}H NMR (400 MHz, $CDCl_3$) δ 9.69 (d, *J* = 7.1 Hz, 1H, C*H*O), 8.07 (d, *J* = 6.9 Hz, 2H, Ar*H*), 7.35 – 7.51 (m, 1H, Ar*H*), 7.29 (d, *J* = 7.0 Hz, 2H, Ar*H*), 7.12 – 7.25 (m, Ar*H* & C*H*=CH-CHO), 6.67 (dt, *J* = 14.7, 6.9 Hz, 1H, CH=C*H*-CHO), 3.84 (s, 3H, OCH_3), 2.44 (s, 3H, ArCH_3). ^{13}C NMR (101 MHz, $CDCl_3$) δ 193.50, 164.51, 152.03, 151.94, 144.66, 142.68, 132.92, 130.44, 129.36, 128.72, 126.26, 123.76, 121.97, 111.54, 56.05, 21.81.

3.3 Cytotoxicity Assays

Cytotoxicity assays was performed as described before[35]. Briefly, A549 and H1299 were cultured in RPMI-1640 medium being supplemented with 10% (v/v) heat inactivated fetal bovine. The cells were maintained in 5% CO_2 humidified incubator at 37 °C. A549 and H1299 cells were seeded at 750 and 1000 cells per well, respectively, into 96-well plates and left for next day for attachment. Media was changed the next day and treatment using the new compounds were added at various concentrations ranging between 0.01 and 60 μM for 96 h. Cell viability was then measured using MTT assay. Optical densities were then measured by the BioTeK SYNERGY HTX multi-mode plate reader at 540 nm. Dose–response curves were generated using the GraphPad Prism 9 Software, and nonlinear regression analysis was used to fit the data. IC_{50} values were determined from these curves.

3.4 Antioxidant Activity

Antioxidant activity was performed as described before[44]. A serial dilution of the synthesized compounds and vitamin C dissolved in DMSO is prepared to give a range of final well concentrations as follows: 200, 100, 50, 25, 12.5, 6.25, 3.125 and 1.5625 μg/mL. A stock solution of DPPH in ethanol (1 mg/mL) is prepared and diluted to 40 μg/mL. To a 96-well plate, 20 μL of each sample is added then followed by 280 μL of the 40 μg/mL DPPH. The 96-well plate was incubated for 30 minutes in dark at RT for 30 minutes. The absorbance was read at 517 nm by the BioTeK SYNERGY HTX multi-mode plate reader. The scavenging activity is calculated according to the equation: Antioxidant activity % = ((Absorbance of DPPH* − Absorbance of the sample) / (Absorbance of DPPH*)) × 100%.

Informed Consent: Not Applicable

Funding and Acknowledgment: We acknowledge Al-Zaytoonah University of Jordan for funding this project under grant number: 32/11/2020-2021. Dedicated to Professor Dr. Wolfgang Weigand on the occasion of his 65th Birthday.

REFERENCES

(1) Kim, C, Kim, B. Anti-Cancer Natural Products and Their Bioactive Compounds Inducing ER Stress-Mediated Apoptosis: A Review. Nutrients 2018, 10 (8).

(2) Xu, D. P, Li, Y, Meng, X. et al. Natural Antioxidants in Foods and Medicinal Plants: Extraction, Assessment and Resources. International Journal of molecular sciences 2017, 18 (1).

(3) Kokoska, L, Kloucek, P, Leuner, O. et al. Plant-Derived Products as Antibacterial and Antifungal Agents in Human Health Care. Current medicinal chemistry 2019, 26 (29), 5501-5541.

(4) Heard, S. C, Wu, G, Winter, J. M. Antifungal natural products. Current opinion in biotechnology 2021, 69, 232-241.

(5) Alsalman, A. H, Aboalhaija, N, Talib, W.et al. Evaluation of the Single and Combined Antibacterial Efficiency of the Leaf Essential Oils of Four Common Culinary herbs: Dill, Celery, Coriander and Fennel Grown in Jordan. Journal of Essential Oil Bearing Plants 2021, 24 (2), 317-328.

(6) Abaza, I, Aboalhaija, N, Alsalman, A. et al.Aroma Profile, Chemical Composition and Antiproliferative Activity of the Hydrodistilled Essential Oil of a Rare Salvia Species (Salvia greggii). Journal of Biologically Active Products from Nature 2021, 11 (2), 129-137.

(7) Farah, A. I, Ahmad, M. N, Al-Qirim, T. M. The Antioxidant and Pro-oxidant Impacts of Varying Levels of Alpha-Lipoic Acid on Biomarkers of Myoglobin Oxidation in Vitro. Jordan Journal of Agricultural Sciences 2020, 16 (4), 89-99.

(8) Al-Qirim, T. M, Zafir, A, Banu, N. Comparative anti-oxidant potential of Rauwolfia serpentina and Withania somnifera on cardiac tissues. The FASEB Journal 2007, 21 (5), A271-A271.

(9) Dilshad, R, Batool, R. Antibacterial and Antioxidant Potential of Ziziphus jujube, Fagonia Arabica, Mallotus phillipensis and Hemidesmus Indicus. Jordan j pharm. Sci. 2022, 15 (3), 413-427.

(10) Femi-Oyewo, M. N, Adeleye, O. A, Bakre, L. G. et al. Evaluation of the Antimicrobial Activity of Strombosia grandifolia Hook.f. ex Benth Extract Hand Sanitizer Formulation. Jordan j pharm. Sci. 2023, 16 (1), 61-71.

(11) Naskar, A, Dasgupta, A, Acharya, K. Antioxidant and Cytotoxic Activity of Lentinus fasciatus. Jordan j pharm. Sci. 2023, 16 (1), 72-81.

(12) Shreaz, S, Wani, W. A, Behbehani, J. M. et al. Cinnamaldehyde and its derivatives, a novel class of antifungal agents. Fitoterapia 2016, 112, 116-31.

(13) Vasconcelos, N. G, Croda, J, Simionatto, S. Antibacterial mechanisms of cinnamon and its constituents: A review. Microbial pathogenesis 2018, 120, 198-203.

(14) Hong, S. H, Ismail, I. A, Kang, S. M. et al. Cinnamaldehydes in Cancer Chemotherapy. Phytotherapy research : PTR 2016, 30 (5), 754-67.

(15) Gan, F. F, Chua, Y. S. Scarmagnani, S, et al. Structure-activity analysis of 2'-modified cinnamaldehyde analogues as potential anticancer agents. Biochemical and biophysical research communications 2009, 387 (4), 741-7.

(16) Kostrzewa, T, Przychodzen, P, Gorska-Ponikowska , M. et al.Curcumin and Cinnamaldehyde as PTP1B Inhibitors With Antidiabetic and Anticancer Potential. Anticancer research 2019, 39 (2), 745-749.

(17) Warsito, W, Murlistyarini, S, Suratmo, S.et al. Molecular Docking Compounds of Cinnamaldehyde Derivatives as Anticancer Agents. Asian Pacific Journal of cancer prevention: APJCP 2021, 22 (8), 2409-2419.

(18) Hariri, M, Ghiasvand, R. Cinnamon and Chronic Diseases. Advances in experimental medicine and biology 2016, 929, 1-24.

(19) Mrityunjaya, M, Pavithra, V, Neelam, R.et al. Immune-Boosting, Antioxidant and Anti-inflammatory Food Supplements Targeting Pathogenesis of COVID-19. Frontiers in immunology 2020, 11, 570122.

(20) Tanaka, Y, Uchi, H, Furue, M. Antioxidant cinnamaldehyde attenuates UVB-induced photoaging. Journal of dermatological science 2019, 96 (3), 151-158.

(21) Hashimoto-Hachiya, A, Tsuji, G, Furue, M. Antioxidants cinnamaldehyde and Galactomyces fermentation filtrate downregulate senescence marker CDKN2A/p16INK4A via NRF2 activation in keratinocytes. Journal of dermatological science 2019, 96 (1), 53-56.

(22) Zhang, J. H, Liu, L. Q, He, Y. L. et al.Cytotoxic effect of trans-cinnamaldehyde on human leukemia K562 cells. Acta pharmacologica Sinica 2010, 31 (7), 861-6.

(23) Najar, B, Shortrede, J. E, Pistelli, L. et al.Chemical Composition and in Vitro Cytotoxic Screening of Sixteen Commercial Essential Oils on Five Cancer Cell Lines. Chemistry & biodiversity 2020, 17 (1), e1900478.

(24) Yu, C, Liu, S.L, Qi, M.H. et al.Cinnamaldehyde/ chemotherapeutic agents interaction and drug-metabolizing genes in colorectal cancer. Molecular medicine reports 2014, 9 (2), 669-76.

(25) Park, J, Baek, S. H. Combination Therapy with Cinnamaldehyde and Hyperthermia Induces Apoptosis of A549 Non-Small Cell Lung Carcinoma Cells via Regulation of Reactive Oxygen Species and Mitogen-Activated Protein Kinase Family. International journal of molecular sciences 2020, 21 (17).

(26) Abbasi, A, Hajialyani, M, Hosseinzadeh, L. et al. Evaluation of the cytotoxic and apoptogenic effects of cinnamaldehyde on U87MG cells alone and in combination with doxorubicin. Research in pharmaceutical sciences 2020, 15 (1), 26-35.

(27) Zhu, R, Liu, H, Liu, C. et al. Cinnamaldehyde in diabetes: A review of pharmacology, pharmacokinetics and safety. Pharmacological research 2017, 122, 78-89.

(28) Xu, R, Xiao, X, Zhang, S. et al.The methyltransferase METTL3-mediated fatty acid metabolism revealed the mechanism of cinnamaldehyde on alleviating steatosis. Biomedicine & pharmacotherapy = Biomedecine & pharmacotherapie 2022, 153, 113367.

(29) Doyle, A. A, Stephens, J. C. A review of cinnamaldehyde and its derivatives as antibacterial agents. Fitoterapia 2019, 139, 104405.

(30) Du, G. F, Yin, X. F, Yang, D. H. et al. Proteomic Investigation of the Antibacterial Mechanism of trans-Cinnamaldehyde against Escherichia coli. Journal of proteome research 2021, 20 (5), 2319-2328.

(31) Yin, L, Chen, J, Wang, K. et al.Study the antibacterial mechanism of cinnamaldehyde against drug-resistant Aeromonas hydrophila in vitro. Microbial pathogenesis 2020, 145, 104208.

(32) Taguchi, Y, Hasumi, Y, Abe, S. et al. The effect of cinnamaldehyde on the growth and morphology of Candida albicans. Medical molecular morphology 2013, 46 (1), 8-13.

(33) Manneck, D, Manz, G, Braun, H. S. et al. The TRPA1 Agonist Cinnamaldehyde Induces the Secretion of HCO(3)(-) by the Porcine Colon. International Journal of molecular sciences 2021, 22 (10).

(34) Załuski, D, Cieśla, Ł, Janeczko, Z. The structure–activity relationships of plant secondary metabolites with antimicrobial, free radical scavenging and inhibitory activity toward selected enzymes. Studies in Natural Products Chemistry 2015, 45, 217-249.

(35) Ibrahim, A. I. M, Ikhmais, B, Batlle, E. et al. Design, Synthesis, Biological Evaluation and In Silico Study of Benzyloxybenzaldehyde Derivatives as Selective ALDH1A3 Inhibitors. Molecules 2021, 26 (19), 5770.

(36) Sudanich, S, Tiyaworanant, S, Yenjai, C. Cytotoxicity of flavonoids and isoflavonoids from Crotalaria bracteata. Natural product research 2017, 31 (22), 2641-2646.

(37) Cabello, C. M, Bair, W. B., Lamore, S. D. et al.The cinnamon-derived Michael acceptor cinnamic aldehyde impairs melanoma cell proliferation, invasiveness, and tumor growth. Free radical biology & medicine 2009, 46 (2), 220-31.

(38) Nair, A. S, Singh, A. K, Kumar, A.et al. FDA-Approved Trifluoromethyl Group-Containing Drugs: A Review of 20 Years. Processes 2022, 10 (10), 2054.

(39) Alkadi, H. A Review on Free Radicals and Antioxidants. Infectious disorders drug targets 2020, 20 (1), 16-26.

(40) Brand-Williams, W, Cuvelier, M. E, Berset, C. Use of a free radical method to evaluate antioxidant activity. LWT - Food Science and Technology 1995, 28 (1), 25-30.

(41) Kedare, S. B, Singh, R. P. Genesis and development of DPPH method of antioxidant assay. Journal of food science and technology 2011, 48 (4), 412-22.

(42) Caritá, A. C, Fonseca-Santos, B, Shultz, J. D.et al. Vitamin C: One compound, several uses. Advances for delivery, efficiency and stability. Nanomedicine: nanotechnology, biology, and medicine 2020, 24, 102117.

(43) Williams, F. M. Clinical significance of esterases in man. Clinical pharmacokinetics 1985, 10 (5), 392-403.

(44) Azhari, S, Xu, Y. S, Jiang, Q. X.et al. Physicochemical properties and chemical composition of Seinat (Cucumis melo var. tibish) seed oil and its antioxidant activity. Grasas y Aceites 2014, 65 (1), e008.

تصميم وتصنيع وفحص النشاط البيولوجي لمشتقات مركب كونيفيريل ألدهيد كمركبات محتملة مضادة للسرطان والأكسدة

ورود حماده اسماعيل[1]†، أسامة هيثم أبوسارة[1]†*، بلقيس اخميس[1]، حسن ابوالفتوح[2] سهير سنقرط[1]، علي ابراهيم مصطفى ابراهيم[1]

[1] كلية الصيدلة، جامعة الزيتونة الأردنية، عمان، الأردن.

[2] قسم الكيمياء، كلية العلوم، الجامعة الهاشمية، الزرقاء، الأردن.

† ساهم كل من ورود حماده إسماعيل وأسامة هيثم أبوسارة في هذا العمل بالتساوي.

ملخص

من المعروف أن النواتج الطبيعية تملك أنشطة مضادة للميكروبات والسرطان والأكسدة. من بين هذه النواتج الطبيعية هي القرفة التي تحتوي على مركب سينامالديهيد. وجدت الدراسات أن مركب السينامالديهايد ومشتقاته لهم أنشطة مضادة للسرطان والأكسدة. كما أظهر مركب كونيفيريل ألدهيد، وهو مركب غير سام للخلايا ومشتق من مركب سينامالديهايد، أن له نشاطا مضادا للسرطان. في هذه الدراسة، تم تصنيع عدد من مشتقات مركب كونيفيريل ألدهيد وتقييم أنشطتها المضادة للسرطان والأكسدة. أظهرت المركبات 1 و2 و4 و8–11 نشاطا ساما للخلايا ضد خلايا H1299، وهي خلايا سرطان الرئة ذات الخلايا غير الصغيرة، وأظهر مركب 4 أعلى فعالية لقتل الخلايا حيث بلغت قيمة نصف التركيز المثبط الأقصى 6.7 ميكرومولار. كما أظهرت مركبات 1 و2 و4 نشاطا مضاد للأكسدة بالمقارنة مع فيتامين سي، حيث وصلت نسبة الكسح للمركبات نصف نسبة الكسح لفيتامين سي في جميع التركيزات التي تم اختبارها للمركبات، وذلك من خلال تجربة فحص مضادات الأكسدة باستخدام مركب DPPH. أظهر مركب كونيفيريل ألدهيد نفسه نشاطا مضادا للأكسدة يعتمد على الجرعة، حيث من المقترح أن ذلك تم عن طريق آلية تثبيت الشوارد الحرة في المركب. وهكذا، أظهرت دراستنا أن مشتقات مركب كونيفيريل ألدهيد تظهر أنشطة مضادة للسرطان والأكسدة، والتي قد تمثل مركبات علاجية محتملة.

الكلمات الدالة: كونيفيريل ألدهيد، مضاد للسرطان، مضاد للأكسدة، DPPH.

* ***المؤلف المراسل:***

أسامة هيثم أبوسارة ، علي ابراهيم مصطفى ابراهيم

o.abusara@zuj.edu.jo , a.ibrahim@zuj.edu.jo

تاريخ الإستلام 2022/12/28 تاريخ قبول النشر 2023/3/8.

Jordan Journal of Pharmaceutical Sciences, Volume 16, No. 2, Supplement 1, 2023

Cholesteryl Ester Transfer Protein Inhibitory Activity of New 4-Bromophenethyl Benzamides

Reema Abu Khalaf [1]*, Areej NasrAllah[1], Ghadeer AlBadawi[1]

[1] Department of Pharmacy, Faculty of Pharmacy, Al-Zaytoonah University of Jordan, Jordan.

ABSTRACT

Cardiovascular diseases, as coronary heart disease, heart failure, and hypertension are the first leading cause of death in the United States and the third globally. CETP is a glycoprotein excreted mainly from the liver and found in plasma. Normal plasma CETP concentration is 1-4 µg/ml, while the ratio increased 70-80% in dyslipidemic patients. There is a growing need for new CETP inhibitors which encourages us to conduct this research. In this work, synthesis and *in vitro* study for four new 4-bromophenethylbenzamides 9a-d were carried out. *In vitro* study showed that the targeted compounds 9a-d exhibit acceptable activity against CETP, where compound 9a has a % inhibition of 40.7 at 10 µM concentration. It was found that the presence of the oxy group in both 9a and 9c enhances their activity which could be attributed to Hydrogen-bond formation with the amino acid residues of the CETP binding site.

Keywords: Benzamides, 4-Bromophenethyl, CETP, Hypercholesterolemia, Inhibitors.

INTRODUCTION

Cardiovascular diseases (CVD), like coronary heart disease, heart failure, and hypertension are the first leading cause for death in the United States and the third globally [1, 2]. The lipoproteins that carry cholesterol through the blood are chylomicrons, very low-density lipoproteins (VLDL), low-density lipoproteins (LDL) and high-density lipoproteins (HDL). Chylomicrons are triglyceride-loaded particles, which function in transferring dietary lipids from the intestine to the liver and tissues; VLDL is also a triglyceride loaded particle, whose function is to carry endogenous triglyceride from the liver to peripheral tissues [3]. It is suggested that VLDL triglyceride is processed to LDL *via* hepatic lipase or lipoprotein lipase [4, 5].

HDL are diverse group of lipoprotein particles. Most of the HDL particles contain apolipoprotein A-I, which is the most common apolipoprotein in plasma. HDL also contains apolipoprotein A-II, the second most common protein in HDL [4]. Many researchers found that elevated level of HDL in blood decreases the opportunity of CVD, *vice versa* high level of LDL and VLDL increases the incidence of CVD [2].

CETP is a glycoprotein excreted mainly from the liver and found in plasma. Normal plasma CETP concentration is 1-4 µg/ml, while it increased 70-80 % in people with dyslipidemia [6]. Lipid control has considerable scope for improvement in patients with dyslipidemia [7]. There are two hypothesized mechanisms for CETP activity: the shuttle model, and the ternary complex model. In the shuttle model, CETP can bind to cholesteryl ester and triglycerides and fills the stores that can be then exchanged with lipoproteins. The ternary complex model assumes that CETP can bind two lipoproteins one on each side, followed by the transfer of lipids between the two lipoproteins. Therefore, CETP raises LDL levels and decreases HDL levels and the inhibition of

[*]***Corresponding author: Reema Abu Khalaf***
reema.abukhalaf@zuj.edu.jo
Received: 28/12/2022 Accepted: 13/3/2023.
DOI: https://doi.org/10.35516/jjps.v16i2.1465

the CETP results in raising the concentration of cholesterol ester in HDL and decreasing its concentration in VLDL and LDL particles. High level of HDL has an atheroprotective effect against CVD [8]. Hyperlipidemia management with statin drugs still the most proper treatment despite of their side effect [9]. While CETP inhibitors are promising drugs that increase HDL cholesterol, and decrease LDL cholesterol in the blood with fewer side effects than statins [10, 11].

However, the first trials with the CETP inhibitors (Figure 1) torcetrapib and dalcetrapib failed to show a reduction in cardiovascular events. Torcetrapib has an effect on the aldosterone level that increases blood pressure, while dalcetrapib had a low enhancement of lipid profile [6, 12]. Besides, evacetrapib study was terminated due to its low efficacy, while anacetrapib is still under further investigation[12].

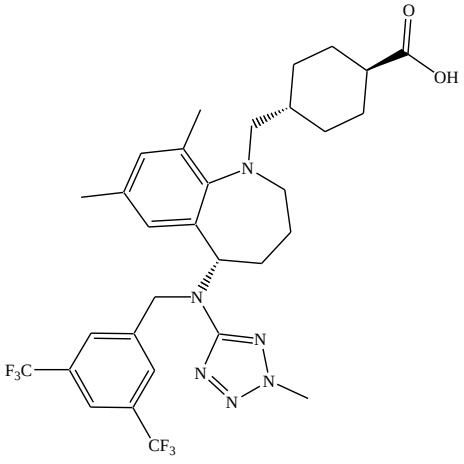

Evacetrapib

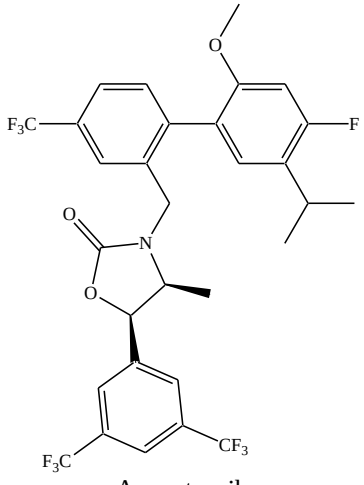

Anacetrapib

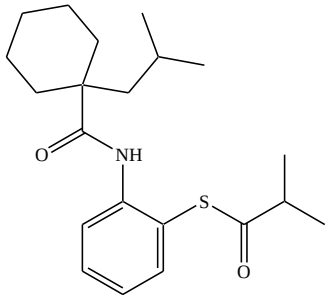

Dalcetrapib

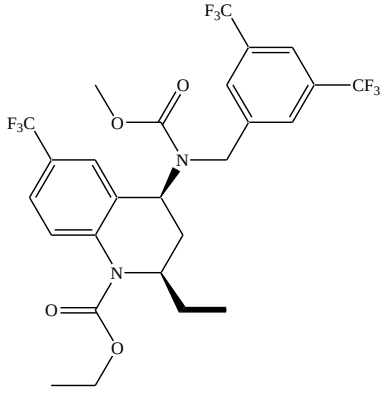

Torcetrapib

Figure 1: Structures of some known CETP inhibitors.

Earlier our group design and synthesize different potential CETP inhibitors (Figure 2) such as: benzylidene-amino methanones [13], benzyl- amino-methanones [14], *N*-(4-benzyloxyphenyl)-4-methyl-benzenesulfonamides, *N*-(4-benzylamino- phenyl)-toluene-4-sulfonic acid esters [15], chlorobenzyl benzamides [16], fluorinated benzamides [17, 18], substituted benzyl benzamides [19, 20] and aryl sulfonamides [21, 22].

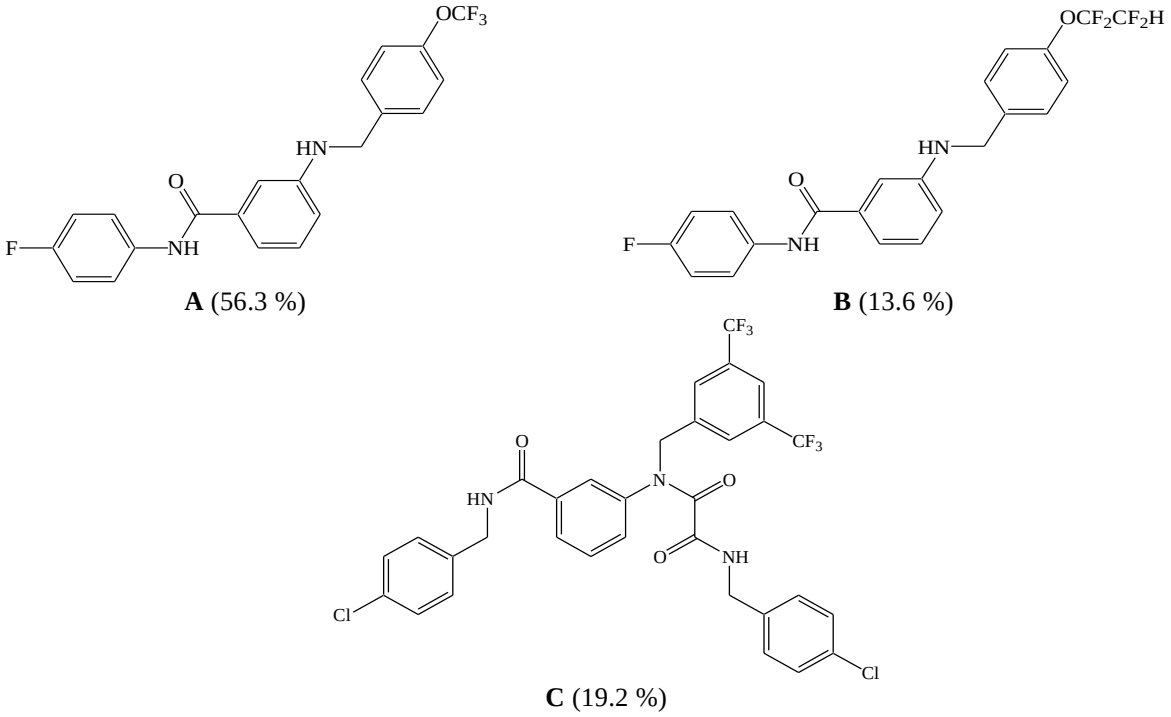

Figure 2: Our previously synthesized potential CETP inhibitors leads (% inhibition of CETP at 10 µM concentration) [16-20]

Our study aims to synthesize new benzamide analogues **9a-d** by varying the substitution with different groups such as -OCF_3, -CF_3, and-CF_2CF_2H, in addition to altering the chain length at the benzyl amine side, followed by *in vitro* biological evaluation of the targeted compounds as CETP inhibitors.

MATERIALS AND METHODS

General

All chemicals, reagents and solvents were of analytical grade. Chemicals and solvents were purchased from the corresponding companies (Alfa Aesar, Acros Organics, Sigma-Aldrich, Fluka, SD fine ChemLimite, and Tedia and Fisher Scientific).

3-Aminobenzoic acid was purchased from (Alfa Aesar materials, Karlsruhe, Germany). Dichloromethane (DCM), triethylamine (TEA), acetone, cyclohexane, ethanol, ethyl acetate, and methanol (CH_3OH) were obtained from (Tedia company, INC, USA). Chloroform, and dimethylformamide (DMF) were purchased from (Fisher Scientific UK limited, UK). Sodium sulfate anhydrous, hydrochloric acid (HCl, 37%), 2-(4-bromophenyl) ethylamine, oxalyl chloride $(COCl)_2$, and sodium borohydride ($NaBH_4$) were obtained from (Sigma-Aldrich, Germany). 1-Bromomethyl-4-trifluromethoxy benzene, 1-bromomethyl-4-trifluromethyl benzene, 4-(1,1,2,2-tetrafluoroethoxy) benzaldehyde, and 1-(bromomethyl)-3,5-bis (trifluoromethyl) benzene were obtained from (Aldrich chemistry, USA). Sodium hydroxide (NaOH) was purchased from (SD fine Chem Limited, India).

Melting points were measured using Gallenkamp melting point apparatus. Infrared (IR) spectra were recorded using Shimadzu IR Affinity1 FTIR spectrophotometer. All samples were prepared with potassium bromide and pressed into a disc. 1H and 13C Nuclear Magnetic Resonance (NMR) spectra were measured on Bruker, Avance DPX- 300, and 500 spectrometers, at The University of Jordan. Chemical

shifts are given in δ (ppm) using TMS as internal reference; the samples were dissolved in deuterated DMSO. High resolution mass spectrometry (HR-MS) was performed using LC Mass Bruker Apex-IV mass spectrometer utilizing an electrospray interface, at The University of Jordan. AFLX800TBI Microplate Fluorimeter (BioTek Instruments, Winooski, VT, USA) was used for the in vitro bioassay.

Thin Layer Chromatography (TLC) was performed on 20 x 20 cm with layer thickness of 0.2 mm aluminum cards pre-coated with fluorescent silica gel GF254 DC-alufolien-kieselgel (Fluka analytical, Germany), and visualized by UV light indicator (at 254 and/ or 360 nm). CETP inhibitory bioactivities were assayed employing a commercially available kit (Fluorometric) (BioVision, Linda Vista Avenue, USA).

Synthesis of the targeted compounds 9a-d

The methyl benzoate intermediates **5a-d** were synthesized as previously described [16-20] and purified by column chromatography using different concentrations of cyclohexane and ethyl acetate. The preparation of the acyl intermediates **7a-d** from methyl esters **5a-d** was carried out as formerly stated [16-20].

*3-(4-(Trifluoromethoxy)benzylamino)-N-(4-bromophenethyl)benzamide **(9a)***

2-(4-Bromophenyl)ethylamine (**8**, 0.48 ml, 2.91 mmol) together with 5 ml of triethylamine and 10 ml of dichloromethane were added to **7a** (0.97 mmol), then the reaction mixture was stirred at room temperature for 5 days. The crude product was purified by column chromatography using chloroform: methanol (98:2) as eluent.

White powder was achieved (0.1gm, % yield = 21%); m.p. = 184-185 ºC; Rf = 0.69 (Chloroform: methanol, 8.5:1.5); 1H-NMR (300 MHz, DMSO): δ 4.09 (s, 2H, CH2), 4.41 (s, 2H, CH2), 4.98 (s, 2H, CH2), 6.78 (s, 1H, CH2NH), 7.26-7.31 (m, 8H, Ar-H), 7.46 (s, 2H, Ar-H), 7.77 (s, 2H, Ar-H), 9.23 (s, 1H, CONH); 13C-NMR (75 MHz, DMSO): δ 41.4 (1C, CH2), 42.6 (1C, CH2), 50.8 (1C, CH2), 120.4 (1C, Ar-C), 121.5 (2C, Ar-C), 127.4 (1C, Ar-C), 128.7 (1C, Ar-C), 129.7 (1C, Ar-C), 130.0 (2C, Ar-C), 130.3 (2C, Ar-C), 131.7 (2C, Ar-C), 133.8 (1C, Ar-C), 136.4 (1C, Ar-C), 138.1 (1C, Ar-C), 139.5 (1C, Ar-C), 143.2 (1C, Ar-C), 148.1 (1C, Ar-C), 163.5 (1C, Ar-C), 165.8 (1C, CONH) ppm; IR (KBr): 3325, 3086, 2924, 2855, 1659, 1528, 1404, 1258 cm-1; HR-MS (ESI, positive mode) m/z [M-Br]+ 413.26614 (C23H20 F3N2O2 requires 413.06602).

*3-(3,5-Bis(trifluoromethyl)benzylamino)-N-(4-bromophenethyl)benzamide **(9b)***

2-(4-Bromophenyl)ethylamine (**8**, 0.18 ml, 1.18 mmol) together with 5 ml of triethylamine and 10 ml of dichloromethane were added to **7b** (0.34 mmol), then the reaction mixture was stirred at room temperature for 5 days. The crude product was purified by column chromatography using cyclohexane: ethyl acetate (6:4) as eluent.

Off white powder was achieved (0.164 gm, % yield = 82 %); m.p. = 87-89 ºC; Rf = 0.71 (Cyclohexane: ethyl acetate, 6:4); 1H-NMR (500 MHz, DMSO): δ 2.79 (s, 2H, CH2), 3.43 (s, 2H, CH2), 4.53 (s, 2H, CH2), 6.62 (s, 1H, CH2NH), 6.73 (s, 1H, Ar-H), 6.99 (s, 1H, Ar-H), 7.06 (s, 1H, Ar-H), 7.14-7.19 (m, 2H, Ar-H), 7.45 (s, 3H, Ar-H), 7.98 (s, 1H, Ar-H), 8.07 (s, 2H, Ar-H), 8.35 (s, 1H, CONH); 13C-NMR (125 MHz, DMSO):δ 34.9 (1C, CH2), 40.9 (1C, CH2), 45.9 (1C, CH2), 111.8 (1C, Ar-C), 115.3 (1C, CF3), 115.5 (1C, CF3), 119.6 (1C, Ar-C), 121.0 (1C, Ar-C), 122.8 (1C, Ar-C), 125.0 (1C, Ar-C), 128.4 (1C, Ar-C), 129.3 (1C, Ar-C), 129.7 (1C, Ar-C), 130.2 (1C, Ar-C), 130.5 (1C, Ar-C), 130.8 (1C, Ar-C), 131.0 (1C, Ar-C), 131.4 (2C, Ar-C), 131.5 (2C, Ar-C), 136.0 (1C, Ar-C), 139.5 (1C, Ar-C), 144.6 (1C, Ar-C), 148.5 (1C, Ar-C), 167.2 (1C, CONH) ppm; IR (KBr): 3318, 3063, 2932, 2870, 1651, 1589, 1543, 1489, 1381, 1327 cm-1; HR-MS (ESI, positive mode) m/z [M-Br]+ 465.12052 (C24H19 F6N2Orequires 465.05849).

*3-(4-(1,1,2,2-Tetrafluoroethoxy)benzylamino)-N-(4-bromophenethyl)benzamide **(9c)***

2-(4-Bromophenyl) ethylamine (**8**, 0.38 ml, 2.25 mmol) together with 5 ml of triethylamine and 10 ml of dichloromethane were added to **7c** (0.75 mmol), then the reaction mixture was stirred at room temperature for 5 days.

Then the crude product was purified by column chromatography using chloroform: methanol (98:2) as eluent.

Viscous yellow liquid was achieved (0.07 gm, % yield = 39.2 %); R_f = 0.71 (Chloroform: methanol, 98:2); H^1-NMR (300 MHz, DMSO): δ 2.65 (s, 2H, CH_2), 3.10 (s, 2H, CH_2), 3.45 (s, 2H, CH_2), 4.95 (s, 1H, CH_2N*H*), 6.56 (s, 1H, CF_2-*H*), 6.74 (s, 1H, Ar-*H*), 6.91-7.13 (m, 5H, Ar-*H*), 7.28-7.40 (m, 5H, Ar-*H*), 7.64-7.70 (m, 1H, Ar-*H*), 8.85 (s, 1H, CON*H*); ^{13}C-NMR (75 MHz, DMSO):δ 34.8 (1C, *C*H_2), 42.0 (1C, *C*H_2), 51.0 (1C,*C*H_2), 119.7 (1C, *C*F_2), 122.0 (2C, Ar-*C*), 126.2 (1C, *C*F_2), 126.4 (1C, Ar-*C*), 128.5 (1C, Ar-*C*), 129.3 (1C, Ar-*C*), 129.7 (2C, Ar-*C*), 130.0 (2C, Ar-*C*), 131.3 (2C, Ar-*C*), 131.4 (1C, Ar-*C*), 135.8 (1C, Ar-*C*), 138.9 (1C, Ar-*C*), 139.4 (1C, Ar-*C*), 141.2 (1C, Ar-*C*), 147.7 (1C, Ar-*C*), 163.3 (1C, Ar-*C*), 165.7 (1C, *C*ONH)ppm; IR (KBr): 3325, 3071, 2924, 2855, 1651, 1528, 1304, 1273 cm^{-1}.

*3-(4-(Trifluoromethyl)benzylamino)-N-(4-bromophenethyl)benzamide **(9d)***

2-(4-Bromophenyl)ethylamine (**8**, 0. 44ml, 2.63mmol) together with 5 ml of triethylamine and 10 ml of dichloromethane were added to **7d** (0.88mmol), then the reaction mixture was stirred at room temperature for 5 days. The crude product was purified by column chromatography using chloroform: methanol (95:5) as eluent.

Off white powder was achieved (0.199 gm, % yield = 47.8 %); m.p. = 88-90 ºC; Rf = 0.79 (Chloroform: methanol, 95: 5); 1H-NMR (300 MHz, DMSO): δ 2.76 (s, 2H, CH2), 3.13 (s, 2H, CH2), 4.09 (br s, 1H, CH2NH), 5.04 (s, 2H, CH2), 6.94-7.21 (m, 4H, Ar-H), 7.39-7.41 (d, J = 6.6 MHz, 6H, Ar-H), 7.63 (s, 1H, Ar-H), 8.61-8.68 (d, J = 7.0 MHz, 1H, Ar-H), 8.92 (s, 1H, CONH); 13C-NMR (75 MHz, DMSO):δ 35.2 (1C, CH2), 42.0 (1C, CH2), 52.5 (1C, CH2), 119.7 (1C, CF3), 122.9 (1C, Ar-C), 125.8 (1C, Ar-C), 126.5 (1C, Ar-C), 127.2 (1C, Ar-C), 128.2 (1C, Ar-C), 129.0 (2C, Ar-C), 129.8 (1C, Ar-C), 131.4 (2C, Ar-C), 131.4 (2C, Ar-C), 135.9 (1C, Ar-C), 138.9 (1C, Ar-C), 139.4 (2C, Ar-C), 141.1 (1C, Ar-C), 141.9 (1C, Ar-C), 165.7 (1C, CONH)ppm; IR (KBr): 3325, 3071, 2963, 2862, 1651, 1543, 1404, 1265 cm-1; HR-MS (ESI, positive mode) m/z [M-Br]+ 397.29759 (C23H20 F3N2Orequires 397.07111).

***In vitro* determination of CETP inhibition**

The assay kit is composed of a donor molecule harboring a self-quenched neutral lipid, an acceptor molecule, and CETP extracted from rabbit serum. The transfer of the fluorescent neutral lipid to the acceptor molecule induces fluorescence. The inhibition of CETP prohibits lipid transfer and thus decreases fluorescence intensity. The assay protocol is described as follows: an aliquot of rabbit serum (1.5 μL) was mixed with a testing sample (160 μL). Next, the donor and acceptor molecules in the assay buffer were added, mixed well, and the volume was adjusted to 203 μL using the assay buffer. Then the mixture was incubated at 37°C for 1 hour. The fluorescence intensity (Excitation λ: 465 nm; Emission λ: 535 nm) was read in a FLX800TBI Microplate Fluorimeter (BioTek Instruments, Winooski, VT, USA).

The synthesized molecules were dissolved in DMSO yielding 10 mM stock solutions. Then the solutions were diluted to the required concentration using distilled deionized water. DMSO concentration was adjusted to 0.1%. The percentage of residual CETP activity was identified in the presence and absence of the tested molecules. Torcetrapib was used as a positive inhibitor. CETP activity is not affected by DMSO. The negative control samples missing rabbit serum were used as a contrast background. The experimental protocol and measurements were carried out in duplicates.

The % inhibition of CETP by the synthesized compounds was calculated using the following equation[13]:

$$\% \text{ Inhibition} = \left[1 - \frac{\text{Inhibitor read - Blank read}}{\text{Positive control- Negative control}} \right] * 100\%$$

RESULTS AND DISCUSSION

Chemistry

Novel series of 4-bromophenethyl benzamides **9a-d** was synthesized (Scheme 1).

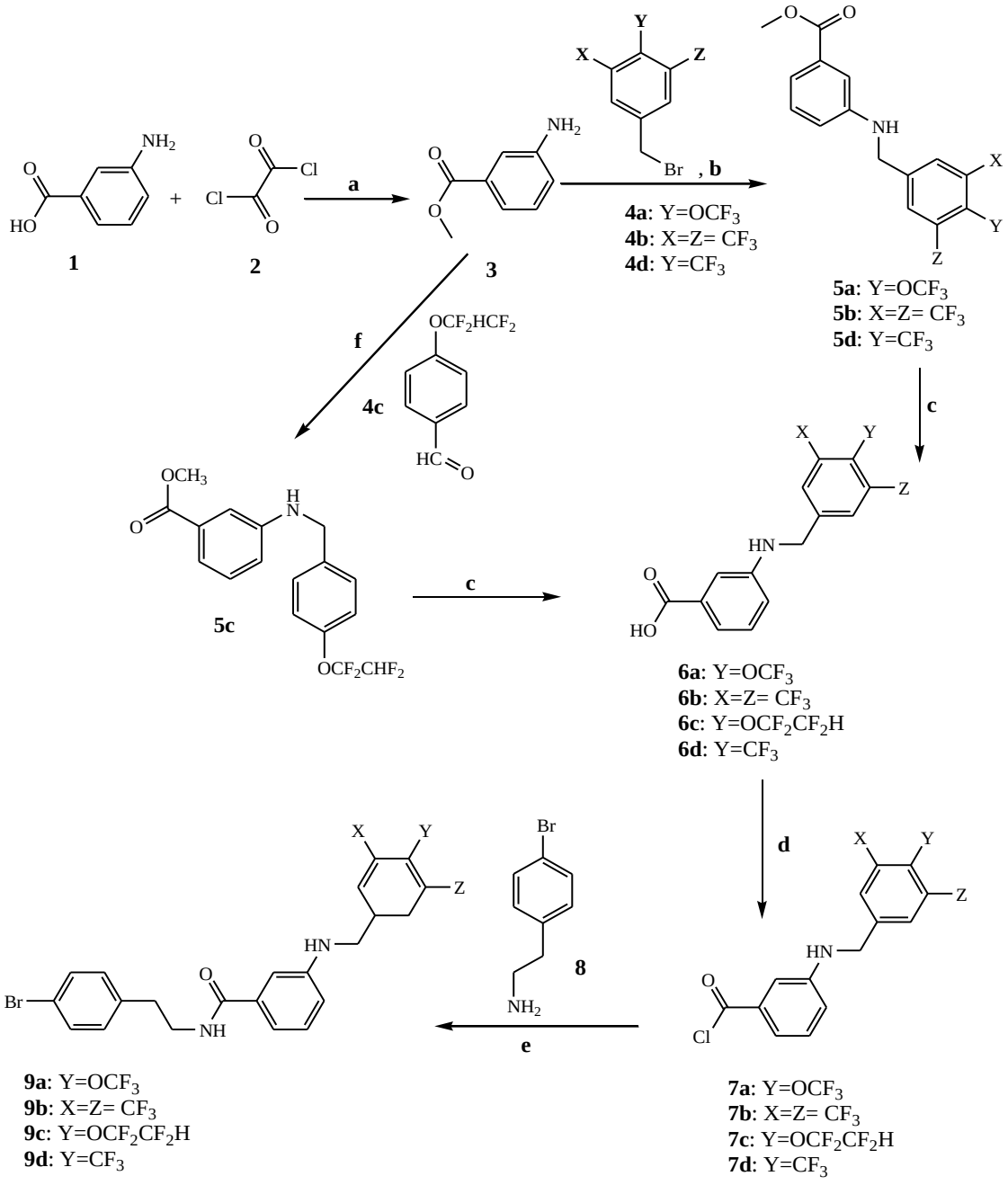

Scheme 1: Synthesis of the targeted 4-bromophenethyl benzamides 9a-d. Reagents and conditions:
(a) CH_3OH/reflux (60-70°C), 24 hours, (b) DCM, TEA, RT, 5 days, (c) (1) 1M NaOH (100°C), overnight, (2) 1M HCl, (d) $(COCl)_2$ /reflux (60-70°C), DCM, 4 days, (e) TEA, DCM, RT, 5 days, (f) DMF/reflux (100-140°C), 7 days/ HCl after 24 hours, CH_3OH, $NaBH_4$, RT, 3 days

The synthesis started with the activation of the carboxylic acid moiety of 3-aminobenzoic acid (**1**) using oxalyl chloride (**2**) in the presence of methanol producing the methyl ester protecting group **3**. Next, the amine nitrogen of 3-amino benzoic acid methyl ester (**3**) attacked the partially positive methylene group of the benzyl bromide **4a**, **4b**, or **4d** in the presence of DCM as a solvent to produce substituted 3-benzylamino benzoic acid methyl ester intermediates **5a**, **5b**, or **5d**. Triethylamine was used as an acid scavenger (HBr).

Imine formation was attained by the nucleophilic attack of the amine nitrogen of 3-aminobenzoic acid methyl ester **3** on the partially positive carbonyl carbon of the 4- (1,1,2,2-tetrafluoroethoxy) benzaldehyde **4c** followed by the elimination of a molecule of water resulting in the acid-catalyzed formation of the imine intermediate. Afterward, reduction of the imine was carried out by sodium borohydride ($NaBH_4$) where a hydride ion attacks the electrophilic carbon of the imine functional group and the anion that forms is then protonated to generate the secondary amine **5c** using methanol as a solvent at room temperature for 3 days.

Afterward, deprotection of the carboxylic acid group of 3-aminobenzoic acid methyl ester intermediates **5a-d** was carried out by alkaline hydrolysis using 1M NaOH under reflux followed by neutralization with concentrated HCl. Then, reactivation of the carboxylic acid moiety of 3-benzylamino benzoic acid intermediates **6a-d** was performed using oxalyl chloride (**2**) to produce acyl chloride derivatives **7a-d** in the presence of DCM and the tetrahedral structure leaves as HCl, CO_2 and CO gases.

Subsequently, amide formation was attained by the nucleophilic attack of the amine moiety of 2-(4-bromophenyl) ethylamine (**8**) on the partially positive carbonyl carbon of the previously produced acyl chloride **7a-d** to get the targeted 4-bromophenethyl benzamide derivatives **9a-9d** (as shown in scheme I). The best yield of 82% was found for compound **9b**, while compound **9a** has the lowest yield of 21%.

***In vitro* determination of CETP inhibition**

The results of CETP inhibition bioassay, presented in Figure 3, demonstrated that compounds **9a-d** exhibited acceptable activity against CETP at 10 µM concentration. The preliminary CETP inhibitory activity of the synthesized compounds was evaluated at 10 µM concentration which is considered a suitable concentration for capturing possible CETP inhibitors as hit compounds that can later undergo further optimization [13].

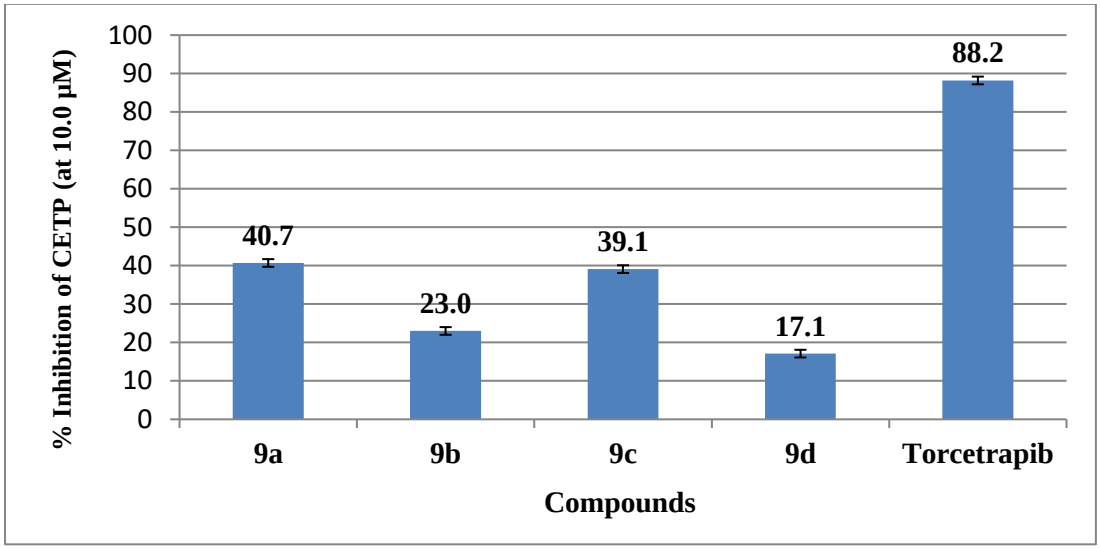

Figure 3. *In vitro* bioactivities of the synthesized 4-bromophenethyl benzamides 9a-d (at 10 µM concentration) and the positive inhibitor Torcetrapib (at 0.08 µM concentration)

As can be seen from Figure 3, compound **9a** with 4-trifluromethoxy group exhibits the highest activity with a % inhibition of 40.7 at 10 µM concentration. Compound **9c** was found to exhibit comparable activity to that of **9a** with a 39.1% inhibition at the same concentration. It is expected that the presence of the oxy group in both compounds, **9a** and **9c**, enhances their activity that can be involved in H-bond formation with the amino acid residues of CETP binding site. On the other hand, compounds **9b** (with 3, 5- ditrifluoromethyl) and **9d** (with 4-trifluoromethyl) showed similar CETP inhibition (23.0% and 17.1% respectively).

CONCLUSION

This work identified 4-bromophenethyl benzamide as a new scaffold targeting CETP activity. Benzamide **9a** showed the highest inhibitory activity with a % inhibition of 40.7 at 10 µM concentration. The study found that presence of oxy moiety such in compounds **9a** and **9c** enhances the activity which can be attributed to H-bond formation with CETP binding site.

Acknowledgments

The authors acknowledge the Deanship of Scientific Research and Innovation at Al-Zaytoonah University of Jordan for sponsoring this project (Fund number 12/08/2021-2022).

Conflict of interest

No conflict of interest is associated with this work.

REFERENCES

(1) Benjamin E.J., Muntner P., Alonso A. et al. Heart Disease and Stroke Statistics-2019 Update: A Report from the American Heart Association. Circulation. 2019; 139(10):e56-e528.

(2) Jansen M., Puetz G., Hoffmann M.M. et al. mathematical model to estimate cholesterylester transfer protein (CETP) triglycerides flux in human plasma. BMC Syst. Biol. 2019; 13(1):1-12.

(3) Yu Y., Kuang Y.L., Lei D. et al. Polyhedral 3D structure of human plasma very low-density lipoproteins by individual particle cryo-electron tomography1. J. Lipid Res. 2016; 57(10):1879-1888.

(4) Yuana Y., Levels J., Grootemaat A. et al. Nieuwland R. Co-isolation of extracellular vesicles and high-density lipoproteins using density gradient ultracentrifugation. J. Extracell. Vesicles. 2014; 3:1-5.

(5) Younis N., Abu-Mallouh S., Almasri I. et al. Pancreatic Lipase Inhibition by Edible Plants Used in Three Middle East Countries: A Mini-Review. Jordan J. Pharm. Sci. 2021; 14(2):179-188.

(6) Kosmas C.E., DeJesus E., Rosario D. et al.CETP Inhibition: Past Failures and Future Hopes. Clin. Med. Insights Cardiol. 2016; 10:37-42.

(7) Jarab A.S., Alefishat E.A., Al-Qerem W. et al. Lipid control and its associated factors among patients with dyslipidemia in Jordan. Int. J. Clin. Pract. 2021; 75(5):e14000.

(8) Shrestha S., Wu B.J., Guiney L. et al. Cholesteryl ester transfer protein and its inhibitors. J. Lipid Res. 2018; 59(5):772-783.

(9) Skoumas J., Liontou C., Chrysohoou C. et al. Statin therapy and risk of diabetes in patients with heterozygous familial hypercholesterolemia or familial combined hyperlipidemia. Atherosclerosis. 2014; 237 (1):140-145.

(10) Dong B., Singh A.B., Fung C. et al. CETP inhibitors downregulate hepatic LDL receptor and PCSK9 expression in vitro and in vivo through a SREBP2-dependent mechanism. Atherosclerosis. 2014; 235 (2):449-462.

(11) Taybeh E.O., Al-Alami Z.M., Albasha A. Statin Use in Jordan: Patients Experience and Attitude toward Adverse Drug Reactions. Jordan J. Pharm. Sci. 2020; 13(2):197-205.

(12) Alkhalil M., Chai J.T., Choudhury R.P. Plaque imaging to refine indications for emerging lipid-lowering drugs. Eur. Heart J. Cardiovasc. Pharmacother. 2017; 3(1):58-67.

(13) Abu Khalaf R., Abu Sheikha G., Bustanji Y. et al. Discovery of new cholesteryl ester transfer protein inhibitors via ligand-based pharmacophore modeling and QSAR analysis followed by synthetic exploration. Eur. J. Med. Chem. 2010; 45(4):1598-1617.

(14) Abu Sheikha G., Abu Khalaf R., Melhem A. et al. Design, synthesis, and biological evaluation of benzylamino-methanone-based cholesteryl ester transfer protein inhibitors. Molecules. 2010; 15(8):5721-5733.

(15) Abu Khalaf R., Abu Sheikha G., Al-Sha'er M., et al. Design, synthesis, and biological evaluation of sulfonic acid ester and benzenesulfonamide derivatives as potential CETP inhibitors. Med. Chem. Res. 2012; 21(11):3669-3680.

(16) Abu Khalaf R., Abd El-Aziz H., Sabbah D., et al. CETP Inhibitory Activity of Chlorobenzyl Benzamides: QPLD Docking, Pharmacophore Mapping, and Synthesis. Lett. Drug Des. Discov. 2017; 14(12):1391-1400.

(17) Abu Khalaf R., Al-Rawashdeh S., Sabbah D.et al. Molecular Docking and Pharmacophore Modeling Studies of Fluorinated Benzamides as Potential CETP Inhibitors. Med. Chem. 2017; 13(3):239-253.

(18) Abu Khalaf R., Awad M., Al-Qirim T. et al. Synthesis and Molecular Modeling of Novel 3, 5-Bis (trifluoromethyl) benzylamino Benzamides as Potential CETP Inhibitors. Med. Chem. 2022; 18(4):417-426.

(19) Abu Khalaf R., Sabbah D., Al-Shalabi E. et al. Biological Evaluation, and Molecular Modeling Study of Substituted Benzyl Benzamides as CETP Inhibitors. Arch. Pharm. 2017; 350(12):e1700204.

(20) Abu Khalaf R., Nasrallah A., Jarrar W. et al. Cholesteryl ester transfer protein inhibitory oxoacetamideo-benzamide derivatives: glide docking, pharmacophore mapping. and synthesis, Braz. J. Pharm. Sci., 2022; 58: e20028.

(21) Abu Khalaf R., Asa'ad M., Habash M. Thiomethylphenyl benzenesulfonamides as potential cholesteryl ester transfer protein inhibitors: Synthesis, molecular modeling and biological evaluation. Curr. Org. Chem., 2022; 26(8):807-815.

(22) Abu Khalaf R., Al Shaiah H., Sabbah D. Trifluoromethylated aryl sulfonamides as novel CETP inhibitors: Synthesis, induced fit docking, pharmacophore mapping and subsequent in vitro validation. Med. Chem., 2023; 19(4):393-404.

النشاط المثبط للبروتين الناقل للكوليستريل استر ل 4-بروموفينيثيل بنزاميدات الجديدة

ريما أبو خلف[1]*، أريج نصر الله[1]، غدير البدوي[1]

[1] قسم الصيدلة، كلية الصيدلة، جامعة الزيتونة الأردنية، عمان، الأردن.

ملخص

تعد أمراض القلب والأوعية الدموية، مثل أمراض القلب التاجية وفشل القلب وارتفاع ضغط الدم، السبب الرئيسي الأول للوفاة في الولايات المتحدة والثالث على مستوى العالم. CETP هو بروتين سكري يفرز بشكل رئيسي من الكبد ويوجد في البلازما. تركيز CETP في البلازما الطبيعي هو 1-4 ميكروغرام / مل، بينما زادت النسبة بين 70-80٪ في مرضى اضطراب دهنيات الدم. هناك حاجة متزايدة لمثبطات CETP الجديدة التي تشجعنا على إجراء هذا البحث. في هذا العمل، تم إجراء التوليف والدراسة في المختبر لأربعة 4-بروموفينيثيل بنزاميدات جديدة 9a-d. أظهرت دراسة في المختبر أن المركبات المستهدفة 9a-d تظهر نشاطًا مقبولًا ضد CETP، حيث يكون للمركب 9a تثبيط بنسبة 40.7 عند تركيز 10 ميكرومولار. وجد أن وجود مجموعة أوكسي في كل من 9a و9cيعزز نشاطها الذي يمكن أن يعزى إلى تكوين رابطة هيدروجينية مع بقايا الأحماض الأمينية في موقع ربط CETP.

الكلمات الدالة: بنزاميدات، 4-بروموفينيثيل، CETP، ارتفاع كوليسترول الدم، مثبطات.

* ***المؤلف المراسل: ريما أبو خلف***

reema.abukhalaf@zuj.edu.jo

تاريخ الإستلام 2022/12/28 تاريخ قبول النشر 2023/3/13.

Jordan Journal of Pharmaceutical Sciences, Volume 16, No. 2, Supplement 1, 2023

Toxic Metals Transfer from Heating Coils to e-liquids: Safety Assessment of Popular e-cigarettes in Jordan

Ala A. Alhusban[1*], Samah A. Ata[1], Lama A. Hamadneh[1], Ola A. Tarawneh[1], Haneen Abuzaid[1], Sokiyna Albustanji[1], Mohammad K. Awad[1]

[1] Department of Pharmacy, Faculty of Pharmacy, Al-Zaytoonah University of Jordan, Jordan.

ABSTRACT

The rate of smokers in Jordan has been among the highest globally. Electronic Nicotine Delivery systems (ENDs) are considered helpful in smoking cessation but also have the potential for metals exposure resulting from their transfer from the metallic coils to the e-liquid upon use. Metal exposure is associated with severe health outcomes. We sought to assess the levels of toxic metals (Cr, Cd, Pb, Ni and Al) transfer from two of the most popular coils used in ENDs among users in Jordan. The validated inductively coupled plasma-optical emission spectroscopy (ICP-OES) with limit of detections (LODs) of 0.10, 0.90, 0.15, 0.13 and 1.00 $mg.kg^{-1}$ was employed to measure the levels of toxic metals in the e-liquid samples. Following a repetitive usage of coils in both tank and pod systems for five continuous days, the cumulative amount of toxic metals; Ni, Cr, Al and Pb levels were significantly increased in all e-liquids used ($p < 0.0001$) compared to the fresh unheated samples. The obtained results showed a time-dependent increase of metals transfer from coils to e-liquids, thus highlighting the need for additional studies to re-assess the safety claims of using ENDs for smoking cessation.

Keywords: Metals, ENDs, e-liquid, ICP-OES, safety assessment.

1. INTRODUCTION

Smoking rates in Jordan are documented to be one of the highest rates globally. Reports stated that 66% of males above 18 years consume tobacco products while 16.5% are using Electronic Nicotine Delivery systems (ENDs) in 2019[1] and raised to 18% in 2021[2]. This rate is expected to reveal further increase since ENDs are considered a beneficial tool in smoking cessation by 69.1% of the adult population aged ≥ 18 years who participated in a national survey [3]. Therefore, tobacco smokers in Jordan are changing their smoking habit to consumption of ENDs at the expense of regular tobacco smoking. It is estimated that one out of ten regular tobacco smokers has either attempted or switched to ENDs [4]. The situation in Jordan is not different from other countries worldwide since ENDs use is increasing worldwide to approximately 68 million users in 2020 [5]. Claims about the safety of ENDs compared to tobacco smoking did not eliminate the potentially harmful effects of ENDs exposure, especially after long-term use [6].

ENDs are electronic devices that produce aerosols by resistance heating of an electronic-liquid (e-liquid) solution via a metallic coil[7]. Frequent metallic coils used include Kanthal (an iron/chromium/aluminium alloy) and Nichrome (a chromium and nickel alloy) [8]. Through the vaporization of e-liquids, toxic metals may be released by the metallic coils and inhaled by the user [9]. ENDs have the potential for metals exposure resulting from their transfer from the metallic coils to the e-liquid[10]. Unprotected exposure to elevated concentrations of heavy

[*]***Corresponding author: Ala A. Alhusban***
ala.alhusban@zuj.edu.jo
Received: 28/12/2022 Accepted: 29/3/2023.
DOI: https://doi.org/10.35516/jjps.v16i2.1466

metals is associated with severe health consequences. For instance, exposure to the neurotoxic lead (Pb) may increase the risk of neurological disorders, such as Parkinson's disease and Alzheimer's disease [11, 12]. Other diseases might also arise upon exposure to metals including nephrotoxicity for Pb and cadmium (Cd) [13]; neurotoxicity for aluminium (Al) [14] and lung cancer for chromium (Cr) and nickel (Ni) [15].

In Jordan, tanks and pods are two of the most used delivery devices for e-liquids that are supplied to users from different sources (brands). They are connected to refillable ENDs provided with different internal designs, components, and materials [16]. The e-liquid mostly contains nicotine, water, propylene glycol, glycerol, flavours, and pH modifiers [17], and mostly are free from toxic metals. However, metals can transfer to e-liquid from the housing and vapor path that is usually made out of stainless steel or the heating element that could be manufactured from kanthal or nichrome, in which a cotton wick is located inside [18].

The transfer of toxic metals to ENDs e-liquid has been documented in the literature [19, 20]. Furthermore, previous studies demonstrated the presence of several metals including Cr, Ni, Pb, Zn, and Mn in ENDs aerosol that originated from ENDs pod system. The designated metals were found in varying levels [10, 21]. Several agencies have set exposure limits for inhalation of such toxic metals including the Agency for Toxic Substance and Disease Registry (ATSDR), the National Institute for Occupational Safety and Health (NIOSH), the Occupational Safety and Health Administration, and the American Conference of Governmental Industrial Hygienists (ACGIH) [22]. However, no permissible limits for toxic metals have been set by various global and local authorities. Additionally, a continuous exposure to e-liquids with more precise and accurate quantification of metal transfer from ENDs coils to e-liquid is still needed.

Studying the toxicity of substances is very important [23-27]. In our previous studies, we investigated the levels of toxic metals in various pharmaceutical preparations from a local market in Jordan, which is claimed to be a relatively safe option for users [28, 29]. Here we report the presence of high levels of toxic metals in e-liquids upon heating ENDs, resulting from the continuous transfer of metals from internal coils used in Jordan market into the e-liquids. Providing an accurate and precise method for time-dependent analysis, the levels of potentially toxic metals were detected using an inductively coupled plasma optical emission spectrometer ICP-OES due to its high accuracy.

2. MATERIALS AND METHODS

2.1. Chemicals and Reagents

A solution consisted of 10% Nitric acid (HNO_3) (69%, w/v% trace metal concentration, Fluka Analytical, France) was used for sample digestion. Standard solutions of Pb, Al, Ni, Cd and Cr, each of 1000 ppm, (Merck, Germany) were used for the preparation of working standard solutions within the linear range for each element and were prepared at 6 concentration levels using the appropriate dilutions of stock solutions for the construction of calibration curves. All plastic and glassware used in experiments were firstly cleaned with proper detergent, washed thoroughly with distilled water, and deionized water, soaked overnight in 10% (v/v) HNO_3, and finally rinsed several times with deionized water immediately before use to remove any traces of contamination by metals. Nicotine was obtained from (Alfa Aesar, UK).

2.2. Sample Collection

ENDs products were obtained from a local market in Amman, Jordan. The products investigated were tank systems (voopoo drag s pro) and pod systems (wenax h1). E-liquid products were purchased from local stores (**Table 1)**

Table 1. The description of brands of e-liquid used for analysis.

Brand of E-liquid	Date of Purchase	Date of Expiration	Labelled Level of Nicotine (mg/mL)	Flavour
e-Liquid 1	10- June-21	Oct-23	25	Apple
e-Liquid 2	10- June -21	May-23	25	Watermelon
e-Liquid 3	10- June -21	Jul-23	25	Mango

E-Liquids were sampled directly from tanks and pods in 24 h sampling periods for consecutive 5 days. In which the ENDs products were filled with e-liquids and were turned on for puffing every 15 minutes for 5 h each day. After 24 h, the tank/pod systems were evacuated and the same procedure was repeated the next day for successive five days.

2.3. Sample preparation

Matrix digestion is vital in all analytical processes for determining trace elements. In this work, 0.5 mL e-liquids were accurately withdrawn from the tank/pod systems into 2 mL PTFE sample cups (PerkinElmer, Waltham, MA, USA) followed by the addition of a freshly prepared 1 mL 10% HNO_3 (w/v) and left for 15 min then shaking for 5 min. to allow matrix digestion. Then 0.5 mL of deionised water was added to the resultant mixture. Then, samples were filtered using a 0.45 µm syringe filter and the filtrate was completed to 5 mL with deionised water. The procedure was repeated three times for the same samples and the control was prepared from the acid mixture as a referee.

2.4. Instrumentation

The determination of metal levels was determined using Optima 2000 DV inductively coupled plasma optical emission spectrometer (ICP-OES, PerkinElmer Corporation, USA). The instrument settings were prepared to work to its optimum operating conditions: the incident power was 1300 W, the Argon gas flow rate of plasma was 15 $L.min^{-1}$, the auxiliary 0.5 $L.min^{-1}$ and the nebulizer was 0.8 $L.min^{-1}$. The flow rate of the sample was set at 1.5 $L.min^{-1}$. The temperature heater temperature was adjusted to 30.5 °C. To detect LOD for each metal, serial dilutions of standards were prepared for each designated metal. The repeatability of the method was calculated by the analysis of one standard solution (0.1 $mg.L^{-1}$) of each metal five times. Furthermore, five standard solutions of each metal were analyzed in-between runs with the RSD values in a range from 1.6 to 2.2%.

The accuracy of the analytical wet digestion procedure should be determined especially after optimizing the conditions. This was carried out through analysis of a reference e-liquid. The reference in concern was prepared in the laboratory comprising propylene glycol, glycerol and pure nicotine in addition to known concentrations of each analyzed metal using the developed method. The results obtained are presented in **Table 2**.

Table 2. Method accuracy assessment using the prepared reference e-liquid

Toxic metal	standardized value $mg.kg^{-1}$	Determined value $mg.kg^{-1}$	Recovery (%)
Cr	4	3.82 ± 0.43	95%
Cd	4	3.75 ± 0.89	94%
Pb	4	3.89 ± 0.39	97%
Ni	4	3.91 ± 0.66	98%
Al	4	3.88 ± 0.80	97%

2.5. Statistical analysis

Results were evaluated using Graph Pad Prism v9.5.1. Representative Figures are shown as mean ± standard deviation (SD). Two-way ANOVA statistical analyses and Dunnett's multiple comparisons test was used to assess significant differences and defined as * ($P < 0.05$), ** ($P < 0.01$), *** ($P < 0.001$), **** ($P < 0.0001$). All experiments were repeated 3 times.

3. RESULTS AND DISCUSSION

In order to accurately report the levels of potentially toxic metals in e-liquids, ICP-OES was used following the optimizing and validating method of analysis. The detected levels of tested toxic metals including Ni, Cr, Cd, Al, and Pb are shown in **Table 3** and **Table 4** along with their representative **Figure 1a** and **Figure 1b** for both tank and pod systems, respectively.

Table 3. Levels of metals in e-liquids in tank systems (n = 3).

#	Products no. and use	Ni mg/kg	Cr mg/kg	Cd mg/kg	Al mg/kg	Pb mg/kg
1.	e-Liquid 1 after 5 days use	11.92 ± 2.6	15.8 ± 4.8	<DL	1.554 ± 0.85	0.951 ± 0.62
2.	e-Liquid 1 after 4 days use	17.72 ± 3.9	12.76 ± 2.4	<DL	1.42 ± 0.38	0.57 ± 0.36
3.	e-Liquid 1 after 3 days use	0.62 ± 0.22	3.38 ± 0.90	<DL	1.56 ± 0.67	0.638 ± 0.53
4.	e-Liquid 1 after 2 days use	0.568 ± 0.17	10.9 ± 2.10	<DL	2.712 ± 0.82	1.082 ± 0.56
5.	e-Liquid 1 after 1 days use	0.052 ± 0.02	0.762 ± 0.36	<DL	1.566 ± 0.79	0.42 ± 0.17
6.	e-Liquid 1 after 0 days use	<DL	<DL	<DL	<DL	<DL
7.	e-Liquid 2 after 5 days use	3.572 ± 1.16	4.8 ± 0.54	<DL	1.56 ± 0.53	0.852 ± 0.24
8.	e-Liquid 2 after 4 days use	0.552 ± 0.11	2.392 ± 0.77	<DL	2.07 ± 0.48	0.032 ± 0.02
9.	e-Liquid 2 after 3 days use	0.54 ± 0.26	2.234 ± 0.93	0.09 ± 0.03	1.984 ± 0.84	0.398 ± 0.18
10	e-Liquid 2 after 2 days use	0.346 ± 0.12	3.952 ± 1.02	<DL	2.76 ± 0.92	1.67 ± 0.67
11	e-Liquid 2 after 1 days use	0.044 0.02	1.954 ± 0.85	<DL	1.204 ± 0.46	0.166 ±0.06
12	e-Liquid 2 after 0 days use	<DL	<DL	<DL	<DL	<DL
13	e-Liquid 3 after 5 days use	1.577 ± 0.77	3.395 ± 1.56	0.02 ± 0.1	1.421 ± 0.60	0.611 ± 0.26
14	e-Liquid 3 after 4 days use	0.733 ± 0.32	1.873 ± 0.95	<DL	1.294 ± 0.49	0.547 ± 0.32
15	e-Liquid 3 after 3 days use	0.441 ± 0.25	2.012 ± 1.04	<DL	1.318 ± 0.72	0.423 ± 0.18
16	e-Liquid 3 after 2 days use	0.036 ± 0.02	1.816 ± 1.01	<DL	1.597 ± 0.61	0.595 ± 0.39
17	e-Liquid 3 after 1 days use	0.029 ± 0.01	0.595 ± 0.74	<DL	0.536 ± 0.48	0.317 ± 0.17
18	e-Liquid 3 after 0 days use	<DL	<DL	<DL	<DL	<DL

DL (Detection limit)

Table 4. Levels of metals in e-liquids in pod systems (n = 3).

#	Products no. and use	Ni mg/kg	Cr mg/kg	Cd mg/kg	Al mg/kg	Pb mg/kg
1.	e-Liquid 1 after 5 days use	1.804 ± 0.99	1.714 ± 0.74	0.004	0.826 ± 0.62	0.83 ± 0.46
2.	e-Liquid 1 after 4 days use	1.609 ± 0.56	1.183 ± 0.30	<DL	0.621 0.36	0.318 0.25
3.	e-Liquid 1 after 3 days use	0.372 ± 0.43	0.338 ± 0.06	<DL	0.702 ± 0.43	0.231 ± 0.09
4.	e-Liquid 1 after 2 days use	0.231 ± 0.39	0.942 ±0.36	<DL	0.775 ± 0.87	0.609 ± 0.16
5.	e-Liquid 1 after 1 days use	0.012 ± 0.01	0.166 ±0.09	<DL	0.365 ± 0.33	0.026 ± 0.01
6.	e-Liquid 1 after 0 days use	<DL	<DL	<DL	<DL	<DL
7.	e-Liquid 2 after 5 days use	2.062 ± 0.88	2.404 ± 0.69	<DL	1.512 ± 0.62	1.71 ± 0.43
8.	e-Liquid 2 after 4 days use	0.552 ± 0.23	2.392 ± 0.85	<DL	2.07 ±0.71	0.032 ± 0.01
9.	e-Liquid 2 after 3 days use	0.54 ± 0.19	2.234 ± 0.52	0.09	1.984 ±0.37	0.398 ± 0.07
10	e-Liquid 2 after 2 days use	0.346 ± 0.15	3.952 ±1.07	<DL	2.76 ± 0.48	1.67 ± 0.49
11	e-Liquid 2 after 1 days use	0.044	1.954 ±0.45	<DL	1.204 ± 0.77	0.166 ± 0.02
12	e-Liquid 2 after 0 days use	<DL	<DL	<DL	<DL	<DL
13	e-Liquid 3 after 5 days use	1.66 ± 0.53	0.474 ± 0.03	<DL	0.5 ± 0.14	1.032 ± 0.61
14	e-Liquid 3 after 4 days use	0.599 ± 0.17	1.177 ± 0.67	<DL	1.046 ± 0.41	0.188 ± 0.04
15	e-Liquid 3 after 3 days use	0.287 ± 0.07	0.919 ± 0.31	<DL	0.814 ± 0.16	0.286 ± 0.01
16	e-Liquid 3 after 2 days use	0.03	1.021 ± 0.81	<DL	0.739 ±0.20	0.402 ± 0.07
17	e-Liquid 3 after 1 days use	0.018	0.405 ± 0.10	<DL	0.202 ±0.04	0.293 ± 0.11
18	e-Liquid 3 after 0 days use	<DL	<DL	<DL	<DL	<DL

During the experimental time of five days, higher but various levels of toxic metals were found in all tested e-liquids (**Figure 1a**, **Figure 1b**), indicating that transfer of toxic metals out of both tank and pod systems started from the first day of using coils with heating. For example, the levels of Cr and Al were significantly higher in e-liquid 2 after the first day of using the coil of both tank and pod systems ($p < 0.0001$ and $p < 0.05$ respectively), while with liquid 1 and 3, such metals started to significantly increase after the second day of usage. This agrees with the finding of Olmedo *et al.* who reported that metal concentrations in the e-liquid increased markedly after it was added to the ENDs device when brought into contact with the heating coil in the generated aerosol and in the liquid that remained in the tank [10].

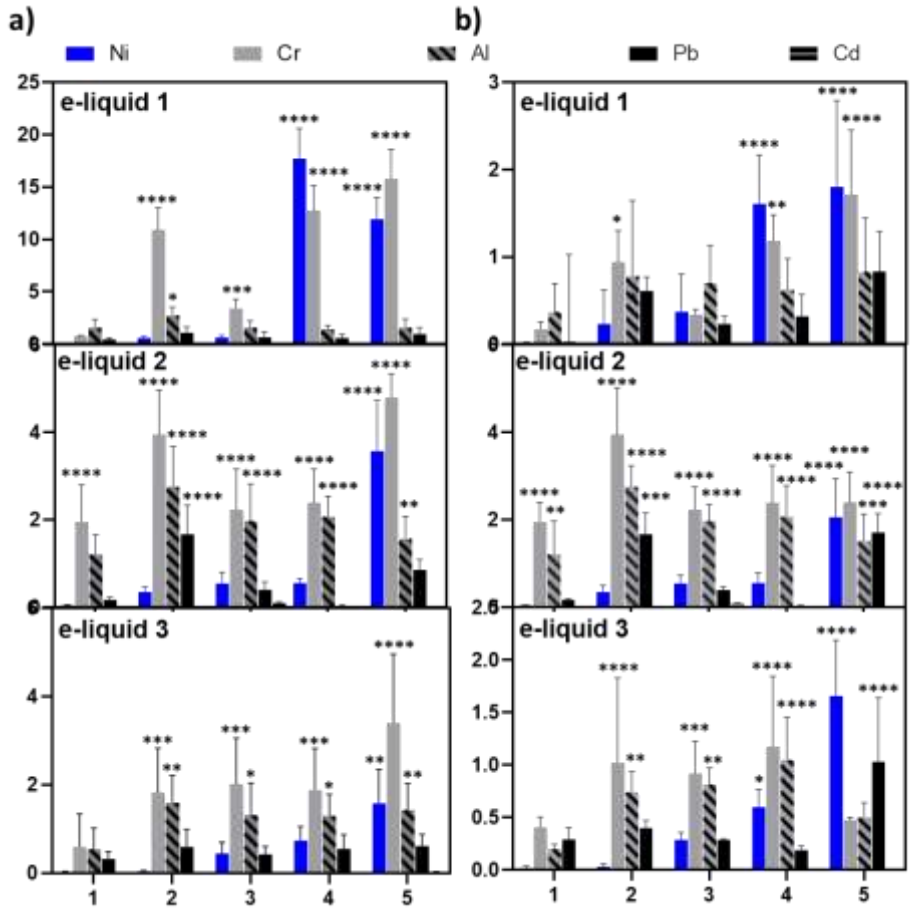

Figure 1: Toxic metals transfer study from tank
(a, and pod **(b** system ENDs' coil into three tested e-liquids for five continuous days. The levels of Ni, Cr, Cd, Al and Pb are reported in mg/kg. Data are reported as mean ± SD (n=3 internal repeats). Significant differences from pre-heated e-liquids (day 0) are expressed as *P < 0.05, **P < 0.01, ***P < 0.001 and ****P < 0.0001.

However, the results also indicate the unpredictable and uncontrollable health problems that users might develop upon using different brands of ENDs. This comes from the point that metals are transferred from the ENDs' coils to the e-liquid and from the e-liquid to the aerosol which is eventually inhaled by the user. Indeed, ENDs are considered a significant source of generating toxic metals that might lead to end-user exposure [30]. Chronic exposure to such metals as continuous usage of ENDs provide the user's body with a dangerous amount of toxic metals that ultimately adversely affect various body system, especially the cardiovascular system [31].

The transfer of most detected metals was not following a specific pattern. This reveals that other factors play an important role in the transfer process of metals from the coil to e-liquids, some might be related to the composite of the used system.

One interesting finding was related to the transfer levels of Ni into the tested e-liquids, as it follows an increasing pattern with time. For instance, the levels of Ni of the three different e-liquids used on day 5 of the experiment were ~55 to 230-fold higher than on day 1 of

the experiment as determined in the used tank system, and ~47 to 150-fold higher in the used pod system. This indicates that Ni is more susceptible to transfer with ageing and repetitive usage of the coil. This exhibits more risk for users who do not change the coil continuously. Indeed, exposure to Ni has been found to be carcinogenic and might predispose bronchitis [20].

The cumulative levels of each toxic metal following five days of usage were compared between tank and pod systems for the same e-liquid brand (**Figure 2**).

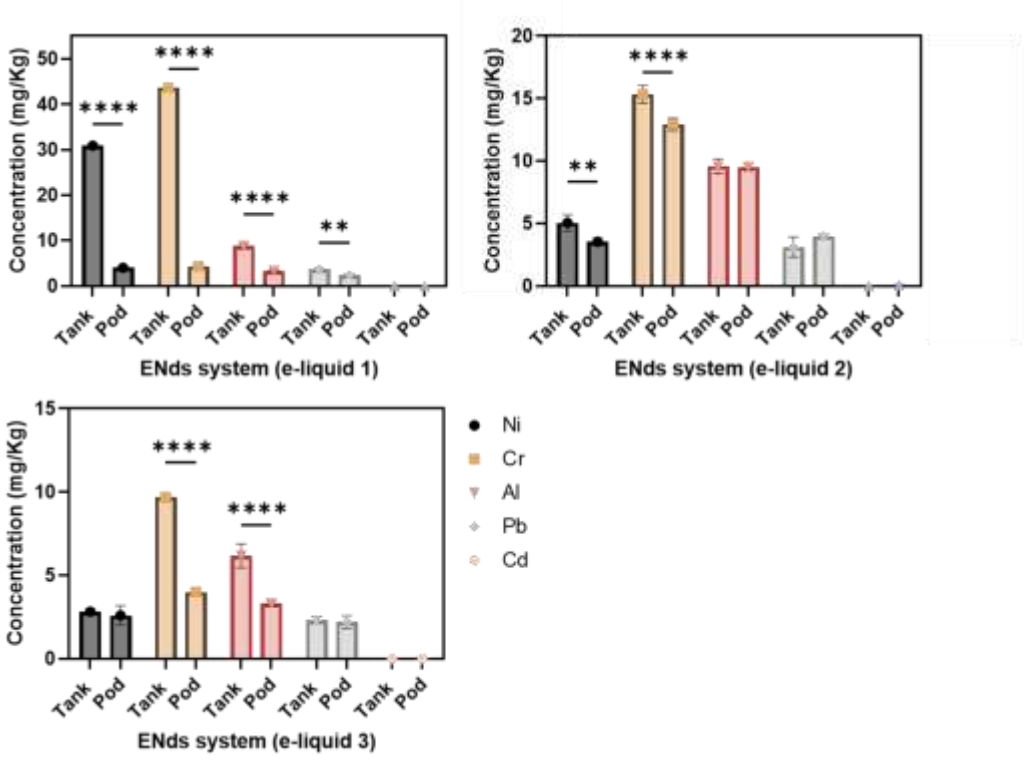

Figure 2: Comparative cumulative concentrations of Ni, Cr, Cd, Al, and Pb for continuous five days in all tested e-liquids between both tank and pod systems ENDs.

Statistical analyses revealed significant higher accumulation of Cr in all tested e-liquids and of Ni and Al of tank compared to pod. Values are reported as mean ± SD (n = 3). ** P < 0.01 and *** P < 0.001.

Interestingly significantly higher levels of Ni and Cr metals were found in e-liquid 1 with tank usage compared to pod ($p < 0.0001$) and in e-liquid 3 ($p < 0.05$) for Cr. This might be attributed to that coils used in tank systems contains more metals in comparison to pod systems [32]. Besides, this highlights that the type of e-liquid used can also contribute to the amount and type of metals leaching from the same coil.

Such results might offer a relatively safer option for users using pod systems ENDs. However inclusive studies comprising a higher number of ENDs and liquid brands are needed before concluding this.

Taking into consideration that ENDs are used in a continuous rather than occasional manner, and except for Cd, the cumulative levels of all detected toxic metals; Ni, Cr, Al and Pb levels after five continuous days of usage were significantly higher in all e-liquids used ($p< 0.0001$) for both systems compared to the fresh unheated samples. Our results support findings obtained by Gray *et al.* who confirm that detectable metals in e-liquids are resulting

from contact between the e-liquid and ENDs device components [19], and Hess *et al.* who found that when ENDs are used, direct contact of the e-liquid comes to the heating coil, resulting in leaching of the coil metals into the e-liquid at higher temperatures [20]. Our findings also emphasise the urge for additional safety studies of using ENDs with chronic users as a safe method for smoking cessation.

4. CONCLUSION

An accurate and precise analytical method based on ICP-OES for the analysis of 5 toxic metals in ENDs e-liquids was developed and validated. Analyses of ENDS e-liquids before any contact with the metallic ENDs coils revealed no metal concentrations and were below LODs. While e-liquids in contact with the metallic coils showed significantly increased metals concentrations including Ni, Cr, Al and Pb ($p < 0.0001$). The increase in metal concentrations was correlated with the increased time of e-liquid contact with the metallic coils in both tank and pod systems. The obtained results confirm that detectable metals in e-liquids are resulting from contact between the e-liquid and heated device metallic coil. The presence of the investigated metals in e-liquid might cause a potential adverse effect to ENDs users and more regulations should be put to ensure the quality of ENDs products to ensure safety to users.

Acknowledgments

This work received financial support from Al-Zaytoonah University of Jordan [grants no. 2022-2023/17/49].

Competing interests

The authors declare no competing interests.

REFERENCES

(1) World Health Organization, W. Empowering the Government of Jordan to strengthen tobacco control using a "One UN approach", WHO. https://open.who.int/2018-19/country/JOR (July 30, 2022),

(2) Al-Balas, H. I.; Al-Balas, M.; Al-Balas, H.et al. Electronic Cigarettes Prevalence and Awareness among Jordanian Individuals. Journal of Community Health 2021, 46, (3), 587-590.

(3) Abdel-Qader, D. H.; Al Meslamani, A. Z. Knowledge and beliefs of Jordanian community toward e-cigarettes: a national survey. Journal of community health 2021, 46, (3), 577-586.

(4) Alhusban, A. A.; Ata, S. A. Simple HPLC method for rapid quantification of nicotine content in e-cigarettes liquids. Acta Chromatographica 2021, 33, (3), 302-307.

(5) Jerzyński, T.; Stimson, G. V.; Shapiro, H.et al.Estimation of the global number of e-cigarette users in 2020. Harm reduction journal 2021, 18, (1), 1-10.

(6) Alasmari, F.; Alexander, L. E. C.; Hammad, A. M.et al. E-cigarette aerosols containing nicotine modulate nicotinic acetylcholine receptors and astroglial glutamate transporters in mesocorticolimbic brain regions of chronically exposed mice. Chemico-Biological Interactions 2021, 333, 109308.

(7) Snoderly, H. T.; Nurkiewicz, T. R.; Bowdridge, E. C.; et al.E-cigarette use: device market, study design, and emerging evidence of biological consequences. International Journal of Molecular Sciences 2021, 22, (22), 12452.

(8) Fowles, J.; Barreau, T.; Wu, N. Cancer and non-cancer risk concerns from metals in electronic cigarette liquids and aerosols. International Journal of Environmental Research and Public Health 2020, 17, (6), 2146.

(9) Szumilas, P.; Wilk, A.; Szumilas, K.et al. The Effects of E-Cigarette Aerosol on Oral Cavity Cells and Tissues: A Narrative Review. Toxics 2022, 10, (2), 74.

(10) Olmedo, P.; Goessler, W.; Tanda, S.et al. Metal concentrations in e-cigarette liquid and aerosol samples: the contribution of metallic coils. Environmental Health Perspectives 2018, 126, (2), 027010.

(11) Wang, T.; Zhang, J.; Xu, Y., Epigenetic basis of lead-induced neurological disorders. International Journal of Environmental Research and Public Health 2020, 17, (13), 4878.

(12) Santa Maria, M. P.; Hill, B. D.; Kline, J., Lead (Pb) neurotoxicology and cognition. Applied Neuropsychology: Child 2019, 8, (3), 272-293.

(13) Satarug, S.; Gobe, G. C.; Ujjin, P.et al. A comparison of the nephrotoxicity of low doses of cadmium and lead. Toxics 2020, 8, (1), 18.

(14) Tietz, T.; Lenzner, A.; Kolbaum, A. E.; Zellmer, S.et al. Aggregated aluminium exposure: risk assessment for the general population. Archives of Toxicology 2019, 93, (12), 3503-3521.

(15) Genchi, G.; Carocci, A.; Lauria, G.et al. Nickel: Human health and environmental toxicology. International journal of environmental research and public health 2020, 17, (3), 679.

(16) Ozga, J. E.; Felicione, N. J.; Douglas, A.et al. Electronic cigarette terminology: Where does one generation end and the next begin? Nicotine and Tobacco Research 2022, 24, (3), 421-424.

(17) Krüsemann, E. J.; Havermans, A.; Pennings, J. L. et al. Comprehensive overview of common e-liquid ingredients and how they can be used to predict an e-liquid's flavour category. Tobacco control 2021, 30, (2), 185-191.

(18) Jităreanu, A.; Cara, I. G.; Sava, A.et al. The impact of the storage conditions and type of clearomizers on the increase of heavy metal levels in electronic cigarette liquids retailed in romania. Toxics 2022, 10, (3), 126.

(19) Gray, N.; Halstead, M.; Gonzalez-Jimenez, N.et al. Analysis of toxic metals in liquid from electronic cigarettes. International journal of environmental research and public health 2019, 16, (22), 4450.

(20) Hess, C. A.; Olmedo, P.; Navas-Acien, A. et al. E-cigarettes as a source of toxic and potentially carcinogenic metals. Environmental research 2017, 152, 221-225.

(21) Pappas, R. S.; Gray, N.; Halstead, M.et al. Toxic metal-containing particles in aerosols from pod-type electronic cigarettes. Journal of analytical toxicology 2021, 45, (4), 337-347.

(22) Mishra, V. K.; Kim, K.-H.; Samaddar, P.et al. Review on metallic components released due to the use of electronic cigarettes. Environmental Engineering Research 2017, 22, (2), 131-140.

(23) Al-Awar, M. S. A. Acute and Sub-Acute Oral Toxicity Assessment of Mixed Extract of Trigonella Foenum-Graecum Seeds and Withania Somnifera Root in Rats. Jordan Journal of Pharmaceutical Sciences 2022, 15, (4), 493-506.

(24) Adel, I.; Jarrar, Q.; Ayoub, R.et al. The Toxicity and Therapeutic Efficacy of Mefenamic Acid and its Hydroxyethyl Ester in Mice: In Vivo Comparative Study: A promising Drug Derivative. Jordan Journal of Pharmaceutical Sciences 2022, 15, (4), 507-522.

(25) Alhusban, A. A.; Breadmore, M. C.; Gueven, N.et al. Time-resolved pharmacological studies using automated, on-line monitoring of five parallel suspension cultures. Scientific Reports 2017, 7, (1).

(26) Alhusban, A. A.; Hammad, A. M.; Alzaghari, L. F.et al. Rapid and sensitive HPLC–MS/MS method for the quantification of dopamine, GABA, serotonin, glutamine and glutamate in rat brain regions after exposure to tobacco cigarettes. Biomed. Chromatogr. 2023, 37, (1).

(27) Hammad, A. M.; Alhusban, A. A.; Alzaghari, L. F.et al. Effect of Cigarette Smoke Exposure and Aspirin Treatment on Neurotransmitters’ Tissue Content in Rats’ Hippocampus and Amygdala. Metabolites 2023, 13, (4), 515.

(28) Massadeh, A. M.; Alhusban, A. A., A developing method for preconcentration and determination of Pb, Cd, Al and As in different herbal pharmaceutical dosage forms using chelex-100. Chemical Papers 2021, 75, (7), 3563-3573.

(29) Alhusban, A. A.; Ata, S. A.; Shraim, S. A., The safety assessment of toxic metals in commonly used pharmaceutical herbal products and traditional herbs for infants in Jordanian market. Biological trace element research 2019, 187, (1), 307-315.

(30) Soulet, S.; Sussman, R. A. A Critical Review of Recent Literature on Metal Contents in E-Cigarette Aerosol. Toxics 2022, 10, (9), 510.

(31) Navas-Acien, A.; Martinez-Morata, I.; Hilpert, M.et al. Early cardiovascular risk in E-cigarette users: the potential role of metals. Current environmental health reports 2020, 7, (4), 353-361.

(32) Zhao, D.; Aravindakshan, A.; Hilpert, M.et al. Metal/metalloid levels in electronic cigarette liquids, aerosols, and human biosamples: a systematic review. Environmental health perspectives 2020, 128, (3), 036001.

انتقال المعادن السامة من ملفات التسخين إلى السائل الإلكتروني: تقييم الأمان للسجائر الإلكترونية الشائعة الاستعمال في الأردن

علاء الحسبان[1]*، سماح عطا[1]، لمى حمادنة[1]، علا الطراونة[1]، حنين ابوزيد[1]، سكينة البستنجي[1]، محمد عواد[1]

[1] قسم الصيدلة، كلية الصيدلة، جامعة الزيتونة الاردنية، الأردن.

ملخص

معدل المدخنين في الأردن من بين أعلى المعدلات على مستوى العالم. تعتبر أجهزة توصيل النيكوتين الإلكترونية مفيدة في الإقلاع عن التدخين وفقًا لمسح وطني حديث. هذه الأجهزة الإلكترونية لديها احتمالية التعرض للمعادن السامة الناتج عن نقلها من الملفات المعدنية إلى السائل الإلكتروني اثناء عملية التسخين. يرتبط التعرض للمعادن بنتائج صحية خطيرة للمستعملين لهذه الأنظمة. الهدف من هذه الدراسة هو تقييم انتقال المعادن السامة وتشمل الالمنيوم، النيكل، الرصاص، الكروم، والكادميوم من ملفات اثنين من أنظمة توصيل النيكوتين الإلكترونية الأكثر استخدامًا في الأردن بين المستخدمين كل 24 ساعة لمدة 5 أيام متواصلة من الأستعمال. تم قياس تراكيز المعادن السامة في عينات السائل الإلكتروني باستخدام جهاز مطياف الانبعاث البصري البلازمي المقترن حثيًا، مع حدود دنيا من التراكيزبعد تطوير طريقة ذات درجة تحقق عالية ومثبتة. وجدت معظم المعادن السامة في اغلب العينات المحللة، بينما تم الكشف عن الكادميوم في عينتين فقط تم تحليلهما. أظهرت النتائج التي تم الحصول عليها على وجود علاقة بين زيادات نقل المعادن من الملفات إلى السوائل الإلكترونية مع طول فترة استخدام أنظمة توصيل النيكوتين الإلكترونية.

الكلمات الدالة: المعادن، ENDs، السائل الإلكتروني، ICP-OES، تقييم السلامة.

* ***المؤلف المراسل: علاء الحسبان***

ala.alhusban@zuj.edu.jo

تاريخ الإستلام 2022/12/28 تاريخ قبول النشر 2023/3/29.

Jordan Journal of Pharmaceutical Sciences, Volume 16, No. 2, Supplement 1, 2023

Metal Chelators as Anticancer Approach: Part I; Novel 7-Anisidine Derivatives with Multidentate at 7-8 Carbons of Fluoroquinolone Scaffold as Potential Chelator Anticancer and Antilipolytic Candidates

Yusuf Al-Hiari[1,2]*, Shereen Arabiyat[3], Violet Kasabri[1], Imad Hamdan[1], Ihab Almasri[4], Mohammad Y. Mohammad[5], Dalya Al-Saad[6]

[1] School of Pharmacy, The University of Jordan, Amman Jordan.
[2] Faculty of Pharmacy, Al-Zaytooneh University of Jordan, Jordan.
[3] Al-Balqa Applied University, Jordan.
[4] Department of Pharmaceutical Chemistry and Pharmacognosy, Faculty of Pharmacy, AL Azhar University-Gaza, Palestine.
[5] Faculty of Pharmacy, Aqaba University of Technology, Jordan.
[6] Department of Basic Sciences and Humanities, Faculty of Science, The American University of Madaba, Jordan.

ABSTRACT

Background: Cancer is one of the greatest troubling maladies currently. It is believed that it is the second reason for death following cardiovascular maladies. Owing to the multiplicity of its types, stages and genetic basis, there is no existing drug to cure all types of cancer. Resistance to present drugs and severe adverse effects are other challenges in the struggle against cancer. In such pursuit, fluoroquinolones (FQs) have the potential as antiproliferative compounds due to safety, low cost, and absence of resistance.

Aims: In this study, we aim to synthesize biologically active compounds that have dual anticancer and anti-lipase potential. Sixteen compounds were prepared, fully characterized, and studied through identification of IC_{50} values against the highly susceptible cancer cell lines.

Methods: In this work we are concerned with synthesizing biologically active compounds that belong to fluoroquinolones (FQs) with dual anti-colorectal cancer and anti-lipase activity, owing to association between cancer and obesity, conduct titration and docking experiments to validate our hypothesis.

Results: *In vitro* findings indicated that these compounds demonstrated promising anticancer activity against tested cell lines in micromolar range with a potency comparable to cisplatin. Compound **11** exhibited approximately doubled potency compared to cisplatin against SW620 colorectal cancer cell line with IC50 3.2 μM which proposes FQs as potent antiproliferative agents. The synthesized Fluoroquinolone (FQ) compounds were further screened for their *in vitro* anti-lipase potential. The findings demonstrated that all the screened compounds have demonstrated remarkable anti-lipase activity, as compared to control molecule orlistat. Compound **9** exhibited comparable activity to orlistat against pancreatic lipase with IC_{50} 0.4 μM which proposes FQs as potent pancreatic lipase inhibitors.

Conclusions: The anticancer potential of these derivatives is referred to their ability to inhibit Topo II which indicates that chelation is the mechanism of inhibition of Topo II emphasized with titration and docking experiments.

Keywords: Metal chelators, Multidentate, Fluoroquinolones, Chelator anticancer.

[*]***Corresponding author: Yusuf Al-Hiari***
hiary@ju.edu.jo
Received: 11/1/2023 Accepted: 29/3/2023.
DOI: https://doi.org/10.35516/jjps.v16i2.1467

INTRODUCTION

Fluoroquinolones have been recognized for more than 40 years as one of the highest active antibacterial agents [1]. Fluoroquinolones elucidated to have other biological activities as antidiabetic[2], antimycobacterial[3], antiviral[4], anticancer[5], as well as pancreatic lipase inhibitors[6]. The ability of quinolones exemplified by Vosaroxin to target type II topoisomerase enzymes suggests them as anticancer agents. Their potential to chelate metal ions represents another way of achieving their pharmacological activities[7]. Ciprofloxacin use for the experimental adjunctive therapy of lung cancer is reported[8]. Moreover, ciprofloxacin derivatives have shown potent *in vitro* antiproliferative activity[9]. Antitumor activity for a series of N1-decyl and C7 secondary amine derivatives of fluoroquinolones was investigated. Most of the compounds were found significantly potent (IC_{50} <0.01-8.8µM). Their antiproliferative activity has been tested against four cancer cell lines: human breast carcinoma (MDA-MD-231), human pancreatic carcinoma (MIA PaCa), human cervical carcinoma (HeLa) and human neuroblastoma cells (IMR32)[10]. Derivatives of 6-fluoro-4-oxopyrido[2,3-*a*] carbazole-3-carboxylic acids were evaluated for their *in vitro* antiproliferative potential against A549 non-small cell lung cancer cells and MCF-7 breast tumor. Some compounds were very potent compared to positive control ellipticine coupled with an absence of cytotoxicity toward normal human-derm fibroblasts (HuDe)[11]. Vosaroxin (Voreloxin) is an anti-cancer quinolone that inhibits topoisomerase-II leading to cell cycle arrest and apoptosis[12]. It has shown efficacy in a range of solid organ and hematopoietic tumors *in vitro*[13]. Referring to the potential biological interest in these heterocyclic compounds[14] **,**numerous FQs derivatives have been synthesized and evaluated for anticancer potential. Many compounds were in the form of hybrid structures. Initial cytotoxicity analyses were conducted for some derivatives against MCF-7 cells, a human breast adenocarcinoma cell line[15]. Such derivatives demonstrated remarkable bio-properties such as antitumor and/or antimicrobial potential[16]. In the same vein, this work involves new FQs as potential pancreatic lipase inhibitors. Pancreatic lipase (PL) is the key enzyme for lipid absorption. It catalyzes the hydrolysis of triacylglycerides in the gastrointestinal tract and is responsible for the hydrolysis of 50–70% of total dietary fats[17,18]. Orlistat, a semisynthetic derivative of lipstatin, is a selective and potent inhibitor of PL. The success of Orlistat has encouraged research to identify newer PL inhibitors that lack unpleasant side effects like oily stool, abdominal pain, flatulence and fecal urgency[19]. Fluoroquinolone (FQ) derivatives were declared as efficacious and powerful antilipolytic agents *in vitro*[6]. Since Colorectal cancer is statistically associated with obesity, this research aims at preparing new FQs with dual inhibitory activity.

A. EXPERIMENTAL

A. Synthesis of novel title compounds (Supplementary attached)

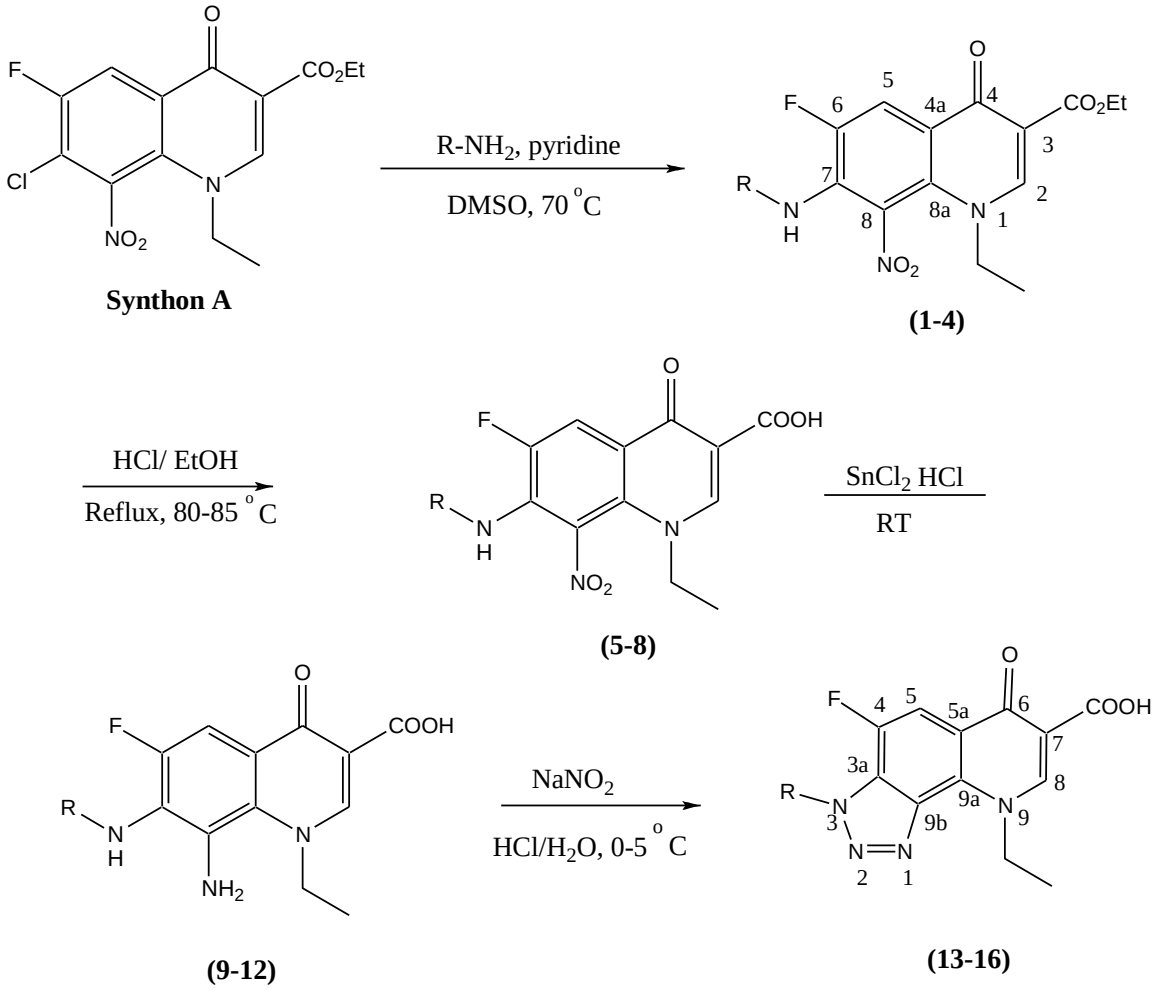

Synthon A

(1-4)

(5-8)

(9-12)

(13-16)

Scheme 1: Synthetic pathway of target compounds (FQ targets); R: *o*-anisidine, *p*-anisidine, *m*-anisidine, 2,4-dimethoxyaniline

Substitution	Ester	Nitro Acid	Amino	Triazolo
***o*-** methoxy phenyl	**1**	**5**	**9**	**13**
***m*-** methoxy phenyl	**2**	**6**	**10**	**14**
***p*-** methoxy phenyl	**3**	**7**	**11**	**15**
2,4- methoxy phenyl	**4**	**8**	**12**	**16**

B- In vitro antiproliferative assay

Obesity associated colorectal cell lines HT29, HCT116, SW620, and SW480 were kindly provided by Dr. Rick F. Thorne (University of Newcastle, Australia) in high-glucose DMEM (Bio Whittaker, Verviers, Belgium) containing 10% FCS. cultured. The CACO2 cell line was provided by Professor Yasser Bustanji, Faculty of Pharmacy, The University of Jordan. The CACO2 cell line was treated with L-glutamine (2 mM), penicillin (100 U/ml), gentamicin (50 µg/ml), streptomycin sulfate (100 mg/ml), 10% FBS and HEPES buffer (10 mM) (Sigma, St. Louis, Missouri, USA). The cytotoxicity assay was performed using sulforhodamine

B (SRB; Santa Cruz Biotechnology, Inc. Texas, USA) A calorimetric assay to assess the mechanisms of cytotoxicity and decreased cell viability[20]. The method outlined in this work has been adapted for toxicity assessment of compounds against adherent cells in a 96-well format. After the incubation period, cell monolayers were fixed with 10% (w/v) trichloroacetic acid (TCAA), stained for 30 min, and excess pigment was removed by repeated washing with 1% (v/v) acetic acid. Protein-bound pigment is dissolved in 10 mM Tris stock solution for optical density detection at 570 nm using a microplate reader. Human periodontal fibroblasts (PDL) are the primary cell culture to confirm selective cytotoxicity with the lowest antiproliferative IC50 values achieved. Cisplatin (1–100 µg/mL, Sigma, St. Louis, MO, USA) was used as a standard antitumor reference compound for comparison[21]. Relative cell viability was recorded as the average percentage of viable cells compared to DMSO-treated cells (control). All tests were performed in triplicate and the calculated antiproliferative potencies were recorded as mean ± SD (n = 3).

D. Docking Methodology

To explore drug-likeness properties and the prospective anticancer activity of the synthesized FQ derivatives (Fig. 2) against human topoisomerase II (TopII), *in silico* computational tools were used. Docking simulations were conducted to predict FQ's-TopII binding modes as potential target. TopII has been identified as an effective target in the treatment of cancers. The enzyme induces topological changes (unwinding) to the DNA molecule through the formation of transient double-stranded breaks in the DNA double helix, which makes topoisomerase essential for cell proliferation. TopII is targeted by several chemotherapeutic agents e.g., doxorubicin; mitoxantrone; etoposide and daunorubicin[22].

D.1 Molecular Modeling

D.1.1. *In silico* determination of drug-likeness properties

The Molinspiration server[23] was used to calculate the physicochemical properties of the designed compounds and to calculate a biological activity score for the six most important drug classes: GPCR ligands, kinase inhibitors, ion channel modulators, nuclear receptors, protease inhibitors, and enzyme inhibitors.

D.1.2. Docking experiment

Two-dimensional (2D) chemical structures of synthesized FQ derivatives (1–16; Scheme 2) were sketched with MarvinSketch[24] and saved in MDL Molfile format. As a result, a collection of energetically accessible conformers was generated using the OMEGA software[25]. OMEGA builds an initial structural model by assembling fragment templates along sigma bonds. The generated conformers were saved in SDF format. A 3D structural model of TopII (PDB ID: 3QX3) was obtained from the Protein Data Bank (www.rcsb.org)[26]. TopII receptor (binding) sites were identified using the MAKE_RECEPTOR module, a "graphical utility for creating or modifying receptors". A receptor is a special file used by FRED that contains target protein structure, active site location and geometry, binding ligand structure, and docking conditions, at least two of which are optional (OEDOCKING 3.2.0.2)[27]. Hydrogen atoms were added to proteins using the Discovery Studio (DS) Protein Residue Visualizer templat[28]. The synthesized compound and intercalating anticancer drug doxorubicin were docked into the TopII receptor site using the FRED program (OEDOCKING 3.2.0.2)[27]. Protein structures and ligand conformers were treated as rigid bodies during the docking process. This involves a thorough evaluation of each possible position of the ligand in the active binding site. The highest rated pose is optimized and given a final rating (Chemgauss4 rating). Doxorubicin showed similar pattern of results compared to positive control and cisplatin as test compound (Fig. 1).

E. PL activity assay

E.1 Preparation of the test compounds and Orlistat for the in vitro PL activity assay

Orlistat (10 mg, Sigma, St. Louis, MO, USA) was

dissolved in DMSO (10 mL) to make a stock solution (1 mg/mL), which was used to quantify 6 different concentrations ranging from 0.625 to 20. We got 6 different stock solutions. µg/ml. As a result, 20 µL aliquots of each working solution were used in the reaction mixture to obtain final working concentrations ranging from 0.0125 to 0.4 µg/mL. The test compounds were then dissolved primarily in DMSO to prepare 3 stock solutions, which were diluted to give 5 stock solutions (0.01-100 mg/ml). A 20 µL aliquot of each stock solution was then used in the reaction mixture to provide the final working concentration range (0.2–2000 µg/mL). A negative control containing 2% DMSO was run in parallel.

E.2 Quantification of PL potential spectrophotometrically

Crude porcine PL type II (0.5 mg/ml) (Sigma, St. Luis, MO, USA, EC 3.1.1.3) was diluted in Tris-HCl buffer (2.5 mM, pH 7.4, Promega Corp WI, USA) to final concentration of 200 units/mL. A 100 µM solution of para-nitrophenyl butyrate (p-NPB, Sigma, St. Louis, MO, USA) in DMSO was used as the PL substrate. An aliquot (0.1 mL) of the PL solution was included in the reaction mixture and the volume was brought to a final 1 mL with Tris-HCl buffer. PLs was pre-incubated with various concentrations of test materials for at least 1 min after substrate inclusion. Reactions were kept at room temperature and initiated by the addition of 5 µl of p-NPB substrate solution. The p-nitrophenol formed during the reaction was denatured using a SpectroScan 80D UV-VIS spectrophotometer (Sedico Ltd., Nicosia, Cyprus) at 410 nm over at least 7 time points (1–4 min), contains denatured enzymes. The catalytic ability of PL was measured calorimetrically by its activity towards the hydrolysis of p-NPB to p-nitrophenol. The activity of PL in this experiment was measured by determining the increase in p-nitrophenol production rate from the slope of the even part of the absorbance vs. time profile. The percentage of PL activity remaining for each test compound compared to control incubations was determined to calculate the concentration required to inhibit PL activity by 50% (i.e., IC50). All assays were performed in triplicate and calculated activities were reported as mean ± standard deviation (n = 3). PL inhibition values (%) were calculated according to the following formula: Inhibition (%) = 100 – [(B/A) × 100], where A is the PL activity in the absence of an inhibitor or test compound and B is the PL activity in the presence of an inhibitor or test compound.

C- Results and Discussion

A. Synthesis

The most versatile position for antibacterial fluoroquinolone is secondary amine at the C-7 position[29]. However, activity has been observed for quinolones with a primary amino group substituted at the C-7 position by our group creating new lipophilic anticancer members[30,31]. The chemistry included nucleophilic aromatic substitution reaction (S_N2 AR) of the primary amino group into C-7 position of quinolone nucleus. Substituted anisidines were introduced at C-7 of 7-chloro-1-cyclopropyl-6-fluoro-8-nitro-4-oxo-1,4-dihydroquinoline-3-carboxylic ester using DMSO and pyridine as catalyst. This step was very straightforward producing good yields of the FQs esters (1-4)[32]. Subsequent acid hydrolysis of the esters and stannous chloride reduction produced the acids (5-8) and the reduced amines (9-12) in high yields. Cyclization was carried out through diazotization reaction (acidic sodium nitrite) of the 8-amino group to produce the triazoles 13-16 in high yields. All compounds were separated and fully characterized by NMR spectra as detailed in supplementary sheets.

B. Modulation of proliferative activity by FQ in obesity associated colorectal cancer cell lines

The epidemiological indication of connotation between cancer and obesity has been officially recognized in the last 10-year report from American Institute for Cancer Research and the World Cancer Research Fund[33]. The reported potential anti-cancer activity of FQ [5, 34] is associated with anti-cancer activity against a panel of colon cancer cell lines (HT29, HCT116, SW620, CACO2, and SW480) led to cancer screening[35]. The significant antiproliferative potential

of four series of FQs evaluated against a panel of cancer cell lines was validated with IC_{50} values against Cisplatin (Table 1). All tested FQs revealed good activity against all CRC cells, with IC_{50} values below 200 μM. The reduced series which contains the 7-8 ethylene diamine bridge showed the lowest IC_{50} values. Significantly reduced derivative **11** cytotoxicity against colorectal cancer cell lines was expressed as equivalent to or superior to that of cisplatin's in 72h incubations (Table 1). Substitutions like anisidine have major contribution to activity. Notably compound **11** with IC_{50} value (±SD) of cytotoxicity in HCT116 (μM) of 35.3±3.0 vs. **cisplatin's** 38.0±0 **was** more potent than cisplatin. The active FQs **11** was pronouncedly **antineoplastic** in SW620 colorectal incubations with IC_{50} values (μM) (±SD) of 3.2±0.8 vs. cisplatin's 5.7±0.9).

Table 1. *In vitro* antiproliferative activity IC_{50} values (μg/mL; μM) of FQs and cisplatin on colorectal cancer cell lines

COMPOUND	HT29	HCT116	SW620	CACO2	SW480	Fibroblasts
(1)	61.2±0.6 (142.4±1.5)	105.1±17.0 (244.9±40)	112.1±3.3 (261.0±1.2)	87.1±0.5 (202.8±1.2)	82.3±16.1 (191.6±38)	174.6±11.9 (406.6±28)
(3)	31.7±3.0 (82.8±7.8)	51.7±2.9 (134.9±7.6)	43.1±3.7 (112.3±9.7)	56.4±6.4 (147.0±16.7)	100.9±7.0 (263.3±18)	60.1±5.4 (156.8±14)
(5)	50.1±0.2 (135.2±0.6)	21.8±2.2 (54.4±5.5)	43.6±2.3 (108.7±5.8)	69.7±15.2 (173.7±38)	15.9±1.6 (39.6±4.0)	54.8±9.2 (136.5±22.8)
(6)	1298.5±152.0 (3235.4±379)	177.3±7.1 (441.7±18)	250.6±19.7 (624.4±49.0)	NI	98.9±11.3 (246.4±28)	94.2±10.3 (234.7±25.6)
(7)	139.1±5.3 (346.6±13.2)	37.4±6.2 (93.2±15.6)	44.4±6.0 (110.7±14.9)	62.7±7.2 (156.2±18)	16.7±2.2 (41.6±5.6)	29.7±2.5 (74.0±6.2)
(8)	250.2±33.7 (580.0±78.1)	NI	341.1±65.2 (790.7±151.1)	7.3±1.4 (17.0±3.2)	96.7±11.5 (224.2±27)	625.0±37.1 (1448.8±86)
(9)	48.3±1.8 (130.0±5)	54.7±147) (147.3±4)	61.3±3.4 (165.1±9)	122.1±11.2 (328.8±30)	40.5±0.7 (109.0±1.9)	48.4±5.5 (130.3±14.8)
(10)	97.3±1.2 (261.9±3)	63.6±6.5 (171.1±17)	56.4±6.2 (151.9±17)	73.8±5.4 (198.7±14.5)	69.6±2.7 (187.3±7.3)	63.2±3.3 (170.3±8.8)
(11)	11.2±1.7 (30.3±4.5)	13.1±1.1 (**35.3±3.0**)	1.2±0.3 (**3.2±0.8**)	20.2±2.5 (54.4±6.8)	12.6±0.3 (34.0±0.7)	18.0±1.4 (48.4±3.8)
(13)	52.1±2.3 (136.2±6.0)	64.9±4.4 (169.7±12)	74±7.5 (193.5±20)	203.9±16.3 (533.2±43)	39.3±2.5 (102.8±7)	68.9±3.5 (180.2±9.2)
(14)	175.9±13.8 (460.1±36.1)	75±3 (196.2±7.7)	46.1±2.4 (120.6±6.2)	176.8±4 (462.4±10)	31±2.5 (81.1±6.6)	39.9±5.4 (104.3±14)
(15)	171±26.1 (447.1±68.1)	122.9±14.2 (321.4±37)	84.7±4.2 (221.5±11)	149.2±14.9 (390.2±39)	84.1±7.1 (220±19)	72.9±6.9 (190.8±18)
Cisplatin	2.1±0.2 (6.9±0.5)	11.4±0.02 (38.0±0.1)	1.7±0.3 (5.7±0.9)	0.4±0.06 (**1.3±0.2**)	1.6±0.2 (**5.3±0.7**)	2.1±0.2 (7.0±0.7)

Results are mean ± standard deviation (n = 3 independent replicates). IC50 values (concentration at which 50% inhibition of cell proliferation occurred compared to non-induced basal 72 h incubation) were calculated in the range 5-200 μg/ml. NI is lack of cytotoxicity.

Supported by previous clues about the mechanism of action of new FQs[36], it was decided to investigate the antiproliferative mechanism and target of these new FQs by comparing their IC_{50} with each other's and with doxorubicin against 5 CRC cell lines (Fig. 1A and B).

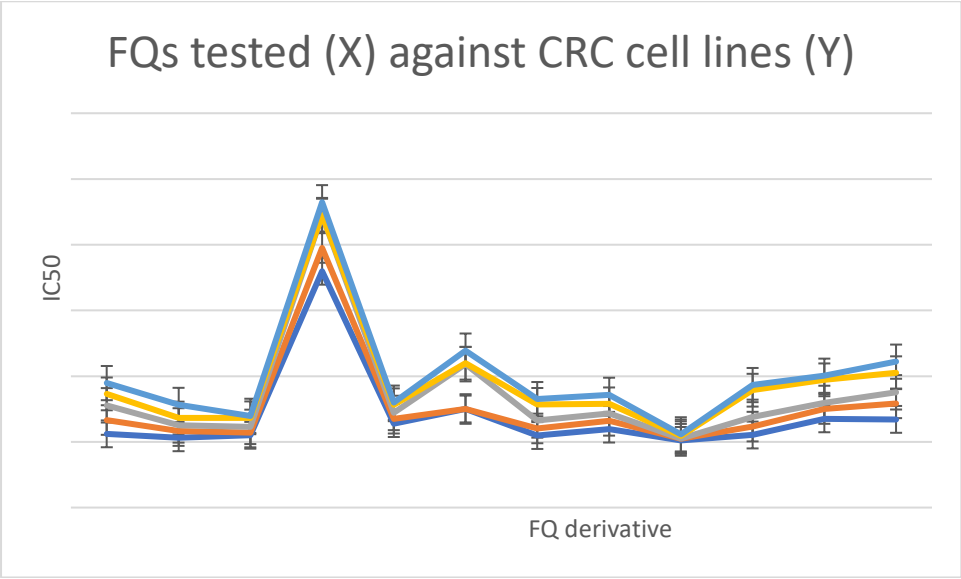

Figure 1A: IC_{50} comparison of synthesized FQs (5-16) against 5 CRC cell lines revealing similar pattern of screened FQs against CRCs.

Capriciously, the new FQs (5-16) showed a similar pattern of inhibition to each other against all CRC cell lines incriminating that they have common mechanism or target (Fig. 1A). To our surprise, such similarity in pattern was also noticed with reference drug doxorubicin against all CRC cell lines (Fig. 1B).

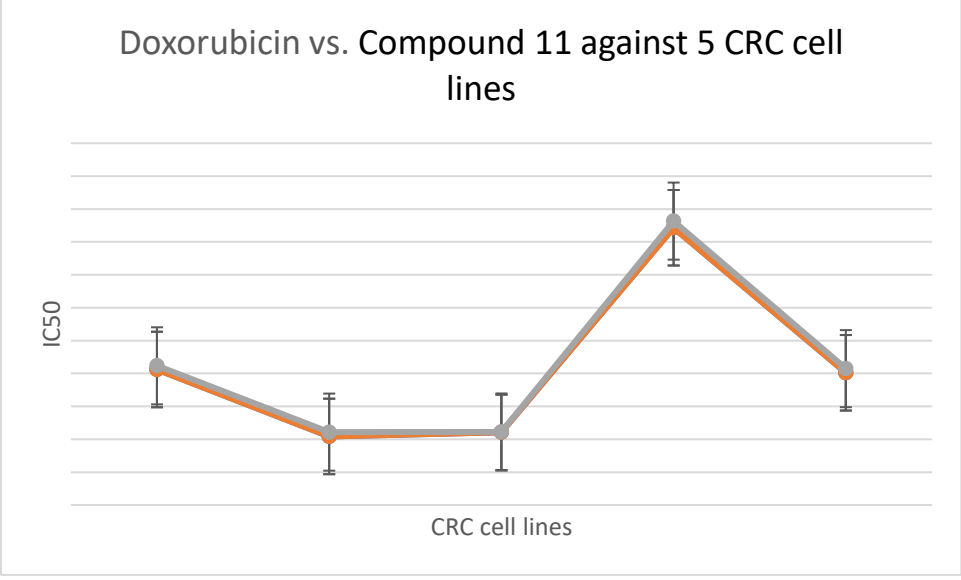

Figure 1B: IC_{50} comparison of synthesized FQs 11 and Doxorubicin against colorectal cancer cell lines.

Figure 1: IC50 A) Similarities in antiproliferative sequence and pattern of activity among tested FQ compounds B) Doxorubicin, and most active 11 against colorectal cancer cell lines (HT29 (1); HCT116 (2); SW620 (3); CACO2 (4); SW480 (5)). IC_{50} data of Doxorubicin used in this table were previously published[36] and further validated in this work

These findings point out clearly that there is structural scaffold similarity between our compounds (mainly 11) and doxorubicin. Since doxorubicin targets topoisomerase II, this means that our FQs work also on topoisomerase II similar to doxorubicin. Herein, we propose that the key structural features of eukaryotic topoisomerase II inhibitors common to our FQs are the C7-8- diamine ethylene chelator bridge serving as H-B donor/acceptor and its chelating similarity to hydroxyl groups in doxorubicin. Both FQ 11 and doxorubicin share a hydrogen bond acceptor-donor substituent, the amino group at C-8, and the isosteric OH of doxorubicin. They all feature such amino groups as part of an extended chelation system between C-7 and C-8 of compound **11** and the β-hydroxyketone of doxorubicin (Figure 2). This site/chelator system has been widely discussed in prokaryotic topoisomerase IV and gyrase inhibitors but seems to have been overlooked in all previously reported SAR scaffolds of eukaryotic topoisomerase II inhibitors. Here, we would like to emphasize the importance of C-8 amino groug in FQ 11 in the development of new anti-tumor FQ agents, and spot the light on the diamine chelate system generated in reduced FQ11 which has a major impact on the antiproliferative activity. Such findings led to explore binding sites on top. II enzyme of both compounds.

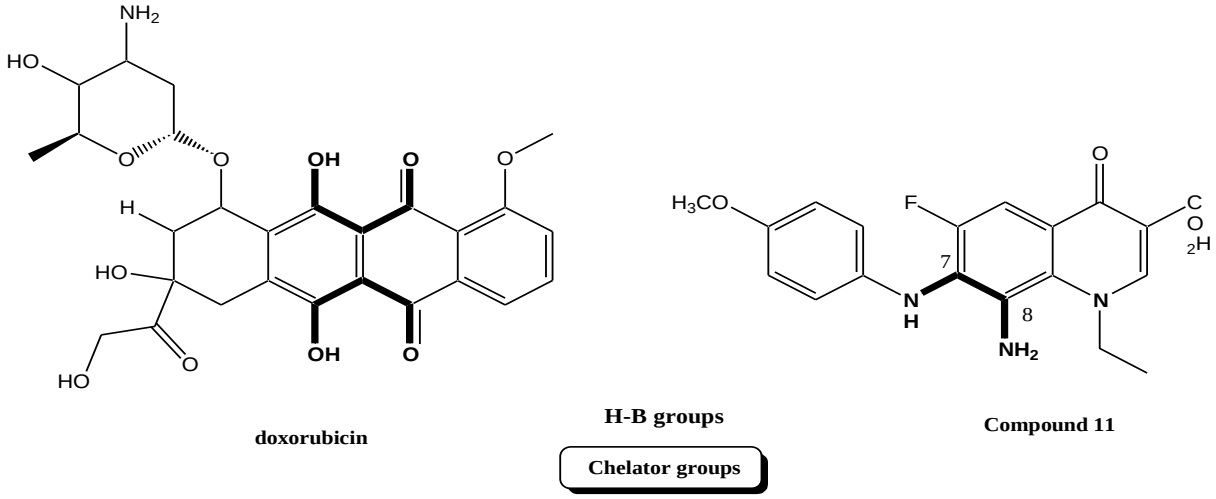

Figure 2: Proposed Chelator groups shared in both FQ 11 and doxorubicin.

D. Docking Experiment

D.1. *In silico* drug-likeliness analysis

Good oral bioavailability is an essential requirement in the identification and development of chemotherapeutic compounds. Therefore, when developing new drugs, it is very important to consider molecular properties that reduce oral bioavailability to support the development of valuable potential drug candidates. Reducing the number of experimental studies required for drug selection and development by using in silico computational tools throughout the drug discovery process to perform in silico ADMET analysis and bioactivity prediction to predict potential drug properties can save you time and money. As a result, several important physicochemical parameters. For example, Lipinski's parameters, the number of rotatable bonds, and the polar surface area (PSA) of synthesized compounds [37, 38], were identified using the computational tool Molinspiration for molecular property predictions.

Absorption rate (% ABS) was determined using the following formula: %ABS = 109 − 0.345 × PSA [10]. The results in table 2 showed that all the synthesized compounds meet Lipinski's rule of five and Veber rule with zero violations [37, 38]. The obtained results suggest that the synthesized compounds hypothetically have good oral bioavailability as suggested by the determined %ABS as shown in table 2.

Table 2. Drug-likeliness prediction of the synthesized compounds utilizing Molinspiration server.

Compound	PSA	NRB	miLogP	HBA	HBD	Mol Vol	MW	%ABS	MBS
1	106.16	6	2.12	8	1	338.92	399.38	72.40%	- 0.13
2	106.16	6	2.15	8	1	338.92	399.38	72.40%	- 0.11
3	106.16	6	2.17	8	1	338.92	399.38	72.40%	- 0.10
4	115.39	7	2.16	9	1	364.46	429.40	69.20%	- 0.12
5	126.39	6	1.80	9	2	330.37	401.35	65.40%	- 0.00
6	126.39	6	1.82	9	2	330.37	401.35	65.40%	0.01
7	126.39	6	1.85	9	2	330.37	401.35	65.40%	0.03
8	135.62	7	1.83	10	2	355.92	431.38	62.21%	- 0.01
9	86.36	5	1.65	6	3	326.87	369.40	79.21%	0.05
10	86.36	5	1.67	6	3	326.87	369.40	79.21%	0.07
11	86.36	5	1.70	6	3	326.87	369.40	79.21%	0.08
12	95.59	6	1.68	7	3	352.42	399.42	76.02%	0.04
13	79.03	4	1.13	7	0	324.23	380.38	81.73%	- 0.08
14	79.03	4	1.15	7	0	324.23	380.38	81.73%	- 0.07
15	79.03	4	0.96	7	0	324.23	380.38	81.73%	- 0.05
16	88.26	5	1.16	8	0	349.77	410.40	78.55%	- 0.07

PSA: polar surface area, NRB: number of rotatable bonds, miLogP: logarithmic partition coefficient, HBA: number of hydrogen bond acceptors, HBD: number of hydrogen bond donors, Mol Vol: molecular volume, MW: molecular weight, %ABS: absorption rate**.** MBS: enzyme inhibitor Molinspiration bioactivity score.

The drug-likeness score of synthesized molecules is ascertained by calculating the activity score for the ion channel modulator, GPCR, kinase inhibitor, enzyme inhibitor, protease inhibitor, and nuclear receptor ligands which has been applied to explore the compounds overall potential to be a good candidate for drug development. It was stated that the bigger the predicted bioactivity score, the higher the probability of specific molecule to be active as a drug. According to bioactivity score, a molecule having bioactivity score ≥ 0.00 is classified active, while classified as moderately active if the score is ≥−0.50 and less than 0.00 and if the score is less than− 0.50 it is presumed inactive[39]. The results of bioactivity data indicated that all the designed molecules are active to moderately active against all target classes and the highest activity was as enzyme inhibitors (Table 2). Interestingly, the most potent compound **11**as the highest bioactivity score as enzyme inhibitor and almost has the highest score against all classes.

D.2 Molecular docking study

Molecular docking studies were performed to focus on

the binding mode of the newly synthesized compound within the DNA binding site of Topo II (PDB code: 3QX3). Docking studies were performed using the FRED program of OEDocking suite [27]. As a validation step of the docking protocol, etoposide (a co-crystallized ligand) was first re-docked. FRED effectively predicted the pose of co-crystallized lower RMSD ligands, suggesting the effectiveness of the docking protocol. To discover the binding properties of synthetic compounds with TopII, we performed the same docking protocol on synthetic compounds within the DNA binding site and evaluated comparable binding modes and binding energies. All synthesized compounds successfully docked into the TopII binding site. A general examination of the docking results showed that the designed compounds exhibited binding patterns comparable to those of both the co-crystallized ligand (etoposide) and doxorubicin, with docking scores ranging from -13.45 to -15.74. was shown (Figure 3). The expected binding mode of compound **11** (the most potent compound) is shown in Figure 4. The planar quinolone unit exhibits pi-pi stacking and multiple hydrophobic interactions with DC-8, DT-9, DA-12, and DG-13, and with amino acids Glu477, Gly478, Ser480, Gly504. Using the action, the DNA was trapped between nucleotides. and Gln778. Moreover, both the amino group at position 8 and the NH of the 4-methoxyaniline moiety interact with Arg503 via hydrogen bonding (Fig. 3A). On the other hand, the proposed binding mode of the anticancer drug doxorubicin, with a predicted value of -14.345, is that the planar aromatic ring system of doxorubicin forms hydrophobic and aromatic stacking interactions with the DNA nucleotides DC-8, DT-9 and DA. made it clear that it has -12, DG-13, and several hydrophobic interactions with different key amino acid residues: Glu477, Gly478, Asp479, Leu502, Arg503, Gln778, Met782 like FQ75. In addition, the terminal 14-OH group of doxorubicin hydrogen bonds to Arg503 and DG-13, like FQ75 (Fig. 3B), while the OH at position 9 hydrogen bonds to his DT-9. In addition, the sugar moiety of doxorubicin was in the minor groove of DNA and hydrogen-bonded to Met782 and DC-8.

Figure 3: Diagram presenting ligand-DNA binding modes showing the overlay of docked poses of FQ11 (blue) and Doxorubicin (green) in the intercalation site (PDB ID: 3QX3).

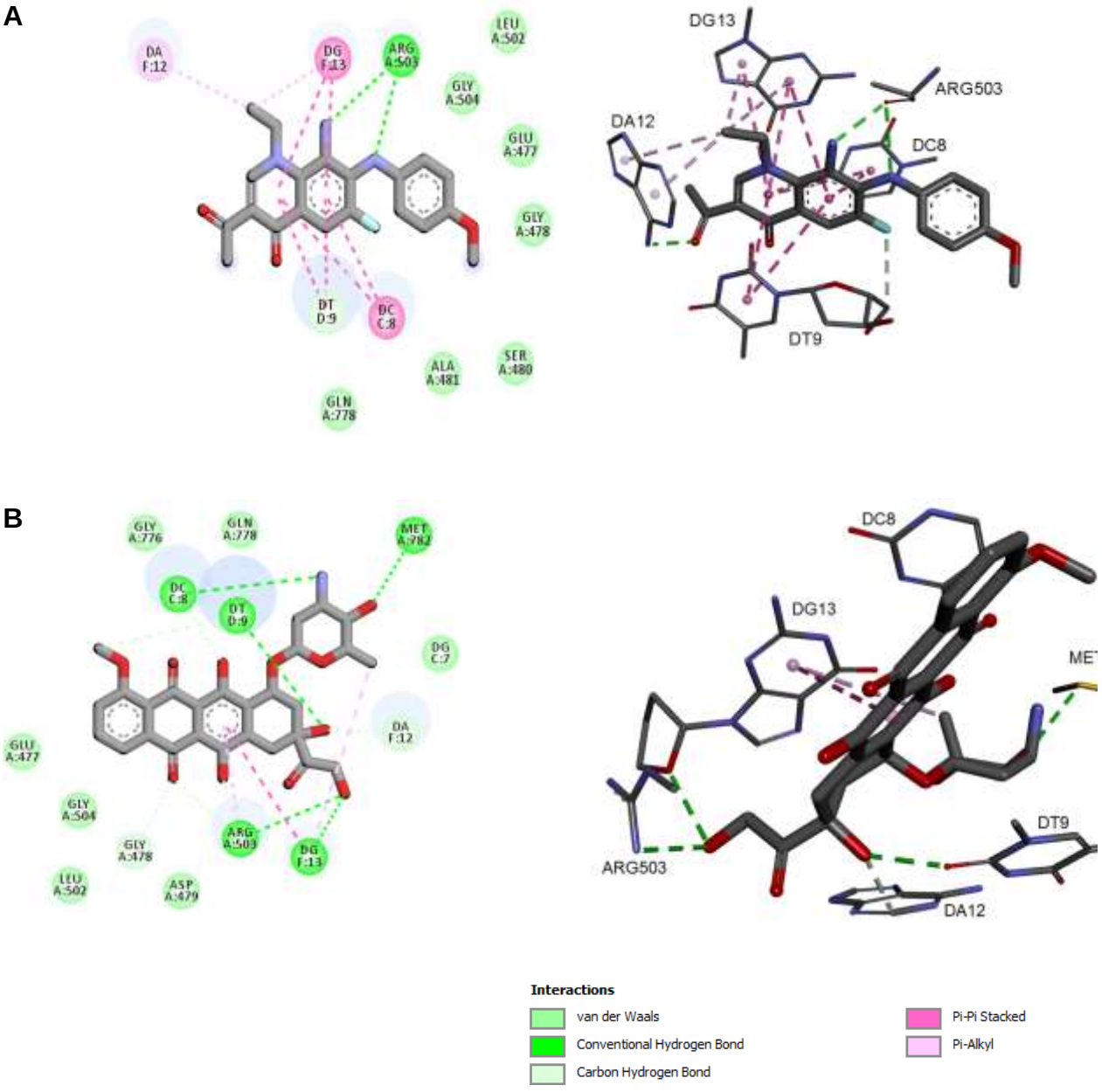

Figure 4: 2D and 3D illustration of the docking binding modes of: (**A**) designed compound FQ11, (**B**) doxorubicin in the Topoisomerase II active site. Hydrogen bonds are indicated by red dashed lines and pi-pi by purple dashed lines.

B. FQs as *In vitro* inhibitors of PL activity

Substantially based to the FQs antilipolytic activity [6, 40] and based on the fact that antilipolytic compounds can protect from Colorectal cancer; this study was directed toward

exploring dual anticancer FQs with antilipolytic effect against PL enzyme. Table 3 shows new FQs as inhibitors of pancreatic triacylglycerol lipase. These compounds have been reported to have dose-dependent anti-PL activity. IC_{50} values for both series of compounds ranged from 0.4 to 614 µM. Surprisingly, the reduced series (9-12) and the triazolo series (13-16) revealed the most potent activity which was comparable to the reference drug. Compound **9** was identified with a minimum IC50 value of 0.4 (±0.03) µM. The reference compound orlistat had an IC_{50} value of 0.2 µM, comparable to the value cited in the literature [41, 42]. Again, the antilipolytic FQs have showed the best anticancer activity exemplified by reduced series 9 -12. Although week to intermediate anti-CRC activity, this suggest primarily that such FQs might be used for such dual activity upon further investigation and optimization.

Table 3. PL-IC50 values of FQ and orlistat (µg/ml; µM)

No.	PL-IC_{50} (µg/mL)	PL-IC_{50} (µM)	No.	PL-IC_{50} (µg/mL)	PL-IC_{50} (µM)
1	16.9±2.4	44.1±6.3	10	14.0±0.7	37.6±1.8
4	21.8±2.7	52.8±6.5	11	4.6±0.5	12.3±1.3
5	9.1±0.1	22.7±0.3	12	8.3±0.2	20.6±3.0
6	4.1±0.6	10.1±1.6	**13**	**2.0±0.2**	**5.3±0.5**
7	57.3±1.2	142.8±3.0	14	12.3±1.9	32.0±5.0
8	4.4±0.3	10.2±0.6	15	56.2±1.0	147.1±2.7
9	**0.14±0.01**	**0.4±0.03**	16	243.3±17.1	614.4±43.4
Orlistat	**0.114±0.01**	**0.2±0.0**			

Results are mean ± standard deviation (n = 3 independent replicates).

Complexation studies:

To understand and confirm the chelation impact within the fluoroquinolones structure; we have decided to conduct Zn-complexation studies on PL enzyme for selected FQs. The acid CA, (7-chloro-1-cyclopropyl-6-fluoro-8-nitro-4-oxo-1,4-dihydroquinoline-3-carboxylic acid) and its precursor ester CE (ethyl 7-chloro-1-cyclopropyl-6-fluoro-8-nitro-4-oxo-1,4-dihydroquinoline-3-carboxylate) were selected such study due to availability in good amounts. Both were complexed with Zn metal (1 to 1 ratio) before adding to the PL enzyme, since FQs are well known to exhibit their antibacterial activity through metal chelation. Ciprofloxacin, the well-known antibacterial FQ, was used to confirm the idea since previously reported to have PL inhibitory activity[6, 43,44]. Then presence of excess metal ions within the test mixture of both FQs and ciprofloxacin, should neutralize the drug and the inhibitory effect would be lessened. The anti-lipase activities of CA, CE and ciprofloxacin are shown in Table 4.

Table 4.PL-IC_{50} values (µg/mL; µM) of FQs and FQs/$ZnCl_2$ complex

FQs test compounds/drugs	IC_{50} value (µg/mL)	IC_{50} value (µM)
Ciprofloxacin	23.55±1.13	71.08±4.46
Ciprofloxacin/$ZnCl_2$ complex	107.5±6.92	248.15±15.97
$ZnCl_2$	64.31±8.35	471.79±61.25
CA /$ZnCl_2$ complex	35.77±2.63	91.23±6.7
CA	5.35±5.8	16.38±1.6
CE	130±6.16	366.49±17.36

Results are mean ± standard deviation (n = 3 independent replicates)

Table 4 shows that both ciprofloxacin and CA exhibited potent inhibitory activity against PL with IC_{50} values of 71.08 and 16.38 µM, respectively. However, upon adding $ZnCl_2$ in-excess within the test mixture of both ciprofloxacin and CA showed significant decline in their inhibitory activity, with IC_{50} values of 248.15 and 91.23 µM, respectively. These data are attributed to pre-complexation of possibly the free COOH of both FQs with Zn ions and subsequently approve the role chelator groups against PL. Further assessing the CE ester derivative**,** PL-IC_{50} value was 366.49 µM (Table 4). These results indicate clearly that PL-inhibitory potential within the FQs tested can be linked to the free chelator groups beard by the molecules. Unfortunately, this study was not possible with active compounds due to low amounts, nor it was possible to conduct on CRC lines due to cell membrane barriers and metal penetration strains.

Conclusion

This work addressed the synthesis of biologically active compounds belonging to FQs with dual anticancer and anti-lipase activity, hypothesized to act via a chelation mechanism or inhibition validated by titration and docking experiments. Sixteen compounds were synthesized, fully characterized and tested by determining IC50 values against the most sensitive cancer cell lines. *In vitro* results showed that these compounds exhibited potent anticancer activity against test cell lines in the micromolar range with potency comparable pattern to doxorubicin. Compound 11 showed approximately 2-fold potency compared to cisplatin against the colorectal cancer cell line SW620 with an IC50 of 3.2 µM, suggesting that FQ is a potent anti-proliferative agent. The antiproliferative activity of these derivatives correlated well with their potential to inhibit topo II, suggesting that chelation is the mechanism of topo II inhibition, underscored by titration and docking experiments. Synthesized FQ derivatives were screened for their in vitro anti-lipase activity. The results showed that all tested compounds exhibited superior anti-lipase activity compared to the control molecule orlistat. Compound 9 exhibited comparable activity to orlistat against pancreatic lipase with an IC50 of 0.4 µM, suggesting that FQs are potent inhibitors of pancreatic lipase.

Acknowledgments

We are grateful for the Deanship of Scientific Research at The University of Jordan and Al-Zaytoonah Private University for providing research facilities and funding. This research was conducted during a sabbatical given to the professor Yusuf Al Hiari by The University of Jordan in the academic year 2021/2022 at Al-Zaytoonah Private University.

Supplementary 1 data : Chemistry spectral data

All chemicals, solvents, and reagents were of analytical grade and used directly without further purification. The starting materials are ethyl 3- (N, N-dimethyl-amino)acrylate and ethylamine purchased from his Acros, Belgium. 2,4-Dichloro-5-fluoro-3-nitrobenzoic acid was purchased from Sigma-Aldrich (St. Louis, MO, USA). Primary aromatic amines: m-anisidine and 2,4-dimethoxyaniline were purchased from Aldrich Chemicals (UK), p-anisidine and o-anisidine from Merck (Darmstadt, Germany). The reducing agent, anhydrous tin chloride crystals ($SnCl_2$), was from Fluka (Switzerland) and the cyclizing agent, sodium nitrate, from Sigma Aldrich (St. Louis, MO, USA). Thin-layer chromatography (TLC) was performed on 10 x 10 cm aluminum plates precoated with fluorescent silica gel GF254 (ALBET, Germany) and visualized using UV light with a wavelength of 254 nm. The mobile phase combination was 94:5:1 chloroform-methanol-formic acid (CHCl3-MeOH-FA) (system 1) and 50:50 (n-hexane-ethyl acetate) (system 2). Melting points (mp) were determined on an open capillary on a Stuart Scientific Electrothermal Melting Point Apparatus (Stuart, Staffordshire, UK) and were recorded uncorrected. Nuclear magnetic resonance (NMR) spectra were obtained on a Varian Oxford-300 (300 MHz) spectrometer, a Bruker Avance DPX-300 spectrometer, a Bruker Avance-400 (400 MHz) Ultra Shield spectrometer, and a Bruker 500 MHz-Avance III (500MHz). Chemical shifts were reported in ppm relative to tetramethylsilane (TMS) as internal standard. Deuterated chloroform (CDCl3) and deuterated dimethylsulfoxide (DMSO-d6) were used as solvents for sample preparation. 1H NMR data are reported as: chemical shifts (ppm), (multiplicities, coupling constants (Hz), number of protons, corresponding protons). Low-resolution mass spectra (LRMS) were analyzed by Applied Biosystems MDS SCIEX API. High-resolution mass spectra (HRMS) were evaluated in positive ion mode using the electrospray ionization (ESI) technique with collision-induced dissociation on a Bruker APEX-4 (7 Tesla) instrument., inject the spray solution (methanol/water 1:1 v/v + 0.1 formic acid) and a syringe pump at a flow rate of 2 µL/min. External calibration was performed using the arginine cluster in the mass range m/z 175-871. Molecular masses were reported as AMU + 1 because the positive mode of ESI 1 adds his AMU to the molecular ion peak. Some compounds were documented as AMU+2 because the positive mode of ESI 1 added AMU to the molecular ion peak and ran the Ion Trap Analyzer. Infrared (IR) spectra were recorded on a Shimadzu 8400F FT-IR spectrophotometer Shimadzu, Kyoto, Japan. Samples were prepared as potassium bromide (KBr) (Sigma, St. Luis, MO, USA) discs.

B1. Synthesis of ethyl -1-ethyl-6-fluoro-7-(2-methoxy-phenylamino)-8-nitro-4-oxo-1,4-dihydro-quinoline-3-carboxylate (1)

3 molar equivalents of *o*-anisidine (2.7 g, 21.9 mmol) were introduced into a solution (starting synthon A, 2.5 g, 7.3 mmol) and 10 ml of dimethylsulfoxide (DMSO) as a vehicle and few drops of pyridine and then was refluxed at 65-70 °C under anhydrous conditions for (2-3) days. The reaction mixture was observed until the starting material totally reacted and then was allowed to crystallize at room temperature. The resulting product was filtered, rinsed and dried in the dark to produce orange crystals. Color of produced compound: orange. Yield ≈ 89% (2.8 g); mp = 199-200 °C; R*f* value in system 1 = 0.68 and in system 2 = 0.4. ^{1}H NMR (300 MHz, DMSO-d_6): 1.23 (2t, 6H, CH_3-1', OCH_2CH_3), 3.68 (s, 3H, OCH_3), 3.99 (q, J =7.13 Hz, 2H, NCH2-1'), 4.21 (q, J = 7.09 Hz, 2H, OCH_2CH_3), 6.82 (dd, J = 7.8 Hz, 8.2Hz, 1H, CH-5"), 6.90 (d, J = 7.81 Hz, 1H, CH-3"), 6.96 (m, 1H, CH-6"), 7.00 (m, 1H, CH-4"), 8.01 (d, ^{3}JH–F = 11.86 Hz, 1H, H-5), 8.06 (s, 1H, NH), 8.59 (s, 1H, H-2). ^{13}C NMR (75 MHz, DMSO-d_6): 14.73 (C-2'),15.77 (OCH_2CH_3), 50.50 (NC-1'), 56.13 (OCH_3), 60.69 (OCH_2), 111.91 (C-3"), 112.24 (C-3), 114.77 (d, 2JC–F =

21.38 Hz, C-5), 120.52 (C-6"), 120.95 (C-4"), 124.37 (C-5"), 124.55 (d, 3JC–F = 5.78 Hz, C-4a), 130.59 (C-8a), 130.99 (C-1"), 132.43 (d, 2JC–F = 16.13 Hz, C-7), 134.47 (C-8), 150.94 (C-2"), 151.43 (C-2), 152.64 (d, ^{1}JC–F = 244.95 Hz, C-6), 164.38 (CO_2Et), 170.62 (C-4). IR (KBr): ν 3396, 3033, 2358, 1714, 1636, 1527, 1317, 1077, 980 cm^{-1}. LRMS (ES, +ve) m/z calculated for $C_{21}H_{20}FN_3O_5$ (429.13): Found 430.6 (100%, M+1), 402.2 (1%), 384.3 (15%), 356.4 (1%), 310.4 (1%), 155.5 (8%), 141.2 (55%), 124.1 (1%), 114.2 (4%), 85.2 (4%), 78.9 (1%), 64.1 (7%).

B2. Synthesis of ethyl -1-ethyl-6-fluoro-7-(3-methoxy-phenylamino)-8-nitro-4-oxo-1,4-dihydro-quinoline-3-carboxylate (2)

3 molar equivalents of *m*-anisidine (3.2 g, 26.3 mmol) were introduced into a solution containing (starting synthon A, 3 g, 8.75 mmol) and 10 ml of dimethylsulfoxide (DMSO) as a vehicle and drops of pyridine and then was refluxed at 65-70 °C under anhydrous conditions for (2-3) days. The reaction mixture was observed until the starting material totally reacted and then was allowed to crystallize at room temperature. The resulting product was filtered, rinsed and dried in the dark to produce dark orange crystals. Color of produced compound: dark orange. Yield ≈ 70% (2.6 g); mp = 170-171 °C; R*f* value in system 1 = 0.75 and in system 2 = 0.43. ^{1}H NMR (300 Hz, DMSO d_6): 1.24 (2t, 6H, OCH_2CH_3, CH_3-2'), 3.65 (s, 3H, OCH_3), 4.02 (q, J= 7.01 Hz, 2H, NCH_2-1'), 4.22 (q, J= 7.05 Hz, 2H, OCH_2), 6.38 (d, J= 8.14 Hz, 1H, H-6"), 6.42 (br s, 1H, H-2"), 6.46 (d, J= 8.18 Hz, 1H, H-4"), 7.07 (dd, J= 8.2 Hz, 8.04 Hz, 1H, H-5"), 8.12 (d, ^{3}JH-F= 11.1 Hz, 1H, H-5), 8.49 (br s, 1H, NH), 8.62 (s, 1H, H-2). ^{13}C NMR (75 Hz, DMSO d_6): 14.74 (C-1'), 15.98 (OCH_2CH_3), 50.29 (C-2'), 55.45 (OCH_3), 60.74 (OCH_2), 103.30 (C-4"), 107.35 (C-2"), 109.62 (C-6"), 112.06 (C-3), 115.57 (d, ^{2}JC-F= 21.45, C-5), 126.64 (d, ^{3}JC-F= 6.08, C-4a), 129.78 (d, ^{4}JC-F= 2.03, C-8a), 130.11 (d, ^{3}JC-F= 9.3, C-8), 130.28 (C-5"), 137.79 (C-7), 145.04 (d, ^{4}JC-F= 1.65, C-1"), 151.82 (C-2), 153.77 (d, ^{1}JC-F= 251.33, C-6), 160.39 (C-3"), 164.33 (CO_2Et), 170.62 (C-4). IR (KBr): ν 3387, 2978, 2255, 1722, 1615, 1522, 1452, 1322, 1060, 988 cm^{-1}. LRMS (ES, +ve) m/z calculated for $C_{21}H_{20}FN_3O_5$ (429.13): Found 430.3 (100%, M+1), 415.3 (5%), 402.2 (1%), 385.3 (39%), 373.7 (1%), 352.1 (4%), 339.2 (7%), 324.4 (8%), 310.3 (1%), 272.3 (1%), 258.2 (11%), 247.3 (1%), 186.5 (7%), 170.4 (1%), 138.4 (4%), 124.2 (19%), 94.0 (1%), 79.7 (3%).

B3. Synthesis of 1 ethyl -1-ethyl-6-fluoro-7-(4-methoxy-phenylamino)-8-nitro-4-oxo-1,4-dihydro-quinoline-3-carboxylate (3)

3 molar equivalents of *p*-anisidine (3.2 g, 26.3 mmol) were introduced into a solution containing (starting synthon A, 3 g, 8.75 mmol) and 10 ml of dimethylsulfoxide (DMSO) as a vehicle and drops of pyridine and then was refluxed at 65-70 °C under anhydrous conditions for (2-3) days. The reaction mixture was observed until the starting material totally reacted and then was allowed to crystallize at room temperature. The resulting product was filtered, rinsed and dried in the dark to give brick red powder. Color of produced compound: brick red. Yield ≈ 93% (3.5 g); mp= 118-119 °C; R*f* value in system 1 = 0.77 and in system 2 = 0.44. ^{1}H NMR (400 MHz, DMSO-d_6): 1.27 (2t, 6H, CH_3-1', OCH_2CH_3), 3.70 (s, 3H, OCH_3), 4.02 (q, J= 6.7 Hz, 2H, NCH_2-1'), 4.24 (q, J= 7.2 Hz, 2H, OCH_2CH_3), 6.48 (d, J= 7.89 Hz, J= 8.03 Hz, 2H, CH-2", CH-6"), 6.82 (d, J= 7.89 Hz, 2H, CH-3", CH-5"), 8.03 (d, ^{3}JH–F = 11.72 Hz, 1H, H-5), 8.53 (s, 1H, NH), 8.60 (s, 1H, H-2). ^{13}C NMR (75 MHz, DMSO-d_6): 15.6 (C-2'), 15.39 (OCH_2CH_3), 52.6 (NC-1'), 55.54 (OCH_3), 61.28 (OCH_2), 110.91 (C-3), 116.9 (d, ^{2}JC-F = 16.92 Hz, C-5), 114.26 (C-4a), 114.75 (2C, C-3", C-5"), 122.6 (2C, C-2", C-6"), 130.43 (d, ^{2}JC–F = 16.35 Hz, C-7), 134.14 (C-8a), 134.77 (C-8), 138.86 (C-1"), 150.4 (d, ^{1}JC-F = 253 Hz, C-6), 151.13 (C-2), 157.31(C-4"), 164.59 (CO_2Et), 171.22 (C-4). IR (KBr): ν 3390, 3077, 2354, 1764, 1614, 1508, 1463, 1089, 928 cm^{-1}. LRMS (ES, +ve) m/z calculated for $C_{21}H_{20}FN_3O_5$ (429.13): Found 430.4 (100%, M+1), 416.1 (1%), 407.5 (5%), 385.3 (36%), 365.6

(1%), 343.3 (3%), 339.3 (4%), 324.5 (3%), 122.4 (45%), 104.2 (12%), 56.1 (1%). 3.2.2.10

B4. Synthesis of ethyl -7-(2,4-dimethoxy-phenylamino)-1-ethyl-6-fluoro-8-nitro-4-oxo-1,4-dihydro-quinoline-3-carboxylate (4)

3 molar equivalents of 2,4-dimethoxyaniline (3.35 g, 21.9 mmol) were introduced into a solution containing (starting synthon A, 2.5 g, 7.3 mmol) and 10 ml of dimethylsulfoxide (DMSO) as a vehicle and drops of pyridine and then was refluxed at 65-70 °C under anhydrous conditions for (2-3) days. The reaction mixture was observed until the starting material totally reacted and then was allowed to crystallize at room temperature and the resulting product was filtered, rinsed and dried in the dark to produce bright orange crystals. Color of produced compound: bright orange. Yield ≈ 80% (2.7 g); mp = 114-115 °C; R*f* value in system 1 = 0.88 and in system 2 = 0.3. ^{1}H NMR (500 MHz, DMSO-d_6): 1.2 (t, J = 7.05 Hz, 3H, CH_3-1'), 1.25 (t, J = 7.1 Hz, 3H, OCH_2CH_3), 3.63 (s, 3H, OCH_3-2"), 3.72 (s, 3H, OCH_3-4"), 3.95 (q, J = 7.05 Hz, 2H, NCH_2-1'), 4.20 (q, J = 7.05 Hz, 2H, OCH_2CH_3), 6.43 (dd, J= 6.2, 2.45 Hz, 1H, CH-5"), 6.55 (d, J = 1.4 Hz, 1H, CH-3"), 7.00 (d, J= 8.45Hz, 1H, , CH-6"), 7.9 (d, 3JH–F = 12.5 Hz, 1H, H-5), 8.16 (s, 1H, NH), 8.54 (s, 1H, H-2). ^{13}C NMR (125 MHz, DMSO-d_6): 14.7 (C-2'),15.69 (OCH_2CH_3), 50.51 (NC-1'), 55.84 (OCH_3-2"), 56.17 (OCH_3-4"), 60.59 (OCH_2), 99.74 (C-5"), 104.84 (C-3"), 112.33 (C-3), 114.38 (d, 2JC–F = 21.06 Hz, C-5), 122.22 (d, ^{3}JC–F = 5.59 Hz, C-4a), 122.78 (C-8a), 124.79 (C-6"), 131.24 (d, ^{3}JC–F = 3.23 Hz, C-8), 131.33 (C-1"), 134.3 (d, ^{2}JC–F = 14.34 Hz, C-7), 151.05 (C-2), 151.32 (d, ^{1}JC–F = 249.89 Hz, C-6), 153.9 (C-2"), 158.14 (C-4"), 164.40 (CO2Et), 170.57 (C-4). IR (KBr): ν 3367, 3034, 2347, 1738, 1633, 1512, 1460, 1344, 1087, 960 cm^{-1}. LRMS (ES, +ve) m/z calculated for $C_{22}H_{22}FN_3O_7$ (459.14): Found 459.9; (M+1, 100%), 416.3 (11.2%), 414.4 (41.6%), 386.2 (1.1%), 367.3 (2.2%), 340.3 (5.6%), 325.3 (1.1%), 74.2 (4.5%), 57.5 (6.7%).

B5. Synthesis of 1-ethyl-6-fluoro-7-(2-methoxy-phenylamino)-8-nitro-4-oxo-1,4-dihydro-quinoline-3-carboxylic acid (5)

A forcefully agitated suspension of (1.2 g, 4.7 mmol) in 12 N HCl (28 mL) and ethanol (12 mL) was heated at 80-85 °C under reflux conditions. Advancement of ester hydrolysis was observed by TLC and was done in 24-36 hours. The reaction mixture was then cooled and, poured onto mashed ice (250 g) and the resultant orange precipitate was taken, washed with cold water (2 x 20 mL) and dried. Yield ≈ 70% (1.3 g). mp = 210-212 °C; R*f* value in system 1 = 0.49. ^{1}H NMR (300 MHz, DMSO-d_6): 1.26 (t, 3H, CH_3-2'), 3.64 (s, 3H, OCH_3), 4.14 (q, J = 7.1Hz, 2H, NCH_2-1'), 6.86 (dd, J = 7.42 Hz, 8.22 Hz, 1H, CH-5"),6.99 (d, J = 7.89 Hz 1H, CH-3"), 7.07 (m, 2H, CH-4",CH-6"), 7.44 (d, ^{3}JH–F = 9.54 Hz, 1H, H-5), 8.51 (s, 1H, NH), 8.88 (s, 1H, H-2), 15.11 (br s, 1H, COOH).^{13}C NMR (75 MHz, DMSO-d_6): 15.96 (C-2'), 51.50 (NC-1'), 56.13 (OCH_3), 109.62 (C-3), 112.03 (C-3"), 113.77 (d, ^{2}JC–F = 21.6 Hz, C-5), 120.59 (d, ^{3}JC–F = 7.2 Hz, C-4a), 120.88 (C-6"), 122.77 (C-4"), 125.76 (C-5"), 129.79 (C-8), 131.54 (C-1"), 132.57 (d, ^{4}JC–F = 3.9 Hz, C-8a), 134.77 (d, ^{2}JC–F = 15.08 Hz, C-7), 152.17 (C-2), 152.17 (C-2"), 152.59 (d, ^{1}JC–F = 252.45 Hz, C-6), 165.55 (CO_2Et), 175.70 (d, ^{4}JC–F = 2.63 Hz, C-4). IR (KBr): ν 3374, 2988, 2714, 2242, 1768, 1625, 1478, 1331, 1074, 936 cm^{-1}. LRMS (ES, +ve) m/z calculated for $C_{19}H_{16}FN_3O_6$ (401.10): Found 402.2 (M+1, 100%), 384.3 (45%), 357.5 (90%), 339.2 (37%), 102.1; (1.1%), 74.3 (3.4%), 57.3 (5.6%).

B6. Synthesis of 1-ethyl-6-fluoro-7-(3-methoxy-phenylamino)-8-nitro-4-oxo-1,4-dihydro-quinoline-3-carboxylic acid (6)

A forcefully agitated suspension of (2, 2.1 g, 4.9 mmol) in 12 N HCl (29.5 mL) and ethanol (12.5 mL) was heated at 80-85 °C under reflux conditions. Advancement of ester hydrolysis was observed by TLC and was done in 24-36 hours. The reaction mixture was then cooled and, poured onto mashed ice (250 g) and the resultant dark orange precipitate was taken, washed with cold water (2 x 20 mL)

and dried. Yield ≈ 78% (1.64 g). mp = 171-173 °C; R*f* value in system 1 = 0.43. ^{1}H NMR (300 Hz, DMSO d_6): 1.24 (m, 3H, CH_3-2'), 3.66 (s, 3H, OCH_3), 4.18 (q, J= 6.95 Hz, 2H, NCH_2-1'), 6.46 (d, J= 8.0 Hz, 1H, H-6"), 6.52 (d, J*m*= 4.2 Hz, 1H, H-2"), 6.53 (d, J*o*= 8.13 Hz, 1H, H-4"), 7.10 (dd, J*o*= 7.93 Hz, J*o*= 7.97 Hz, 1H, H-5"), 8.24 (d, ^{2}JH-F= 11.14 Hz, 1H, H-5), 8.79 (br s, 1H, NH), 8.95 (s, 1H, H-2), 14.52 (br s, 1H, COOH). ^{13}C NMR (75 Hz, DMSO d_6): 16.15 (C-1'), 51.43 (C-2'), 55.52 (OCH_3), 104.38 (C-4"), 108.35 (C-2"), 109.57 (C-6"), 110.7 (C-3), 115.01 (d, ^{2}JC-F= 21.53, C-5), 123.18 (d, ^{3}JC-F= 7.2, C-4a), 130.15 (C-5"), 130.69 (d, ^{4}JC-F= 1.8, C-8a), 132.15 (d, ^{2}JC-F= 16.35, C-7), 137.0 (C-8), 144.18 (d, ^{4}JC-F= 1.9, C-1"), 152.2 (C-2), 153.9 (d, ^{1}JC-F= 252.9, C-6), 160.32(C-3"), 165.45 (COOH), 175.81 (d, ^{4}JC-F= 2.25, C-4). IR (KBr): ν 3360, 3077, 2843, 2353, 1714, 1644, 1485, 1307, 1078, 930 cm^{-1}. LRMS (ES, +ve) m/z calculated for $C_{19}H_{16}FN_3O_5$ (401.10): Found 402.2 (100%, M+1), 385.2 (11%), 384.3 (31.5%), 357.5 (5.6%), 355.3 (1%), 337.9 (1%), 102.2 (2%), 75.3 (4.5%), 60.8 (6.7%), 57 (6.7%).

B7. Synthesis of 1-ethyl-6-fluoro-7-(4-methoxy-phenylamino)-8-nitro-4-oxo-1,4-dihydro-quinoline-3-carboxylic acid (7)

A forcefully agitated suspension of (3, 2.6 g, 6 mmol) in 12 N HCl (36.5 mL) and ethanol (15.5 mL) was heated at 80-85 °C under reflux conditions. Advancement of ester hydrolysis was observed by TLC and was done in 24-36 hours. The reaction mixture then was cooled, poured onto mashed ice (250 g) and the resultant yellow precipitate was taken, washed with cold water (2 x 20 mL) and dried. Yield ≈ 60% (1.45 g). mp = 250-252 °C; Rf value in system 1 = 0.47. ^{1}H NMR (300 MHz, DMSO-d_6): 1.25 (t, J=6.87 Hz, 3H, CH_3-1"), 3.69 (s, 3H, OCH_3), 4.14 (q, J= 6.95 Hz, 2H, NCH_2-1'), 6.82 (d, J= 8.86 Hz, 2H, CH-2", CH-6"), 6.99 (d, J= 8.32 Hz, 2H, CH-3", CH-5"), 8.13 (d, ^{3}JH–F = 12.02 Hz, 1H, H-5), 8.85 (s, 1H, NH), 8.91 (s, 1H, H-2), 14.16 (br s, 1H, COOH). ^{13}C NMR (75 MHz, DMSO-d_6): 16.05 (C-2'), 51.58 (NC-1'), 55.78 (OCH_3), 109.59 (C-3), 114.60 (d, ^{2}JC–F = 21.83 Hz, C-5), 114.92 (C-4a), 114.75 (2C, C-3", C-5"), 120.12 (C-7), 122.45 (2C, C-2", C-6"), 134.14 (C-8a), 134.77 (C-8), 138.81 (C-1"), 151.78 (C-2), 153.17 (d, ^{1}JC–F = 253.13 Hz, C-6), 156.47 (C-4"), 165.56 (COOH), 175.69 (C-4). IR (KBr): ν 3380, 3070, 2648, 2322, 1716, 1621, 1485, 1312, 1122, 970 cm^{-1}. LRMS (ES, +ve) m/z calculated for $C_{19}H_{16}FN_3O_5$ (401.10): Found 402.2 (100%, M+1), 385.3 (30%), 379.2 (2%), 357.6 (26%), 355 (3.4%), 339.1 (25%), 310.3 (1%), 296.4 (2%), 241.1 (1%), 127.3 (1%), 102.2 (2%), 74.3 (3.4%), 61.1 (1%), 59.2 (13.5%), 57.3 (6.7%).

B8. Synthesis of 7-(2,4-dimethoxy-phenylamino)-1-ethyl-6-fluoro-8-nitro-4-oxo-1,4- dihydro-quinoline-3-carboxylic acid (8)

A forcefully agitated suspension (4, 2 g, 4.35 mmol) in 12 N HCl (28 mL) and ethanol (12 mL) was heated at 80-85 °C under reflux conditions. Advancement of ester hydrolysis was observed by TLC and was done in 24-36 hours. The reaction mixture then was cooled, poured onto mashed ice (250 g) and the resultant orange precipitate was taken, washed with cold water (2 x 20 mL) and dried. Yield ≈1.5 g (84 %). mp = 212-215 °C; R*f* value in system 1 = 0.7. ^{1}H NMR (300 Hz, DMSO d_6): 1.25 (t, J= 7.02 Hz, 3H, CH_3-2'), 3.62 (s, 3H, OCH_3-2"), 3.72 (s, 3H, OCH_3-4"), 4.13 (q, J= 7.01 Hz, 2H, NCH_2-1'), 6.46 (dd, J= 8.48 Hz, 4.2 Hz, 1H, H-5"), 6.55 (s, 1H, H-3"), 7.07 (d, J*o*= 8.57 Hz, 1H, H-6"), 8.01 (d, JH-F= 12.48 Hz, 1H, H-5), 8.58 (br s, 1H, NH), 8.86 (s, 1H, H-2), 14.70 (br s, 1H, COOH). ^{13}C NMR (75 Hz, DMSO d_6): 15.97 (C-2'), 51.65 (NC-1'), 55.89 (OCH_3-2"), 56.21(OCH_3-4"), 99.25 (C-3"), 104.90 (C-5"), 109.56 (C-3), 113.39 (d, ^{2}JC-F= 21.5 Hz, C-5), 118.74 (d, ^{4}JC-F= 6.83, C-8a), 121.81 (C-1"), 126.14 (C-6"), 130.04 (C-8), 132.15 (C-4a), 136.22 (d, ^{2}JC-F= 13.8, C-7), 151.44 (C-2), 151.64 (d, ^{1}JC-F= 254.85, C-6), 154.62 (d, ^{5}JC-F= 2.03, C-2"), 158.81 (C-4"), 165.63 (COOH), 175.61 (d, ^{4}JC-F= 2.7, C-4). IR (KBr): ν 3392, 3060, 2843, 2274, 1776, 1633, 1474, 1319, 1120, 915 cm^{-1}. LRMS (ES, +ve) m/z calculated for $C_{20}H_{18}FN_3O_7$

(431.11): Found 432.2 (100%, M+1), 416.1 (12.5%), 415.4 (62.5%), 401.3 (6.25%), 389.7 (2%), 387.2 (89.6%), 369.3 (14.6%), 296.3 (4%), 279.4 (2%), 251.5 (2%), 233.4 (2%), 74.4 (4%), 57.3 (8%).

B9. Synthesis of 8-amino-1-ethyl-6-fluoro-7-(2-methoxy-phenylamino)-4-oxo-1,4-dihydro-quinoline-3-carboxylic acid (9)

A mixture of (5, 0.65 g, 1.6 mmol) in 6.4 mL of 12 N HCl was stirred in ice bath (0-5 °C) for 15 minutes. Subsequently, the ice bath was removed and (1.2 g, 6.4 mmol) stannous chloride ($SnCl_2$) was introduced gradually and the reaction mixture stirred during the night and was observed by TLC until completion. The reaction mixture then was poured on mashed ice to yield a yellow precipitate that is collected by filtration and dried. Yield = 0.38 g (≈ 65%). mp = 215-217°C (decomposition); R*f* value in system 1 = 0.19. ^{1}H NMR (300 MHz, DMSO-d_6): 1.19 (t, 3H, CH_3-1'), 3.84 (s, 3H, OCH3), 4.81 (m, 2H, NCH_2-1'), 5.51 (br s, 2H, NH2), 6.18 (dd, J*o* = 6.73 Hz, 1H, CH-3"), 6.70 (dd, J*o* = 8.05 Hz, J*o* = 7.84 Hz, 2H, CH-4", CH-5"), 6.94 (d, J*o* = 7.79 Hz 1H, CH-6"), 7.02 (s, 1H, NH), 7.41 (d, ^{3}JH–F = 11.99 Hz, 1H, H-5), 8.88 (s, 1H, H-2), 14.60 (br s, 1H, COOH). ^{13}C NMR (75 MHz, DMSO-d_6): 16.19 (C-2'), 52.61 (NC-1'), 56.10 (OCH^3), 99.92 (d, ^{2}JC–F = 23.48 Hz, C-5),107.37 (C-3), 111.49 (C-3"), 112.75 (C-6"), 119.68 (C-4"), 121.75 (C-5"), 122.90 (d, ^{2}JC–F = 16.58 Hz, C-7), 126.21 (d, ^{3}JC–F = 9.3 Hz, C-4a), 127.25 (C-8a), 134.52 (C-8), 139.88 (C-1"), 148.18 (C-2"), 151.46 (C-2), 157.30 (d, ^{1}JC–F = 244.95 Hz, C-6), 166.55 (COOH), 177.44 (d, ^{4}JC–F = 2.85 Hz, C-4). IR (KBr): ν 3363, 3088, 2941, 1604, 1512, 1436, 1273, 1157, 1054, 1021 cm^{-1}. LRMS (ES, +ve) m/z calculated for $C_{19}H_{18}FN_3O_4$ (371.16): Found 372.4 (100%, M+1), 354.2 (51%), 339.3 (38%), 328.4 (42%), 102.2 (1%), 74.2 (2.2%), 59.2 (3.4%).

B10. Synthesis of 8-amino-1-ethyl-6-fluoro-7-(3-methoxy-phenylamino)-4-oxo-1,4-dihydro-quinoline-3-carboxylic acid (10)

A mixture of (6, 1.5 g, 3.7 mmol) in 4 mL of 12 N HCl was stirred in ice bath (0-5 °C) for 15 minutes. Subsequently, the ice bath was removed and (2.8 g, 15 mmol) stannous chloride ($SnCl_2$) was added gradually and the reaction mixture stirred during the night and was observed by TLC until completion. The reaction mixture then was poured on mashed ice to yield a yellow precipitate that is collected by filtration and dried. Yield = 0.9 g (≈ 65%). mp = 295-297 °C (decomposition); R*f* value in system 1 = 0.27. ^{1}H NMR (300 Hz, DMSO d_6): 1.16 (m, 3H, CH_3-2'), 3.6 (s, 3H, OCH_3), 4.16 (q, J= 7.11 Hz, 2H, NCH_2-1'), 5.94 (br s, 2H, NH_2), 6.46 (d, J*o*= 8.0 Hz, 1H, H-6"), 6.52 (d, J*m*= 2.5 Hz, 1H, H-2"), 6.53 (d, J*o*= 8.13 Hz, 1H, H-4"), 7.10 (dd, J*o*= 7.93 Hz, J*o*= 7.97 Hz, 1H, H-5"), 8.24 (d, ^{2}JH-F= 11.14 Hz, 1H, H-5), 8.79 (br s, 1H, NH), 8.95 (s, 1H, H-2), 15.88 (br s, 1H, COOH). ^{13}C NMR (75 Hz, DMSO d_6): 16.15 (C-1'), 51.43 (C-2'), 55.52 (OCH_3), 104.38 (C-4"), 108.35 (C-2"), 109.57 (C-6"), 110.7 (C-3), 115.01 (d, ^{2}JC-F= 21.53, C-5), 123.18 (d, ^{3}JC-F= 7.2, C-4a), 130.15 (C-8), 130.69 (d, ^{4}JC-F= 1.8, C-8a), 132.15 (d, ^{2}JC-F= 16.35, C-7), 137.0 (C-5"), 144.18 (d, ^{4}JC-F= 1.9, C-1"), 152.2 (C-2), 153.9 (d, ^{1}JC-F= 252.9, C-6), 160.32(C-3"), 165.45 (COOH), 175.81 (d, ^{4}JC-F= 2.25, C-4). IR (KBr): ν 3363, 3086, 2938, 2360, 1624, 1510, 1450, 1124, 1062, 1031 cm^{-1}. LRMS (ES, +ve) m/z calculated for $C_{19}H_{18}FN_3O_4$ (371.16): Found 372.4 (100%, M+1), 354.2 (51%), 339.3 (8%), 328.4 (42%), 102.2 (1%), 74.2 (2.2%), 59.2 (3.4%).

B11. Synthesis of 8-Amino-1-ethyl-6-fluoro-7-(4-methoxy-phenylamino)-4-oxo-1,4-dihydro-quinoline-3-carboxylic acid (11)

A mixture of (7, 0.4 g, 1 mmol) in 4 mL of 12 N HCl was stirred in ice bath (0-5 °C) for 15 minutes. After that, the ice bath was removed and (0.75 g, 4 mmol) stannous chloride ($SnCl_2$) was added portion wise and the reaction mixture stirred overnight and was monitored by TLC until completion. The reaction mixture then was poured on

mashed ice to precipitate to a red product that is collected by filtration and dried. Yield = 0.12 g (≈ 33%). mp = 295-297 °C (decomposition); R*f* value in system 1 = 0.25. ^{1}H NMR (300 MHz, DMSO-d_6): 1.25 (t, 3H, CH_3-1"), 3.69 (s, 3H, OCH_3), 4.59 (q, J= 6.98 Hz, 2H, NCH_2-1'), 6.23 (br s, 2H, NH_2), 6.93 (dd, J*o*= 8.79 Hz, 2H, CH-2", CH-6"), 7.22 (dd, J*o*= 8.29 Hz, 2H, CH-3", CH-5"), 7.47 (d, ^{3}JH–F = 11.53 Hz, 1H, H-5), 8.42 (s, 1H, NH), 8.72 (s, 1H, H-2), 15.46 (br s, 1H, COOH).^{13}C NMR (75 MHz, DMSO-d_6): 16.05 (C-2'), 51.58 (NC-1'), 55.78 (OCH_3), 105.59 (C-3), 106.65 (d, ^{3}JC–F = 20.33 Hz, C-5), 114.45 (2C, C-3", C-5"), 118.86 (d, ^{3}JC–F = 6.68 Hz, C-4a), 125.21 (C-8a), 129.25 (2C, C-2", C-6"), 129.96 (d, ^{2}JC–F = 16 Hz, C-7), 136.14 (C-8), 144.96 (C-1"), 147.89 (C-4"), 149.98 (C-2), 153.17 (d, ^{1}JC–F = 253.13 Hz, C-6), 166.89 (COOH), 176.96 (C-4). IR (KBr): ν 3356, 2924, 2854, 2291, 1625, 1531, 1458, 1377, 1180, 1033 cm^{-1}. LRMS (ES, +ve) m/z calculated for $C_{19}H_{18}FN_3O_4$ (371.16): Found 372.2 (4%, M+1), 368.4 (32%), 364.6 (18%), 357.5 (43%), 352.2 (100%), 339.0 (18%), 74.4 (14%), 59.1 (39%).

B12. Synthesis of 8-amino-7-(2,4-dimethoxy-phenylamino)-1-ethyl-6-fluoro-4-oxo-1,4-dihydro-quinoline-3-carboxylic acid (12)

A mixture of (8, 1.35 g, 3 mmol) in 12 mL of 12 N HCl was stirred in ice bath (0-5 °C) for 15 minutes. The ice bath was then removed and (2.4 g, 12 mmol) stannous chloride ($SnCl_2$) was added gradually and the reaction mixture stirred during the night and observed by TLC until completion. Later, the reaction mixture was poured on mashed ice to yield light brown precipitate that is collected by filtration and dried. Yield = 0.22 g (≈ 18%). mp = 285-287 °C (decomposition); R*f* value in system 1 = 0.15. ^{1}H NMR (300 Hz, DMSO-d_6): 1.22 (t, J= 8.2 Hz, 3H, CH_3-2'), 3.4 (s, 3H, OCH_3-2"), 3.62 (s, 3H, OCH_3-4"), 4.3 (m, 2H, NCH_2-1'), 5.6 (br s, 2H, NH_2), 6.88 (d, J= 8 Hz, 1H, H-5"), 7.1 (s, 1H, H-3"), 7.4 (d, J= 7.2 Hz, 1H, H-6"), 8.3 (d, JH-F= 14.75 Hz, 1H, H-5), 8.6 (br s, 1H, NH), 8.82 (s, 1H, H-2), 14.96 (br s, 1H, COOH). ^{13}C NMR (75 Hz, DMSO-d_6): 14.3 (C-2'), 52.6 (C-1'), 56.2 (OCH_3-2"), 57.8(OCH3-4"), 100.6 (C-3"), 105.4 (C-5"), 110.42 (C-3"), 144.7 (d, ^{2}JC-F= 18.25 Hz, C-5), 116.2 (C-4a), 121.3 (C-1"), 125.25 (C-6"), 131.0 (C-8a), 133.6 (C-8), 135.4 (C-7), 148.6 (C-2), 150.55 (d, ^{1}JC-F= 253 Hz, C-6), 154.62 (C-2"), 160.35 (C-4"), 166.4 (COOH), 173.6 (d, ^{4}JC-F= 2 Hz, C-4). IR (KBr): ν 3351, 2933, 2854, 2279, 1604, 1527, 1470, 1410, 1375, 1038 cm^{1}. LRMS (ES, +ve) m/z calculated for $C_{20}H_{20}FN_3O_5$ (401.14): Found 401.4 (15%), 396.6 (5%), 390.7 (1%), 384.2 (3%), 382.3 (7%), 380.6 (50.6), 387.2 (100%), 374.4 (11%), 369.2 (39%), 361.4 (9%), 356.2 (8%), 343.4 (11%), 334.3 (5%), 329.4 (7%), 326.5 (1%), 310.3 (4%), 284.7 (1%), 279.4 (9%), 270.4 (5%), 256.3 (4%), 233.3 (5%), 178.4 (3%), 154.5 (3%), 141.2 (20%), 122.4 (3%), 102.2 (11%), 78.9 (3%), 74.3 (2%).

B13. Synthesis of 9-ethyl-4-fluoro-3-(2-methoxy-phenyl)-6-oxo-6,9-dihydro-3H- [1,2,3] triazolo[4,5-h] quinoline-7-carboxylic acid (13)

Compound 13 was synthesized by cyclizing the previously reduced acid. (9, 0.25 g, 1 mmol) in 20 ml HCl with stirring for 15 minutes in an ice bath(0-5 °C) for 15 minutes. $NaNO_2$ (0.07 g, 1 mmol) dissolved in 10 mL H_2O is added gradually. The reaction mixture was stirred during the night. Improvement of cyclization reaction was checked by TLC and was completed in 24 hours. After that, the reaction mixture was cooled, poured onto mashed ice (250 g) and the resulting light brown precipitate was collected, washed with cold water (2 x 20 mL) and dried. Yield= 0.14 g (≈ 37 %). mp = 219-220 °C; R*f* value in system 1= 0.32. ^{1}H NMR (300 MHz, DMSO-d_6): 1.54 (t, J = 6.47 Hz, 3H, CH_3-1'), 3.78 (s, 3H, OCH_3), 5.27 (s, 2H, NCH_2-1'), 7.22 (dd, J*o* = 7.41 Hz, J*o* = 7.50Hz, 1H, CH-5"), 7.37 (d, J*o* = 8.26 Hz, 1H, CH-3"), 7.71 (m, 2H, CH-4", CH-6"), 8.24 (d, ^{3}JH–F = 23.77 Hz, 1H, H-5), 9.17 (s, 1H, H-8), 15.18 (br s, 1H, COOH). ^{13}C NMR (75 MHz, DMSO-d_6): 16.15 (C-2'), 53.39 (NC-1'), 56.60 (OCH_3), 109.26 (d, ^{2}JC–F = 19.35 Hz, C-5), 110.31 (C-7), 113.24

(C-3"), 121.32 (C-6"), 123.51 (C-9a), 124.50 (C-5a), 128.76 (C-4"), 129.0 (d, ^{2}JC–F = 15.9 Hz, C-3a), 130.67 (C-9b), 133.20 (C-5"), 139.25 (C-1"), 146.10 (d, ^{1}JC–F = 252.53 Hz, C-4), 149.73 (C-8), 154.40 (C-2"), 166.00 (COOH), 176.46 (C-6). IR (KBr): ν 3428, 3067, 2655, 1760, 1622, 1495, 1162, 1084, 1003 cm^{-1}. LRMS (ES, +ve) m/z calculated for $C_{19}H_{15}FN_4O_4$ (382.1): Found 383.3 (23%, M+1), 365.5 (100%), 337.2 (8%), 306.2 (7%).

B14. Synthesis of 9-ethyl-4-fluoro-3-(3-methoxy-phenyl)-6-oxo-6,9-dihydro-3H- [1,2,3] triazolo[4,5-h]quinoline-7-carboxylic acid (14)

Compound 14 was synthesized by cyclizing the previously reduced acid. (10, 0.74 g, 2 mmol) in 20 ml HCl with stirring for 15 minutes in an ice bath (0-5 °C) for 15 minutes. $NaNO_2$ (0.14 g, 2 mmol) dissolved in 10 mL H_2O is added gradually. The reaction mixture was stirred during the night. Improvement of cyclization reaction was checked by TLC and was completed in 24 hours. After that, the reaction mixture was cooled, poured onto mashed ice (250 g) and the resulting light brown precipitate was collected, washed with cold water (2 x 20 mL) and dried. Yield= 0.4 g (≈ 52 %). mp = 240-242 °C; R*f* value in system 1= 0.35. ^{1}H NMR (300 Hz, DMSO d_6): 1.52 (t, J= 6.2 Hz, 3H, CH_3-2'), 3.91 (s, 3H, OCH_3), 5.26 (d, J= 5.96 Hz, 2H, NCH2-1'), 7.23 (d, J*o*= 8.08 Hz, 1H, H-6"), 7.38 (d, J*o*= 7.38 Hz, 1H, H-4"), 7.44 (d, Jm= 3.5 Hz, 1H, H-2"), 7.57 (d, J*o*= 7.92 Hz, J*o*= 7.18 Hz 1H, H-5"), 8.11 (d, ^{3}JH-F= 13.53 Hz, 1H, H-5), 9.13 (s, 1H, H-8), 12.0 (br s, 1H, COOH). ^{13}C NMR (75 Hz, DMSO d_6): 16.1 (C-2'), 53.42 (C-1'), 56.23 (OCH_3), 109.32 (d, ^{2}JC-F= 20 Hz, C-5), 110.22 (C-7), 112.08 (C-2"), 116.68 (C-4"), 118.33 (C-6"), 123.38 (d, ^{4}JC-F= 5.85 Hz, C-9a), 127.78 (d, ^{3}JC-F= 16.05 Hz, C-5a), 130.59 (C-5"), 136.96 (C-3a), 139.59 (C-9b), 144.32 (C-1"), 146.0 (d, ^{1}JC-F= 253.35 Hz, C-4), 149.77 (C-8), 160.17 (C-3"), 165.84 (COOH), 176.27 (C-6). IR (KBr): ν 3389, 3064, 2895, 1720, 1618, 1482, 1136, 1078, 1016 cm^{-1}. LRMS (ES, +ve) m/z calculated for $C_{19}H_{15}FN_4O_4$ (382.1): Found 383.3 (100%, M+1), 374.5 (3.4%), 365.5 (30%), 355.3 (1%), 339.3 (1%), 279.4 (9%), 258.3 (1%), 251.6 (1%), 233.3 (3.4%), 163.3 (9%), 102.2 (10%), 79.9 (5.6%), 74.1 (1%), 60.1 (1%).

B15. Synthesis of 9-Ethyl-4-fluoro-3-(4-methoxy-phenyl)-6-oxo-6,9-dihydro-3H- [1,2,3] triazolo[4,5-h] quinoline-7-carboxylic acid (15)

Compound 15 was synthesized by cyclizing the previously reduced acid. (11, 0.8 g, 2.1 mmol) in 20 ml aqueous HCl, stirred overnight in ice bath (0-5 °C) for 15 minutes. $NaNO_2$ (0.14 g, 2.1 mmol) dissolved in 10 mL H_2O is added gradually. The reaction mixture was stirred during the night. Improvement of cyclization reaction was checked by TLC and was completed in 24 hours. After that, the reaction mixture was cooled, poured onto mashed ice (250 g) and the resulting grayish green precipitate was collected, washed with cold water (2 x 20 mL) and dried. Yield= 0.6 g (≈ 75 %). mp = 305-307 °C; R*f* value in system 1= 0.3. ^{1}H NMR (400 MHz, DMSO-d_6): 1.24 (m, 3H, CH_3-1"), 4.02 (s, 3H, OCH_3), 5.23 (m, 2H, NCH_2-1'), 7.2 (2H, CH-3", CH-5"), 7.42-7.47 (m, 2H, CH-6", CH-2"), 8.16 (1H, H-5), 9.18 (s, 1H, H-8), 15.46 (br s, 1H, COOH). ^{13}C NMR (75 MHz, DMSO-d_6): 16.09 (C-2'), 53.21 (NC-1'), 56.83 (OCH_3), 107.25 (C-7), 109.73 (d, ^{2}JC–F = 19.58 Hz, C-5), 110.37 (2C, C-3", C-5"), 127.77 (2C, C-2", C-6"), 130.72 (C-9b), 131.04 (C-9a), 131.99 (C-5a), 138.22 (C-3a), 138.81 (C-1"), 149.87 (C-8), 151. 25 (d, ^{1}JC–F = 249 Hz, C-4), 162.32 (C-4"), 166.00 (COOH), 176.52 (C-6). IR (KBr): ν 3366, 2978, 2710, 1745, 1625, 1496, 1135, 1073, 1015 cm^{-1}. LRMS (ES, +ve) m/z calculated for $C_{19}H_{15}FN_4O_4$ (382.1): 385.2 (25%, M+3), 366.3 (25%), 364.6 (55%), 336.2 (5%), 186.6 (15%), 122.4 (100%), 104.2 (25%).

B16. Synthesis of 3-(2,4-dimethoxy-phenyl)-9-ethyl-4-fluoro-6-oxo-6,9-dihydro-3H- [1,2,3] triazolo[4,5-h] quinoline-7-carboxylic acid (16)

Compound 16 was synthesized by cyclizing the previously reduced acid (12, 0.5 g, 1.2 mmol) in 20 ml HCl

with stirring for 15 minutes in an ice bath (0-5 °C) for 15 minutes. $NaNO_2$ (0.09 g, 1.2 mmol) dissolved in 10 mL H_2O is added gradually. The reaction mixture was stirred during the night. Improvement of cyclization reaction was checked by TLC and was completed in 24 hrs. After that, the reaction mixture was cooled, poured onto mashed ice (250 g) and the resulting off-white precipitate was collected, washed with cold water (2 x 20 mL) and dried. Yield= 0.35 g (≈ 70 %). mp = 320-322 °C; R*f* value in system 1= 0.58. ^{1}H NMR (400 Hz, DMSO d_6): 1.14 (m, 3H, CH_3-2'), 3.89 (s, 6H, OCH_3-2", OCH_3-4"), 5.32 (m, 2H, NCH_2-1'), 7.23 (d, J= 8.32 Hz, 4.2 Hz, 1H, H-6"), 7.46 (s, 1H, H-3"), 7.78 (d, J*o*= 8.28 Hz, 1H, H-5"), 8.17 (d, JH-F= 10.6 Hz, 1H, H-5), 9.22 (s, 1H, H-8), 14.70 (br s, 1H, COOH). ^{13}C NMR (75 Hz, DMSO d_6): 14.50 (C-1'), 51.80 (C-2'), 54.59 (OCH_3-2"), 55.21(OCH_3-4"), 104.9 (C-5"), 109.5 (d, ^{2}JC-F= 21.5 Hz, C-5), 110.2 (C-7), 113.42 (C-3"), 118.74 (C-9b), 121.81 (C-1"), 126.16 (C-6"), 130.04 (C-9a), 132.15 (C-5a), 136.22 (d, ^{2}JC-F= 13.8, C-3a), 148.12 (C-8), 151.64 (d, ^{1}JC-F= 255, C-5), 154.62 (C-2"), 158.81 (C-4"), 165.63 (COOH), 175.61 (C-6). IR (KBr): ν 3390, 2973, 2643, 2382, 1726, 1621, 1469, 1319, 1089 cm^{-1}. LRMS (ES, +ve) m/z calculated for $C_{20}H_{17}FN_4O_5$ (412.12): Found 412.3 (24%), 411.5 (72%), 404.4 (8%), 399.3 (16%), 397.6 (1%), 390.6 (2%), 384.2 (26%), 383.3 (9.2), 369.2 (3%), 365.5 (37%), 336.3 (3%), 308.6 (2%), 282.5 (2%), 259.3 (2%), 251.5 (1%), 203.5 (2%), 195.4 (4%), 180.4 (1%), 163.3 (3%), 158.2 (9%), 149.0 (4%), 130.5 (3%), 102.2 (1%), 78.9 (2%), 74.3 (1%).

REFERENCES

(1) Appelbaum, P. C. & Hunter, P. A. The fluoroquinolone antibacterials: past, present and future perspectives. International Journal of Antimicrobial Agents, 2000; 16 (1), 5-15.

(2) Edmont, D. S., Rocher, R., Plisson, C. et al.Synthesis and evaluation of quinoline carboxyguanidines as antidiabetic agents. Bioorganic & Medicinal Chemistry Letters, 2000; 10 (16), 1831-1834.

(3) Zhao, Y.-L., Chen, Y.-L., Sheu, J.-Y.et al.Synthesis and antimycobacterial evaluation of certain fluoroquinolone derivatives. Bioorganic & Medicinal Chemistry, 2005; 13 (12), 3921-3926

(4) Lucero, B. D. A., Gomes, C. R. B., Frugulhetti, I. C. D. P. P. et al. Synthesis and anti-HSV-1 activity of quinolonic acyclovir analogues. Bioorganic & Medicinal Chemistry Letters, 2006; 16 (4), 1010-1013.

(5) Shaharyar, M., Ali, M. A. & Abdullah, M. M. Synthesis and antiproliferative activity of 1-[(sub)]-6-fluoro-3-[(sub)]-1, 3, 4-oxadiazol-2-yl-7-piperazino-1, 4-dihydro-4-quinolinone derivatives. Medicinal Chemistry Research, 2007; 16 (6), 292-299.

(6) Al-Hiari, Y. M., Kasabri, V. N., Shakya, A. K. et al. Fluoroquinolones: novel class of gastrointestinal dietary lipid digestion and absorption inhibitors. Medicinal Chemistry Research, 2014a; 23 (7), 1-11.

(7) Sissi, C. & Palumbo, M. The quinolone family: from antibacterial to anticancer agents. Current Medicinal Chemistry-Anti-Cancer Agents, 2003; 3 (6), 439-450.

(8) Kloskowski, T., Gurtowska, N., Nowak, M.et al. The influence of ciprofloxacin on viability of A549, HepG2, A375. S2, B16 and C6 cell lines in vitro. Acta Poloniae Pharmceutica, 2011; 68 859-865.

(9) Azema, J. L., Guidetti, B., Dewelle, J.et al. 7-((4-Substituted) piperazin-1-yl) derivatives of ciprofloxacin: synthesis and in vitro biological evaluation as potential antitumor agents. Bioorganic & Medicinal Chemistry, 2009; 17 (15), 5396-5407.

(10) Kumar, A. R., Lingaiah, B. P. V., Rao, P. S.et al.. Synthesis and biological evaluation of novel N1-decyl and C7-sec amine substituted fluoroquinolones as antitubercular and anticancer agents. Indian Journal of Chemistry, 2015; 54 1495-1501.

(11) Al-Trawneh, S. A., Zahra, J. A., Kamal, M. R.et al. Synthesis and biological evaluation of tetracyclic fluoroquinolones as antibacterial and anticancer agents. Bioorganic & Medicinal Chemistry, 2010; 18 (16), 5873-5884.

(12) Abbas, J. A. & Stuart, R. K. Vosaroxin: a novel antineoplastic quinolone. Expert Opinion on Investigational Drugs, 2012; 21 (8), 1223-1233.

(13) Hawtin, R. E., Stockett, D. E., Byl, J. A. W.et al. Voreloxin is an anticancer quinolone derivative that intercalates DNA and poisons topoisomerase II. PLoS One, 2010; 5 (4), e10186.

(14) Sweidan K, Sabbah DA, Bardaweel S, et al. Facile synthesis, characterization, and cytotoxicity study of new 3-(indol-2-yl) bicyclotetrazatridecahexaens. Can J Chem 2017; 95(8):858-862.

(15) Al-Hiari, Y. M., Abu-Dahab, R. & El-Abadelah, M. M. Heterocycles [h]-Fused Onto 4-Oxoquinoline-3-Carboxylic Acid, Part VIII [1]. Convenient Synthesis and Antimicrobial Properties of Substituted Hexahydro [1, 4] diazepino [2, 3-h] quinoline-9-carboxylic acid and Its Tetrahydroquino [7, 8-b] benzodiazepine Analog. Molecules, 2008; 13 (11), 2880-2893.

(16) Al-Hiari, Y. M., Shakya, A. K., Alzweiri, M. H. Synthesis and biological evaluation of substituted tetrahydro-1h-quino [7, 8-b][1, 4] benzodiazepine-3-carboxylic derivatives. FARMACIA, 2014b; 62 (3), 570-588.

(17) Winkler, F. K., D'arcy, A. & Hunziker, W. Structure of human pancreatic lipase. Nature, 1990; 343 (6260), 771-774.

(18) Lowe, M. E. Structure and function of pancreatic lipase and colipase. Annual Review of Nutrition, 1997; 17 (1), 141-158.

(19) Birari, R. B. & Bhutani, K. K. Pancreatic lipase inhibitors from natural sources: unexplored potential. Drug Discovery Today, 2007; 12 (19), 879-889.

(20) Vichai, V., and Kirtikara, K. Sulforhadamine B colorimetric assay for cytotoxicity screening. Nature Protocols, 2006; 1, 1112-1116.

(21) Kasabri, V., Afifi, F. U., Abu-Dahab, R. In vitro modulation of metabolic syndrome enzymes and proliferation of obesity-related-colorectal cancer cell line panel by Salvia species from Jordan. Revue Roumaine de Chimie, 2014; 59 693-705.

(22) Nitiss, J. L. Targeting DNA topoisomerase II in cancer chemotherapy. Nature Reviews Cancer, 2009; 9(5), 338-350.

(23) Molinspiration server (www.molinspiration.com): Molinspiration property engine v2021.10

(24) MarvinSketch16.10.24 ChemAxon - Software Solutions and Services for Chemistry & Biology 2016.

(25) OMEGA, O. 2.5. 1.4: OpenEye Scientific Software, Santa Fe, NM. Google Scholar There is no corresponding record for this reference.

(26) Wu, C. C., Li, T. K., Farh, L.et al. Structural basis of type II topoisomerase inhibition by the anticancer drug etoposide. Science, 2011; 333(6041), 459-462.

(27) OEDOCKING 3.2.0.2: Open Eye Scientific Software, Santa Fe, NM. http://www.eyesopen.com

(28) BIOVIA, Dassault Systemes, BIOVIA Discovery Studio Visualizer, v17.2.0.16349, San Diego: Dassault systems, 2016.

(29) Mitscher, L. A. Bacterial topoisomerase inhibitors: quinolone and pyridone antibacterial agents. Chemical Reviews, 2005; 105 (2), 559-592.

(30) Al-Hiari, Y. M., Qaisia, A. M., Shuheil, M. Y. A.et al. Synthesis and Antibacterial Potency of 4-Methyl-2, 7-dioxo-1, 2, 3, 4, 7, 10-hexahydropyrido [2, 3-f] quinoxaline-8-carboxylic acid, Selected [a]-Fused Heterocycles and Acyclic Precursors. Zeitschrift fuer Naturforschung B: Chemical Sciences, 2007b ; 62 (11), 1453-1458.

(31) Al-Hiari, Y. M., Qandil, A. M., Al-Zoubi, R. M.et al. (2010), 7-(3-Chlorophenylamino)-1-cyclopropyl-6-fluoro-8-nitro-4-oxo-1, 4-dihydroquinoline-3-carboxylic Acid. Molbank, 2010 (2), M669.

(32) Arabiyat, S., Kasabri, V., Al-Hiari, Y.et al. Antilipase and antiproliferative activities of novel fluoroquinolones and triazolofluoroquinolones. Chemical Biology & Drug Design, 2017; 90(6), 1282-1294.

(33) World Cancer Research, F. & American Institute for Cancer, R. Food, nutrition, physical activity, and the prevention of cancer: a global perspective. American Institution for Cancer Research, 2007.

(34) Kathiravan, M. K., Khilare, M. M., Nikoomanesh, K.et al. Topoisomerase as target for antibacterial and anticancer drug discovery. Journal of Enzyme Inhibition and Medicinal Chemistry, 2013; 28 (3), 419-435.

(35) Arabiyat, S., Kasabri, V., & Al-Hiari, Y. Antilipolytic-Antiproliferative Activity of Novel Antidiabesity Triazolo/Fluoroquinolones. Jordan J. of Pharm. Scie., 2020; 13(1).

(36) Khaleel, S., Al-Hiari, Y., Kasabri, V.et al. Antiproliferative Properties of 7, 8-Ethylene Diamine Chelator-Lipophilic Fluoroquinolone Derivatives Against Colorectal Cancer Cell Lines. Anti-Cancer Agents in Medicinal Chemistry (Formerly Current Medicinal Chemistry-Anti-Cancer Agents), 2022; 22(5), 1012-102835.

(37) Lipinski CA, Lombardo F, Dominy BW, Feeney PJ. Experimental and computational approaches to estimate solubility and permeability in drug discovery and development settings. Adv Drug Deliv Rev. 2001; 46(1-3):3-26

(38) Veber DF, Johnson SR, Cheng HY.et al.Kopple KD. Molecular properties that influence the oral bioavailability of drug candidates. J Med Chem. 2002; 45(12):2615-23.

(39) Nath, A., Kumer, A., Zaben, F.et al. Investigating the binding affinity, molecular dynamics, and ADMET properties of 2, 3-dihydrobenzofuran derivatives as an inhibitor of fungi, bacteria, and virus protein. Beni-Suef University Journal of Basic and Applied Sciences, 2021; 10(1), 1-13.

(40) Arabiyat, S., Kasabri, V., Al-Hiari, Y.et al. Dual glycation-inflammation modulation, DPP-IV and pancraetic lipase inhibitory potentials and antiproliferative activity of novel fluoroquinolones. Asian Pacific journal of cancer prevention: APJCP, 2019; 20(8), 2503.

(41) Bentley, D., Young, A.-M., Rowell, L.et al. Evidence of a drug-drug interaction linked to inhibition of ester hydrolysis by orlistat. Journal of Cardiovascular Pharmacology, 2012; 60 (4), 390-396.

(42) Habtemariam, S. The anti-obesity potential of sigmoidin A. Pharmaceutical Biology, 2012; 50 (12), 1519-1522.

(43) Arabiyat, S., Al-Hiari, Y., Bustanji, Y.et al. In Vitro modulation of pancreatic lipase and proliferation of obesity related colorectal cancer cell line panel by novel synthetic triazoloquinolones. Rev. Roum. Chim, 2016; 61(11-12), 871-879.

(44) Al-Hiari, Y., Sweileh, B., Shakya, A.et al. Synthesis of 1-Benzyl-1, 2, 3, 4-Tetrahydroisoquinoline, Part I: Grignard Synthesis of 1-(Substitutedbenzyl)-1,2,3,4-Tetrahydroisoquinoline Models with Potential Antibacterial Activity, Jordan J. of Pharm. Sci., 2009; 2(1), 1-21, 2009.

تخلب المعادن كميكانيكية لعلاج السرطان: الجزء الأول؛ مركبات جديدة من مشتقات 7- انيسيدين مع متعدد التخلب في ذرات الكربون 7-8 في نموذج حلقة الفلوروكوينولون كمضاد محتمل للسرطان ومضاد محتمل لتسكير الدهون

يوسف الحياري [1، 2]، شيرين عربيات [3]، فيوليت كسابري [1]، عماد حمدان [1]، ليهاب المصري [4]، محمد ياسين محمد[5]، داليا السعد [6]

[1] كلية الصيدلة، الجامعة الأردنية، عمان، الأردن.
[2] كلية الصيدلة، جامعة الزيتونة الأردنية، الأردن.
[3] جامعة البلقاء التطبيقية، الأردن.
[4] قسم الكيمياء الصيدلانية والعقاقير، كلية الصيدلة، جامعة الأزهر- غزة، فلسطين.
[5] كلية الصيدلة، جامعة العقبة للتكنولوجيا، الأردن.
[6] قسم العلوم الأساسية والإنسانية، كلية العلوم، الجامعة الأمريكية في مادبا، الأردن.

ملخص

الخلفية: السرطان هو أحد أعظم الأمراض المزعجة في الوقت الحالي. يُعتقد أنه السبب الثاني للوفاة بعد أمراض القلب والأوعية الدموية. نظرا لتعدد أنواعها ومراحلها وأساسها الجيني، فلا يوجد دواء موجود لعلاج جميع أنواع السرطان. تعتبر مقاومة الأدوية الحالية والآثار الضارة الشديدة من التحديات الأخرى في مكافحة السرطان. في مثل هذا المسعى، تمتلك الفلوروكينولونات (FQs) إمكانات كمركبات مضادة للتكاثر بسبب السلامة والتكلفة المنخفضة وغياب المقاومة.

الهدف: في هذه الدراسة، نهدف إلى تصنيع مركبات نشطة بيولوجيًا لها إمكانات مزدوجة مضادة للسرطان ومضادة لليبيز. تم تحضير ستة عشر مركبًا، وتم تصنيفها بالكامل، ودراستها من خلال تحديد قيم IC50 ضد خطوط الخلايا السرطانية شديدة الحساسية.

المنهجية: في هذا العمل، نحن مهتمون بتجميع المركبات النشطة بيولوجيًا التي تنتمي إلى الفلوروكينولونات (FQs) مع نشاط مزدوج مضاد لسرطان القولون والمستقيم ومضاد لليبيز، نظرًا للارتباط بين السرطان والسمنة، وإجراء تجارب المعايرة ومحاكاة الارتباط للتحقق من صحة فرضيتنا

النتائج: أشارت النتائج في المختبر إلى أن هذه المركبات أظهرت نشاطًا واعدًا مضادًا للسرطان ضد خطوط الخلايا المختبرة في نطاق الميكرومولار بقوة مماثلة لسيسبلاتين. أظهر المركب 11 فاعلية مضاعفة تقريبًا مقارنة بالسيسبلاتين ضد خط خلايا سرطان القولون والمستقيم SW620 مع IC50 3.2 ميكرومتر والذي يقترح FQs كعوامل فعالة مضادة للتكاثر. تم فحص مركبات الفلوروكينولون المُصنَّعة (FQ) بشكل إضافي لمعرفة إمكاناتها المضادة لليباز في المختبر. أظهرت النتائج أن جميع المركبات التي تم فحصها أظهرت نشاطًا ملحوظًا مضادًا لليبيز، مقارنةً بجزيء التحكم أورليستات. أظهر المركب 9 نشاطًا مشابهًا لأورليستات ضد الليباز البنكرياس مع IC50 0.4 ميكرومتر والذي يقترح FQs كمثبطات قوية لليبيز البنكرياس

الخلاصة: تشير الإمكانات المضادة للسرطان لهذه المشتقات إلى قدرتها على تثبيط أنزيم Topo II مما يشير إلى أن عملية الاتحاد مع المعادن الثقيلة هي آلية تثبيط أنزيم Topo II التي يتم التأكيد عليها من خلال تجارب المعايرة ومحاكاة الارتباط.

الكلمات الدالة: مخلبات المعادن، متعدد التخلب، الفلوروكوينولونات، مضاد سرطاني مخلب.

---

* ***المؤلف المراسل: يوسف الحياري***

hiary@ju.edu.jo

تاريخ الإستلام 2023/1/11 تاريخ قبول النشر 2023/3/29.

Jordan Journal of Pharmaceutical Sciences, Volume 16, No. 2, Supplement 1, 2023

Synthesis and Biological Evaluation of Carbonic Anhydrase III and IX Inhibitors using Gas Chromatography with Modified pH-Sensitive Pellets

Buthaina Hussein[1&*], Laurance M. S. Bourghli [1&*], Muhammed Alzweiri[2], Yusuf Al-Hiari[2], Mohammad Abu Sini[1], Soraya Alnabulsi[3], Batool Al-Ghwairi[1]

[1] Department of Pharmacy, Faculty of Pharmacy, Al-Zaytoonah University of Jordan, Jordan.
[2] Department of Pharmaceutical Sciences, Faculty of Pharmacy, The University of Jordan, Amman, Jordan.
[3] Department of Medicinal Chemistry and Pharmacognosy, Faculty of Pharmacy, Jordan University of Science and Technology, Jordan.
[&] Both authors contributed equally.

ABSTRACT

Fifteen compounds were synthesized and tested as potential carbonic anhydrase III (CAIII) and carbonic anhydrase IX (CAIX) inhibitors, six of which are novel. Amides (**a1-4**), hydroxamic acids (**b1-2**), and imines (**c1-9**) derivatives were evaluated for their inhibitory activity against CAII and CAIX using gas chromatography with modified pH-sensitive pellets. The derivatives showed inhibition percentages between 12-56% for CAIII and 44-59% for CAIX, compared to 49% and 63% for captopril (the positive control), respectively. Imines showed the best inhibition of CAIII, while all derivatives showed comparable activity against CAIX. It is hypothesized that the nitrogen atom in imine, amide, or hydroxamic acid moieties in the vicinity of an ionizable group is in coordination with the zinc ion in the active site. Furthermore, the candidates were tested for their antimicrobial and antifungal activity. Generally, they showed low to zero activity against some gram-positive and negative bacteria. This supports the theory of their ability to bind to human carbonic anhydrase but not to bacterial one. These compounds could serve as useful scaffolds to develop more potent and selective carbonic anhydrase inhibitors as anti-obesity and anticancer candidates.

Keywords: Carbonic anhydrase III, Carbonic anhydrase IX, inhibitors, amides, hydroxamic acids, imines, zinc chelation.

Introduction

Carbonic anhydrases (CAs) are metalloenzymes spread in archaea, bacteria, plants, and eukaryotes[1, 2] Up to date, there are eight distinct classes of CAs α, β, γ, δ, η, ζ, and ι [1]. CAs catalyze the reaction involving the conversion of carbon dioxide to bicarbonate and protons, which is essential for pH regulation, electrolytes, gases, and anion balance[1,3]. Furthermore, CAs exhibit weak esterase activity[4].

The classes (α, β, γ, and ι) are the ones that exist in bacteria[5], β-CAs are the most distributed class in bacteria[6], where they are required for CO_2 transport[7, 8], and the growth of the microbe in general[5]. α and β CAs are abundant in fungi and yeasts, which have a crucial role in the fungi's survival. Sulfonamides, dithiocarbamates, and thiols were reported to show activity on fungi such as *candida albican* [9].

α-CA isoform is expressed in human cells and has a significant role in human pathology[4]. Human CA inhibitors such as sulfonamides have been in clinical use for decades as diuretics, anti-obesity, antiglaucoma, antiepileptic, and even anti-cancer[1, 10], [11-13]. Twelve isoforms out of fifteen known human CAs are catalytically active[3].

[*]***Corresponding author:***
Buthaina Hussein, Laurance M. S. Bourghli
buthina.hussein@zuj.edu.jo , laurance.bourghli@zuj.edu.jo
Received: 10/1/2023 Accepted: 30/3/2023.
DOI: https://doi.org/10.35516/jjps.v16i2.1470

Carbonic anhydrase III (CAIII), which belongs to α-CAs, is considered one of the weakest carbonic anhydrases regarding its catalytic activity in converting CO_2 to carbonic acid [3, 13, 14]. It has also shown weak binding with sulfonamides, the classical CAs inhibitors[13, 14]. Regulation of adipogenesis is one of the proposed physiological roles for CAIII. In addition to its high expression in adipocytes[3], Mitterberger *et al.* figured out that CAIII knocked-down adipocytes are associated with gene expressions leading to altering lipid metabolism[15], making CAIII a reasonable candidate for agents targeting hyperlipidemia[10, 16, 17].

On the other hand, Carbonic anhydrase IX (CAIX) is a tumor-associated isoform, significantly expressed in a wide variety of solid tumors[2]. Its expression is associated with hypoxic cancer types [3]. Its contribution to pH regulation helps protect the tumor cell from acidosis and contributes to the chemoresistance of some basic anticancer agents [18-20].

Up to date, several classes of CAs inhibitors are known[21, 22]. Metal complexing anions[1], unsubstituted sulfonamide and sulfamate[6, 21, 22], sulfamic acid, phenylboronic acid [23], dithiocarbamates[5], carboxylic acids [5], sulfonamides and their derivatives have been the most class investigated[21, 22]. Sulfa drugs are an old class of antibacterial agents. However, sulfonamides have many other pharmacological actions rather than antimicrobial such as anti-diabetes, antifungal, antimalarial, diuretics (e.g., hydrochlorothiazide), Alzheimer's disease [24] and rheumatoid arthritis (Sulfasalazine)[9]. This extended targets of sulfonamides in addition to their ability to inhibit both the human and bacterial carbonic anhydrase, such as ethoxzolamide and acetazolamide which were found to inhibit *Helicobacter Pylori* and vancomycin-resistant *Enterococcus spp*. respectively[5], rising up more side effects and make sulfonamides not ideal CAs inhibitor [10]. This encourages the rationale of finding new classes rather than sulfonamide to inhibit carbonic anhydrase. Accordingly, previous projects conducted by our team to find out new selective agents including vanillic acid, benzoic acid and nicotinic acid derivatives [10, 16, 17] where it was revealed the importance of carboxylic acid moiety in coordinating to Zn atom. In this study a group of variant moieties were synthesized and biologically tested against CAIII and CAIX.

2. Results and Discussion

2.1 Synthesis

Based on the fact that the zinc atom is responsible for the binding mode of the CAs enzymes to their inhibitors[25], this study focuses on finding new zinc binder moieties rather than sulfonamide and testing them as potential CAIII and CAIX inhibitors. Amide, imine, and hydroxamic acid derivatives were synthesized and biologically tested[26-28].

As shown in **scheme** (**1**), amide derivatives (**a1-2**) were synthesized by the direct amidation reaction between the carboxylic acid and the amines. The carbonyl group is activated using DCC, and HOBT catalyzes the reaction[29-31]. The synthesis of amides (**a3-4**) was performed by the direct nucleophilic addition reaction of the corresponding amine with maleic anhydride[32, 33].

Hydroxamic acid derivatives (**b1-2**) [34, 35] were synthesized by converting the corresponding carboxylic acid into the acid chloride using oxalyl chloride, then treating the crude acid chloride with hydroxylamine hydrochloride[36].

Imines (Schiff bases; **c1-c9**), shown in **scheme (2),** were prepared by the classical nucleophilic addition reaction of a 1^{o} amine with an aldehyde[36]. *o*-Vanillin, vanillin, and quinoline-8-carbaldehyde were used to synthesize imines **c1**, **c2**[37], **c3**[38], **c4**[39], **c5**[40], **c6**[41], **c7**[42], **c8**, and **c9**[43].

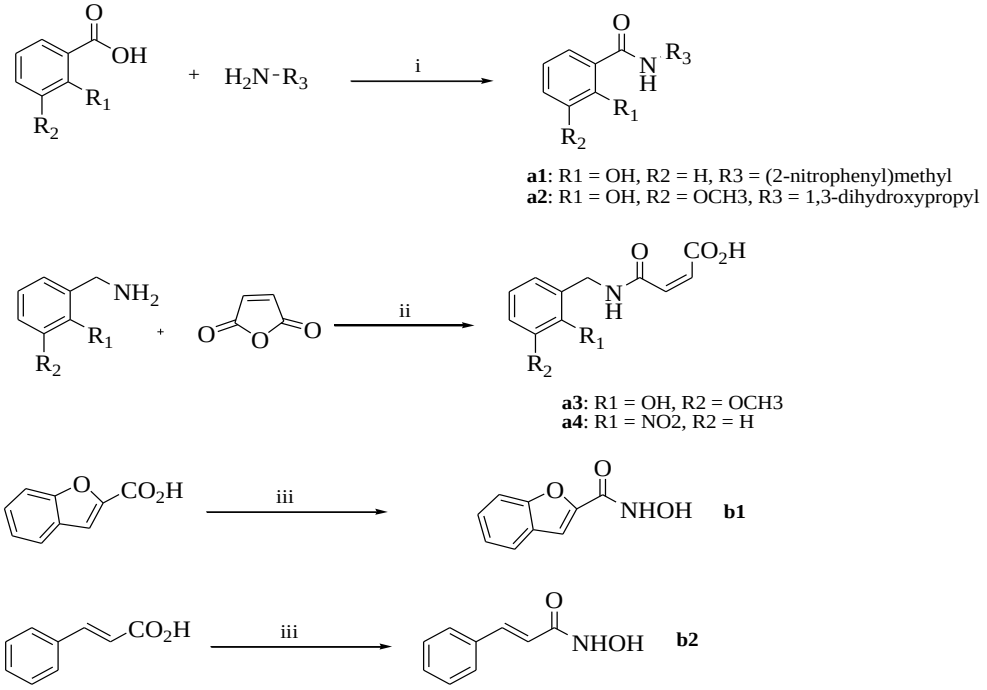

a1: R1 = OH, R2 = H, R3 = (2-nitrophenyl)methyl
a2: R1 = OH, R2 = OCH3, R3 = 1,3-dihydroxypropyl

a3: R1 = OH, R2 = OCH3
a4: R1 = NO2, R2 = H

b1 **b2**

Scheme 1: Chemical synthesis of the different amide and hydroxamic acid derivatives: i) DCC, HOBt/THF, stir, r.t, ii) 1) TEA, MeOH, rt 2) 1M HCl iii) 1) oxalyl chloride, DMF, DCM 2) $NH_2OH.HCl$, KOAc, rt

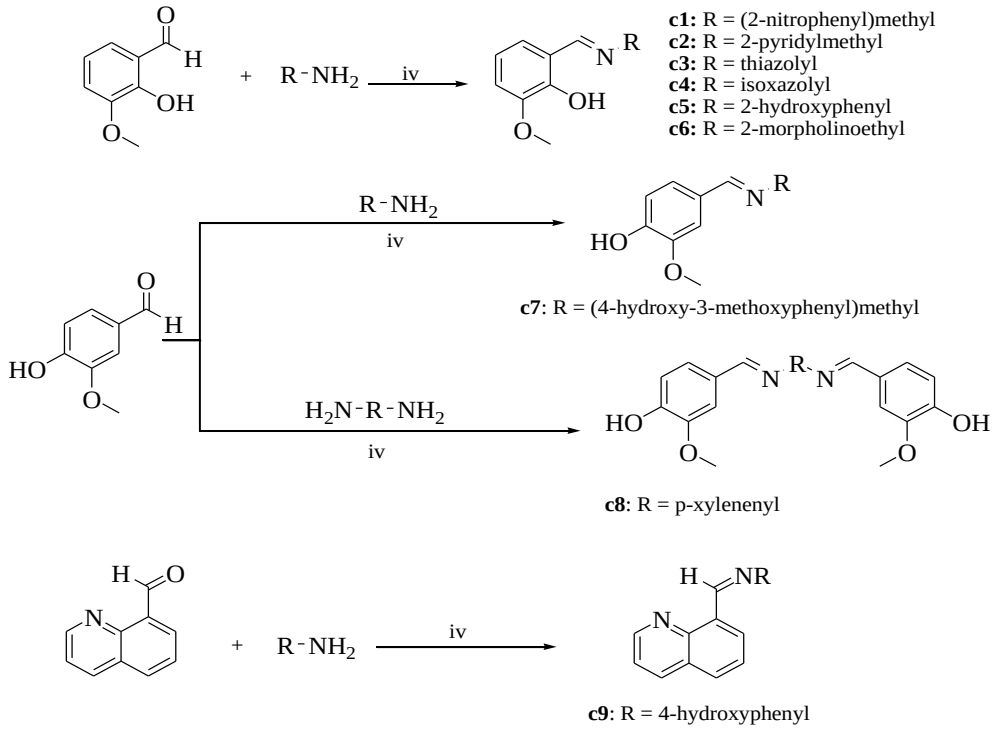

c1: R = (2-nitrophenyl)methyl
c2: R = 2-pyridylmethyl
c3: R = thiazolyl
c4: R = isoxazolyl
c5: R = 2-hydroxyphenyl
c6: R = 2-morpholinoethyl

c7: R = (4-hydroxy-3-methoxyphenyl)methyl

c8: R = p-xylenenyl

c9: R = 4-hydroxyphenyl

Scheme 2: Chemical synthesis of the different imine derivatives: iv) CH_3OH or CH_3CH_2OH

2.2 Inhibition of Enzyme Activity

Fifteen compounds were screened for their inhibitory activity against CAIII and CAIX using the new method adopted by our team. Alzweiri et al. presented a novel gas chromatography-based approach with good GC-FID detection sensitivity[44, 45]. The approach is based on using pH-sensitive pellets to assess CA esterase activity. These Pellets comprise a volatile chemical (limonene) encapsulated in a calcium alginate matrix and a pH-sensitive polymer such as eudragit E. As the medium becomes more acidic, reaching pH 5, the action enzyme activity increases the emission of the volatile chemical limonene. The suggested inhibitor will lower the enzyme's activity and, therefore, release limonene. The fluctuation in the amount of the volatile chemical reflects the tested drug's action against CAs[17]. Captopril was employed as a positive control because, as previously documented by our research, it has strong action against CA[4].

Table 1: Inhibition percentage of the proposed inhibitors against CAIII and CAIV

	CAIII Inhibition% (1 µM)	**CAIX Inhibition% (1 µM)**
a1	46.1	58.35
a2	45.02	51.48
a3	17.49	46.12
a4	31.08	44.79
b1	24.38	59.64
b2	not tested	not tested
c1	56.6	54.87
c2	24.0	48.28
c3	31.36	55.93
c4	26.23	54.59
c5	14.8	55.14
c6	44.42	49.61
c7	47.18	54.19
c8	12.3	51.29
c9	42.87	53.55
Captopril	49.38	63.52

Table (1) shows the inhibition percentage of the synthesized derivatives. The imine **c1** shows the best inhibition percentage against CAIII (56.6%) at 1 µM, whereas imine derivative **c2** showed a percent inhibition of only 24%, and that of **c5** dropped to 14.8%. Similarly, the percentage inhibition of **a4** (31.08%) is about twice as much as that of **a3** (17.49%). This variation in the inhibitory action could be attributed to the existence of the highly polar nitro group in close vicinity to the nitrogen atom of either the imine or the amide, which in turn may allow for the chelation of the zinc ion.

Looking at the imine derivative **c6** with a percentage inhibition of 44.42%, this could be attributed to a similar analogy that the nitrogen atom of the morpholine ring could be positioned in close vicinity to the imine nitrogen through rotation around the carbon-carbon single bond in an eclipsed conformation, allowing once more for the chelation to the zinc ion.

The close vicinity between the imine nitrogen and the quinolone nitrogen in derivative **c9**, allowing for the chelation

to the zinc ion, may also explain the somewhat high percent inhibition of this derivative with 42.87%.

The importance of the vicinity of two chelating groups for the successful binding to the zinc ion may be exemplified by the low percentage inhibition (12.3%) of the imine derivative **c8**. In this derivative, there is no close donor atom to the imine nitrogen, thus limiting the possible chelation to the zinc ion, which needs a bidentate ligand for chelation.

This hypothesis could be extended to explain the percent inhibition of **a1** (46.1%) and **a4** (31.08%). Both derivatives have a nitro group in the vicinity of the amide nitrogen, forming a bidentate suitable to bind to the zinc ion. Regarding the amide derivative **a2**, with a percent inhibition of 45.02%, the free rotation around the carbon-carbon single bond of the primary alcohol brings the donor oxygen atom in close vicinity to the amide nitrogen, allowing for the chelation of the zinc ion.

For CAIX, the percentage inhibition, in general, was higher than for CAIII with almost all the derivatives. The inhibition percentages were around (40-60)%. Captopril has higher % inhibition; 49.38% for CAIII and 63.52% for CAIX. This could be explained by the difference in the active site where the CAIII is narrow and cone-like and has less catalytic activity than other CAs. CAIX has a hydrophobic region about 10-15 A° away from the zinc atom and is close to the entrance of the active site[46]. These differences in the size and shape of the active site may rely on the differences in the activity and the ability of the CAIX to interact with the different scaffolds used in this project. The proposed SAR could be summarized as in **scheme (3)** below:

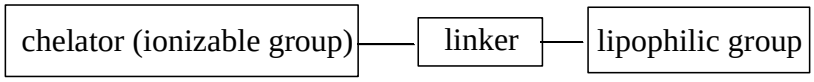

Scheme 3: Summary of the proposed SAR of the tested compounds as CA inhibitors

The chelator could be varied, such as the imine and the adjacent nitro group, or the imine and the adjacent amine group, or the amide and the adjacent nitro group, or even the amide with the adjacent hydroxyl group. These could be seen in **c1**, **c6**, **a1**, and **a2,** respectively. At the same time, the lipophilic part of the derivatives could be much more important for the CAIX than for CAIII as the pocket is small and narrow. Consequently, not all the derivatives show comparable inhibition percentage for both enzymes. The lipophilic part varied between the benzene ring, benzofuran (**b1**), and quinoline (**c9**).

In general, the inhibition percentages reported in this work show a good ability to inhibit CAIII and CAIX with comparable results to the captopril (the positive control) and some reported results by our team. For example, nicotinic acid derivatives which showed oxygen coordinate to the zinc atom gave inhibition percentage range between 40-90 % at 10 µM[45].

2.3 Antimicrobial and Antifungal Activity

The previous results encouraged testing some synthesized compounds against their ability to inhibit bacterial growth. Bearing in mind that β-CAs active site poses little similarity with human α-CAs increasing the possibility of finding selective α-CAs inhibitors[8]. The synthesized compounds were tested to find their antimicrobial activity. Kirby-Bauer Disk, Diffusion Susceptibility Test was performed to know the inhibition zone for the samples. While the Broth dilution method (196 microplates well) was used to determine the lowest concentration of an antimicrobial agent that prevents visible growth of the microorganism, the result was calculated by calculating the mean value. **Table** (**2**) lists the derivatives that showed activity against different bacterial strains and *Candida albicans*. Imine derivatives (**c1-4**) were inactive against bacterial strain but showed good activity against *candida albicans* with MIC ranging from (0.625-1.25 mM) compared to 0.15 mM for Nestatine as a control.

Meanwhile, hydroxamic acid derivatives (**b1-2**) showed antimicrobial activity with a low millimolar compared to the control, while **b1** showed activity against *C. albicans* with equal MIC to that of imines. Unfortunately, **b2** did not show the same activity. The amide derivatives (**a1-4**) were inactive at these concentrations. It is known that hydroxamic acids have good antimicrobial, antifungal and antitumor activity owing to their ability to bind to many metalloenzymes. They also have low toxicity and weak acid properties[47-49]. These results support the hypothesis of the ability of these agents to inhibit CAs via zinc complexation. Thus, the track will keep open for further modification on these derivatives to enhance their activity.

Table 2: Antimicrobial activity by disc diffusion method (mm) and Minimum inhibition concentration (MIC) for the tested compounds against different organisms.

	Disc Diffusion method (mm)			Minimum Inhibition Concentration (MIC)		
Tested compound	***Escherichia coli* (mm)**	***Staphylococcus aureus* (mm)**	***Candida albicans* (mm)**	***Escherichia coli* (mM)**	***Staphylococcus aureus* (mM)**	***Candida albicans* (mM)**
c1	0	0	16	-----	-----	1.25
c2	0	0	15	-----	-----	0.625
c3	0	0	16	-----	-----	1.25
c4	0	0	16	-----	-----	1.25
b1	12	8	19	1.25	2.5	1.25
b2	0	8	0	------	2.5	-------
Levofloxacin	24	32	0	0.00488	0.025	-------
Amoxicillin/ Clavulanic acid	20	42	0			
Trimethoprim/ Sulfamethoxazol	24	21	0			
Nystatin	0	0	21	------	------	0.15

The synthesized compounds showed inactivity to low activity against some gram-positive and negative bacteria, which is considered good as we propose their ability to inhibit the human carbonic anhydrases rather than the bacterial ones.

3. Experimental

3.1. Synthesis

3.1.1. General procedure for the synthesis of amide derivatives (a1-2)

After adding the amine to a solution of the carboxylic acid (1 mmoL) in dry THF (15 mL) and stirring, the DCC (1.2 mmoL) and HOBT (1.2 mmoL) were added (1 mmoL). Overnight, the reaction mixture was left to stir at room temperature. Ethyl acetate was extracted from the white precipitate and diluted with water (30 mL) (x3). After brine washing, drying ($MgSO_4$), and rotational evaporation, the combined organic extracts were ready for use. The amide product crystallized out of the ethyl acetate/hexane mixture and appeared white.

N-(2-Nitrobenzyl)-2-hydroxybenzamide (a1)

It was collected as a white solid (0.56 g, 57%), m.p. 110-112°C. ^{1}H NMR (400 MHz, DMS-d_6): δ 12.10 (1H, s, OH), 9.35 (1H, s, NH), 8.06-8.08 (1H, d), 7.90-7.92 (1H, d), 7.73-7.75 (1H, m), 7.57-7.62 (2H, m), 7.43 (1H, m), 6.93-6.95 (2H, m), 4.81 (2H, s, CH_2N). HRMS (ESI): m/z calculated for $C_{14}H_{12}N_2O_4$ + H^+ 273.2641; found 273.0763.

N-(1,3-Dihydroxypropan-2-yl)-4-hydroxy-3-methoxybenzamide (a2)

Collected as white solid (0.18 g, 24%), m.p. 133-136°C.^{1}H NMR (400 MHz, DMS-d_6): δ 9.43 (1H, br s, OH), 7.62-7.65 (1H, d), 7.35 (1H, s), 7.28-7.30 (1H, d, NH), 6.71-6.73 (1H, d), 4.55-4.58 (2H, t, 2 x CH_2OH), 3.81-3.88 (1H, m, NHC*H*), 3.74 (3H, s, OCH_3), 3.43-3.49 (4H, t, 2 x CH_2OH). ^{13}C NMR (100 MHz, DMS-d_6): δ 165.87, 149.29, 146.98, 125.71, 120.79, 114.62, 111.43, 60.41, 55.67, 53.68. m/z calculated for $C_{11}H_{15}NO_5$ 241.24; found 241.09.

3.1.2. General procedure for the synthesis of amide derivatives (a3-4)

The amine (1.3 mmoL) was dissolved in methanol (7 mL) and triethylamine (3 mL), and then maleic anhydride was added while the mixture was agitated (1.3 mmoL). The product precipitated after being agitated in a reaction mixture containing 10 mL of 1M HCl slowly throughout the previous night. Products were filtered, washed many times, and dried in an oven overnight.

(Z)-4-(2-Hydroxy-3-methoxybenzylamino)-4-oxobut-2-enoic acid (a3)

They were prepared as previously mentioned. However, the product was extracted after adding 1M HCl using dichloromethane. The desired chemical was obtained as a white solid (0.21g, 68%) when the mixed organic extracts were washed with water, dried (MgSO4), and evaporated.^{1}H NMR (400 MHz, DMS-d_6): *δ* 9.38-9.40 (1H, t, NH), 8.07 (1H, br s, OH), 6.73-6.91 (3H, m), 6.47-6.50 (1H, d), 6.26-6.29 (1H, d), 4.34-4.35 (2H, d, CH_2N), 3.79 (3H, s, OCH_3). HRMS (ESI): m/z calculated for $C_{12}H_{13}NO_5 - H^+$ 250.2274; found 250.0681.

(Z)-4-((2-Nitrobenzyl)amino)-4-oxobut-2-enoic acid (a4)

It was collected as a white powder (0.25 g, 77%), m.p. 142-144°C. ^{1}H NMR (400 MHz, DMS-d_6): *δ* 9.29 (1H, br s, NH), 8.06-8.08 (1H, dd), 7.72-7.76 (1H, dt), 7.64-7.66 (1H, d), 7.55-7.59 (1H, dt), 6.43-6.46 (1H, d), 6.24-6.27 (1H, d), 4.66-4.67 (2H, d, CH_2N). ^{13}C NMR (100 MHz, DMS-d_6): δ 166.66, 165.98, 148.37, 134.32, 133.56, 132.02, 131.71, 130.51, 129.06, 125.15 (chemical shift for CH_2N carbon is combined with DMS signal peaks). HRMS (ESI): m/z calculated for $C_{11}H_{10}N_2O_5 + H^+$ 251.2155; found 251.0588.

*3.1.3. General procedure for the synthesis of hydroxamic acid derivatives (*b1-2)

Carboxylic acid (1 mmoL) and dichloromethane (1 mmoL) in dichloromethane (100 mL) were chilled to 0 degrees Celsius. Afterward, oxalyl chloride (2.5 mmoL) was injected gradually, sparking a rapid release of gas. After stirring for an hour, the reaction mixture was combined with a THF/water solution of hydroxylamine hydrochloride (4.0 mmoL) and triethylamine (6.0 mmoL) (50:10). The ingredients were combined and agitated for 30 minutes before being added to 2 N HCl. Extracting the product using dichloromethane (x 2), then washing the mixed organic layer with brine, drying it (MgSO4), and rotary-evaporating it. Aqueous ethanol was used to create the crystals.

N-Hydroxybenzofuran-2-carboxamide (b1)

Collected as white solid (0.16g, 58%), m.p. 150-153°C. ^{1}H NMR (400MHz, DMS-d_6) δ 11.47 (1H, br s), 9.28 (1H, br s), 7.76-7.78 (1H, d), 7.64-7.66 (1H, d), 7.44-7.49 (2H, m), 7.32-7.36 (1H, m). m/z calculated for $C_9H_7NO_3$ 177.16; found 177.04.

N-Hydroxycinnamamide (b2)

Collected as white solid (0.17g, 60%), 255°C (with decomposition). ^{1}H NMR (400MHz, DMS-d_6) δ 7.55-7.57 (2H, d), 7.40-7.46 (6H, m), 6.46-6.50 (1H, d). m/z calculated for $C_9H_9NO_2$ 163.17; found 163.06.

3.1.4. General procedure for the synthesis of imine derivatives (c1-c9)

To a stirred solution of the corresponding amine (10.6 mmoL) in ethanol or methanol (20 mL) was added the

aldehyde (9.7 mmoL). The reaction was stirred for (1-2) days, and then the yellow precipitate was filtered, washed with ethanol, and dried.

***(E)-2-((2-Nitrobenzylimino)methyl)-6-methoxyphenol* (c1)**

Potassium acetate (0.55 g, 5.60 mmoL) was added to the solution, and the product was crystallized from dichloromethane/ether to afford the product as yellow-orange crystals (0.28 g, 18%), m.p. 70-71°C. ^{1}H NMR (400 MHz, DMS-d_6): δ 13.21 (s, OH, 1H), 8.72 (s, CH=N, 1H), 8.09-8.07 (d, 1H), 7.80-7.76 (t, 1H), 7.65-7.59 (m, 2H), 7.09-7.07 (d, 2H), 6.88-6.84 (t, 1H), 5.11 (s, CH_2N, 2H), 3.79 (s, OCH_3, 3H). HRMS (ESI): m/z calculated for $C_{15}H_{14}N_2O_4$ + H^+ 287.2907; found 287.0912.

***(E)-2-Methoxy-6-((pyridin-2-ylmethyl)imino)methyl)phenol* (c2)**

Collected as yellow solid (0.56 g, 24%), m.p. 85-87°C. ^{1}H NMR (400 MHz, DMS-d_6): δ 13.60 (1H, br s, OH), 8.73 (1H, s, CH=N), 8.55-8.57 (dd, 1H), 7.80-7.84 (1H, dt), 7.40-7.42 (1H, d), 7.31-7.34 (1H, t), 7.05-7.09 (2H, dd), 6.81-6.85 (1H, t), 4.92 (2H, s, CH_2N), 3.78 (3H, s, OCH_3). ^{13}C NMR (100 MHz, DMS) δ 168.04, 158.17, 151.99, 149.77, 148.52, 137.52, 123.75, 123.02, 122.56, 118.92, 118.36, 115.42, 63.83, 56.22. HRMS (ESI): m/z calculated for $C_{14}H_{14}N_2O_2$ – H^+ 241.2653; found 241.0950.

***(E)-2-Methoxy-6-((thiazol-2-ylimino)methyl)phenol* (c3)**

Collected as yellow crystals (0.24 g, 39%), m.p. 91-93°C. ^{1}H NMR (400 MHz, DMS-d_6): δ 11.32 (br s, OH, 1H), 9.30-9.33 (1H, d, CH=N), 7.65-7.74 (2H, dd), 7.41-7.43 (1H, m), 7.17-7.19 (1H, m), 6.92-6.94 (1H, m), 3.83 (3H, s, OCH_3). HRMS (ESI): m/z calculated for $C_{11}H_{10}N_2O_2S$ + H^+ + H_2O 253.2986; found 253.0562.

***(E)-2-((Isoxazol-3-ylimino)methyl)-6-methoxyphenol* (c4)**

Collected as yellow solid (0.30g, 40%) m.p. 165-166°C. ^{1}H NMR (400 MHz, DMS-d_6): δ 11.90 (1H, br s, OH), 9.18-9.20 (1H, d), 8.94 (1H, s, CH=N), 7.32-7.34 (1H, m), 7.19-7.21 (1H, m), 6.94-6.98 (2H, m), 3.85 (3H, s, OCH_3). HRMS (ESI): m/z calculated for $C_{11}H_{10}N_2O_3$ + H^+ 219.2167; found 219.0751.

***(E)-2-(2-Hydroxy-3-methoxybenzylideneamino)phenol* (c5)**

Collected as orange solid (0.30g, 40%). ^{1}H NMR (400 MHz, DMS-d_6): δ 14.06 (1H, s, OH), 9.78 (1H, s, OH), 8.94 (1H, s, CH=N), 6.85-7.36 (7H, m), 3.79 (3H, s, OCH_3). m/z calculated for $C_{14}H_{13}NO_3$ 243.26; found 243.08.

***(E)-2-Methoxy-6-((2-morpholinoethylimino)methyl)phenol* (c6)**

Collected as yellow solid (0.36g, 84%). ^{1}H NMR (400 MHz, DMS-d_6): δ 13.79 (1H, br s, OH), 8.52 (1H, s, CH=N), 6.98-7.01 (2H, m), 6.74-6.78 (1H, m), 3.77 (3H, s, OCH_3), 3.69-3.72 (2H, t), 3.55-3.57 (2H, m), 3.34 (2H, m), 2.57-2.67 (2H, t), 2.43-2.50 (4H, m). m/z calculated for $C_{14}H_{20}N_2O_3$ 264.32; found 264.14.

***(E)-4-((4-Hydroxy-3-methoxybenzylimino)methyl)-2-methoxyphenol* (c7)**

Collected as yellow solid (0.26g, 73%). ^{1}H NMR (400 MHz, DMS-d_6): δ 9.53 (1H, br s, OH), 8.86 (1H, br s, OH), 8.27 (1H, s, CH=N), 7.34 (1H, m), 7.14 (1H, m), 6.69-6.86 (4H, m), 4.58 (2H, s, CH_2N), 3.78 (3H, s, OCH_3), 3.75 (3H, s, OCH_3). m/z calculated for $C_{16}H_{17}NO_4$ 287.31; found 287.12.

***4-((E)-((E)-4-(((E)-4-Hydroxy-3-methoxybenzylideneamino)methyl)benzylimino)methyl)-2-methoxyphenol* (c8)**

Collected as orange solid (0.47g, 88%). ^{1}H NMR (400 MHz, DMS-d_6): δ 13.6 (2H, br s, 2xOH), 8.90 (2H, s, 2xCH=N), 6.82-7.35 (10H, m), 4.81 (4H, s, 2xCH_2N), 3.77 (6H, s, 2xOCH_3). m/z calculated for $C_{24}H_{24}N_2O_4$ 404.46; found 404.17.

***(E)-4-(Quinolin-8-ylmethyleneamino)phenol* (c9)**

Collected as yellow solid (0.13g, 38%). ^{1}H NMR (500 MHz, DMS-d_6): δ 9.84 (1H, s, OH), 9.55 (1H, s, CH=N), 9.03 (1H, m), 8.46-8.50 (2H, dd), 8.14-8.15 (1H, d), 7.73 -7.76 (1H, t), 7.62-7.65 (1H, m), 7.26-7.28 (2H, m), 6.83-6.85 (2H, m). ^{13}C NMR (100 MHz, DMS-d_6): δ 156.9, 154.4, 151.1, 146.6, 143.7, 137.2, 133, 131.5, 128.5, 127.3, 127, 123.1, 122.4, 116.3. m/z calculated for $C_{16}H_{12}N_2O$ 248.28; found 248.09.

3.2 Inhibition of enzyme activity

Fifteen compounds were screened for their inhibitory activity against CAIII and CAIX using the method developed by Alzweiri et al. The method is based on GC-FID[45, 50]. The method utilizes pH-sensitive pellets for evaluating the esterase activity of CAs.

3.3 Antimicrobial activity

3.3.1 Materials and methods

E. coli ATCC8739, *Pseudomonas aeruginosa* ATCC9027, *Proteus mirabilis* ATCC12453, *Bacillus subtilis* ATCC6633, and *Staphylococcus aureus* ATCC6538 were utilized as bacteria, while *Candida albicans* ATCC10231 was used as yeast. All of these strains were acquired from the American Type Culture Collection. Nutrient agar (NA, Biolab, Budapest, Hungary) and Sabouraud Dextrose Agar (SDA, Biolab, Budapest, Hungary) slants were used to cultivate the bacterial and yeast strains, respectively, at 37°C.

3.3.2 Antimicrobial assay

Disc diffusion method

In vitro tests using the Kirby-Bauer agar diffusion technique determined whether or not the synthesized compounds exhibited antibacterial activity against Gram-positive and Gram-negative bacteria and Candida[51, 52]. To culture bacteria, Mueller-Hinton agar was used, and to culture yeast, Sabouraud Dextrose agar was used, as suggested by the NCCLS recommendations[53, 54].

One hundred microliters (100 µl) of microbial suspension was plated onto the Mueller-Hinton agar medium after 10 ml of new media was used to cultivate the test bacteria/Candida to a concentration of about 108 cells/ml for bacteria (0.5 McFarland standards) (MHA, oxoid, Wade Road, UK).

As previously noted, the compounds were evaluated using sterile blank discs with a diameter of 6 millimeters (antibiotic assay discs, Whatman-model 2017-006[54]. After the discs were dried, they were injected with 20 µL of 20 mM of the chemical and put on plates. Bacterial and fungal pathogens were inoculated onto plates, and after 24 hours at 37ºC, the widths of the inhibitory zones were measured. The results of each antimicrobial test were averaged from two independent runs. Positive controls for antimicrobial and Candida activity were established using standard antibiotics such as levofloxacin (5 mcg/disc), amoxicillin/clavulanic acid (30mcc), trimethoprim/sulfamethoxazole (1.25/23.75 µg), and nystatin (100mcg/disc). As a sham, we utilized discs soaked in 20 µl of DMSO. It was possible to quantify the sizes of the inhibitory zones. **Table 2** lists the synthesized compounds and their inhibitory activities against these species.

Serial dilution method (broth microdilution assay)

The MIC was calculated using the broth microdilution method, as recommended by the National Committee for Clinical Laboratory Standards [55]. After overnight incubation in broth, inocula of the bacterial strains or Candida were made, and the turbidity of the suspensions was set to 0.5 McFarland units. In a 96-well microtiter plate, the compounds were diluted serially. The diluent utilized was Mueller Hinton broth (MHA, Oxoid, Wade Road, UK). Compounds were found in quantities spanning from 2.5 to 0.00488 mM. Mueller Hinton broth was used to inoculate wells with test strains of bacteria and Candida (with final concentrations of 2.0×10^6 CFU/ml for bacteria and 2.0×10^5 CFU/ml for Candida). For 24 hours, the plate was kept at 37ºC. A well was set up with the growth media and the bacteria or Candida as a control. Positive controls included levofloxacin and

nystatin, while negative controls included DMSO. The test wells and the positive and negative controls were examined to assess the level of microbial growth. Antibacterial and antifungal actions were inferred from the lack of microbiological development. According to **Table 2**, the minimal inhibitory concentration (MIC) is defined as the lowest concentration of a substance at which observable growth of microorganisms occurs.

Conclusion

In summary, 15 compounds were synthesized and tested as CAIII and CAIX inhibitors. Compounds **c1**, **c6**, **a1**, and **a2** that have a bidentate chelating efficiency gave the best inhibition activity against CAIII, whereas all compounds had a satisfactory inhibiton activity against CAIX. Based on these results, it can be concluded that other functional groups other than the sulfonamide group could be developed as potential CAs inhibitors. It should be noted that Schiff bases synthesized in this work showed different percentage inhibition with CAIII and CAIX. As such, this may give potential to design selective inhibitors. CAs active site need further investigation, and the synthesized compounds could be used as a good starting point for other, non-sulfonamide CA inhibitors.

Acknowledgments

This project was funded by Al-Zaytoonah of Jordan.

Conflict of Interest

The authors confirm no conflict of interest.

Abbreviations

CA: carbonic anhydrase
CAIII: carbonic anhydrase III
CAIX: carbonic anhydrase IX
DCC: Dicyclohexylcarbodiimide
HOBT hydrate: 1-hydroxybenzotriazole hydrate
TEA: triethylamine
THF: tetrahydrofuran

REFERENCES

(1) Andrea Petrenia VDL, C. Andrea Scalonic, et al.Anion inhibition studies of the Zn (II)-bound i-carbonic anhydrase from the Gram-negative bacterium Burkholderia territorii. J Enzyme Inhib Med Chem. 2021;36(1):372-6.

(2) Hamadneh L, Hikmat S, Al-Samad LA, et al. Synthesis, Characterization and Antimicrobial Activity of Novel Symmetrical and Unsymmetrical Thiadiazole Derivatives as Potential Carbonic Anhydrase Inhibitor in E. Coli. Journal of Global Pharma Technology. 2009;11(02):171-80.

(3) Nocentini A, Donald WA, Supuran CT. Human carbonic anhydrases: tissue distribution, physiological role, and druggability. Carbonic Anhydrases. Academic press; 2019. p. 151-85.

(4) Alzweiri M. Inhibitory binding of angiotensin converting enzyme inhibitors with carbonic anhydrase III. Chromatographia. 2020;83(12):1517-24.

(5) Supuran CT, Capasso C. Antibacterial carbonic anhydrase inhibitors: an update on the recent literature. Expert Opin Ther Targets. 2020;30(12):963-82.

(6) Supuran CT. Inhibition of bacterial carbonic anhydrases and zinc proteases: from orphan targets to innovative new antibiotic drugs. Curr Med Chem. 2012;19(6):831-44.

(7) Rasti B, Mazraedoost S, Panahi H, et al.New insights into the selective inhibition of the β-carbonic anhydrases of pathogenic bacteria Burkholderia pseudomallei and Francisella tularensis: a proteochemometrics study. Mol Divers 2019;23(2):263-73.

(8) Murray AB, Aggarwal M, Pinard M, et al. Patrauchan M, Supuran CT, et al. Structural Mapping of Anion Inhibitors to β-Carbonic Anhydrase psCA3 from Pseudomonas aeruginosa. ChemMedChem. 2018;13(19):2024-9.

(9) Plosker GL, Croom KF. Sulfasalazine. Drugs. 2005;65(13):1825-49.

(10) Alzweiri M, Al-Hiari Y. Evaluation of vanillic acid as inhibitor of carbonic anhydrase isozyme III by using a modified Hummel–Dreyer method: approach for drug discovery. Biomed Chromatogr. 2013;27(9):1157-61.

(11) Angeli A, Donald WA, Parkkila S, et al. Activation studies with amines and amino acids of the β-carbonic anhydrase from the pathogenic protozoan Leishmania donovani chagasi. Bioorganic Chemistry. 2018;78:406-10.

(12) Chiaramonte N, Bua S, Ferraroni M, et al. 2-Benzylpiperazine: A new scaffold for potent human carbonic anhydrase inhibitors. Synthesis, enzyme inhibition, enantioselectivity, computational and crystallographic studies and in vivo activity for a new class of intraocular pressure lowering agents. Eur J Med Chem. 2018;151:363-75.

(13) Harju AK, Bootorabi F, Kuuslahti M, et al. Carbonic anhydrase III: A neglected isozyme is stepping into the limelight. J Enzyme Inhib Med Chem. 2013;28(2):231-9.

(14) Mahon BP, McKenna R. Carbonic Anhydrases as Biocatalysts. Chapter 5: Carbonic Anhydrase III, pages: 91-108: Elsevier; 2015.

(15) Mitterberger MC, Kim G, Rostek U, et al. Carbonic anhydrase III regulates peroxisome proliferator-activated receptor-γ2. Exp Cell Res. 2012;318(8):877-86.

(16) Mohammad HK, Alzweiri MH, Khanfar MA, et al.6-Substituted nicotinic acid analogues, potent inhibitors of CAIII, used as therapeutic candidates in hyperlipidemia and cancer. Med Chem Res. 2017;26(7):1397-404.

(17) Alzweiri M, Al-Balas Q, Al-Hiari Y. Chromatographic evaluation and QSAR optimization for benzoic acid analogues against carbonic anhydrase III. J Enzyme Inhib Med Chem. 2015;30(3):420-9.

(18) Supuran CT, Winum JY. Carbonic anhydrase IX inhibitors in cancer therapy: an update. Future Med Chem. 2015;7(11):1407-14.

(19) Mahon BP, Pinard MA, McKenna R. Targeting carbonic anhydrase IX activity and expression. Molecules. 2015;20(2):2323-48.

(20) McDonald PC, Winum J-Y, Supuran CT, et al. Recent developments in targeting carbonic anhydrase IX for cancer therapeutics. Oncotarget. 2012;3(1):84.

(21) Rasti B, Mazraedoost, S., Panahi, H., et al.New insights into the selective inhibition of the β-carbonic anhydrases of pathogenic bacteria Burkholderia pseudomallei and Francisella tularensis: a proteochemometrics study. Mol Divers 2018;23:263–73.

(22) Capasso C, Supuran CT. Bacterial, fungal and protozoan carbonic anhydrases as drug targets. Expert Opin Ther Targets. 2015;19(12):1689-704.

(23) Köhler S, Ouahrani-Bettache, S., Winum, J.V. Brucella suis carbonic anhydrases and their inhibitors: Towards alternative antibiotics? J Enzyme Inhib Med Chem. 2017;32(1):683-7.

(24) Apaydın S, Török M. Sulfonamide derivatives as multi-target agents for complex diseases. Bioorg Med Chem Lett. 2019;29(16):2042-50.

(25) Supuran CT. Carbon-versus sulphur-based zinc binding groups for carbonic anhydrase inhibitors? J Enzyme Inhib Med Chem. 2018;33(1):485-95.

(26) Zhang L, Zhang J, Jiang Q.et al. Zinc binding groups for histone deacetylase inhibitors. J Enzyme Inhib Med Chem. 2018;33(1):714-21.

(27) Kusamoto H, Shiba A, Tsunehiro M. et al. A simple method for determining the ligand affinity toward a zinc-enzyme model by using a TAMRA/TAMRA interaction. Dalton Trans. 2018;47(6):1841-8.

(28) Liu Z-Q, Ng YM, Tiong PJ, et al. Five-coordinate zinc (II) complex: synthesis, characterization, molecular structure, and antibacterial activities of bis-[(E)-2-hydroxy-N′-1-(4-methoxyphenyl) ethylidenebenzohydrazido] dimethylsulfoxidezinc (II) complex. International Journal of Inorganic Chemistry. 2017;2017.

(29) Takahashi T, Miyazawa M. Synthesis and structure–activity relationships of serotonin derivatives effect on α-glucosidase inhibition. Med Chem Res. 2012;21(8):1762-70.

(30) Stachulski AV, Santoro MG, Piacentini S, et al. Second-generation nitazoxanide derivatives: thiazolides are effective inhibitors of the influenza A virus. Future Med Chem. 2018;10(8):851-62.

(31) Stachulski AV, Pidathala C, Row EC, et al. Thiazolides as novel antiviral agents. 1. Inhibition of hepatitis B virus replication. J Med Chem. 2011;54(12):4119-32.

(32) Trujillo-Ferrara J, Vazquez I, Espinosa J, et al.Reversible and irreversible inhibitory activity of succinic and maleic acid derivatives on acetylcholinesterase. Eur J Pharm Sci. 2003;18(5):313-22.

(33) Ameduri B, Boutevin B, Malek F. Synthesis and characterization of styrenic polymers with pendant pyrazole groups. II. J Polym Sci Part A Polym Chem. 1994;32(4):729-40.

(34) Bayer T, Chakrabarti A, Lancelot J, et al. Synthesis, crystallization studies, and in vitro characterization of cinnamic acid derivatives as SmHDAC8 Inhibitors for the treatment of schistosomiasis. ChemMedChem. 2018;13(15):1517-29.

(35) Ai T, Xu Y, Qiu L, et al. Hydroxamic acids block replication of hepatitis C virus. J Med Chem. 2015;58(2):785-800.

(36) Aakeröy CB, Sinha AS, Epa KN, et al.versatile and green mechanochemical route for aldehyde–oxime conversions. ChemComm. 2012;48(92):11289-91.

(37) Shukla SN, Gaur P, Bagri SS, et al. Pd (II) complexes with ONN pincer ligand: Tailored synthesis, characterization, DFT, and catalytic activity toward the Suzuki-Miyaura reaction. J Mol Struct. 2021;1225:129071.

(38) Elshaarawy RF, Mustafa FH, Sofy AR, et al. New synthetic antifouling coatings integrated novel aminothiazole-functionalized ionic liquids motifs with enhanced antibacterial performance. Journal of Environmental Chemical Engineering. 2019;7(1):102800.

(39) Prashanthi Y, Kiranmai K. Spectroscopic characterization and biological activity of mixed ligand complexes of Ni (II) with 1, 10-phenanthroline and heterocyclic schiff bases. Bioinorganic Chemistry and Applications. 2012;2012.

(40) Shang X, Li J, Guo K, et al. Development and cytotoxicity of Schiff base derivative as a fluorescence probe for the detection of l-Arginine. J Mol Struct. 2017;1134:369-73.

(41) Petek H, Albayrak Ç, İskeleli NO, et al.Crystallographic and conformational analyses of zwitterionic form of (E)-2-methoxy-6-[(2-morpholinoethylimino) methyl] phenolate. J Chem Crystallogr. 2007;37(4):285-90.

(42) Bhanja A, Moreno-Pineda E, Herchel R, et al. Self-assembled octanuclear [Ni 5 Ln 3](Ln= Dy, Tb and Ho) complexes: synthesis, coordination induced ligand hydrolysis, structure and magnetism. Dalton Trans. 2020;49(23):7968-76.

(43) Reihsig J, Krause H-W. Über organische Katalysatoren, LXXIV. Chelatkatalyse XVII. Journal für Praktische Chemie. 1966;31(3-4):167-78.

(44) Alzweiri M, Sweidan K, Al-Helo T. Synthesis and evaluation of new 2-oxo-1, 2-dihydroquinoline-3-carboxamides as potent inhibitors against acetylcholinesterase enzyme. Med Chem Res. 2022;31(9):1448-60.

(45) Alzweiri M, Al-Helo T. Gas Chromatography with Modified pH-Sensitive Pellets in Evaluating Esterase Activity of Carbonic Anhydrase III Enzyme: Drug Discovery Approach. Chromatographia. 2021;84 (12):1113-20.

(46) Mboge MY, Chen Z, Wolff A, et al. Selective inhibition of carbonic anhydrase IX over carbonic anhydrase XII in breast cancer cells using benzene sulfonamides: Disconnect between activity and growth inhibition. PLoS One. 2018;13(11):e0207417.

(47) Summers JB, Mazdiyasni H, Holms JH, et al. Hydroxamic acid inhibitors of 5-lipoxygenase. J Med Chem. 1987;30(3):574-80.

(48) Pepeljnjak S, Zorc B, Butula I. Antimicrobial activity of some hydroxamic acids. Acta Pharmaceutica. 2005;55(4):401-8.

(49) Yekkour A, Meklat A, Bijani C, et al. A novel hydroxamic acid-containing antibiotic produced by a Saharan soil-living Streptomyces strain. Letters in applied microbiology. 2015;60(6):589-96.

(50) Abu Hajleh MN, Alzweiri, M., Bustanji, Y. K.et al. Biodegradable Poly (lactic-co-glycolic acid) Microparticles Controlled Delivery System: A Review. Jordan J Pharm. Sci. 2020;13(3):317-35.

(51) Bayer A, Kirby W, Sherris J, et al.Antibiotic susceptibility testing by a standardized single disc method. Am J Clin Pathol. 1966;45(4):493-6.

(52) Mahmoud IS, Altaif, K. I., Abu Sini, M. K., et al. Determination of Antimicrobial Drug Resistance among Bacterial Isolates in Two Hospitals of Baghdad Jordan J Pharm. Sci. 2020;13(1):1-9.

(53) Wayne P. Clinical and laboratory standards institute: performance standards for antimicrobial disk susceptibility tests. Approved standard M2–A9, Clinical and laboratory standards institute. 2006.

(54) Antonio-Velmonte AJG, M. Local production of low cost quality antibiotic susceptibility disks for the Philippines. Philos J Microb Infect Dis. 1988;17 66-75.

(55) National Committee for Clinical Laboratory Standards Performance standards for antimicrobial susceptibility testing: eleventh informational supplement, National Committee for Clinical Laboratory Standard. PA, USA: Wayne; 2003.

التوليف والتقييم البيولوجي لمثبطات الأنهايدريز الكربونية III و IV عن طريق كروماتوغرافيا الغاز باستخدام كريات معدلة حساسة لدرجة الحموضة

بثينة حسين [1]&*، لورانس البرغلي [1]&*، محمد الزوبري [2]، يوسف الحياري [2]، محمد أبو صيني [1]، سريا النابلسي [3]، بتول الغويري [1]

[1] قسم الصيدلة، كلية الصيدلة، جامعة الزيتونة الأردنية، الأردن.

[2] قسم العلوم الصيدلانية، كلية الصيدلة، الجامعة الأردنية، عمان، الأردن.

[3] قسم الكيمياء الطبية والعقاقير، كلية الصيدلة، جامعة العلوم والتكنولوجيا الأردنية، الأردن.

& ساهم كل من بثينة حسين و لورانس البرغلي في هذا العمل بالتساوي.

ملخص

تم تصنيع خمسة عشر مركبًا واختبارها كمثبطات محتملة للأنهايدريز الكربوني III (CAIII) والأنهايدريز الكربوني IX (CAIX)، ستة منها مركبات جديدة. تم تقييم مشتقات الأميدات (a1-4) والأحماض الهيدروكسيمية (b1-2) والإيمينات (c1-9) لنشاطها المثبط ضد CAIII وCAIX عن طريق كروماتوجرافيا الغاز باستخدام كريات معدلة حساسة لدرجة الحموضة. أظهرت المشتقات نسب تثبيط تتراوح بين 12–56٪ لـ CAIII و44–59٪ لـ CAIX، مقارنة بـ 49٪ و63٪ لكابتوبريل (المركب المرجعي) على التوالي. أظهرت الإيمينات أفضل تثبيط لـ CAIII، بينما أظهرت جميع المشتقات نشاطًا مشابهًا ضد CAIX. من المفترض أن ذرة النيتروجين في شقوق الإيمين أو الأميد أو الحمض الهيدروكسيمي بالقرب من مجموعة قابلة للتأين بالتنسيق مع أيون الزنك في الموقع النشط. علاوة على ذلك، تم اختبار المركبات بالنسبة لنشاطهم المضاد للميكروبات والفطريات. بشكل عام، أظهرت المركبات نشاطًا منخفضًا او عدم النشاط ضد بعض البكتيريا موجبة وسالبة الجرام. هذا يدعم نظرية قدرتها على الارتباط بالأنهايدريز الكربوني البشري ولكن ليس الأنهايدريز الكربوني الخاص بالبكتيريا. يمكن أن تكون هذه المركبات بمثابة نماذج مفيدة لتطوير مثبطات الأنهايدريز الكربونية أكثر فعالية وانتقائية كمضادات للسمنة ومضادة للسرطان.

الكلمات الدالة: كربونيك أنهايدريز III، كربونيك أنهايدريز IX، مثبطات، أميدات، أحماض هيدروكسيمية، إيمينات، مخلّب الزنك.

* ***المؤلف المراسل:***

بثينة حسين ، لورانس البرغلي

Laurance.bourghli@zuj.edu.jo , buthina.hussein@zuj.edu.jo

تاريخ الإستلام 2023/1/10 تاريخ قبول النشر 2023/3/30.

Abstracts

الملخصات

Precision Medicine and Pharmacogenetics: Stratification and Improved Outcome in Non-Small Cell Lung Cancer

Aamir Ahmad*

Dermatology Institute and Translational Research Institute, Academic Health System, Hamad Medical Corporation, Qatar.
University of Alabama at Birmingham, USA.

DOI: https://doi.org/10.35516/jjps.v16i2.1474

ABSTRACT

Lung cancer is the most common cancer globally, accounting for a quarter of all cancer-related deaths. Non-small cell lung cancer (NSCLC) is the major lung cancer subtype. Research in the last few decades has led to the identification of key molecular targets resulting in targeted therapies, such as the use of tyrosine kinase inhibitors (TKIs) targeting epidermal growth factor receptors (EGFR). EGFR-TKIs themselves have evolved through few generations based on the knowledge gained from gene mutations in the EGFR leading to therapy resistance. As part of pharmacogenetics, it is well known that patients often respond differentially to different therapies, based on their genetic makeup. This has opened up avenues for precision medicine in the treatment of NSCLC patients with the identification of EGFR mutations and the most optimum treatment strategy. Since time is of the essence, it is critical that the NSCLC patients be administered a therapy that they are most likely to respond to. Evolving data validates this notion and it is expected that such an approach will invariably lead to improved patient outcomes.

Spatiotemporal ^{1}H NMR Spectroscopy of 3D Cell Models

R. Hergenröder[1]*, R. Hollmann[1], H. Raschke[1], J. Lambert[1], M. AlWahsh[2]

[1] Leibniz-Institut für Analytische Wissenschaften - ISAS, Bunsen-Kirchhoff-Str. 11, Germany.
[2] Faculty of Pharmacy, Al-Zaytoonah University of Jordan, Jordan.

DOI: https://doi.org/10.35516/jjps.v16i2.1476

ABSTRACT

The emergence of three-dimensional cell cultures representing tissue features closely, that are weakly reproduced by standard two-dimensional systems, requires adapting established analytical techniques to investigate these challenging new models. It is especially desired to obtain spatially resolved data for living organoids giving insight into transport processes and biochemical characteristics of domains differently provided with nutrition supply and waste product removal. Within this work we present an NMR-based approach to dynamically obtained radial metabolite profiles for cell spheroids, one of the most frequently used 3D models. Our approach combines an easy to reproduce custom-made measurement design maintaining incubator conditions without inhibition of the NMR experiment, with a spatial selective NMR pulse sequence. To overcome the inherently low sensitivity of NMR spectroscopy we modified the selective sequence to achieve faster acquisition and employed a commercially available cryo NMR probe. Finally, radial metabolite profiles could be obtained via double Abel inversion of the measured one-dimensional intensity profiles. Applying this method to Ty82 cancer cell spheroids clearly demonstrates the spatial resolution, for instance confirming exceedingly high lactate and strongly decreased glucose concentrations in the oxygen-depleted core of the spheroid. Furthermore, we dynamically investigate the process of cell death and metabolite degradation after maintaining a spheroid under incubator conditions for several days.

Chronic Inhalation of Pod-based e-cigarette Aerosols on Inflammatory Biomarkers in the Central Nervous and Peripheral Systems

Youssef Sari

University of Toledo, USA.

DOI: https://doi.org/10.35516/jjps.v16i2.1482

ABSTRACT

Electronic cigarettes (e-cigs) use has been dramatically increased recently, especially among youths. In this study, we evaluated the effect of one- and three-months continuous exposure to e-cig vapor (JUUL pods), containing high nicotine concentration, on the expression of glutamate receptors and transporters and mainly the associated neuroinflammatory markers in drug reward brain regions such as nucleus accumbens (NAc) core (NAc-core), NAc shell (NAc-shell) and hippocampus (HIP) in female C57BL/6 mice. We revealed that three months' exposure to mint or mango flavored-JUUL (containing 5% nicotine, 59 mg/ml) induced upregulation in metabotropic glutamate receptor 1 (mGluR1) and postsynaptic density protein 95 (phosphorylated and total PSD95) expression, and downregulation of mGluR5 and glutamate transporter 1 (GLT-1) in the NAc-shell. Three months' exposure to JUUL induced upregulation of mGluR5 and GLT-1 expression in the HIPP. We further revealed that mice exposed to JUUL Mango and JUUL Mint for one month had significantly increased TNF-α expression in the NAc-core and NAc-shell, with elevation in IL-1β as well. NAc-shell also showed significantly increased levels of IL-6 and HMGB-1 for both flavors. There were significantly increased levels of TNF-α in the NAc-core and NAc-shell for both Mint- and Mango-exposed JUUL mice for three months. NAc-shell also showed significantly increased levels of IL-1β, IL-6, HMGB-1, and RAGE after three months of JULL exposure, while the hippocampus showed significantly decreased levels of HMGB-1 for both flavors. These findings demonstrated that exposure to e-cig vapor containing high nicotine concentrations induced differential effects on glutamatergic system as well as induction of proinflammatory markers in the brain.

Pharmacogenetics and Personalized Medicines

Nancy Hakooz

School of Pharmacy-University of Jordan.

DOI: https://doi.org/10.35516/jjps.v16i2.1483

ABSTRACT

Personalized or precision medicine has been used to describe the right drug to the right person at the right dose at the right time. One important aspect of personalized medicines is the genetic makeup of the individual. Pharmacogenetics investigates the role of individual genes in drug disposition. The use of pharmacogenetics will increase drug efficacy with minimum side effects. Several tables have been published by the FDA that list the pharmacogenetic associations with certain drugs. These tables suggest that certain subgroups of patients with certain genetic variants are likely to have "altered drug metabolism, and in certain cases, differential therapeutic effects, including differences in risks of adverse events" (https://www.fda.gov/medical-devices/precision-medicine/table-pharmacogenetic-associations#about).These tables include: Section 1: Pharmacogenetic associations for which the data support therapeutic management recommendations such as celecoxib and CYP2C9 polymorphisms. Section 2: Pharmacogenetic associations for which the data indicate a potential impact on safety or response such as codeine in CYP2D6 poor metabolizers will result in a lower concentration of the active form morphine. Section 3: Pharmacogenetic associations for which the data demonstrate a potential impact on pharmacokinetic properties only. In this list, the implications of the genotypes have not been well established for example atorvastatin and SLCO1B1 phenotypes may result in a higher systemic concentration of the drug. In the US pharmacogenetic tests are available as direct-to-consumer (DTC) tests. With DTC tests, individuals can send in a saliva sample and get results directly at their homes (Drelles et al 2021). Although the evidence on the effects of such tests and pharmacogenetic counseling is available and mounting in many clinical practices all around the world but is still to be implemented in the clinical practice in Jordan.

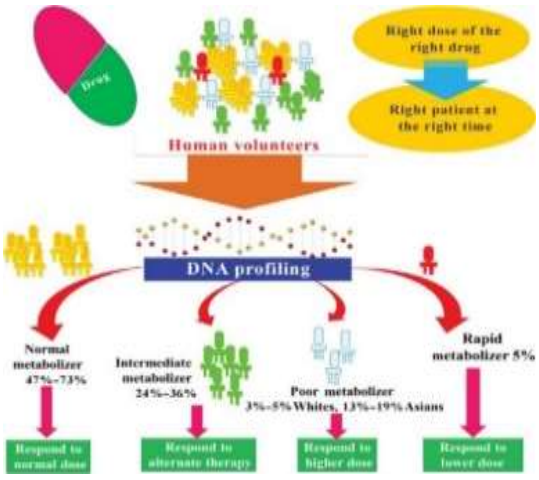

References

Drelles et al: Impact of Previous Genetic Counseling and Objective Numeracy on Accurate Interpretation of a Pharmacogenetics Test Report. Public Health Genomics 2021;24:26-32. doi: https://doi.org/10.1159/000512476

Gas Chromatography with Modified pH-sensitive Pellets in Evaluating the Activity of Some Enzymes Attributed with a Change in the Medium pH

Muhammed Alzweiri

Faculty of Pharmacy, The University of Jordan, Amman, Jordan

DOI: https://doi.org/10.35516/jjps.v16i2.1484

ABSTRACT

A new evaluation method based on gas chromatography (GC) is considered for the screening of the inhibitory activity of various compounds against certain enzymes using immobilized pH-sensitive matrix pellets. This approach of analysis is being utilized in developing sensitive GC methods for enzymes attributed to pH change in their media. Particularly, for those which require accurate and sensitive assay methods. The method has been implemented in drug discovery research related to antagonism of carbonic anhydrase, isozyme 3 (CAIII). This isozyme has a strong potential in treating obesity, hyperlipidemia and cancer. The method was also used in investigation of various peptide derivatives with an epoxide warhead for their anti-lipase activity. Recently, the method has been used in evaluating some tacrine analogues for their inhibition against acetylcholinesterase enzyme. The latter is important in treating Alzheimer's disease (AD) which is a worldwide mental disorder manifested with dementia symptoms and anticipated to be the second causality of deaths by 2040.

Design, Synthesis and Biological Evaluation of Novel Pyrazolotriazolopyrimidine Derivatives as Potential Anticancer Agents

Ihab M. Almasri

Department of Pharmaceutical Chemistry and Pharmacognosy, Faculty of Pharmacy,
Al Azhar University-Gaza, Palestine.

DOI: https://doi.org/10.35516/jjps.v16i2.1485

ABSTRACT

Three novel pyrazolo-[4,3-e][1,2,4]triazolopyrimidine derivatives (**1**, **2**, and **3**) were designed, synthesized, and evaluated for their in vitro biological activity. All three compounds exhibited different levels of cytotoxicity against cervical and breast cancer cell lines. However, compound **1** showed the best antiproliferative activity against all tested tumor cell lines, including HCC1937 and HeLa cells, which express high levels of wild-type epidermal growth factor receptor (EGFR). Western blot analyses demonstrated that compound **1** inhibited the activation of EGFR, protein kinase B (Akt), and extracellular signal-regulated kinase (Erk)1/2 in breast and cervical cancer cells at concentrations of 7 and 11 µM, respectively. The results from docking experiments with EGFR suggested the binding of compound **1** at the ATP binding site of EGFR. Furthermore, the crystal structure of compound 3 (7-(4-bromophenyl)-9-(pyridin-4-yl)-7H-pyrazolo[4,3-e][1,2,4]triazolo[1,5-c]pyrimidine) was determined by single crystal X-ray analysis. Our work represents a promising starting point for the development of a new series of compounds targeting EGFR.

Keywords: Pyrazolo[1,2,4]triazolopyrimidine, EGF-receptor inhibitor, breast cancer, cervical cancer, molecular modeling, crystal X-ray analysis.

Knowledge and Attitudes towards Antibiotic Usage

Hatem A Hejaz

Department of Pharmacy, Faculty of Pharmacy, Arab American University, Palestine.

DOI: https://doi.org/10.35516/jjps.v16i2.1486

ABSTRACT

Background: Antibiotic resistance is a global problem, and the World Health Organization (WHO) has made this problem one of its priorities for solving. Repeated and improper use of antibiotics is the main reason for the bacteria's resistance to the drugs.

Objectives: This study aimed to evaluate the knowledge, and attitudes of Palestinians regarding antibiotic usage and awareness about resistance.

Methods: This was a cross-sectional study that targeted Palestinians from different cities. We used an online questionnaire which distributed randomly for data collection. The questionnaire consists of 52 questions to measure the knowledge, attitudes, and awareness of antibiotic use and resistance. Statistical Package for the Social Sciences (SPSS) version 25 was used to analyze the data collected.

Results: A total of 744 participated in the study and completed the questionnaire, and the majority of them (60.5 %; n= 450 out of 744) were from the Hebron Governorate. The major of the respondents also were females (n= 653, 87.8%) and their age between 20-35 years old (n= 498, 66.9%) with a bachelor degree (n= 502, 67.5%). The majority of them (75.5%, n= 560) think that antibiotics should be given only by prescription, and about half of the people (52%= n= 387) believe that antibiotics are not safe. Most participants relied on the physician for dispensing the antibiotic (60.1%, n= 455) but the same percentage of them use leftover antibiotics that have been used previously. Four hundred eighty-three (65%, n= 483) who completed the questionnaire heard about the antibiotic resistance term from medical staff, and their main primary sources of information about antibiotics and medicines were from health staff too (50%, n= 371), then internet (25%, n= 185). Some people (16%, n= 119) mentioned that pharmacists have a role in educating them and providing all the necessary information, or advice about the use of medicines and the dangers of medication misuse. Most of the participants obtained the antibiotics by prescription from a doctor (n= 339, 45.6%), then from the Pharmacist (n= 91, 12.2%), and 63 persons (8.5%) purchases them on their own. Quite a high number of participants (n= 348, 46.8%) stop taking antibiotics when they start feeling better. According to the results obtained, social media was the primary source of information regarding antibiotic resistance.

Conclusions: Higher education, younger age, gender, profession, and a high monthly income were associated significantly with good knowledge and a positive attitude toward antibiotic use. Educational interventions for appropriate antibiotic use are needed all the time and enforcing antibiotics regulations should be also considered to reduce antibiotic resistance.

Planar Waveguide NMR Gradients (B_0 and B_1) for spatiotemporal Investigations of Anticancer Drug Concentration in 3D Cancer Cell Cultures

Ahmad Telfah[1], Nour Sharar[1], Hanan Jafar[2], Roland Hergenröder[1]

[1] ISAS - Institute for Analytical Sciences, Bunsen-Kirchhoff-Str. 11, 44139 Dortmund, Germany, telfah.ahmad@isas.de.
[2] Cell Therapy Center (CTC), The University of Jordan, Amman, Jordan.

DOI: https://doi.org/10.35516/jjps.v16i2.1487

ABSTRACT

Despite the progression in cancer therapeutic approaches, cancer is still the leading cause of death worldwide with a steadily increasing incidence rate. In Jordan, CRC is the most common type of cancer among men and the second most common among women, while being one of the most accruing cancers in Germany.

The difficulties in cancer treatments arise from the poor correlation between in vivo and in in vitro anti-cancer drug testing results and cancer cells resistance to chemotherapy, which are attributed to the heterogeneity of cancer cells, and the interaction of cancer cells with non-cancerous cells in the tumor microenvironment (TME). In addition to, the several mechanisms, that governs DNA damages repair, epigenetics, epithelial to mesenchymal transition (EMT).

Cell culture techniques have been developed to construct in vitro multicellular cancer spheroids (MTCS) that mimic cell-cells interaction and the cellular organization in the TME. They also illustrate the proliferation gradient of solid tumors, and the nutrition and gas supply to cancer cells at different depth in the spheroid. Therefore, they are considered an excellent in vitro cancer model to study the efficiency and to investigate the penetration depth of the anti-cancer materials.

Nuclear Magnetic Resonance (NMR) spectroscopy is a reliable analytical method that gives comprehensive and rich chemical information, along with high speciation performance. It is one of the major noninvasive tools for metabolomics, therefore it has been utilized to study the metabolic profiling of freshly isolated- non-destructed tissues, and living in vitro cellular models.

A micro-imaging technique for real-time NMR investigations is developed to study the penetration depth, rate, and effective diffusion coefficients of anti-cancer materials through cancer spheroids. This technique is based on our patented invention of planar waveguide micro slot NMR detector with on board thermal regulator integrated and a microfluidic device. Based on this innovative development, we are able to perform real-time magnetic resonance spectroscopic imaging (MRSI) on a living synthetic tissue constructed in micrometer scale to monitor drug penetration and diffusion, while providing spectroscopic information about the production and degradation of metabolites in picomoles concentrations.

Community Pharmacists' Perspectives toward Continuing Professional Development: A Qualitative Study

Rima Hjazeen

School of Pharmacy, The University of Jordan, Amman Jordan.

DOI: https://doi.org/10.35516/jjps.v16i2.1488

ABSTRACT

Objectives: This study's principal aim was to investigate community pharmacists' views of continuing professional development (CPD) and to explore pharmacists' perceptions of the most common facilitators and barriers to participation in continuing education (CE).

Methods: A series of seven focus group sessions were undertaken with groups of four to seven community pharmacists. Focus group transcripts were thematically analyzed using a qualitative data analysis method.

Results: Four key themes were identified: (1) community pharmacists' attitudes toward CPD; (2) perceived motivating factors for CPD; (3) experienced barriers to CPD; (4) and potential strategies for improving pharmacists' CPD.

Conclusion: Practicing pharmacists need support now, and changes to undergraduate education are warranted to keep abreast of current developments and changes to practice. Despite limitations, the distinctive nature of this study would have a valuable contribution to the field of professional development. It can inform theory, policy, and practice relating to pharmacists' CPD at both a professional level and governmentally, helping the relevant parties make informed decisions.

Keywords: Continuing professional development, continuing education, community pharmacist, qualitative, focus group.

Progress in the Design and Development of Phosphoinositide-3-Kinase (PI3Kα) Inhibitors

Dima A. Sabbah

Department of Pharmacy, Faculty of Pharmacy, Al-Zaytoonah University of Jordan, Jordan.

DOI: https://doi.org/10.35516/jjps.v16i2.1489

ABSTRACT

Background: The phosphatidylinositol 3-kinase (PI3Kα) has been spotlighted as a potential oncogene and therapeutic target for anticancer drug design.

Objective: Target compounds were designed employing ligand- and structure-based drug design approaches to address the effect of the compounds' backbones and functionalities on their biological activity.

Methods: Synthesis of the targeted compounds, biological evaluation tests against human cancer cell lines, and molecular docking studies.

Results: Fortunately, 20 novel series of diverse scaffolds were prepared and characterized by means of FT-IR, ^{1}H and ^{13}C NMR, HRMS, and elemental analysis. In addition, the identity of one core nucleus was successfully interpreted with the aid of X-ray crystallography. Biological activity of prepared compounds was investigated *in vitro* against human cancer cell lines. Results that these compounds inhibit cell proliferation and induce apoptosis through an increase in caspase-3 activity and a decrease in DNA cellular content. Furthermore, ligand-based pharmacophore modeling showed that the newly synthesized analogues match PI3Kα inhibitors fingerprint and the molecular docking studies against PI3Kα revealed that the analogues fit PI3Kα kinase catalytic domain and form H-bonding with key binding residues.

Conclusion: The harvested series exhibited a potential PI3Kα inhibitory activity in human cancer cell lines.

Patient-Centeredness in Pharmaceutical Care

Ahmad Al-Rusasi

Al-Noor Drug Store, Jordan.

DOI: https://doi.org/10.35516/jjps.v16i2.1490

ABSTRACT

Background information: Pharmacy is a longstanding profession, although there have been changes in pharmacists' roles over time. The change toward a patient-centered approach is recognized as an entirely different concept from the technical concept of dispensing.

The pharmacist's natural attitude primarily relies on pharmacologic knowledge of medications, the product, the use of counseling as the major approach with patients, and an emphasis on medication adherence as a goal. Though, besides a pharmacologic understanding, the knowledge of the patient and the knowledge of the experience of the patient, from his or her own perspective, are essential to help the pharmacist assess and ensure that a medication is indicated, effective, safe, and convenient. Therefore, to be able to work with patients in a patient-centered manner, the pharmacist must acknowledge a broader scope of knowledge that will account for a more comprehensive approach.

Conclusion: To practice in a truly patient-centered manner, pharmacist must understand that patients want to be heard and seen as individuals with unique experiences and responses to medications. This knowledge is needed to enhance pharmacists' basic pharmacotherapeutic understanding and provide for care of patients as individuals with unique experiences and stories and situated in community, culture, and society. Likewise, to help patients with their medications, pharmacist must begin to understand medications as patients experience them. This includes understanding their experiences with illness as well as their feelings about medications.

Development of Successful Physiologically-Based Pharmacokinetic (PBPK) Models

Nasir Mohammad Yasir Idkaidek

Faculty of Pharmacy, University of Petra, Amman, Jordan.

DOI: https://doi.org/10.35516/jjps.v16i2.1491

ABSTRACT

Physiologically-based pharmacokinetic (PBPK) modeling is a strong mathematical tool that integrates body physiology, drug physicochemical properties and pharmacokinetics to predict detailed drug profiles in different parts of the body. PBPK modeling can also be used to predict the effects of drug-drug interactions and diseases on drug pharmacokinetics. The use of special modules enables the extrapolation to different routes and also different species. PBPK steps for successful modeling will be discussed with examples using GastroPlus program. Such in-silico work can minimize the number and risks of in vivo clinical studies done on healthy subjects or on patients.

Investigations of potential pharmaceutical biofillers based on pregelatinized starch-reinforced with pine-extracted cellulose

E. Albarahmieh*, S. Tabbalat, and R. Muhaisen

* German Jordanian University, Jordan; e-mail: Israa.barahmieh@gju.edu.jo

DOI: https://doi.org/10.35516/jjps.v16i2.1492

ABSTRACT

Starch unique physical properties and abundance makes it an ideal candidate as diluent or filler in tablets. Therefore, this work aims to produce a modified starch known as 'pregelatinized' with the support of renewable cellulosic wood and characterize its properties in an effort to improve its application versatility that notably appeal to the pharmaceutical industry for greener and more sustainable excipients.

Level of Knowledge and Extent of Use of Anabolic-Androgenic Steroids among Physical Education University Students: A Cross-Sectional Study from Palestine

Suhaib Hattab[1*], Saed Zyoud[2], Bashar Saleh[3], Laith Qasarweh[4], Mahmoud Draidi[4]

[1] Department of Biomedical Sciences, Physiology, Pharmacology & Toxicology Division, Faculty of Medicine and Health Sciences, An-Najah National University, Nablus, Palestine.
[2] Department of Clinical and Community Pharmacy, Faculty of Medicine and Health Sciences. An-Najah National University, Nablus, Palestine.
[3] Department of Physical Education, An-Najah National University, Nablus, Palestine.
[4] Department of Medicine, Faculty of Medicine and Health Sciences, An-Najah National University, Nablus, Palestine.

DOI: https://doi.org/10.35516/jjps.v16i2.1493

ABSTRACT

Background: Androgenic-anabolic steroids (AAS) use has increased in the last years, especially among athletes, due to their effect on body shape and performance. These agents could have serious side effects among this highly susciptable population.

Methods: Cross-sectional study that included physical education students at An-Najah National University over the period of November 2020 to January 2021, using an electronic questionnaire. The main outcome was to measure the level of knowledge and use of AAS.

Results: A total of 380 students were included. The mean age of the students was 21 years (SD= 4.2), and study participants were distributed almost equally according to sex. About one fourth of the students were smokers. Eighty percent of the study participants are from West Bank while the remaining 20 % are from Jerusalem and 48 territories. Furthermore, most of the students live with their families, half of them live in cities, while about 40% live in villages and only 8% in camps. The average level of knowledge about AAS was 2.95 over 8 (37/100) with a median of three. Furthermore, only 36 (10%) participants had satisfactory knowledge, scoring 80% or more. Regarding the use of AAS, eleven participants (2.9%), all males, confirmed that they are currently using AAS. Additionally, about 28 (7%) had previously used them while 30 (8%) are planning to try them in the future. Overall, 221(58%) confirmed using vitamins and minerals.

Conclusion: Our study showed that the majority of participants have a substantial lack of information regarding the potential side-effects of AAS while the level of use is comparable with other populations.

Spectrum and Antibiotic Resistance in the Community and Hospital-Acquired Urinary Tract Infected Adults

Adham Abu Taha

Faculty of Medicine and Health Sciences, An Najah National University, Palestine.

DOI: https://doi.org/10.35516/jjps.v16i2.1494

ABSTRACT

Background: Urinary tract infection (UTI) is the most common infection in the community. The causative agents and antibiotic resistance differ between community-acquired and hospital-acquired urinary tract infections.

Objectives: This study aimed at identifying the etiologic agents in both community-acquired as well as hospital-acquired urinary tract infections and to determine the antibiotic resistance pattern of the most frequent organisms.

Methods: This is a retrospective cross sectional study of positive urine cultures of adult patients attending An-Najah National University Hospital (NNUH) between the period of Jan 2019 and Dec 2020.

Each patient's age, sex, and urine culture results were obtained from the microbiology lab of NNUH. Microbiology reports included the isolated microorganisms and their antibiotic susceptibility patterns.

Results: A total of 798 patients were included in the study, of which 472 (59.1%) were female. *Escherichia coli* was the most common uropathogen, accounting for 37.8% of the CAUTI and 25.1% of the HAUTI. In CAUTI, *E. coli* was followed by *E. faecalis* (16.4%), *Klebsiella pneumoniae* (13.7%), *E. faecium* (6.5%), and *Streptococcus agalactia* (4.9%). Among HAUTIs, the second most common was *Klebsiella pneumoniea* (21.4%) followed by *E. faecium* (19.3%), *E. faecalis* (13.4%), and *Pseudomonas aeruginosa* (7%). The rates of ESBL-producing strains of *E. coli* were similar between CAUTI (54.1%) and HAUTI (53.2%).

E. coli from CAUTI and HAUTI was sensitive to carbapenems, amikacin, and nitrofurantoin. The antibiotics with the highest resistance rates were ampicillin, cefuroxime, cotrimoxazole, and ciprofloxacin. Resistance rates were higher in HAUTI than in CAUTI.

Conclusions: The UTI etiological profiles and antibiotic resistance patterns varied between CAUTI and HAUTI; thus, a different antibiotic therapy for various categories should be considered when initiating empirical antimicrobial therapies.

Keywords: Adults, Urinary tract infection, Hospital-acquired urinary tract infection, Community-acquired urinary tract infection, Antibiotic resistance

Prevalence, Risk Factors and Complications of Preeclampsia at Rafidia Governmental Surgical Hospital in Palestine: Case-Control Study

Iyad Ali

Department of Medical Sciences, Faculty of Medicine and Health Sciences, An-Najah National University, Nablus, Palestine.

DOI: https://doi.org/10.35516/jjps.v16i2.1494

ABSTRACT

The development of hypertensive disorders is the most common medical complication during pregnancy. Preeclampsia (PE) causes multi-organ dysfunction and can lead to premature delivery, fetal death, and permanent organ damage in women. The purpose of this study is to estimate the prevalence of PE among the pregnant women who were followed at Rafidia Governmental Surgical Hospital (RGSH) in Nablus-Palestine for a year period from October 2020 to October 2021. During that period, we carried out an observational case-control study and assessed the risk factors, complications, and PE management in RGSH. The study included 170 patients with 85 preeclamptic and 85 randomly selected non-preeclamptic women from 5462 deliveries. PE group age ranged from 17 to 45 years old. PE prevalence increased with increasing gestational age (24% and 75% among women who were <37 and ≥ 37 of age, respectively), where maternal age and abortion incidents were associated with severe PE. First or multiple pregnancies were also factors linked to severe PE. Our findings support the body of evidence that PE is considered as a preventable high causative risk of fetal mortality and morbidity.

Keywords: Preeclampsia, diagnosis, risk factors, management, pregnancy.

Development of Child-Friendly Oral Formulations Containing Celecoxib: Biopharmaceutical Considerations for Formulation Scientists

Ramzi Shawahna[1,2*], Ahed Zyoud[3], Aseel Haj-Yahia[1], Raheek Taya[1]

[1] Faculty of Medicine & Health Sciences, An-Najah National University, Nablus, Palestine
[2] An-Najah BioSciences Unit, Center for Poison Control, Chemical and Biological Analyses, An-Najah National University, Nablus, Palestine.
[3] Faculty of Science, An-Najah National University, Nablus, Palestine.

DOI: https://doi.org/10.35516/jjps.v16i2.1496

ABSTRACT

Purpose: Recently, different international regulatory agencies and task forces have encouraged the pharmaceutical industry to develop child-friendly oral dosage forms. The biopharmaceutical classification system (BCS) has emerged as a tool that facilitates the development of traditional, reformulated, and novel oral dosage forms. Little research was conducted to evaluate the applicability of the BCS in developing child-friendly oral dosage forms. This study was conducted to assess the effects of age-related developmental changes in the composition and volume of gastrointestinal fluids on the solubility and performance of oral formulations containing celecoxib.

Methods: Solubility studies were conducted at 37 ºC in the pH range of 1.2 to 6.8 in 13 different age-appropriate biorelevant media that reflected the gastric and proximal small environments in fasted and fed states for adults and pediatric populations. Quantities of celecoxib were determined using a validated HPLC method. The permeability class of celecoxib was determined using *in vivo* pharmacokinetic parameters, and experimental and computational molecular descriptions.

Results: The solubility of celecoxib in the adult fed-state simulated gastric fluid was lower than that in the pediatric fed-state gastric media representative of neonates (birth to 28 days) fed soy-based formula. Similarly, the solubility of celecoxib in adult fasted-state simulated intestinal media was lower than that in the pediatric fasted-state intestinal media formulated with bile salt concentrations 50% of the adult levels. However, solubility values of celecoxib were lower in the other pediatric media compared to adult media. The age-appropriate pediatric to adult solubility ratios were outside the 80 to 125% range in 3 and was borderline in 1 out of 9 pediatric to adult solubility ratios.

Conclusions: The solubility ratios of celecoxib exhibited significant variability in about 44.4% of the media. This indicated that significant age-related variability could be predicted for oral formulations containing celecoxib intended for pediatric use. Formulation scientists should consider the significant biopharmaceutical considerations when developing child-friendly oral formulations.

Keywords: BCS, initial gastric volume, pediatric, permeability, solubility.

Crosslinking of Water-Soluble Cyclodextrin with Hyaluronic Acid for Targeted Drug Delivery

Fedaa Adaileh

The University of Jordan, Jordan.

DOI: https://doi.org/10.35516/jjps.v16i2.1497

ABSTRACT

Introduction: Most of the cytotoxic anticancer drugs belong to substances with both low solubility in aqueous fluids and poor cellular uptake, which lead to lack of specific therapy with apparent side effects. Therefore, there is a need to develop a novel drug delivery that can remotely and selectively release their payload. Curcumin(CUR) is an antibiotic, also a powerful inhibitor of the proliferation of several tumor cells.

Aims: The aim of the present work is to highlight and discussed hyaluronic acid (HA) to be grafted with Mono-6-deoxyl-6-ethylenediamino-γ-cyclodextrin (ɣ-CD-EDA) to shape a hydrogel that ought to structure inclusion complexes with curcumin, bettering its water-solubility and serving as a model drug delivery system

Methods: Distinct copolymers had been organized HA grafted with ɣ-cyclodextrin (ɣ-CD-EDA) to form a hydrogel with various HA: ɣ-CD-EDA ratios and characterized,

by means of ^{1}H-NMR spectroscopy, zeta potential, Thermogravimetry analysis (TGA) Differential scanning calorimetry (DSC), and transmission electron microscopy (TEM). Furthermore, drug loading Encapsulation efficiency (EE%), and release kinetics, and stability. Also, cytotoxicity and uptake were assessed by flow cytometry, MTT assay and confocal laser microscopy. Wound healing activity was once improved using three cell MDA-MB-231, MCF-7, and fibroblast. Measuring the effect of HA-γ-CD-EDA1-CUR, γ-CD-EDA1-CUR, and CUR free on the Production and Secretion of inflammatory cytokines

Result: CUR loading potential used to be at once correlated with extended HA-ɣ-CD-EDA composition and morphological adjustments have been discovered upon CUR binding. The host substances and their CUR inclusion complexes are no longer cytotoxic, and consequently beneficial for CUR and drug delivery**.** Moreover, HA-γ-CD-EDA1-CUR, γ-CD-EDA1-CUR, and CUR wound healing activity was once improved, and human promonocytic THP-1 cells produce inflammatory mediators such as IL-1β, IL10,IL8, TNF-α,IRAKI and IL6 results showed that the combination HA-γ-CD-EDA$_1$-CUR could be suitable to reduce inflammation and the complex promoted the anti-inflammatory effect by the inhibition of inflammatory mediators.

Conclusion: HA grafted with ɣ-cyclodextrin (ɣ-CD-EDA) to form a hydrogel was designed, formulated, and full characterized. Nanoparticles were stable at physiological pH and have released payload. Encapsulation of CUR into polymer increased its selectivity, distribution, and accumulation into the cancer cells. HA-CD-EDA$_1$conjugated curcumin if incorporated in suitable matrix has a potential utility for treatment of wound, and down regulation in THP-1 cells.

Keywords: Cancer, Targeted Therapy, Hydrogel, Inflammation, Wound healing, Cyclodextrin, Hyaluronic.

The Use of Zebrafish and in Vivo PAL as a Novel Discovery Platform for Psychoactive Agents

Frederick Williams

University of Toledo, USA.

DOI: https://doi.org/10.35516/jjps.v16i2.1498

ABSTRACT

Our research is utilizing the zebrafish model to study molecular processes and animal models of human diseases. These studies discussed here start to assess how different bath salts and methamphetaminecause death upon overdose by addressing the molecules that may bind to the illicit drugs. We have accomplished this by developing an in vivo photo-affinity labelling (PAL) system and studying the drugs in our system. The zebrafish has been lauded as a unique and powerful tool to examine development in a vertebrate animal and address molecular aspects of human disease for decades. We will examine recent published data from our laboratory utilizing the PAL system we developed.

Preparation of Semi-Solid Dosage Forms Containing Psidium Guava Leaves Extract as Antimicrobial Preservative

Fuad Al-Rimawi*, Mohammad Atieh

Chemistry Department, Faculty of Science and Technology, Al-Quds University, Jerusalem, Palestine.

DOI: https://doi.org/10.35516/jjps.v16i2.1499

ABSTRACT

Guava leaves extract has several medicinal activities as antimicrobial, antioxidant, anti-cancer and anti-inflammatory. Several studies have been proposed to use guava leaves extract in several preparations. However, applying guava leaves extract as a preservative in a pharmaceutical product has not been studied previously. In the present work, Guava leaves extract was used as natural preservative instead of chemical ones (methyl and propyl paraben). Guava leaves were extracted with ethanol 95% as extraction solvent with a percentage yield of 20%. This extract was tested by HPLC; several phenolic compounds were detected. To determine the ability to use this extract as a preservative, antimicrobial effectiveness test (preservative efficacy test) was conducted for extracted powder in purified water at different concentrations (0.5, 1.0, 1.5, and 2.0 % w/w), against three bacteria, one gram-positive (S. aureus), two gram-negative (P. aeruginosa, E. coli) and two fungi: one yeast (Candida albicans) and one mold (Aspergillus (Niger) brasiliensis). Results showed that 2% was effective and passed the test of preservative effectiveness test; this concentration was used in semi-solid pharmaceutical products. For this purpose, six different preparations (Ketoconazole shampoo, Clotrimazole Cream, Permethrin Cream, Gentamycin Cream, Ibuprofen gel, Indomethacin emulgel) were used. Chemical preservative was replaced by natural one (guava leaves extract powder) to serve as a preservative. Three out of the six preparations (Ketoconazole shampoo, Clotrimazole Cream, Ibuprofen gel,) passed preservative efficacy test. These preparations were fully checked-up by chemical (drug content,) physical (odor, physical appearance) and biological test (total count test) for three months at accelerated conditions. These results confirmed that these pharmaceutical preparations were stable and effective. As a conclusion Guava leaves extract can be used at 2% as natural preservative instead of chemical ones which have adverse side effects on human health.

A Comparative Study of in Vitro Lipoxygenase Inhibition and DPPH (1, 1-Diphenyl-2-Picrylhydrazyl) Free Radical Scavenging Activity of *Silybum marianum* and [*Notobasis syriaca* (L.) Cass.] Fruits and *Linum usitatisimum* Seeds

M. Alshieka, R. Jandali, Mohammad Isam Hasan Agha

Faculty of Pharmacy, Damascus University, Syria.

DOI: https://doi.org/10.35516/jjps.v16i2.1500

ABSTRACT

Silybum marianum and *Notobasis Syriaca* belong to the most widespread thorny plants in the Middle East, the Mediterranean, and large areas of Asia. Both plants are derived from the Asteraceae family, while Flax seed (*Linum usitatissmum* L.) is belong to the family of Linaceae.

The aim of this study was to compare the scavenging activity of free radicals, and to evaluate the anti-inflammatory activity of the fruit in vitro compared with flax seed. Methanol and ethanol extracts were prepared and the activity of scavenging free radicals was studied using DPPH, and the anti-inflammatory activity was investigated in-vitro using soybean lipoxygenase, in comparison with quercetin and Lignin as standards.

The fruit extract from *Notobasis Syriaca* has the highest capacity to scavenge free radical DPPH (IC_{50}=22.1 µg/ml), and it has higher ability to inhibit soybean lipoxygenase in-vitro (IC_{50}= 2.7 µg/ml) than fruit extract from *Silybum marianum* (IC_{50}= 9.8 µg/ml). This study showed that *Silybum marianum* and *Notobasis Syriaca* have a high ability to scavenge free radicals; and that both plants possess anti-inflammatory properties, while the scavenging potential of free radicals expressed in terms of IC_{50} (µg/ml) of flax seed showed extraction with a mixture of equal volumes of diethyl ether and ethyl acetate after direct acid hydrolysis exhibited higher antioxidant capacity (IC_{50}=22.257±0.095 µg/ml). The median inhibitory concentration (IC_{50}) was calculated according to the LOX enzyme inhibitory method. The IC_{50} value of a mixture of equal volumes of diethyl ether and ethyl acetate after direct acid hydrolysis extract of flaxseeds is 73.689±0.585 µg/ml.

As final conclusion it was found that flax seed extract has the highest anti-inflammatory activity.

Keywords: Lignans, antioxidant, flax seeds, *Silybum marianum*, *Notobasis Syriaca* DPPH, lipoxygenase inhibitory activity.

The Immunostimulatory Effect of Probiotic Conditioned Medium on RAW264.7 Murine Macrophages

Muna Barakat[1], Mohammad AA Al-Najjar[1], Shaymaa Abdulrazzaq[1], Wamidh H. Talib[1], Tamara Athamneh[2]

[1] Faculty of Pharmacy, Applied Science Private University, Jordan.
[2] Institute Council, Jordan University of Science and Technology, Jordan.

DOI: https://doi.org/10.35516/jjps.v16i2.1501

ABSTRACT

Background: Probiotics are a mixture of good live bacteria and/or yeasts that naturally survive in our bodies. Recently, loads of studies have focused on their role in the immune system and digestive tract. Accordingly, there are many commercially available probiotic products in the market. This study examines the immunostimulatory effect of commercially available-probiotic conditioned medium (PCM) on RAW264.7 murine macrophages.

Methods: Probiotic conditioned medium has been prepared by culturing the commercially available probiotic in a cell culture medium overnight at 37°C, followed by centrifugation and filter-sterilization to be tested on RAW264.7 murine macrophages. The immunostimulatory effect of different ratios (50, 75, 100) of PCM was examined using MTT assay, pro-inflammatory cytokine (tumor necrosis factor TNF-alpha) production in macrophages., migration, and Phagocytosis assays.

Results: At all the examined PCM ratios, the percentages of cell viability were >80%. Regarding the migration scratch, TNF-alpha and phagocytosis assays, PCM demonstrated a concentration-dependent pattern in the immunostimulatory effect. However, the ratio of 100 PCM illustrated a significant (p-value<0.05) stimulatory effect compared to the positive and negative control.

Conclusion: The findings of this study confirm the stimulatory activity of probiotic conditioned medium, which may contribute directly to the immune-boosting effect of the probiotic supplements.

Plasma Carnitine, Choline, γ-Butyrobetaine, and Trimethylamine N-oxide, but not Zonulin, are reduced in overweight/obese Patients with Pre/diabetes or Impaired Glycemia

Violet Kasabri,
University of Jordan, Jordan.

DOI: https://doi.org/10.35516/jjps.v16i2.1503

ABSTRACT

Background and Aims: Zonulin**,** carnitine, choline, γ-butyrobetaine (γ-BB), and trimethylamine N-oxide (TMAO) are intricately involved in metabolic anomalies and type 2 diabetes mellitus (T2D). This study aimed to compare and correlate the plasma levels of zonulin**,** carnitine, choline, γ-butyrobetaine, and TMAO, along with the adiposity, atherogenicity, surrogate insulin resistance (sIR), and proinflammatory hematological indices of newly diagnosed drug-naive pre-diabetic and diabetic patients vs. apparently healthy normoglycemic controls.
Methods: In a cross-sectional study, 30 normoglycemic subjects (controls) and 16 pre-diabetic (PreDM) and 14 type 2 diabetes (T2D) cases, that were gender and age-matched, were enrolled. Zonulin**,** carnitine, choline, γ-BB, and TMAO plasma levels were appraised using colorimetric assays. A comparison between the study groups was conducted by ANOVA while Spearman rank correlations between the metabolic risk biomarkers and between the risk markers and adiposity, sIR, atherogenicity, and proinflammatory hematological indices were also examined.
Results: Significant intergroup discrepancies in plasma carnitine, choline, γ-BB, and TMAO (but not zonulin) could be recognized in the cases vs. controls. Fasting blood glucose (FPG), glycated hemoglobin (A1C), triglycerides (TG), body mass index (BMI), lipid accumulation product (LAP), visceral adiposity index (VAI), atherogenic index of plasma (AIP), and all sIR were outstandingly higher in the cases vs. controls. Blood indices lacked a scoring value to discriminate cases from controls. Inadvertently, no relation was found between plasma carnitine, choline, γ-BB, TMAO, or zonulin in cases. Among the rest of the markers and sIR indices; The triglyceride-glucose-body mass index (TyG*BMI) related reciprocally to zonulin. Noticeably, among adiposity indices, TyG*BMI, triglyceride glucose-waist circumference (TyG*WC), and metabolic score for insulin resistance (MetS-IR) positively associated with waist circumference (WC), hip circumference (HC), BMI, body adiposity index (BAI), and waist-to-height ratio (WHtR). Exceptionally LAP proportionally correlated with all sIR. TyG*WC and MetS-IR correlated directly with the conicity index (CI). WHR directly associated with triglyceride-glucose (TyG) index and TyG*WC. Remarkably, the TyG index (but not TyG*BMI, TyG*WC, or MetS-IR) positively associated with all atherogenicity indices and RDW (but none of other blood indices). TMAO correlated inversely ($P < 0.05$) and moderately with choline. Distinctively, carnitine associated negatively with TC ($P < 0.05$). Both choline and carnitine related similarly and directly with PLR but inversely with lymphocytes ($p < 0.05$). Effectively, γButyrobetaine associated with both WC and the TyG-WC index equally negatively ($P < 0.05$). Substantially, γButyrobetaine correlated inversely with both atherogenic LDL-C/HDL-C ratio and MPV ($P < 0.05$). No pronounced relations were detected between the five microbiome signature determinants and glycemic control parameters (FBG and A1C %), sIR (TyG, TyG-BMI or MetS-IR), adiposity (WHR, WHtR, CI, BAI, LAP, or VAI), atherogenicity indices (TC/HDL-C ratio, non-HDL-C/HDL-C ratio, or AIP), or blood indices (NLR or MLR).**Conclusion:** Given the intergroup discrepancies in sIR, plasma zonulin, carnitine, choline, γ-BB, and TMAO along with their elective correlations with indices and clinical parameters of metabolic dysregulations, our study cannot rule out any possible molecular crosstalk and interplay of the biomarkers studied with the pathophysiology of prediabetes/diabetes. All in all, plasma zonulin, carnitine, choline, γ-BB, and TMAO with sIR can be putative surrogates for molecular cardiometabolic risk biomarkers to use as prognostic/predictive tools for the diagnosis/prevention and potential targets for prediabetes/diabetes management modalities.

Keywords: Zonulin trimethylamine-N-oxide, choline, carnitine, γ-butyrobetaine (γ-BB), trimethylamine-N-oxide (TMAO), flavin monooxygenase 3, atherogenic index of plasma, intestinal barrier integrity, metabolomics.

Recent Advancements in the Management of Neuropathic Pain

***Anas Hamdan*[*1], *Rafael Galvez*[2]**

[1] Department of Anesthesia and Resuscitation Technology, Faculty of Medicine and Health Sciences, An-Najah National University, Nablus, Palestine.
[2] Pain Clinic, Hospital Virgen de las Nieves, Granada, Faculty of Medicine. Granada. Instituto de Investigacion Biosanitaria IBS.Granada. Spain.

DOI: https://doi.org/10.35516/jjps.v16i2.1505

ABSTRACT

Neuropathic pain is defined as 'pain arising as a direct consequence of a lesion or disease affecting the Somatosensory system, regarding the most important aspects of analgesic treatment in NP its strongly advised to make use of a confirmatory questionnaire for NP Dx, such as DN4 or LANSS, as the Screening Tools. Administer analgesic medications in accordance with the strong evidence presented in NP. Keep in mind the medications that have been given the approval for NP. Tricyclic antidepressants, selective serotonin reuptake inhibitors (SNRIs; duloxetine, venlafaxine), and gabapentinoids; pregabalin and gabapentin; alone or in combination with topical (lidocaine patch, capsaicin patch) are all indicated as first-line analgesics for patients with peripheral NP. If a medication from the first line is unsuccessful, try another medication from the same group or move on to the second line. Tramadol and oxycodone are both considered to be analgesics of the second line. Tapentadol as a replacement drug in cases of persistent pain, it may be necessary to mix medications that work via distinct mechanisms of action. Alternatively, in the event that pharmacology is unsuccessful, analgesic invasive treatments may be combined with drugs.

Treatment of Macrophages with Gram-Negative and -Positive Bacterial Secretomes Induce Distinct Metabolic Signatures

Alaa Abuawad

Applied Science Private University, Jordan.

DOI: https://doi.org/10.35516/jjps.v16i2.1508

ABSTRACT

Infectious diseases represent major health and economic challenges globally. Emergence of multiple drug-resistant bacteria in the community and hospital has become a worldwide concern that requires novel approaches for rapid diagnosis and treatment. Metabolomics approach is a powerful tool providing important chemical information about the cellular phenotype of living systems, and the changes in their metabolic pathways in response to various perturbations. Metabolomics has become an important tool to study host-pathogen interactions and to discover potential novel therapeutic targets. In this study, untargeted LC-MS metabolic profiling was applied to differentiate between the impact of the secretome of the Gram-positive *S. aureus* SH1000 and Gram-negative *P. aeruginosa* PAO1 bacterial pathogens on THP-1 macrophages. The results showed that *S. aureus* and *P. aeruginosa* secretome affected alanine, aspartate and glutamate metabolism; sphingolipid metabolism; glycine and serine metabolism; GL metabolism; and tryptophan metabolism with different trends in THP-1 macrophages. However, the impact of both bacterial secretome on arginine and proline metabolism was similar. These data could contribute to a better understanding of pathogenesis and resistance of these bacteria and could pave the way for developing new therapeutics that selectively targeting Gram-positive or Gram-negative bacteria.

Investigations of Lipid Droplets Role in Attenuating Chemotherapeutic Responses to 5-FU in Cancer Cells *in vitro*

Duaa Sabbah

Petra University, Jordan.

DOI: https://doi.org/10.35516/jjps.v16i2.1509

ABSTRACT

Cancer has been considered as a main cause of death worldwide. Despite the effectiveness of traditional anticancer therapies such as 5-Flurouracil (5-FU), poor therapeutic outcomes are reported in many cases, due to tumor recurrence and chemoresistance. Intracellular lipid accumulation as lipid droplets (LDs) is now a well-recognized hallmark of cancer. However, the influence of LDs accumulation in cancer progression and treatment remains to be elucidated. Adjuvant use of non-chemotherapeutic drugs (e.g. NSAIDs and corticosteroids) with anticancer drugs to manage cancer related symptoms, may though serve as factors modulating the therapeutic response to anticancer agents via LDs related mechanisms. The aim of this study is to evaluate possible strategies influencing chemoresistance by attenuating LDs biogenesis and function. LDs levels in eight human cancer cell lines were measured. The existence of correlation between the cellular levels of LDs and cytotoxicity of ten chemotherapeutic agents was evaluated. A moderate correlation between basal LDs levels and the half inhibitory concentration (IC50) values of 5-FU on selected cell lines was established (r^2= 0.5235). Nevertheless, LDs levels were significantly elevated following exposure to 5-FU. A549 human lung cancer cells showed the highest increase in LD accumulation (***P >0.001) compared to their basal levels of LDs. LDs levels were also assessed following exposure to 5-FU in the presence of sub-lethal doses of celecoxib (CXB), dexamethasone (DEX), and simvastatin (SMV). Interestingly, CXB and DEX exposure to 5-FUtreated cells resulted in an alleviation in the antiproliferative activities of 5-FU in MDA-MB-468 and HCT116 but not in A549 cells. While, SMV exposure to 5-FU-treated cells resulted in reduced antiproliferative activities of 5-FU in MDA-MB-468 only. These results strongly suggest that increased LDs levels caused by CXB, DEX, and SMV may contribute in the development of a resistance mechanism exist only in some cancer types, which therefore, attenuates responses to 5- FU. The inhibition of phospholipid metabolism by DEX, as well as the inhibition of 3-hydroxy-3- methylglutaryl-CoA reductase (HMGCR) by SMV were expected to result in the up regulation of triacylglycerol (TAG), leading to LDs accumulation. This study highlights the importance of assessing drug-drug interaction before designing integrated therapy regimens for cancer patients receiving 5-FU treatment. Further studies are needed to discover the role of TAG inhibition on the sensitivity of cancer cells against 5-FU.

Phytochemical Screening and Diuretic Activity of selected Palestinian Medicinal plants in Mice using an Aqueous Extract
Division of Physiology, Pharmacology and Toxicology

Belal Rahhal, Isra Taha, Insaf Najajreh, Walid Basha, Hamzeh Alzabadeh, Ahed Zyoud, Areen Sharaga, Zanab Alratrout, Nima Yunis, Ola Kanaan, Jenan Raddad, Tasneem Yousef

Faculty of Medicine and Health Sciences, An- Najah National University, Nablus- Palestine.

DOI: https://doi.org/10.35516/jjps.v16i2.1510

ABSTRACT

Purpose: Man used various natural materials as a remedy for the treatment of various diseases and recently witnessed a vastly growing and renewed interest in herbal medicine globally. In Palestinian folk medicine, *Crataegus aronia*, *Rosmarinus officinalis* known as rosemary and Nigella sativa *is* used as a diuretic and for treatment of hypertension. This study aimed to assess the preliminary phytochemical properties and the diuretic effect of the aqueous extracts of these plants in mice after its intraperitonial administration.

Methods: It is an experimental trial applied on mice (n=8, Male, CD-1, weight range: [25-30 gram]), which are divided into two groups (4 in each). The first group administered with the plant extract (500 mg/kg), and the second with normal saline as negative control group. Then urine output and electrolyte contents were quantified up to 6 hours for the three groups and then compared to the control one.

Results: Preliminary phytochemical screening reveals the presence of tannins, alkaloids and flavoniods as major phytoconstituents in aqueous extract. Significant diuresis was noted in those received the aqueous extract of *Crataegus aronia* ($p < 0.05$) compared to controls. Moreover, aqueous extract had an acidic pH and a mild increase in the electrolyte excretion (Na, K).On the contrary, the aqueous extracts from the Rosemary and Nigella sativa showed no diuretic activity.

Conclusions: Our results revealed that *Crataegus aronia* aqueous extract has a significant potential diuretic effect. Further studies are needed to evaluate this diuretic effect in the relief of diseases characterized by volume overload.

Community Pharmacists' Knowledge, Attitude, and Practices Towards Dispensing Antibiotics without Prescription (DAwP) in the West Bank, Palestine

Mohammad Dweib

College of Pharmacy and Medical Sciences, Hebron University, Palestine.

DOI: https://doi.org/10.35516/jjps.v16i2.1516

ABSTRACT

Introduction: Non-prescription dispensing of antibiotics is common in the West Bank and this could contribute to the emergence of microbial resistance.

Objectives: To evaluate knowledge, attitude, and practices of community pharmacists towards dispensing antibiotics without prescription (DAwP) in the West Bank, Palestine.

Methods: A cross-sectional survey was conducted between April and May 2022 using a structured, validated, and pilot-tested questionnaire. Participants were community pharmacists who completed a 28-item questionnaire either in English or Arabic language based on their personal preference. The data was analyzed using descriptive and inferential analyses. Main outcome measure Knowledge, perception and practices towards dispensing antibiotics without prescription.

Results: Of the 650 community pharmacists approached, 580 completed the questionnaire (response rate: 89.3%). More than half (53.5%) of the pharmacists were not aware that DAwP is illegal practice. Lack of patient willingness to consult a physician for a non-serious infection (71.2%) and an inability to afford a consultation with a physician (63.4%) were the most common reasons claimed for DAwP. A statistically significant association was found between the number of antibiotics dispensed and educating patients about the importance of adherence and completion of the full course of antibiotics ($p < 0.05$).

Conclusions: In general, community pharmacists have inadequate understanding of the regulations prohibiting the over-the-counter sale of antibiotics in the West Bank, explaining the high rate of DAwP in the region. A complicated approach consisting of educational interventions and improving the access to and affordability of healthcare facilities for the general public is required to efficiently reduce DAwP and its negative consequences on public health.

Nuclear Magnetic Resonance for Targeted Metabolomics and Biochemical Sensor

Ahmed Bahti[1], Ahmad Telfah[1,2,3], Nour Sharar[3], Hanan Jafar[3], Roland Hergenröder[1]

[1] ISAS - Institute for Analytical Sciences, Bunsen-Kirchhoff-Str. 11, 44139 Dortmund, Germany.
[2] Technische Universität Dortmund, August-Schmidt-Str.4, 44227 Dortmund, Germany.
[3] Cell Therapy Center (CTC), The University of Jordan, Amman, Jordan.

DOI: https://doi.org/10.35516/jjps.v16i2.1519

ABSTRACT

NMR spectroscopy is quantitative, highly reproducible, non-selective and non-destructive. However, NMR costs and complexity hinder a use as point-of-care and biochemical sensor instrumentation. Low field NMR (LF-NMR) is an inexpensive and low footprint technique to obtain physical, chemical, electronic and structural information on small molecules, but suffers from poor spectral dispersion, especially when applied to the analysis of mixtures. Subspectral editing employing optimal control pulses is a suitable approach to cope with the severe signal superpositions in complex mixture spectra at low field.

We have calculated the optimal control pulse shapes at 0.5 T NMR frequency using the Krotov algorithm. Downsizing the complexity of the algorithm from exponential to polynomial is shown to be possible by using a system approach with each system corresponding to a (small) molecule. In this way compound selective excitation pulses can be calculated. The signals of substructures of the cyclopentenone molecule were excited using optimal control pulses calculated by the Krotov algorithm demonstrating the feasibility of subspectral editing. Likewise, for a mixture of benzoic acid and alanine, editing of the signals of either benzoic acid or alanine employing optimal control pulses was shown to be possible.

The obtained results are promising and can be extended to the targeted analysis of complex mixtures such as biofluids or metabolic samples at low field strengths opening access for benchtop NMR to point of care settings. Moreover, the LF-NMR was improved to allow a unique detection and reliable quantification of metabolites in biofluids like blood, urine, cerebrospinal fluid, or even tissue. In contrast to standard large scale NMR equipment the portable LF-NMR allows for an analysis of the chemical composition of biofluid samples directly at the patient (point-of-care).

LF-NMR can be freely programmable for detecting and detecting and sensing sets of small molecules which deliver information on the health status of a person. Such an analytical tool would be useful for the prediction, diagnosis, monitoring and prognosis of diseases, and for supervision of therapeutic interventions.

Implication of Nanotechnology for Pulmonary Delivery of Docetaxel

Alaa Aziz Fraj Abudayah

Jordan University of Science and Technology, Jordan.

DOI: https://doi.org/10.35516/jjps.v16i2.1527

ABSTRACT

Docetaxel (Taxotere®) is a taxoid antineoplastic agent used in the treatment of various cancers. Docetaxel belongs to class IV drugs in the Biopharmaceutics Classification System (BCS), and their clinical use is limited due to their extreme hydrophobicity, low water solubility, low bioavailability, and high toxicity. This study aims to prepare nanoparticles for pulmonary delivery of Docetaxel with enhanced solubility and dissolution targeting pulmonary tissues. Accordingly, PLGA-Docetaxel nanoparticles (NPs) were prepared by nanoprecipitation method and coated with Carboxymethyl chitosan to investigate its effectiveness as inhaled anticancer therapy. Four formulations had been prepared to reach the highest loading capacity (LC%) and encapsulation efficiency (EE%) and to study the effect of the amount of Carboxymethyl chitosan on the drug release. The sizes, charges, homogeneity, surface morphology, LC% and EE% of the NPs were determined. The NPs were characterized using FTIR and XRD. In vitro release profiles of Docetaxel from PLGA NPs, at pH 5.5, 6.5, and 7.4 were determined. The sizes of the four formulations ranged between 227.7± 9.5 and 306.4 ± 27.4. All prepared formulations showed acceptable monodispersity with positive charges. The EE% was above 99% and the LC% ranged between 31-63%. The in vitro release of Docetaxel show an inverse relation to the amounts of Carboxymethyl chitosan used and the pH of the dissolution medium. In conclusion, coating PLGA NPs with Carboxymethyl chitosan may be used as a good carrier for pulmonary delivery of Docetaxel

Elaeagnus Angustifolia Plant Extract inhibits Epithelial- mesenchymal Transition in Human Colorectal Cancer via β-catenin/JNK signaling Pathways

Arij Fouzat Hassan[1], Ashraf Khalil [1], Ala-Eddin Al Moustafa[2,3,4*]

[1] College of Pharmacy, Qatar University, Qatar; ah1304418@qu.edu.qa (A.F.); akhalil@qu.edu.qa (A.K.)
[2] Biomedical Research Center, Qatar University, Qatar; aalmoustafa@qu.edu.qa (A.-E.A.M.)
[3] College of Medicine, QU Health, Qatar University, Qatar; aalmoustafa@qu.edu.qa (A.-E.A.M.)
[4] Oncology Department, Faculty of Medicine, McGill University, Montreal, QC, Canada; aamousta-fa@qu.edu.qa (A.-E.A.M.)

DOI: https://doi.org/10.35516/jjps.v16i2.1528

ABSTRACT

Elaeagnus angustifolia (*EA*) is a traditional plant that has been used as an alternative medicine for centuries. *EA* roles as anti-cancer has been investigated against different types of cancer, however, its effect against human cancer has not been investigated yet. Therefore, we investigated the aqueous *EA* extract effect on colorectal cancer (CRC) cell lines (HCT-116 and LoVo) and examined its underlying mechanisms of action *in vitro*. Our results showed that *EA* inhibited cell proliferation and disturbed cell-cycle progression of both CRC cell lines comparing to the control. Moreover, *EA* extract significantly reduced colony formation in addition to migration and invasion ability of both CRC cell lines this is confirmed by significant upregulation of E-cadherin and Pan-cadherin as well as down regulation of Vimentin. Further, β-catenin/JNK signaling pathway was analyzed and we found that *EA* extract significantly blocked the activity of total and phosphorylated β-catenin and JNK1/2/3.

Novel NMR Technique for In-Vitro Toxicity Testing of a 3D Cancer Model

Mohammad AlWahsh[1,2,3], Robert Knitsch[1], Rosemarie Marchan[4], Jörg Lambert[1], Elen Tolstik[1], Hannes Raschke[1], Dina Mahadaly[3], Alexander Marx[2], Djeda Belharazem[2], Roland Hergenröder[1]

[1] Leibniz-Institut für Analytische Wissenschaften—ISAS-e.V., 44139 Dortmund, Germany.
[2] Institute of Pathology and Medical Research Center (ZMF), University Medical Center Mannheim, Heidelberg University, Germany.
[3] Department of Pharmacy, Faculty of Pharmacy, Al-Zaytoonah University of Jordan, Jordan.
[4] Department of Toxicology, Leibniz Research Center for Working Environment and Human Factors at the TU Dortmund (IfADo), Germany.

DOI: https://doi.org/10.35516/jjps.v16i2.1529

ABSTRACT

The metabolic pathogenesis of thymic carcinomas (TCs) is poorly understood and adjuvant therapy has limited success in metastatic disease and tumor recurrence. Most studies on TCs use two-dimensional (2D) cell culture models, which are not considered as physiologically relevant, and consequently translation to the in-vivo situation remains challenging. Tissue-specific architecture, based in part on interactions with the microenvironment is an essential component of tumors and may be better recapitulated in three-dimensional (3D) cell culture models. Therefore, our goal is to establish 3D thymoma models which will then be used to understand the pharmacokinetics and pharmacodynamics of anticancer drug therapy via metabolic profiling of living cells. Our novel approach using NMR allows for the measurement of small tissue-like models, which are normally not feasible with standard analytical techniques. The currently-available methods only provide a "snap-shot" of the measured time point and tend to be destructive, e.g. dissecting or optical cleaning of the specimen to gain 3D Information – a limitation we overcome with our current method using NMR spectroscopy. In addition, anticancer therapy is only partially effective, mainly due to inherent or drug-induced resistance of tumor cells to standard chemotherapeutics and radiotherapy. Therefore, novel therapeutic strategies are urgently needed.

The Potential Effects of the Essential Oil of Coriander Seeds on Bacterial Biofilm and Immune Cells

Eliza Hasen

Applied Science Private University, Jordan.

DOI: https://doi.org/10.35516/jjps.v16i2.1530

ABSTRACT

Background: Nowadays, the pharmacological activities of many natural phytochemicals have a huge impact on pharmaceutical research and drug development. Hence, numerous studies have been conducted to investigate plants' efficacy, fractions, and isolated pure compounds to discover new therapeutic agents. Aim: This study aimed to evaluate the potential activity of coriander essential oil (CEO) on bacterial biofilm and immune cells. Methods: CEO has been extracted from the seeds through the hydrodistillation method, and its chemical composition was analyzed using gas chromatography (GC) and Nuclear magnetic resonance (NMR). The antibacterial activity of CEO was assessed using different bacterial strains (P. aeruginosa, S. aureus, S. epidermidis and E. coli), both in planktonic and biofilm forms. In addition, this activity has been investigated individually and in combination with selected antibiotics (Gentamicin and Ciprofloxacin), using the bacterial enumeration following the MBEC Assay® protocol. Pyocianin (PYO) has been measured using a plate reader on 690 nm absorbance, where wells tested were treated with different CEO concentrations (12.5, 25, 50 and 100 mg/mL). An MTT assay was also used to examine the CEO'seffect on the viability of RAW 246.7 murine macrophages. Data were analyzed using GraphPad Prism 9 software. Results: Six major compounds were identified in CEO; Linalool was the most predominant. Regarding the activity of the CEO on planktonic bacteria, cell count was obtained and calculated as log reductions; significant log reductions ($p<0.05$) were measured on 300 mg/mL of CEO for all P. aeruginosa, S. aureus, S. epidermidis and E. coli, 2.00, 6.73, 6.93 and 7.68 respectively. While for the bacterial biofilm, a significant ($p<0.05$) log reduction in the cell count was obtained at 300 mg/mL of CEO for all of P. aeruginosa, S. aureus, S. epidermidis and E. coli, 2.22, 5.33, 5.83 and 6.76, respectively. Minimum inhibitory concentrations (MIC) of the combination of antibiotics Gentamicin (0.60, 0.15, 1.22, 0.3 µg/mL) or Ciprofloxacin (0.075, 0.03, 0.004 and 0.002 µg/mL) for all P. aeruginosa, S. aureus, S. epidermidis and E. coli, respectively, with 50 mg/mL of CEO on planktonic and biofilm bacteria. PYO measurements obtained showed anti-quorum sensing activity of CEO, the absorbance detecting PYO levels, was decreasing as the concentration of CEO was increasing, absorbances were (0.66, 0.075, 0.097 and 0.11), whereas the control of P. aeruginosa was (0.124). On the other hand, the antibacterial/antibiofilm concentrations were cytotoxic (percentage of viability <80%) to macrophages and the safe level was (0.30 mg/mL) of CEO. Conclusion: These results indicated that CEO may have a promising role in bacterial biofilm eradication, which may help manage and prevent chronic infections in the future. However, more investigations are required to understand the exact mechanism and improve its safety on immune cells.

Formulation and evaluation of controlled-release, carrageenan-based powder formulations filled into hard gelatin capsules

Abdullah Barakat[1], Yahya Abu-Hameda[1], Salah Aljamal[1], Suha Al Muhaissen[1], Lorina Bisharat[1,2], Alberto Birardi[2], Hatim S. AlKhatib[1]

[1] School of Pharmacy, The University of Jordan, Amman, Jordan.
[2] DFE Pharma, Goch, 47574, Germany.

DOI: https://doi.org/10.35516/jjps.v16i2.1531

ABSTRACT

Hard gelatin capsules (HGCs) are typically used as immediate release dosage forms, however, controlled drug release can from HGCs be obtained by the application of film coating onto the capsule shells or by filling them with controlled release multi-particulates (e.g. pellets and mini-tablets).

The filling of a hydrophilic gelling polymer into the capsule is an alternative approach to the time-consuming preparation and filling of multi-particulates. Carrageenan is a linear, sulfated polysaccharide that is commonly used as a thickener in pharmaceutical formulations.

The release behavior of propranolol HCl – carrageenan powder mixtures filled into hard gelatin capsules was investigated as a function of drug – to – polymer ratio, the capsule fill weight, grade of carrageenan used. In addition, the effect of the drug release testing method (USP apparatus I or II), rotation speed, pH of the release medium and ionic strength of the release medium on drug release were investigated.

The electrostatic interaction of propranolol HCl with carrageenan was also investigated using equilibrium dialysis method to determine the binding capacity and the stability constant of the complex formed.

Viscarin GP 109 was found to provide a fast-gelling behavior with excellent controlled release properties. Drug loading and ionic strength of the medium significantly influenced drug release. Release in USP apparatus 1 was slower than that in USP apparatus 2. Propranolol HCl formed an insoluble complex with carrageenan with a high binding capacity and stability

Preparation and characterization of drug-loaded, electrospun nanofiber mats formulated with zein or zein-based mixtures for wound healing applications.

Salah Aljamal[1], Shrouq Sotari[2], Ola Tarawneh[3], Nabil Al-Hashimi[4], Saja Hamed[4], Mahmoud Al-Hussein[5] and Hatim S. AlKhatib[1]

[1] School of Pharmacy, The University of Jordan, Amman, Jordan.
[2] Cell Therapy Center, The University of Jordan Amman, Jordan.
[3] Faculty of Pharmacy, Al-Zaytoonah University of Jordan, Jordan.
[4] Faculty of Pharmaceutical Sciences, The Hashemite University, Jordan.
[5] Physics Department and Hamdi Mango Center for Scientific Research, The University of Jordan, Amman, Jordan.

DOI: https://doi.org/10.35516/jjps.v16i2.1532

ABSTRACT

Electrospun zein mats are known to have poor mechanical and water uptake properties limiting their usefulness as wound dressings.

In this study, the effects of the solvent system used, the incorporation of the polymeric additives; polyethylene glycol 20000 (PEG20K) and polyvinylpyrrolidone K30 (PVPK30); and the crosslinking agent Tannic Acid (TA) on the mechanical and water uptake characteristics of zein – based nanofiber mats were investigated.

The incorporation of either PEG20K or PVPK30 resulted in an improvement in water vapor sorption and a reduction in water contact-angle of the nanofiber mats. In addition, the incorporation of PEG20K and PVPK30 reduced the ultimate tensile strength, and Young's modulus while increasing the percent elongation of the nanofiber mats. The use of tannic acid as a crosslinking agent led to an increase in the water vapor sorption, ultimate tensile strength, and Young's modulus of the nanofiber mats.

Mats with smaller average fiber diameter, greater ultimate tensile strength, higher Young's modulus, and greater water vapor sorption were obtained when using 80% (v/v) aqueous ethanol as a solvent system during the preparation of the nanofiber mats when compared to those produced using 60% (v/v) aqueous ethanol. In addition, using solutions with lower zein concentration resulted in mats with lower average fiber diameter, lower ultimate tensile strength and Young's modulus, and higher percent elongation.

Selected formulations were loaded with tetracycline hydrochloride and drug release was evaluated in bulk liquid and using Franz diffusion cells. The use of Franz diffusion cells allowed the discrimination between formulation performance as a function of composition and water uptake properties. Drug release from nanofiber mats was also confirmed by observing the formation of an inhibition zone in cultures of E. coli and S. aureus using the agar diffusion assay.

Improved performance of zein nanofiber mats was achieved using polymeric modifiers and crosslinking with tannic acid improving their suitability for wound dressing applications.

Preparation, in vitro and in vivo evaluation of solid-in-oil dispersion-based formulation the anti-glaucoma drug, timolol maleate

Noor Barakat[1], Mai Jaber[2], Hatim S. AlKhatib[1]

[1] School of Pharmacy, The University of Jordan, Amman, Jordan.
[2] Faculty of Pharmaceutical Sciences, The Hashemite University, Jordan.

DOI: https://doi.org/10.35516/jjps.v16i2.1533

ABSTRACT

Lowering Intraocular pressure (IOP) is a main therapeutic objective in glaucoma patients because IOP is an important risk factor for glaucoma progression. The objective of this work was to formulate and evaluate, in vitro and in vivo, a stable and effective Solid in Oil (S/O) topical formulation of the antiglaucoma drug, timolol maleate (TM). S/O dispersions were prepared by emulsification of aqueous TM solutions in cyclohexane using different amount of the span 85 then lyophilizing the emulsion to produce TM – Span 85 complexes. The complexes were then dispersed in castor oil using tip sonicator to produce S/O nanodispersions. S/O nanodispersions were evaluated in terms of particle size, polydispersity index, encapsulation efficiency, morphology, physical stability, as well as transcorneal permeation and accumulation of TM. In addition, the in vivo tolerability and efficacy of the prepared formulation in lowering intraocular pressure were evaluated in rabbits.

Spherical nanoparticles of TM with a particle size of about 134-155 nm were successfully prepared and found to be physically stable. The encapsulation efficiency was high and was found to be dependent on the level of Span 85 used.

In comparison to TM solution, S/O nanodispersion enhanced TM permeation and decreased accumulation in transcorneal diffusion studies. In addition, application TM S/O nanodispersion onto rabbit eyes resulted in a significant reduction in IOP in comparison to TM aqueous solution.

QCAR$_x$E: Qatar-based cardiovascular risk assessment using the English/Arabic version of the EPI·R$_x$ISK™ mobile application

Lana Abdulkarim Kattan

Qatar University, Qatar.

DOI: https://doi.org/10.35516/jjps.v16i2.1534

ABSTRACT

Background: Cardiovascular disease (CVD) is the leading cause of death worldwide, accounting for almost one-third of the total global deaths. Early CVD risk assessment and management (RAM) has demonstrated to be effective in decreasing CVD-related burden. However, CVDRAM services face many challenges and barriers in the community. Mobile technology has been advocated to facilitate access to CVDRAM for both healthcare providers and patients to overcome these barriers. Nevertheless, there is limited availability and use of CVDRAM-related mobile technology in the Middle East region.

Objectives: To develop and implement an English and Arabic version of a mobile and a web application for CVDRAM in both, community pharmacies and selected primary care centres in Qatar.

Methodology: This study was conducted in two phases. In Phase 1, translation of the EPI·RxISK™ CV risk calculator (ERC) into the Arabic language was conducted based on guidelines developed by the International Society for Pharmacoeconomics and Outcomes Research. The English/Arabic version of the ERC was pilot tested by potential end users, consisting of a sample of community pharmacists (CRxs) and members of the public (MOP) accessing community pharmacy services. Semi-structured interviews were conducted based on the constructs of the Mobile Application Rating Scale (MARS) and data were analyzed using deductive content analysis. In Phase 2, a prospective observational study (QCARxE) is underway to explore the feasibility of using the ERC in patients accessing primary health care services for CVDRAM, including community pharmacies and primary health care centers (PHCC).

Results: In Phase 1, a total of 10 CRxs and 5 MOP were interviewed. The data derived from the interviews indicate that the ERC web and mobile application were overall, positively perceived as having quality engagement, functionality, aesthetics, information and subjective quality attributes. To date, a total of 36 patients have enrolled in the QCARxE study (20 from PHCC and 16 from community pharmacies). At their initial CVD risk assessment visit, the mean CVD risk score for these patients was 28.3%, and the most prevalent risk factor was obesity (mean BMI = 30.2 kg/m²).

Conclusion: The themes derived from the interviews indicate that the ERC was overall, positively perceived. Preliminary data derived from the QCARxE study indicated a significant proportion of patients accessing primary health care services are at high CVD risk. It is speculated that the use of the ERC will enable patients to become better aware of their CVD risk and improve access to risk factor interventions.

Identification and Separation of the Degradation Products of Vildagliptin Tablets and Raw Material using LC-MS and NMR, and then Exploration of the Corresponding Degradation Pathways

Enas Alqudah, Malak Abbadi, Sawsan Alqadoomi, Ibtihal Abo Hameda, Sharif Arar, Kamal Sweidan*

Department of Chemistry, School of Science, The University of Jordan, Amman, Jordan.

DOI: https://doi.org/10.35516/jjps.v16i2.1535

ABSTRACT

A gradient high performance liquid chromatography (HPLC) method has been developed for the qualitative and quantitative analyses of vildagliptin related substances. This method is based on using of RP-C18 (250 × 4.6 mm×5µm) and gradient elution with phosphate buffer and methanol as mobile phase. Various forced degradation studies were conducted to establish an impurity profile for vildagliptin in the tablet formula. Three degradation products were produced upon exposing vildagliptin to different degradation conditions (acidic, basic, oxidative, photolytic, aqueous and thermal); their structures were characterized using LC-MS and NMR (^{1}H NMR, ^{13}C NMR and DEPT) techniques. Some excipient components, examined in this study, had major effect towards producing any extra new degradation products.

Keywords: Vilaglibtin, tablet form, excipients, forced, degradation, impurity profile, 2D-NMR.

Video-based teach-to-goal intervention on inhaler technique on adults with asthma and COPD: a *randomized controlled trial*

Mohammad Al-Kharouf[1], Mariam Abdeljalil[1], Nathir Obeidat[2], Khaled Al Oweidat[2], Oriana Awwad[1*]

[1] Department of Biopharmaceutics and Clinical Pharmacy, School of Pharmacy, the University of Jordan, Amman, Jordan.
[2] Department of Internal Medicine, Faculty of Medicine, University of Jordan, Respiratory and sleep Medicine, Jordan University Hospital, Amman, Jordan.

DOI: https://doi.org/10.35516/jjps.v16i2.1538

ABSTRACT

The incorrect use of inhalers is highly associated with poor patient outcomes. This randomized controlled trial investigated the impact of a novel video-based teach-to-goal (TTG) intervention on the following outcomes; mastery of inhaler technique, disease control, medication adherence, and disease-related QoL over time among patients with asthma and COPD.

After baseline assessment, participants received either a verbal (control group) or a video-based (intervention group) TTG strategy and were assessed after three months for the impact of the intervention on the intended outcomes. At baseline, intervention (n=51) and control (n=52) groups had comparable characteristics. At follow-up, inhaler technique and medication adherence improved among the intervention group compared to control group ((93.4% vs 67%) and (88.2% to 61.5%), respectively ($p<0.05$)) as well as to baseline ((93.4% to 49.5%) and (88.2% to 66.7%), respectively ($p<0.05$)). Similarly, disease control was also ameliorated among the intervention group compared to baseline (35.3% to 54.9%) ($p<0.05$). QoL scores improved significantly among asthma patients (intervention group) at follow-up in comparison to baseline. Better scores were also observed for COPD patients compared to controls, ($p<0.05$).

Interventions using video-based TTG education are effective in enhancing and retaining the inhaler technique over time, with a positive impact on disease outcomes among patients with asthma and COPD.

Keywords: Asthma, Chronic Obstructive Pulmonary Disease, Patient Education, Teach-To-Goal Education, Video-Based, Randomized Controlled Trial.

Development and Physiochemical Characteristics of Vitamin C-loaded Microneedles

Raffa Aborayya, Amani abu kwaik, Yasmeen aladhami, Mais Naser, Ola Tarawneh, Rania Hamed

Department of Pharmacy, Faculty of Pharmacy, Al-Zaytoonah University of Jordan, Jordan.

DOI: https://doi.org/10.35516/jjps.v16i2.1539

ABSTRACT

Vitamin C, ascorbic acid, is a water-soluble vitamin that is considered as one of the most potent antioxidant agent. It delays early skin aging, protects against harmful free radicals, improves wrinkles appearance under-eye circles, and reduces redness and hyperpigmentation. One of the most common way to deliver vitamin C to the body's tissue is through skin layers. Nevertheless, the effect of such ingredient might be limited due to the stratum corneum barrier which decreases the ability to reach the site of action. In this study, we provide an innovative strategy of utilization dissolving microneedles (MNs) to enhance skin-drug delivery system and overcome problems associated with the conventional formulations. A delivery system of micro-molds which provide a diverse range of three-dimensional (3D) MNs were used for the fabrication of vitamin C patches. Vitamin C MNs were examined for mechanical force tolerance, drug release, dimensional evaluation, dissolution, insertion, and permeation tests. Drug, polymers, and stabilizers were mixed at different ratios. Hydrogels were filled into the molds, centrifuged and left for air dry for 24-48 h. Appearance was visualized under light microscope. Patches were analyzed to determine percent assay of drug loaded, mechanical force, and penetration through the skin. The amount of vitamin C loaded into MNs was found to be 102%. MNs were easily inserted and dissolved through skin within 30 s. The dissolution rate of MNs were tested by using rat skin to determine the release of vitamin C within several time intervals. The in vitro release of vitamin C loaded MNs showed cumulative release percentage up to 70% in 9-10 h. Therefore, MNs as dermal drug delivery system was successfully developed, providing efficient release of vitamin C through the skin.

Barriers and facilitators of inappropriate surgical antimicrobial prophylaxis in endourological procedures: a qualitative study from Jordan

Sondos Abdaljaleel[1], Rima Hijazeen[1], Mariam Abdel Jalil[1], Oriana Awwad[1], Ghazi Edwan[2], Mohammad Amaireh[3]

[1] Department of Biopharmaceutics and Clinical Pharmacy, Faculty of Pharmacy, University of Jordan, Amman, Jordan.
[2] Department of Urology, The University of Jordan, Amman, Jordan.
[3] Department of Urology, Islamic Hospital, Amman, Jordan.

DOI: https://doi.org/10.35516/jjps.v16i2.1540

ABSTRACT

Background: Inappropriate surgical antimicrobial prophylaxis (SAP) practice increases patients' morbidity, healthcare cost, and antimicrobial resistance. Several guidelines have been published to set guidance for SAP before endourological procedures. Such guidelines include the American Urological Association (AUA, 2019) and the European Association of Urology (EAU, 2020). Literature reported that compliance with the recommendations of these guidelines has been suboptimal.

Aims: to investigate healthcare professionals' (HCPs) perspectives on the barriers to international guideline adherence regarding SAP for endourological procedures and the potential strategies to optimize adherence to guidelines recommendations.

Methodology: This study was a qualitative study based on face-to-face semi-structured interviews conducted with urologists in multiple medical centers across Jordan using a preformulated interview guide regarding barriers and facilitators to the adherence to international guidelines of preoperative SAP during endourological procedures.

Results: Nineteen urologists were interviewed. Interviews identified many barriers influencing HCP adherence to guidelines, these included factors related to patients, HCPs, the healthcare system, or other external barriers. Also, during the interviews, HCPs suggested many strategies to enhance SAP practice which included increasing patients' awareness about their actual need for antibiotics, providing training sessions for HCPs about appropriate SAP before endourological procedures, developing national guidelines and conducting local clinical studies, and promoting awareness of the clinical pharmacist's role. In addition to imposing national policy to control antibiotic use and prevent over-the-counter (OTC) prescriptions.

Conclusion: Factors related to nonadherence to guidelines were determined. Such knowledge will constitute the backbone for planning appropriate antimicrobial stewardship programs that involve all stakeholders and address all those aspects to optimize SAP prescribing and reduce antibiotic misuse.

Compliance with Antimicrobial Prophylaxis Guidelines in Endourological Procedures: Frequency and Related Outcomes

Sondos Abdaljaleel[1], Mariam Abdeljalil[1], Oriana Awwad[1], Ghazi Al Edwan[2], Mohammad Amaireh[3], Manar Hamdan[1], Ahmad Khattab[1], Tasneem Al-Hourani[1]

[1] Department of Biopharmaceutics and Clinical Pharmacy, School of Pharmacy, The University of Jordan, Amman, Jordan.
[2] Department of Urology, The University of Jordan Hospital, Amman, Jordan.
[3] Department of Urology, Islamic Hospital, Amman, Jordan.

DOI: https://doi.org/10.35516/jjps.v16i2.1541

ABSTRACT

Introduction: Surgical antimicrobial prophylaxis (SAP), when used appropriately based on evidence-based guidelines, reduces the rate of infectious complications following endourological procedures without compromising patient outcomes.

Aims: to audit the appropriateness of the current SAP used in endourological surgeries based on international guidelines and report their associated outcomes (urinary tract infection (UTI) and bloodstream infection (BSI)).

Methodology: The adherence to international guidelines recommendations; AUA 2019 and EAU 2020, regarding indication, duration, choice, and dose of the antibiotics used in endourological procedures were assessed in two medical centers in Amman/Jordan. Also, patients were asked to conduct laboratory urine test to determine the rate of infectious complications within one-month post-procedure.

Results: Three hundred sixty-one patients were recruited for the study. The adherence rate to guidelines regarding indication, choice, and dose of pre-operative antibiotics was 90.3%, 2.8%, and 77.8% respectively. The duration was concordant with guidelines in only 3.4% of participants. A total of 41.8% of patients completed follow-up. Among those, 4.6% developed bacterial UTIs, and 0.7% developed BSI.

Conclusion: Adherence to SAP guidelines in endourological procedures is far from optimal, especially by an inappropriate selection of broad-spectrum antibiotics as the agent of choice and prolonged use of antibiotics after the procedure in the absence of any documented infectious complication.

Identifying factors associated with increased rate of mortality of COVID-19 patients among Jordanian population: A multicenter case-controlled retrospective study

Walid Al-Qerem, Mohammad Safar, Ibrahim Safar, Mahmood Al-Ibadah

Department of Pharmacy, Faculty of Pharmacy, Al-Zaytoonah University of Jordan, Jordan.

DOI: https://doi.org/10.35516/jjps.v16i2.1542

ABSTRACT

Coronavirus 2019 (Covid-19) is a serious infectious disease that affects humans globally. Identifying factors that increase the prevalence of mortality are of interest for the healthcare providers. Therefore, the present study aimed to evaluate many risk factors and its association with mortality among COVID-19 patients.

A total of 353 patients enrolled in this multicentered case-controlled retrospective study that was conducted in two designated hospitals in Amman, Jordan on patients admitted between 25 October 2020 to 26 September 2021. According to a stepwise binary logistic regression analysis found that patients who took Meropenem ($p<0.001$) and beta blockers ($p=0.004$) had lower incidence to be discharge during hospitalization. Also, diabetic patients ($p<0.001$) had lower discharge rate. We concluded that patients with secondary bacterial infection during the course of hospitalization, patients who needed to take beta blockers and diabetic patients are at higher risk of mortality.

Effect of Surface Modification with Na Lauryl Sulfate on The Water-Uptake and Release Properties of Na Tripolyphosphate-Cross Linked Chitosan Beads

Wasan Alwahsh[1,2], Mai Jaber[1], Suha Al Muhaissen[1], Bashar Al-Khalidi[1], Shariza Sahudin[2], Hatim S. AlKhatib[1]

[1] School of Pharmacy, The University of Jordan, Amman, Jordan.
[2] Department of Pharmaceutics, Faculty of Pharmacy, Universiti Teknologi Mara, Puncak Alam Campus, Malaysia.

DOI: https://doi.org/10.35516/jjps.v16i2.1543

ABSTRACT

In this study we evaluated the effect of Na Lauryl sulfate (SLS) on the water-uptake and release properties of Na Tripolyphosphate (TPP)-cross linked chitosan beads. Chitosan beads were prepared by dropping riboflavin-loaded, chitosan (CS) solution into a curing medium composed of either an aqueous solution of TPP, SLS or a combination of these solutes. The resultant beads were characterized in terms of their size, drug encapsulation efficiency, water uptake properties by gravimetry and image analysis. Drug release properties of the prepared beads were studied using USP Apparatus 1 in media with different pH and ionic strength. Composites (CS/TPP, CS/SLS, and CS/TPP/SLS) were also evaluated using DSC, FTIR and contact angle measurements. Encapsulation efficiency was found to be 93%, 93.2% and 93.1% for CS/TPP, CS/SLS, and CS/TPP/SLS beads respectively and did not show any dependence on the composition of the curing medium for riboflavin. FTIR data suggested the presence of electrostatic interactions between positively charged amine group of CS and the negatively charged TPP and SLS. Drug release from the prepared beads was prolonged with CS/SLS beads releasing the drug faster than CS/TPP beads. The slowest drug release was observed in the case of CS/TPP/SLS beads. Drug release from the different types of beads was pH-dependent with the fastest release observed in 0.1 N HCl. Gravimetric water uptake was highest for CS/SLS beads followed by CS/TPP and CS/TPP/SLS respectively. Swelling study using image analysis showed a similar trend to the gravimetric water uptake results. The drug release and water uptake results could be explained by the effect of SLS on the wettability of the beads and the ability of the release medium to hydrate them which was confirmed by the high contact angle between water and CS/TPP/SLS composites.

Aspirin Effect on Tobacco Smoke Withdrawal-Induced Anxiety In Female Rats

Lujain F. Alzaghari, Alaa M. Hammad

Department of Pharmacy, Faculty of Pharmacy, Al-Zaytoonah University of Jordan, Jordan.

DOI: https://doi.org/10.35516/jjps.v16i2.1544

ABSTRACT

Chronic exposure to cigarette smoke produces neuroinflammation and long-term changes in neurotransmitter systems, especially glutamatergic systems. We examined the effects of cigarette smoke on astroglial glutamate transporters as well as NF-κB expression in mesocorticolimbic brain regions including the prefrontal cortex (PFC) and the nucleus accumbens (NAc). The behavioral consequences of cigarette smoke exposure on withdrawal-induced anxiety-like behavior were assessed using open field (OF) and light/dark (LD) tests. Sprague-Dawley rats were randomly assigned to 5 experimental groups: a control group exposed only to standard room air, a cigarette smoke exposed group treated with saline vehicle, two cigarette smoke exposed groups treated with aspirin (15mg/kg and 30mg/kg, respectively). Lastly, a group treated only with aspirin (30 mg/kg). Cigarette smoke exposure was performed for 2hr/day, 5days/week, for 31days. Behavioral tests were conducted weekly, 24hrs after cigarette smoke exposure, during acute withdrawal. At the end of week 4, rats were given either saline or aspirin 45 min before cigarette exposure for 11 days. Cigarette smoke increased withdrawal-induced anxiety, and 30 mg/kg aspirin attenuated this effect. Cigarette smoke exposure increased the relative mRNA and the protein level for nuclear factor κB (NFκB) in the PFC and the NAc, and aspirin treatment reversed this effect. In addition, cigarette smoke decreased the relative mRNA and the protein levels of glutamate transporter 1 (GLT-1) and the cystine-glutamate transporter (xCT) in the PFC and the NAc, while aspirin treatment normalized their expression. Thus, cigarette smoke caused neuroinflammation, alterations in relative mRNA glutamate transporter expression, and increased anxiety-like behavior, and these effects were attenuated by aspirin treatment.

Development and Characterization of Anticancer Model Drug Conjugated to Biosynthesized Zinc Oxide Nanoparticles Loaded into Different Topical Skin Formulations

Ruwa Zuhier Obaid[1], Rana Abu-Huwaij[2], Rania Hamed[1]

[1] Department of Pharmacy, Faculty of Pharmacy, Al-Zaytoonah University of Jordan, Jordan.
[2] Faculty of Pharmacy, Arab Amman University, Amman, Jordan.

DOI: https://doi.org/10.35516/jjps.v16i2.1545

ABSTRACT

Doxorubicin (DOX) is an anthracycline antineoplastic agents, which interacts with DNA and shows sever toxicity due to its lack of specificity. The cytotoxic effect of zinc oxide nanoparticles (ZnO NPs) is mainly concerned in changing the cytoskeleton and nucleoskeleton of proteins and/or producing reactive oxygen species (ROS) in cells exposed to ZnO NPs. The green synthesis of ZnO NPs from plant extracts has been recently employed as a simple, eco-friendly, safe, and cost- and time-effective approach with higher stability and reproducibility. *Phoenix dactylifera*, due to its chemical component (tannins, phenolic acid, and carotenoids), was employed in the preparation of ZnO NPs. The main objective of this study is to greenly synthesize ZnO NPs conjugated with DOX (DOX-ZnO NPS) and loaded into various types of gel preparations (hydrogel and oleogel). *P.dactylifera* solution extract was mixed with 0.6M zinc acetate at 1:1 v/v ratio to prepare ZnO NPs. The prepared NPs was characterized by UV-vis spectroscopy, particles size, PDI, and zeta potential. The maximum wavelength of ZnO NPs was detected at 360 nm. Dialysis method was used to determine the effect of ZnO NPs on enhancing DOX release. The cumulative amount of DOX was calculated via UV-vis spectroscopy at 480 nm after 48 h. Spherical nanoparticles of size range 15.35–28.74 nm and -22mV zeta potential was obtained. The rheological results showed that both gel formulations exhibited a pseudoplastic (shear-thinning) flow and viscoelastic behavior. The *in vitro* release studies showed that ZnO NPs enhanced the release of DOX, where the amount of DOX released from DOX-ZnO NPs hydrogel and oloegel was higher than that of DOX-hydrogel and oleogel. In addition, DOX-ZnO NPs hydrogel showed a faster release that DOX-ZnO NPs oleogel. Therefore, an eco-friendly and low-cost greenly synthesized ZnO NPs were successfully developed, conjugated with DOX, and loaded into hydrogels and oleogels for dermal delivery.

الناشر

الجامعة الأردنية
عمادة البحث العلمي
عمان 11942 الأردن
فاكس: 00962 6 5300815

رقم الإيداع لدى دائرة المكتبة الوطنية
(2008/23.3/د)

عمادة البحث العلمي

المجلة الأردنية في العلوم الصيدلانية

تعريف بالمجلة الأردنية في العلوم الصيدلانية

تأسست المجلة الأردنية في العلوم الصيدلانية بقرار لجنة البحث العلمي/ وزارة التعليم العالي والبحث العلمي رقم 367/2/10 تاريخ 2007/1/11 بشأن إصدار "**المجلة الأردنية في العلوم الصيدلانية**" ضمن إصدارات المجلات الأردنية الوطنية، وهي مجلة علمية عالمية متخصصة ومحكمة، وتصدر بدعم من صندوق دعم البحث العلمي والجامعة الأردنية تعنى بنشر البحوث العلمية الأصيلة المقدمة إليها للنشر في كافة مجالات العلوم الصيدلانية والعلوم الأخرى المرتبطة بها. وتصدر عن عمادة البحث العلمي وضمان الجودة في الجامعة الأردنية باسم الجامعات الأردنية كافة، خدمة للمتخصصين والباحثين والمهتمين في هذه المجالات من داخل الأردن وخارجه. وهي مجلة تصدر أربع مرات في العام أعتبارا من 2021، ومواعيد صدورها (آذار وحزيران وأيلول وكانون أول) من كل عام.

وباسمي وباسم أعضاء هيئة التحرير نود أن نشكر الزملاء الذين أسهموا بإرسال أبحاثهم إلى مجلتنا وتمكنا من إخراج العدد الأول. ونأمل من جميع الزملاء بإرسال ملاحظاتهم الإيجابية إلينا لنتمكن من النهوض بمجلتكم بالشكل الذي يليق بها.

وهذه دعوة إلى كافة الزملاء لإرسال اسهاماتهم العلمية من الأبحاث الأصيلة إلى عنوان المجلة.

والله ولي التوفيق

رئيس هيئة التحرير
أ.د. إبراهيم العبادي
قسم الصيدلة الحيوية والسريرية
كلية الصيدلة- الجامعة الأردنية
عمان 11942-الأردن